MONITORING OF CEREBRAL OXYGENATION, CEREBROVASCULAR REACTIVITY AND CIRCULATORY FUNCTION IN PRETERM INFANTS

Cristine Sortica da Costa

This dissertation is submitted for the degree of

Doctor of Philosophy

Trinity Hall

University of Cambridge

Supervised by Professors Topun Austin and Marek Czosnyka

February 2018

This dissertation is the result of my own work and includes nothing that is the outcome of work done in collaboration except where specifically indicated in the text or acknowledgments. I further state that no substantial part of my dissertation has already been submitted, or, is being concurrently submitted for any such degree, diploma or other qualification at the University of Cambridge or any other University or similar institution except as declared in the preface and specified in the text.

This dissertation does not exceed the word limit of 60 000 words.

Cristine Sortica da Costa

February 2018

“In all chaos there is a cosmos, in all disorder a secret order.”

C.G. Jung

Dedicated to my sister,

Claudia

TABLE OF CONTENTS

SUMMARY

Brain injury in the preterm infant is associated with death and lifelong disability. Cerebral hypoxia and fluctuations in cerebral blood flow (CBF), particularly in the first two days of life, have been implicated in the pathophysiology of haemorrhagic and ischaemic brain injury. Monitoring of haemodynamic changes during the early transitional circulation from in-utero to ex-utero life is currently based on standard measurements of systemic oxygenation and arterial blood pressure, with no reliable assessment of end-organ perfusion. Several studies have suggested the use of near-infrared spectroscopy (NIRS) and functional echocardiography as methods to assess cerebral perfusion and systemic blood flow. Although thresholds of cerebral hypoxia and systemic hypoperfusion have been proposed, values for cerebral oxygenation and CBF may differ for individual patients depending on several factors, such as gestational age, severity of illness and postnatal age. The aim of this thesis is to assess methods of monitoring cerebral oxygenation, cerebral vascular reactivity and cardiac function within the first two days of life, using NIRS and functional echocardiography measurements.

This thesis is divided in four sections:

1) The feasibility of monitoring cerebral oxygenation and cerebrovascular reactivity using cotside software is demonstrated in a series of case reviews. The challenges of recruiting preterm infants within the first hours of life and the heterogeneous characteristics of this population are discussed. In addition, the association between the cerebral oxygenation and impaired cerebrovascular reactivity within the first 48 hours of life and outcome of brain injury and mortality is investigated.

2) Combining measurements of systemic blood flow with end organ perfusion should be the uppermost goal in monitoring haemodynamic changes in preterm infants. The concept of optimal mean arterial blood pressure ($MABP_{OPT}$) or optimal cerebral perfusion pressure (CPP_{OPT}) has been

proposed by studies in adults with traumatic brain injury. Deviations from CPP_{OPT} have been associated with poor outcome. In this thesis, $MABP_{OPT}$ in preterm infants was defined based on an index of cerebrovascular reactivity. Deviations below $MABP_{OPT}$ were associated with intraventricular haemorrhage and mortality.

3) Most studies using cerebral NIRS or systemic measurements of blood flow use linear analysis. However, a complex biological system, such as the human brain, includes many complex regulatory mechanisms that interact in a non-linear way, resulting in effects that cannot be understood wholly through the analysis of its individual constituents. This thesis investigated the complexity of brain and systemic signals by using multi-scale entropy analysis. Lower complexity of brain signals was observed in infants who developed intraventricular hemorrhage or died.

4) Functional echocardiography has increasingly been performed by neonatologists to monitor circulatory changes in preterm infants. Preterm infants are at increased risk to develop low systemic and cerebral blood flow within the first two days of life. Several studies have attempted to correlate static measurements of cardiac function with cerebral oxygenation. In addition, threshold values of systemic and cerebral blood flow have been described. However, most studies on thresholds of cardiac output in preterm infants included stable infants with different gestational and chronological ages. In this thesis we describe the changes in systemic and cerebral blood flow in a cohort of preterm infants within the first 48 hours of life who had invasive monitoring of arterial blood pressure for clinical reasons. The patterns of changes in cardiac output and cerebral oxygenation in infants who had and did not have intraventricular haemorrhage are discussed. Furthermore, the relationship between the presence of haemodynamically significant ductus arteriosus and brain injury is assessed.

The final part of this thesis discusses the implications of these results and directions for future studies.

ACKNOWLEDGEMENTS

Firstly, I would like to thank all parents who gave consent for their preterm infants to participate in the studies included in this thesis.

I would like to thank my supervisors Professors Topun Austin and Marek Czosnyka for the time, patience and dedication in guiding me in this project. I also would like to thank Dr Peter Smielewski, an important mentor, who taught me the concepts of signal processing and statistics. I am immensely grateful for the scientific and personal support they all gave me throughout the last six years and for continuously inspiring me.

I would like to thank all my colleagues and friends from NeoLab and Brain Physics Group. In particular Chuen Wai Lee, Maria Chalia and Laura Dempsey with whom I shared the frustrations and happiness of recruitment, data analysis and writing. Andrea Edwards for her support especially with the paperwork to obtain research ethical approvals for the studies. Michal Placek for his help to perform the multiscale entropy analysis for Chapter 7. Danilo Cardim for his friendship and help to perform the statistical analysis for Chapter 8. Mee Mia Kim, Homa Majd, Tom and Jo Mackerrell, amazing friends for life that I made in Trinity Hall. I would like to thank all doctors and nurses from the Neonatal Unit at the Rosie Hospital in Cambridge. In particular Dr Susan Broster and Dr Wilf Kelsall for the immense support in my medical career and friendship. I would like to thank Paul Higgins for his love, patience and support during the tough years of data collection and data analysis.

I would like to thank Cambridge Trust and CAPES for my PhD Scholarship and Sparks for financially supporting Sister Claire Kemp and Dr Gordon Stevenson to help me with data collection and data analysis.

I would like to thank my parents, Luiz Carlos and Neiva and my aunt, Neide, for always encouraging me to progress in my career and achieve my dreams. And finally my sister Claudia, who was born prematurely and has always taught me to love unconditionally.

LIST OF PUBLICATIONS

Manuscripts published or submitted for publication

1. Ng IHX, da Costa CS, Zeiller FA, Smielewski P, Czosnyka M, Austin T. *Burden of hypoxia and intraventricular haemorrhage in extremely preterm infants.* **Under submission, 2018.**

2. da Costa CS, Czosnyka M, Smielewski P, Austin T. *Optimal mean arterial blood pressure in extremely preterm infants within the first 24 hours of life.* **The Journal of Pediatrics, 2018 Sept; Epub ahead of print. (PMID: 30243537)**

3. Rhee CJ, da Costa CS, Austin T, Brady KM, Czosnyka M, Lee JK. *Neonatal cerebrovascular autoregulation*. **Pediatric Research, 2018 Sept; Epub ahead of print. Review (PMID: 30196311)**

4. Sortica da Costa C, Placek MM, Czosnyka M, Cabella B, Kasprowicz M, Austin T, Smielewski P. *Complexity of brain signals is associated with outcome in preterm infants.* **Journal of Cerebral Blood Flow and Metabolism, 2017 Oct; 37(10): 3368-3379 (PMID: 28075691)**

5. da Costa CS, Greisen G, Austin T. *Is near-infrared spectroscopy clinically useful in the preterm infant?* **Archives of Disease in Childhood Fetal and Neonatal Edition, 2015 Nov; 100(6): F558-61 (PMID: 26215405)**

6. da Costa CS, Czosnyka M, Smielewski P, Mitra S, Stevenson GN, Austin T. *Monitoring of Cerebrovascular Reactivity for Determination of Optimal Blood Pressure in Preterm Infants.* **The Journal of Pediatrics, 2015 Jul; 167(1): 86-91 (PMID: 25891381)**

Conferences Presentations

1. **43rd Annual Fetal and Neonatal Physiological Society Meeting, 2016, Cambridge, UK: "***Complexity of Brain Signals is Associated with Outcome in Preterm Infants"* – oral presentation

2. **Anglo-French Neonatal Societies Summer Meeting, 2016, Cambridge, UK:** *"Complexity of Brain Signals is Associated with Outcome in Preterm Infants"* – oral presentation

3. **12th World Congress of Perinatal Medicine, Madrid, Spain, Nov 2015:** *"Optimal Mean Arterial Blood Pressure in Preterm Infants Less than 24 Hours of Age"* – poster presentation

4. **9th International Conference on Brain Monitoring and Neuroprotection in the Newborn, Cork, Ireland, Oct 2015:** *"Determining the relationship between threshold of cerebral hypoxia and adverse outcome in preterm infants"* – poster presentation

5. **1st Congress of Joint European Neonatal Societies (jENS), Budapest, Hungary, 2015:** *"Optimal Mean Arterial Blood Pressure in Preterm Infants Less than 24 Hours of Age"* – oral presentation

6. **XXII Encontro International de Neonatologia da Santa Casa de São Paulo, São Paulo, Brazil, May 2015:** *"Autoregulação do Fluxo Cerebral no Recém-Nascido Pre-termo* – invited speaker (talk in Portuguese)

7. **54th ESPR Annual Meeting, Porto, Portugal, Oct 2013:** *"Defining Optimal Blood Pressure Based on a Novel Cerebrovascular Regulation Index in Preterm Infants"* – oral presentation

8. **Neonatal Society Summer Meeting, Edinburgh, Scotland, Jun 2013:** *"Defining Optimal Blood Pressure Based on a Novel Cerebrovascular Regulation Index in Preterm Infants"* – oral presentation

SCHOLARSHIP & GRANTS

1. Cambridge Overseas Trust & Capes Scholarship – *"Circulatory function and cerebrovascular control of blood flow and oxygen delivery to the brain in newborn infants undergoing intensive care"* (2012-2016).

2. Trinity Hall Graduate Grant for Research expenses – (2016)

LIST OF FIGURES

LIST OF TABLES

LIST OF ABBREVIATIONS

CBF: cerebral blood flow

CBV: cerebral blood volume

CDO_2: cerebral oxygen delivery

$CMRO_2$: cerebral oxygen consumption

CO: cardiac output

COEF: cerebral oxygen extraction fraction

COx: cerebral oximetry index

CPP: cerebral perfusion pressure

CRIB II: Clinical Risk Index for Babies II

CRP: c-protein reactive

CSF: cerebrospinal fluid

CT: computed tomography

CtOx: oxidised cytochrome oxidase

CVR: cerebral vascular resistance

EEG: electroencephalogram

FTOE: fraction tissue oxygen extraction

GMH-IVH: germinal matrix and intraventricular haemorrhage

Hb: deoxyhaemoglobin

HbO_2: oxyhaemoglobin

HIE: hypoxic ischaemic encephalopathy

HR: heart rate

hsPDA: haemodynamically significant persistent ductus arteriosus

HVx: haemoglobin volume index

ICP: intracranial pressure

LPA: left pulmonary artery

LVO: left ventricle output

MABP: mean arterial blood pressure

$MgSO_4$: magnesium sulphate

MPA: main pulmonary artery

MRI: magnetic resonance imaging

MSE: multiscale entropy

Mx: mean flow in the middle cerebral artery index

NEC: necrotizing enterocolitis

NIRS: Near-infrared spectroscopy

NO: nitric oxide

O_2: Oxygen

$PaCO_2$: partial pressure of carbon dioxide in arterial blood

PaO_2: pressure partial of oxygen in arterial blood

PDA: persistent ductus arteriosus

PET: positron emission tomography

PET: positron emission tomography

PFO: persistent foramen ovale

PHI: parenchymal haemorrhagic infarct

PPHN: persistent pulmonary hypertension of the newborn

PPROM: preterm prolonged rupture of membranes

PRx: pressure reactivity index

PVL: periventricular leukomalacia

rSO_2: regional cerebral oxygen saturation

RVO: right ventricle output

SaO_2: peripheral arterial oxygen saturation

SRS: spatially resolved spectroscopy

SVC: superior vena cava

SVR: systemic vascular resitance

TBI: traumatic brain injury

tCO_2: transcutaneous carbon dioxide

THx: total haemoglobin index

TOHRx: tissue oxygenation heart rate reactivity index

TOI: tissue oxygenation index

TOx: tissue oxygen reactivity index

1. MOTIVATION, AIMS AND HYPOTHESES

1.1. MOTIVATION

Preterm birth is a major cause of neonatal mortality and long-term disabilities. Approximately 14.9 million infants are born prematurely worldwide per year and the complications from preterm birth are the second most common cause of death in children under five years of age[1, 2]. Although advances in neonatal medicine over the last two decades have contributed to decrease the mortality rates, the number of preterm infants who survive with respiratory, visual or neurological sequelae remains high[3-5]. The emotional and financial burden of having a child affected by complications of prematurity is huge, especially for those who survive with poor neurodevelopmental outcome such as cerebral palsy and cognitive impairment[6]. Most of these neurological complications result from early injury to the developing brain. Therefore, efforts in continuing to optimise neonatal care and improve outcome for infants who survive the neonatal period should focus on early brain monitoring and neuroprotection.

1.2. AIMS AND HYPOTHESIS

The aim of this thesis is to investigate methods to monitor early cerebral oxygenation, cerebrovascular reactivity and cardiac function using near-infrared spectroscopy (NIRS) and functional echocardiography. The main transitional changes in systemic and cerebral blood flow from in-utero to ex-utero life occur within the first 48 hours of age. These changes are characterised by fluctuation in systemic and in cerebral blood flow. The degree of cerebral hypoperfusion has been associated with the development of brain injury and mortality in the preterm population. Therefore, early monitoring of systemic and cerebral blood flow may provide better understanding of the pathophysiology of brain injury and predict outcome.

This thesis aimed to test the following hypothesis:

Hypothesis I: Monitoring of cerebral oxygenation and cerebral vascular reactivity within the first 48 hours of age can provide information on cerebral hypoxia and impaired cerebrovascular reactivity between infants with and without intraventricular haemorrhage (IVH) and infants who died and survived.

The use of sophisticated cotside software that collects NIRS and physiological signals and allows real-time data analysis can provide information on the pathophysiology of brain injury in preterm infants. The use of ICM+ software® to collect and analyse data in preterm infants was an important part of the work presented in this thesis and will be discussed with the presentation of cases. In this part of the thesis, the association between cerebral hypoxia and impaired cerebrovascular reactivity with brain injury and death is explored.

Hypothesis II: Optimal mean arterial blood pressure in preterm infants can be defined by monitoring cerebrovascular reactivity using NIRS.

Defining optimal cerebral perfusion pressure and optimal mean arterial blood pressure by the strength of cerebrovascular reactivity has been described in adult patients. This part of the thesis focuses on defining optimal mean arterial blood in preterm infants based on an index of cerebrovascular reactivity measured using NIRS, and investigating the association between deviations from optimal values and outcome.

Hypothesis III: Complexity of cerebral near-infrared signals in preterm infants less than 24 hours old can predict the development of IVH and mortality in this population.

The use of multi-scale entropy analysis to measure complexity of physiological signals has been applied to distinguish healthy from pathological status. This part of the thesis focuses on applying multiscale entropy to cerebral NIRS signal and investigating the association between complexity of brain signals and outcome in preterm infants.

Hypothesis IV: Measurements of cardiac output and ductal patency combined with measurements of cerebral oxygenation and cerebrovascular reactivity can determine the significance of low systemic blood flow on development of IVH.

Decrease in cerebral and systemic blood flow is associated with the development of brain injury in preterm infants. This part of the thesis describes measurements of cardiac output, superior vena cava and ductal patency within the first 48 hours of life. The pattern of the changes in systemic blood flow, and cerebral oxygenation and the correlation between these measurements, between infants who had and did not have IVH is investigated.

2. INTRODUCTION

2.1. PRETERM BRAIN INJURY

Brain injury in the preterm infant is associated with an increased risk of death and poor neurodevelopmental outcome. The advances in neonatal care over the last twenty years have contributed to decrease the mortality rate and to reduce severe motor disabilities in survivors. Nevertheless, the number of preterm infants who survive the neonatal period with poor long term neurodevelopmental outcome resulting from early brain injury remains high[4, 7-9].

2.1.1. Intraventricular haemorrhage

The preterm brain is particularly susceptible to germinal matrix and intraventricular haemorrhage (GMH-IVH) and parenchymal haemorrhagic infarct (PHI), usually occurring within the first three to four days of life. The overall incidence of GMH-IVH has declined since the 1980s but the absolute number of new cases every year remains high. The incidence of GMH-IVH remains around 25% to 30% for all preterm infants born with birth weight < 1500 grams and 45% of those with birth weight < 1000 grams. The incidence of the most severe forms of GMH-IVH is approximately 5%[7, 10].

The haemorrhage arises from bleeding from the vessels in the subependymal germinal matrix, a layer of cells surrounding the lateral ventricles that is also known as ganglionic eminence. The germinal matrix is a very gelatinous and vascularised area of high cellular proliferation in the developing fetal brain, where neuronal precursors arise between 10 to 20 weeks of gestation followed, in the third trimester, by glial cell precursors that become oligodendrocytes and astrocytes. This area involutes progressively, decreasing from a width of 2.5 mm at 23 to 24 weeks to 1.4 mm at 32 weeks to nearly complete extinction by 36 weeks of gestation. The germinal matrix is characterised by intense angiogenesis, induced by high levels of vascular endothelial growth factor (VEGF) and angiopoietin (ANGPT)-2, which may contribute to its

vascular fragility and vulnerability to haemorrhage. In addition, the expression of fibronectine is reduced in the germinal matrix, which may contribute to the fragility of the vasculature in this area[11].

The development of GMH-IVH is closely related to the arterial and venous supply to the germinal matrix. The arterial supply to the subependymal germinal matrix is derived from the anterior cerebral artery (via Heubner's artery), the middle cerebral artery (deep striatal branches primarily and penetrating branches from surface meningeal branches) and the internal carotid artery (via anterior choroidal artery). This rich arterial network supplies the rich capillary bed of the germinal matrix, which is formed by thin and irregular endothelial-lined vessels that are very sensitive to hypoxia and changes in cerebral perfusion pressure. This microvascular bed is continuous to a deep vascular system that ends in the vein of Galen. The venous drainage of the subependymal germinal matrix is mainly through the terminal vein that is also the principal terminus of the medullary, choroidal and thalamostriate veins that drain blood from cerebral white matter, choroid plexus, striatum and thalamus. The blood flow makes a U-turn in the subependymal region at the level of the foramen of Monro, the location where most types of haemorrhage develop (Figure 2.1). This U-shape characteristic is thought to be important for the development of periventricular infarction[8].

Figure 2.1 Development of cerebral vasculature

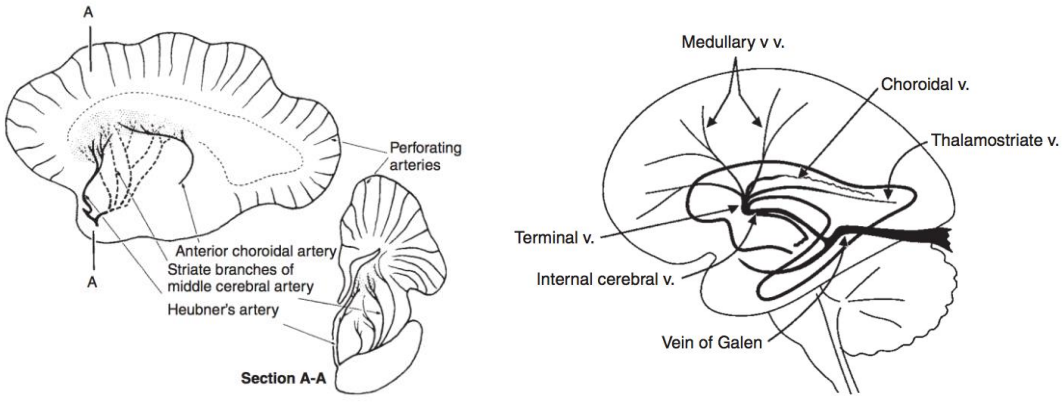

The figure on the left shows the arterial supply to subependymal germinal matrix. The figure on the right shows the venous drainage of subependymal matrix with the peculiar U-shape anatomy. (Adapted from *Neurology of Newborn, Volpe 2008)*[8].

The bleeding in the germinal matrix may disrupt the ependymal lining and extend into the ventricles, causing different degrees of IVH (Table 2.1). The destruction of the germinal matrix due to haemorrhage and thus damage to its glial cells may lead to detrimental effects in later brain development. Severe IVH may be complicated by ventricular dilatation, with later development of post-haemorrhagic hydrocephalus, or by PHI in the periventricular white matter, or by both complications[8] (Figure 2.2). The ventricular dilatation, and possible later hydrocephalus, is a consequence of an obstruction to the cerebrospinal fluid flow caused by excessive bleeding and clot formation in the basilar cisterns in the posterior fossa, in the aqueduct of Sylvius and in the arachnoid villi. The PHI has been described as an "extension" of the GMH-IVH, however microscopic studies have revealed that perivascular haemorrhage follow the U-shaped distribution of the medullary veins in the periventricular cerebral white matter and tend to be concentrated near the ventricular angle where these veins become confluent. Therefore, the periventricular haemorrhagic necrosis is actually a venous infarction. The most common injury in the white matter caused by PHI is large porencephalic cysts that can be isolated or accompanied by smaller cysts (Figure 2.3E)[8, 12].

Figure 2.2 Germinal matrix haemorrhage (GMH) and intraventricular haemorrhage (IVH) with PHI

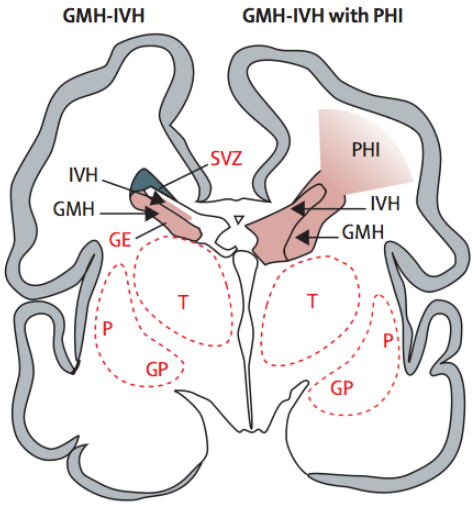

In red is shown GMH that extended into the ventricle causing IVH (left). Large GHM-IVH can result in PHI (right). Subventricular zone (SVZ), the ventral germinative epithelium of the ganglionic eminence (GE), thalamus (T) and putamen (P)/globus pallidum (GP) are shown (Adapted from *Volpe 2009, Lancet Neurology*)[13].

Cranial ultrasound is the non-invasive technique of choice to diagnose GMH-IVH. The severity of GMH-IVH is usually described following the modified Papile classification (Table 2.1 and Figure 2.3)[14]. Despite suggestions that this classification should be replaced by a more descriptive and precise nomenclature, the Papile criteria remains widely used in both clinical or research settings[15, 16]. However, 'IVH grade IV' should ideally be replaced by 'IVH grade I, II or III with or without PHI', as PHI may occur in the presence of any degree of haemorrhage[13].

Table 2.1 Severity of GMH-IVH according to Papile criteria[14]

Severity	Description
Grade I	Haemorrhage is confined to the germinal matrix region
Grade II	Haemorrhage occupies ≤ 50% of the lateral ventricle volume
Grade III	Haemorrhage fills > 50% of the lateral ventricle, usually causing distension and dilatation of the ventricles
Grade IV	Presence of an infarction in the periventricular white matter ipsilateral to a large GMH-IVH

Most infants will have a 'silent' clinical presentation at the onset of GMH-IVH; therefore, clinical diagnosis may be a challenge. According to cranial ultrasound studies, 50% of the affected infants will develop GMH-IVH within the first 24 hours of life and 90% of the lesion can be visualised by 72 hours. Maximal extension of the initial lesion can be seen after three to five days of the initial insult and all lesions should be visible by day seven of life[17]. Some infants may present haemodynamic compromise such as hypotension and general hypoperfusion, which may be accompanied by subtle changes in the level of consciousness, movement, tone, respiration and in more rare cases, infants may present acute deterioration with stupor, coma, de-cerebrating posturing, generalised tonic seizure and quadriparesis[18].

All degrees of GMH-IVH have been associated with an increased risk of poor outcome. IVH grade I and II may be correlated with better outcome compared to IVH grade III and IV. However, in a recent systematic review and meta-analysis, Mukerji et al. (2015) have reported that even mild GMH-IVH has been associated with death or moderate to severe neurodevelopment impairment[7]. On the other hand, severe GMH-IVH has been associated with worse outcome in all domains, such as death, motor and cognitive impairment at both 18 to 24 months and 3 to 18 years neurodevelopmental follow-up[7]. Morita et al. (2015), using diffusion tension imaging studies, have demonstrated an association between IVH grade I and II and cerebellar and cerebral white matter impairment. They have also observed that these areas were more vulnerable to disruption due to IVH in younger preterm infants compared to older preterm infants[19]. Bolisetty et al. (2014) have shown that infants who developed GMH-IVH had increased rates of neurosensory impairment, developmental delay, cerebral palsy and deafness when compared to infants with no GMH-IVH[20].

Figure 2.3 Ultrasound image of GMH-IVH grades

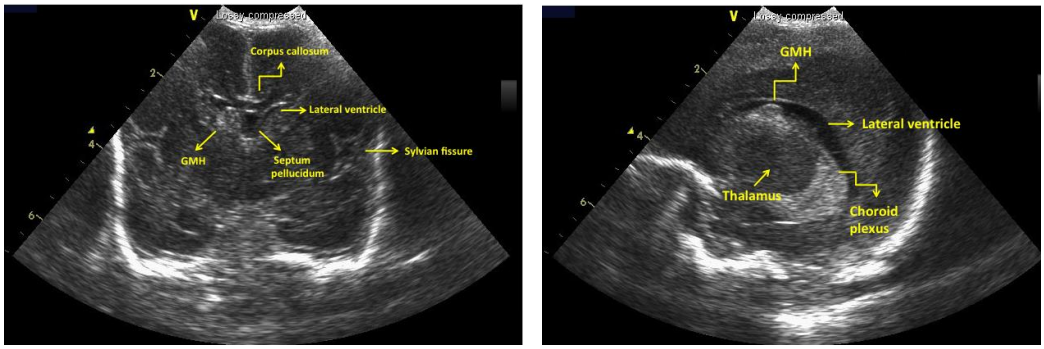

A. Grade I: coronal view on the left and sagittal view on the right

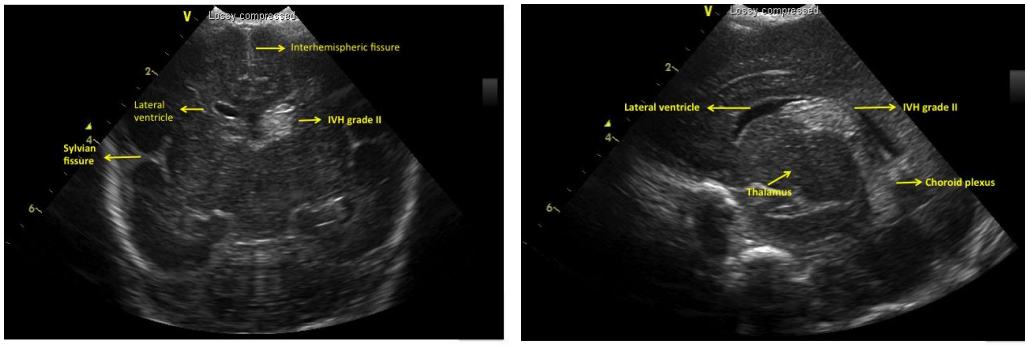

B. Grade II: coronal view of the left and sagittal on the right

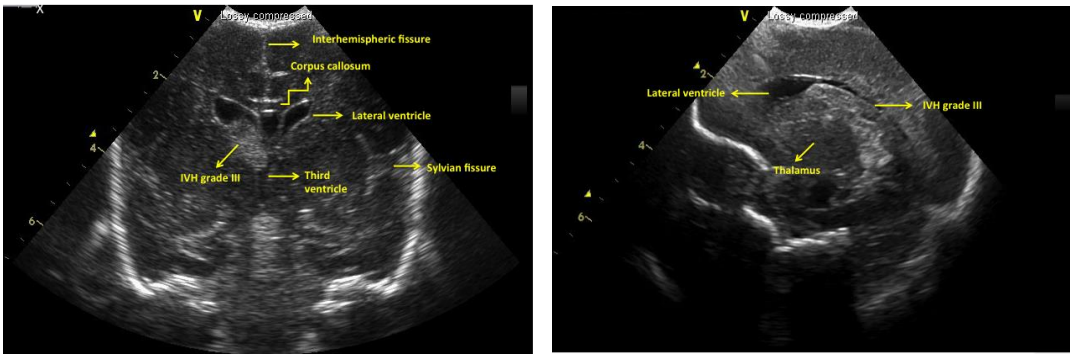

C. Grade III: coronal view on the left and sagittal view on the right

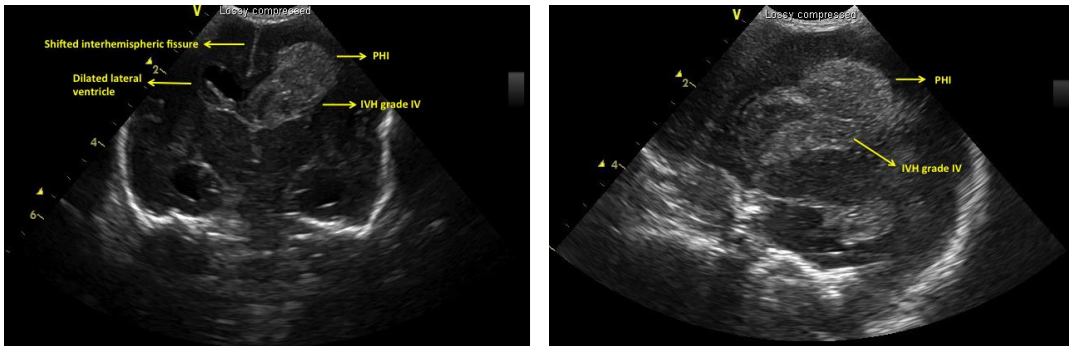

D. Grade IV: coronal view on the left and sagittal view on the right

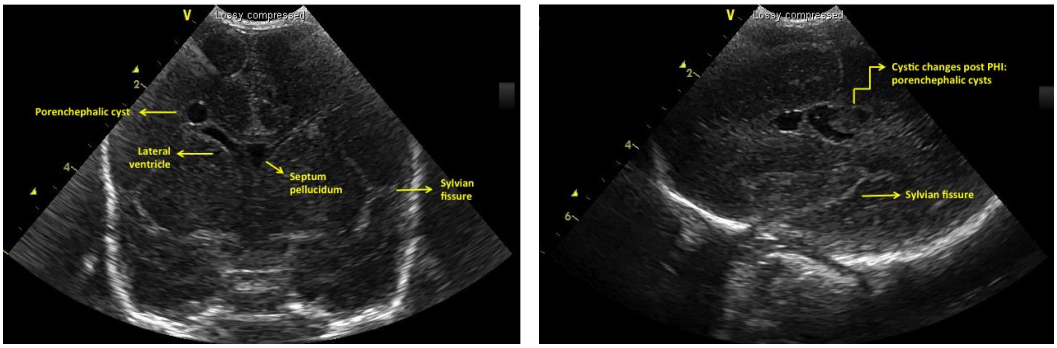

E. Cystic parenchymal changes post PHI: porenchephalic cysts can be seen on the coronal and sagittal views

All cranial ultrasound images presented here were recorded from infants recruited to the studies included in this dissertation. I collected and reported all images (more details in Chapter 4).

2.1.2. White matter injury

Periventricular leukomalacia (PVL) refers to ischaemic brain injury in preterm infants[21, 22]. Banker & Larroche (1962) were the first to name the ischaemic changes observed in the histology of preterm brain's tissue as periventricular leukomalacia. The term PVL was chosen because they observed white (*leukos*) spots and softening (*malacia*) areas in the periventricular white matter[23]. PVL can occur as an isolated phenomenon or in association with GMH-IVH. The pathogenesis of PVL is multifactorial and less well understood than the mechanisms related to GMH-IVH; ischaemia, inflammation and free radical release have all been associated with its aetiology[13].

PVL is characterised by two components: focal and diffuse. The focal component consists in necrosis deep in the periventricular white matter with loss of all cellular elements. The focal necrotic lesions may be initially macroscopic in size and then evolve to cystic formation after several weeks. They usually occur in areas that are considered arterial border zones, lying between the long penetrating branches of the middle, anterior and posterior cerebral arteries that terminate in the deep periventricular white matter. These vascular end zones may predispose the premature brain to injury in the presence of cerebral ischaemia. Following an acute hypoxic-ischaemic insult, coagulation necrosis at the sites of focal periventricular lesions is observed. Over the subsequent days, the cellular response includes macroglia infiltration, proliferation of hypertrophic astrocytes, endothelial hyperplasia and appearance of foamy macrophages. The tissue dissolution and cavity formation are usually seen in about one to two weeks from the initial insult. These cavity lesions, that are large enough to be seen on cranial ultrasound, are usually described as 'cystic PVL' and they should not be confounded with periventricular haemorrhagic infarction, which is mainly a venous disturbance that occurs mostly in association with GMH-IVH[24-26].

In developed countries, where advanced antenatal and neonatal care is broadly available, severe cystic lesions are currently seen in less than 5% of preterm infants with birth weight < 1500 grams[27, 28]. However, focal necrosis can often be microscopic in size and evolve over several weeks to glial scars that are not easily

seen on cranial ultrasound and sometimes may be even difficult to be visualised on brain MRI. This form of PVL accounts for the majority of the cases and is known as 'non-cystic PVL' or diffuse white matter injury[13, 26].

Figure 2.4 Cystic and non-cystic periventricular leukomalacia

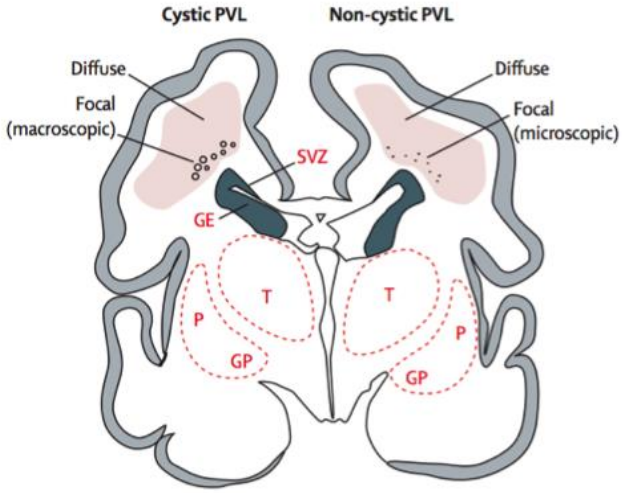

The small circles on the left are the cystic PVL lesions and the small black dots on the right are the non-cystic PVL lesions. Dorsal cerebral subventricular zone (SVZ), ganglionic eminence (GE), thalamus (T) and putamen (P)/globus pallidum (GP) are shown. (Adapted from *Volpe 2009, Lancet Neurology*)[13].

Two decades ago, white matter infarct with axonal degeneration and loss of cortical neurons was the most common cause of early brain injury associated with cerebral palsy. More recently, studies have shown a reduction to less than 1% in white matter infarcts but an increase in more diffuse lesions[29-32]. This diffuse white matter injury seems to occur from selective vulnerability of pre-myelinating oligodendrocytes to cerebral hypoxia. A reactive proliferation of new oligodendrocytes occurs, however these cells do not have the capacity to fully differentiate into mature myelin-producing cells, resulting in hypomylination with ventriculomegaly is a possible later consequence of PVL[13, 26]. Cystic PVL is associated with spastic diplegia and diffuse white matter injury has been correlated with cognitive deficits, usually in the absence of major motor disabilities[26, 28].

Figure 2.5 Bilateral periventricular leukomalacia

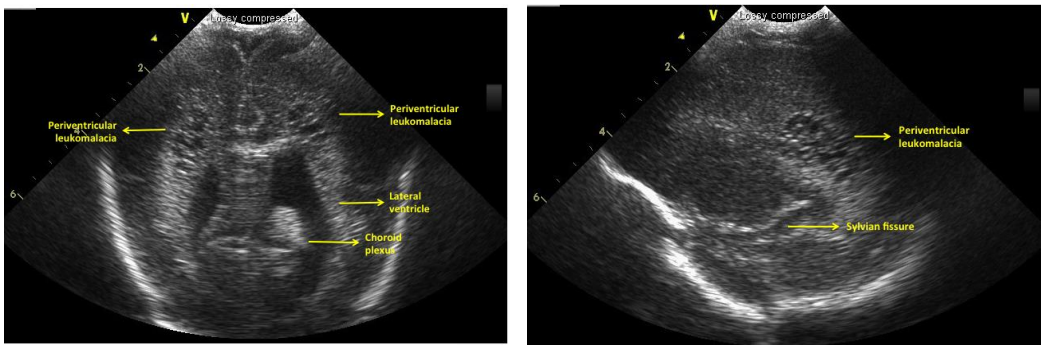

On the right the posterior coronal view shows cystic PVL and on the left side the sagittal view shows the equivalent cystic. Both images were recorded from an infant recruited to the studies included in this dissertation.

2.1.3. Pathophysiology of brain injury

The aetiology of brain injury in the preterm infant is complex and multifactorial. Fluctuations in cerebral blood flow and cerebral oxygenation, as well as infection and inflammation, have been implicated in the pathophysiology of haemorrhagic and ischaemic brain lesions[22, 33, 34].

Pathogenesis of GMH-IVH

Cerebral ischaemia has been recognised as an important factor associated with the pathophysiology of GMH-IVH[35]. Hypoperfusion of the germinal matrix can cause impairment in the integrity of the vascular endothelium. A subsequent period of reperfusion in this area, which is metabolically active with limited structural support, may lead to an increase in intravascular pressure, making the vulnerable vessels to bleed[8].

The work done by Goddard-Finegold et al. (1982) and Ment et al. (1982) has reinforced the concept of ischaemia/reperfusion injury in the pathophysiology of GMH-IVH. By using the newborn beagle puppy model, they have shown that GMH-IVH occurred in animals that became hypertensive after receiving rapid volume expansion with or without previous systemic hypotension[36, 37]. Perlman et al. (1983), using the ultrasound Doppler technique, were the first to describe a 'fluctuating' pattern in cerebral flow velocity in infants who developed GMH-IVH[38]. The presence

of a persistent pressure-passive circulation in sick preterm predisposes them to sudden increases in cerebral blood flow (CBF) in association with increases in arterial blood pressure[39, 40]. Moreover, elevations in venous pressure have also been considered an important mechanism in development of GMH-IVH[38, 41, 42]. Recent evidence has suggested that disturbances in arterial and venous circulation may be modulated by additional factors, such as inflammation (chorioamnionitis) as a negative influence or antenatal glucocorticoids, as a positive influence[43-46].

Pathophysiology of white matter injury

Cerebral ischaemia, maternal intrauterine or neonatal infection and fetal or neonatal inflammation have been associated with the pathogenesis of PVL[25].

Severe hypotension, along with low cerebral blood flow and impaired cerebral autoregulation are the main contributing factors to the development of white matter brain injury[47-49]. The active development of the peripheral penetrating vasculature occurs during the last 16 weeks of gestation. This may predispose the more immature infants to focal white matter injury even in the presence of very low degree of hypoperfusion and ischaemia[50]. The immature white matter vasculature has poor vasoreactivity to changes in pressure; therefore preterm infants with impaired cerebral autoregulation are also at risk of developing PVL[51, 52]

Severe early hypocarbia (low $PaCO_2$) can cause potent cerebral vasoconstriction and it has been associated with PVL[53, 54]. Shankaran et al. (2006) have shown that cumulative hypocarbia during the first week of life in preterm infants born < 1250 grams has been associated with increased likelihood to develop PVL[55]. Infection and inflammation can induce injury or death of pre-oligodendrocytes cells by systemic upregulation of pro-inflammatory cytokines and diffuse activation of microglia within the immature white matter[25].

2.2. CEREBRAL BLOOD FLOW AND CEREBROVASCULAR REACTIVITY IN THE PRETERM BRAIN

Preterm infants are at risk of developing low systemic and cerebral blood flow (CBF) during the first 24 hours of age due to the haemodynamic changes following birth[56]. However, the nadir and duration of a decreased CBF may be a determinant factor for the development of brain injury in some infants. In addition, abrupt increases and fluctuations in CBF may contribute to 'reperfusion injury' – possibly due to loss of cerebral autoregulation – which has been strongly associated with GMH-IVH[57].

A decrease in CBF with increased cerebral oxygen extraction fraction (COEF) occurs immediately after birth in newborn infants. Garfunkel et al. (1954) were the first to measure CBF and cerebral oxygen consumption ($CMRO_2$) in newborn infants[57]. Using the method published by Kety-Schmidt (1944) observed values of 15-23 ml $100g^{-1}$ min^{-1} and 1.1-2.1 ml $100g^{-1}$ min^{-1} for CBF and $CMRO_2$, respectively. The Kety-Schmidt method was based on the inhalation of nitric oxide (NO). CBF was calculated on the assumption that the rate at which the cerebral venous blood content of nitric oxide approaches the arterial blood content will depend on the volume of blood flowing through the brain[58]. Since then, several methods have been used to assess CBF in term and preterm infants. Meek et al. (1998) used near-infrared spectroscopy (NIRS) to measure CBF in preterm infants. Applying a modified Fick principle (Figure 2.6), where oxygen is the intravascular tracer, they reported values of 6.3-15.2 ml 100^{-1} min^{-1} for CBF in mechanically ventilated preterm infants within the first day of life. These measurements were comparable with values of CBF obtained using Xenon clearance technique (between 5.2-18.7 ml $100g^{-1}$ min^{-1}) and positron emission tomography (PET) (between 4.7-17 ml $100g^{-1}$ min^{-1})[59, 60]. Interestingly, values for CBF in preterm infants in the first 24 hours after birth may be lower than the minimal estimated CBF required for minimal neuronal viability and metabolism in the adult brain (15 ml 100^{-1} min^{-1})[61]. In the preterm brain the minimal CBF to maintain neuronal viability has been estimated at less than 5 ml $100g^{-1}$ min^{-1} [62, 63].

Figure 2.6 Measurement of CBF using NIRS (Fick principle)

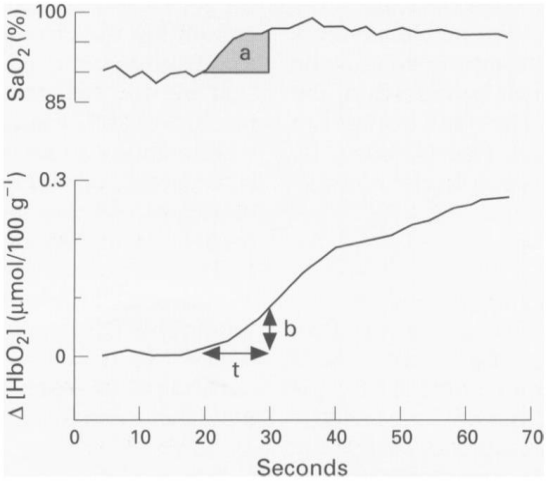

The figure shows an increase in peripheral arterial oxygen (SaO_2) and a subsequent increase in the concentration of oxyhaemoglobin ($\Delta[HbO_2]$). CBF is calculated by dividing the change in $\Delta[HbO_2]$ (b) by the area (a). Adapted from *Pryds et al. (1996)*[64].

CBF increases over the first days of life as a normal adaptation to postnatal circulation[65]. In growing preterm infants, studies have demonstrated that global CBF rises to a range of 10-20 ml $100g^{-1}$ min^{-1}, which is about one third of values observed in the healthy adult brain (50-75 ml 100^{-1} min^{-1})[66].

CBF is dependent on the relationship between cerebral perfusion pressure (CPP) and cerebrovascular resistance (CVR) (Equation 2-5). However, this relationship is not linear, but curvilinear as explained by Darcy's and Poiseuille's Laws.

As described by the Darcy's Law, the flow rate of liquid (Q) is directly proportional to the pressure difference between the inlet and outflow ($P_i - P_o$), which is also known as perfusion pressure (Equation 2-1). In the Darcy's law, K is a constant called the hydraulic conductance and its reciprocal is the hydraulic resistance (R) (Equation 2-2). The Darcy's Law is equivalent to Ohm's Law (in the field of electricity)[67].

The approximately relationship between CBF and CPP could be explained by Poiseulle's Law (Equation 2-3). Poiseuille observed that resistance to liquid (blood) through a straight rigid tube is directly proportional to the viscosity (resistance to flow) of the liquid (η) and the length of the tube (ι), but varies inversely with the flow power of the tube radius (r) (Equation 2-3).

Equation 2-1

$$Q = K.(Pi - Po)$$

Equation 2-2

$$Q = K.(Pi - Po) / R$$

Equation 2-3

$$R = 8\eta l/\pi^4$$

The combination of the Darcy's law with Poiseuille's Law gives us the following mathematical relationship (Equation 2-4):

Equation 2-4

$$Q = (Pi - Po).8\eta l/\pi^4$$

Therefore, for a given fluid (e.g. blood), the larger the diameter of a tube the higher the flow rate for a given pressure difference. Moreover, for a given pressure gradient, the higher is the viscosity of the blood the smaller the flow rate.

Some of the limitations for the application of the Poiseuille's Law in human physiology are: its strict relationship to laminar flow, the assumption of constant pressure gradient and the presence of cylindrical tubes (vessels) with parallel walls. Laminar flow is observed in most of the cardiovascular system (usually in arteries), however once turbulence has occurred, more pressure is required to achieve a given increase in flow. In addition physiological circulation is maintained by a pulsatile and oscillatory pressure, hence pressure gradient is not constant.

Equation 2-5

$$CBF = \frac{CPP}{CVR}$$

CPP is the difference between cerebral arterial and venous blood pressure (Equation 2-6). Cerebral arterial blood pressure is usually assumed to be identical to mean arterial blood pressure (MABP) in other major arteries in the body. Cerebral venous pressure is assumed to be equal to intracranial pressure (ICP).

Equation 2-6

$$CPP = MABP - ICP$$

CVR is dependent on blood vessel size, blood viscosity and characteristics of blood flow in the vessel. MABP is influenced by cardiac output and total peripheral vascular resistance, which differs from CVR.

Cerebral oxygen supply is tightly coupled to cerebral energy demand under normal conditions, however in many pathological states this coupling may be deranged, leading to hypoxia. Cerebral oxygen supply is the product of arterial oxygen content (CaO_2) and cerebral blood flow (CBF) (Equation 2-7):

Equation 2-7

$$Cerebral\ O_2\ delivery = CBF\ .\ CaO_2$$

CaO_2 is the sum of oxygen bound to haemoglobin and dissolved oxygen (Equation 2-8).

Equation 2-8

$$CaO_2 = b \times SaO_2 \times cHb + a \times PaO_2$$

Where β (1.39) is the oxygen capacity of haemoglobin (each gram of haemoglobin is capable of carrying 1.39 mL of O_2), SaO_2 is arterial oxygen saturation, cHb is arterial haemoglobin concentration, α (0.003) is the solubility coefficient of oxygen in the human blood and PaO_2 is partial pressure of oxygen in arterial blood. CaO_2 is mainly dependent on oxygen bound to haemoglobin, as the amount of dissolved O_2 is minimal.

Adjustments of cerebral O_2 supply due to changes in cerebral O_2 demand occur mainly due to changes in CBF. However, when there is a reduction in oxygen delivery, the metabolic demand is met by increasing the oxygen extraction in the blood and can be expressed as CFOE (Equation 2-9):

Equation 2-9

$$CFOE = \frac{CaO_2 - CvO_2}{CaO_2}$$

Where CaO_2 is cerebral arterial oxygen content and CvO_2 is cerebral venous oxygen content.

Changes in a cerebral hemodynamic and oxygen supply may affect cerebral oxygenation and consequently cerebral energy metabolism (Table 2.2). A reduction in oxygen delivery can be caused by a decrease in haemoglobin concentration (anaemic hypoxic), a reduced uptake of oxygen (hypoxic hypoxia) or impaired cerebral blood flow (ischaemic hypoxia). A disruption in oxygen delivery can cause an energy deficit, leading to cessation of neuronal activity and neuronal death[68].

Table 2.2 Relationship between cerebral oxygen delivery, consumption and extraction

CDO_2			CDO_2	$CMRO_2$	CFOE	Comments
CBF	cHb	SaO_2				
→	→	↓	↓	→	↑	***Hypoxic hypoxia*** no compensatory increase in CBF
↑	→	↓	→	→	→	***Hypoxic hypoxia*** compensatory increase in CBF
→	↓	→	↓	→	↑	***Anaemic hypoxia*** no compensatory increase in CBF
↑	↓	→	→	→	→	***Anaemic hypoxia*** compensatory increase in CBF
↓	→	→	↓	→	↑	***Ischaemic hypoxia*** CDO_2 still adequate to maintain CMRO2
↓↓	→	→	↓↓	→	↑↑	***Ischaemic hypoxia*** CDO_2 no longer adequate to maintain $CMRO_2$

CDO_2: cerebral oxygen delivery; $CMRO_2$: cerebral oxygen consumption; CFOE: cerebral fraction oxygen extraction; CBF: cerebral blood flow; cHb: arterial haemoglobin concentration; SaO_2: arterial oxygen saturation (Adapted from *Topun Austin, 'Assessment of cerebral oxygenation in newborn infants using optical techniques' PhD dissertation, University College London, 2008*).

In adults and animal studies using PET, an increase in CFOE has been seen in areas of the brain surrounding ischaemic lesions, a condition known as 'misery perfusion'[69]. Similarly, the neonatal brain has the ability to adapt to conditions of low perfusion. Newborn infants have increased CFOE on the first day of life and higher CFOE has been observed in preterm infants compared to term infants[70-72]. It has been suggested that this high CFOE in the early postnatal period may be close to maximum levels and therefore any further reduction in systemic blood flow or CBF would not result in any increased oxygen extraction and potentially increase the risk of hypoxic-ischaemic injury. Alderliesten et al. (2013) have shown that infants who developed severe IVH with PHI had higher CFOE values on the first day of life when compared to control infants[73]. However, the maximum level of CFOE in neonates remains unknown.

In preterm infants, CBF is higher in the thalami and brain stem than in the white matter according to studies using single photon emission computer tomography (SPECT) and MRI perfusion techniques[74, 75]. Borch et al. (1998) studied preterm infants born between 25 and 32 weeks and observed that regional CBF to the white matter was 0.39 of global CBF while flow to the basal ganglia was 2.33 of global CBF[75]. This difference between grey and white matter perfusion may be explained by the incomplete development of deep vascular anatomy. Moreover, it is already known that CBF in preterm infants is likely to be near the threshold for neuronal viability, therefore the relative hypoperfusion of the white matter may explain its vulnerability to hypoxic-ischaemic injury.

Early studies using the Xe^{133} clearance technique have demonstrated that decreased levels of CBF, impaired cerebral pressure reactivity and abnormal CBF-CO_2 reactivity were associated with the development of severe brain injury[76]. Similarly, Meek et al. (1999) using NIRS, have described lower CBF within the first 24 hours of age in infants who developed severe GMH-IVH compared to infants who had no lesions[77] (Figure 2.7).

Infants who are born very preterm, with lower gestational age or are clinically very sick are at increased risk of presenting with prolonged pressure-passive cerebral circulation (Figure 2.8)[40, 78]. Therefore, a sudden increase in CBF may be implicated in the development of brain lesions in this population. Milligan et al. (1980) using invasive jugular vein occlusion plethysmography, showed the association between a sudden rise in MABP and CBF following blood transfusion in preterm infants who developed GMH-IVH[79]. More recently, studies using NIRS demonstrated that infants who had impaired cerebral autoregulation within the first hours or days of life were more likely to develop GMH-IVH[80, 81]. Wong et al. (2012) has shown that in severely sick preterm infants, impaired cerebral autoregulation and pressure passive perfusion may occur even with small blood pressure fluctuations[82].

Figure 2.7 Association between cerebral blood flow and GMH-IVH

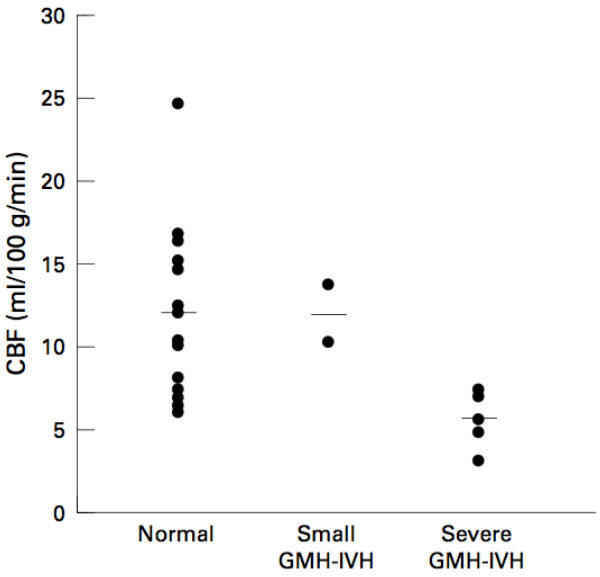

Median (range) CBF in infants with GMH-IVH was 5.8 (3.2 – 7.5) mL/100g/min in infants who had severe IVH and 12.1 (6.1 – 24.5) mL/100g/min in infants who had normal cranial ultrasound (P < 0.01) (Adapted from *Meek et al., Arch Dis Child Fetal Neonatal Ed, 1999)*[77].

Figure 2.8 Coherence between ultra-low frequency waves of MABP and TOI

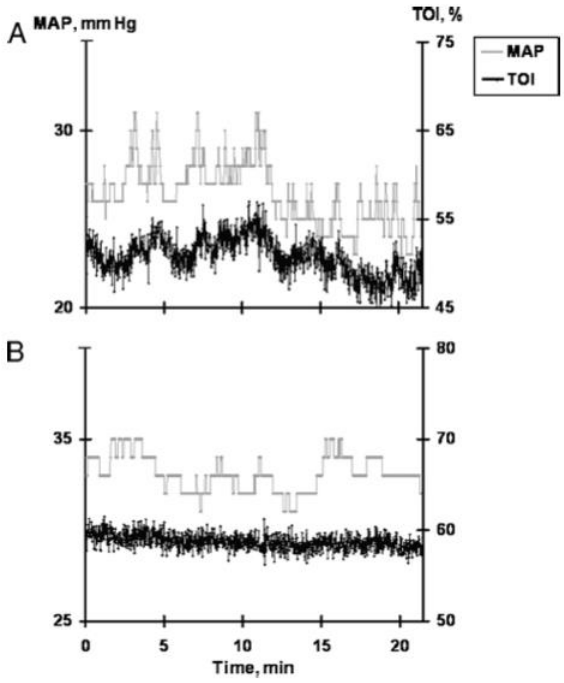

Figure A shows the high coherence between MABP and tissue oxygenation index (TOI) (impaired autoregulation). Correlating changes between these two waves are observed. Figure B shows low coherence between MABP and TOI (intact autoregulation). Despite changes on MABP waves, TOI signal remains stable. Adapted from *Wong et al. (2008)*[78].

2.2.1. Mechanisms involved in the regulation of CBF

Neurovascular coupling

The relationship between neuronal activity and cerebral blood flow was first described in 1890. Roy & Sherrington (1890) directly measured the change in cerebral blood volume caused by electrical stimulation of exposed sensory nerves in dogs[83]. The model used to explain activity-dependent flow is the 'neurovascular unit' in which an astrocyte anatomically bridges a collection of synapses and penetrating arterioles. Neurovascular coupling is spatially specific and characterized by a fast response, where vascular diameter changes within one second from neuronal activation[84]. However, haemodynamic response to neuronal activation seems to be incompletely developed in the infant brain. In preterm infants during the first 48 hours of life there is no correlation between CBF and spontaneous changes in $CMRO_2$, but instead, changes in cerebral oxygen extraction rather than CBF meet changes in oxygen requirement[72, 85]. The mechanisms associated with changes in CBF-metabolism coupling during brain development may be related with changes in astrocytes numbers, size and their connectivity with each other and with blood vessels[86, 87]. In addition, the capacity of arterioles to increase local CBF in response to neurovascular-coupling is likely to increase with age[88]. More recently, Kozberg et al. (2016) have demonstrated a lack of coupled blood flow responses to neural activity in the developing brain during the early postnatal age in mice, suggesting that in the newborn brain, neural activity can lead to a relative hypoxia in areas of neural activation with consequent deplete of local oxygen consumption to levels below the baseline for early developing stages[89, 90].

Vasoreactivity to carbon dioxide (CO_2) and oxygen (O_2)

Hypercapnia (high $PaCO_2$) may cause GMH-IVH by inducing vasodilation and engorgement of the microvasculature[91]. It may also limit vasodilator responses to hypotension and hypoxemia, by inducing abnormal cerebral autoregulation[92]. CO_2-induced vasodilation is a strong vasoregulatory mechanism present from approximately 26 weeks of gestation, according to animal studies[86]. In healthy term infants, CBF changes by 25% per kPa of $PaCO_2$, however in preterm infants changes in CBF range from 10%-30% per kPa of $PaCO_2$ [76, 93]. Hypocapnia (low $PaCO_2$)

induces vasoconstriction until levels of $PaCO_2$ reach approximately 1.2 kPa. Below this level, no further vasoconstriction occurs [94].

The cerebrovascular response to hypoxia is characterized by cerebral vasodilation, with an increase in CBF by two to three-fold. O_2 vasoreactivity depends on intact endothelium and NO production. The ability to increase CBF in response to hypoxia is present from approximately 28 weeks of gestation, according to studies in fetal sheep[95]. Global hypoxia induces redistribution of blood flow to the brain. In late gestational age, the fetal compensatory mechanisms to hypoxia are characterized by a decreased in heart rate with consequent fall in the oxygen consumption. The fetal blood flow is redistributed from the peripheral vasculature towards vital organs, such as the brain[96]. This mechanism is known as 'brain sparing effect' and it has been demonstrated by using Transonic flowmetry to measure simultaneously carotid and femoral blood flow in fetal sheep[97]. Fetal bradycardia and peripheral vasoconstriction in response to hypoxia are triggered by carotid chemoreflexes. However, the magnitude of the fetal peripheral vasoconstrictor response to acute hypoxia is the result of combined carotid chemoreflexes, endocrine response (increase in plasma catecholamines, vasopressin, angiotensin II and neuropeptide Y) and vascular oxidant tone (presence of reactive oxygen species that regulates blood flow). The circulatory response to fetal hypoxia changes as the fetus approaches gestational age at term, in association with the increase in plasma cortisol. In preterm infants, the antenatal exposure to synthetic glucocorticoids may change the pattern and magnitude of the fetal heart rate and promote maturation in the fetal circulatory response to acute hypoxia stress in a similar way as advancing gestational age does[96, 98, 99]. In contrast, hyperoxia reduces CBF. In preterm infants CBF may be decreased by 15% to 30% per kPa of PaO_2 and this decrease in CBF may persists beyond the time that blood oxygenation was raised.

Myogenic mechanisms (cerebral autoregulation)

The myogenic reflex is one of the mechanisms involved in the regulation of cerebral blood flow. It depends on the intrinsic ability of vascular smooth muscle cells to constrict or dilate in response to changes in transmural pressure[100, 101]. A number of endothelial derived vasoactive substances may contribute to cerebral autoregulation. Following a decrease in transmural pressure, endothelial-derived NO, carbon

monoxide and calcium-activated potassium channels induce vasodilation and, hence, an increase in cerebral blood flow[102]. The NO/NO synthase pathway has been related to the maintenance of CBF stability[103-106]. Disruption of this mechanism has been shown in states of impaired cerebral autoregulation. The contribution of endothelial NO in pressure regulation increases with age and therefore it may be less efficient in the preterm infant, where other mechanism may possibly dominate[107].

The next section will describe the mechanism of cerebral autoregulation in more detail.

2.3. CEREBRAL AUTOREGULATION

Cerebral autoregulation is the mechanism that maintains cerebral blood flow (CBF) relatively constant despite changes in cerebral perfusion pressure. It is a homeostatic property of the cerebral arteries and arterioles to constrict or dilate in response to an increase or decrease in transmural pressure, respectively ensuring adequate perfusion and oxygenation to the brain. It was originally believed that CBF varied passively with changes in perfusion pressure (Monro-Kellie doctrine)[108]. However, in 1938 Mogens Fog was the first to directly observe the changes in the diameter of the pial vessels in response to variation in blood pressure through a window in the skull of cats[109]. Lassen first used the term cerebral autoregulation in his famous review paper published in 1959. Using data from 11 different published studies, Lassen plotted mean values of CBF against mean values of MABP (Figure 2.9). The plotted data points yielded a curve where CBF remained constant over a range of MABP (the Lassen's curve)[110].

Figure 2.9 Cerebral autoregulation and cerebral pressure passive curves

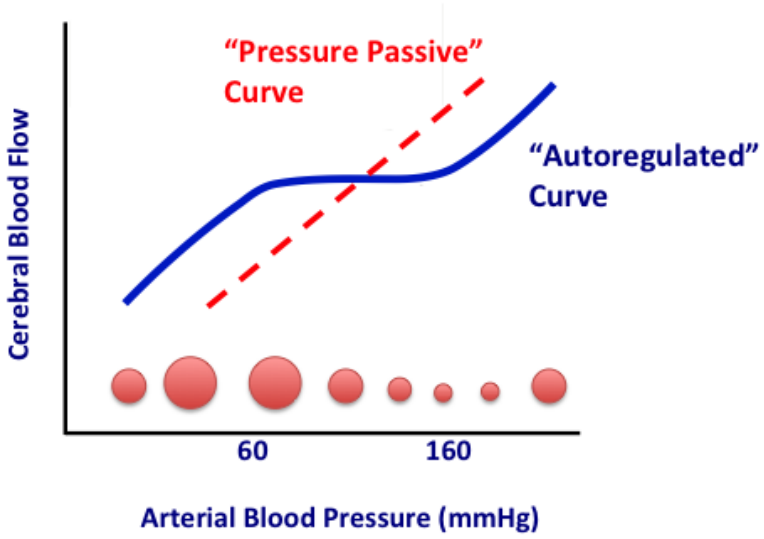

In blue is the autoregulatory curve of Lassen that represents the intrinsic mechanism of the brain to maintain cerebral blood flow relatively constant despite changes in arterial blood pressure (plateau). The circles represent the dilatation and constriction of the cerebral blood vessels in response to changes in arterial blood pressure. In red is the passive pressure curve that represents absence of the autoregulatory mechanism.

Disruption of the autoregulatory mechanism will lead to the development of a 'pressure-passive circulation', where fluctuations in systemic arterial blood pressure are transmitted directly to the cerebral microvasculature. In adults with intact cerebral autoregulation, changes in MABP between 60 and 160mmHg or in CPP between 50 and 150mmHg, produce little or no change in CBF[110]. Beyond the lower limit of autoregulation (LLA) and the upper limit of autoregulation (ULA), hypotension can cause brain ischemia and cell death and hypertension can cause hyperaemia and cerebral oedema.

2.3.1. Cerebral autoregulation in preterm infants

In the preterm brain, the presence and mechanisms of cerebral autoregulation and the thresholds of MABP remain poorly understood (Figure 2.10). The first evidence of impaired autoregulation in the newborn infant was shown by Lou et al. (1979), in Copenhagen, using ^{133}Xenon clearance to measure cerebral blood flow a few hours after birth in preterm babies with different degrees of respiratory disease syndrome[39]. Since then, several studies have suggested that cerebral autoregulation is impaired not only in sick infants but also in clinically well preterm infants [39, 76, 80, 111].

Figure 2.10 Possible cerebral autoregulation curve in preterm infants

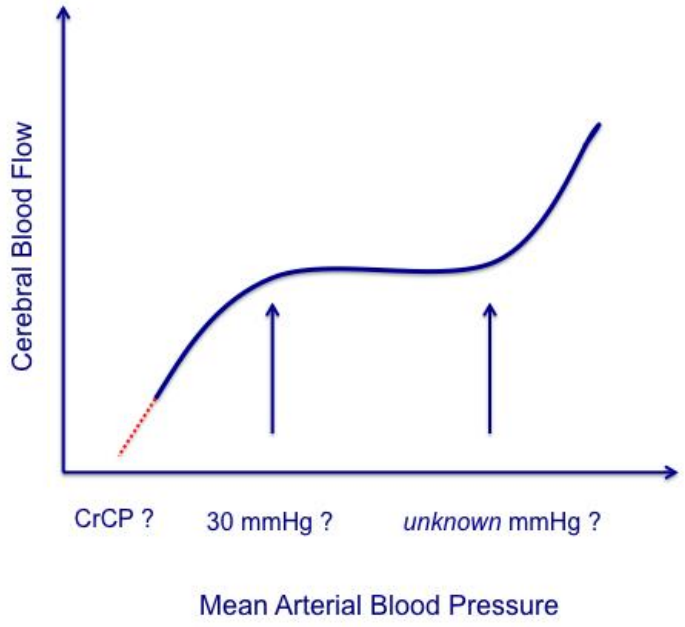

The limits of lower and higher MABP in the plateau area of the curve remain uncertain. Adapted from *Greisen et al. (2016)*[112].

Loss of autoregulation is associated with brain injury and increased risk of mortality in newborn infants, children and adults[81, 113, 114]. In adults, following traumatic brain injury (TBI), impaired cerebral autoregulation has been considered an independent predictor of poor outcome[114]. Data from preterm infants have shown that cerebral autoregulation fluctuates in the first week of life, and that the degree of 'pressure passivity' is associated with the development of significant GMH-IVH[81].

NIRS has been extensively used to assess cerebral autoregulation in neonates. The most common methods to investigate the relationship between MABP and CBF have been frequency and time-domain analysis. The question whether the two methods are equivalent or one is superior to the other remains debatable, however, in a recent study including 60 preterm infants, time-domain analysis appeared more robust compared with coherence function analysis[115].

The frequency-domain analysis was first used by Giller (1990) to assess cerebral autoregulation as a dynamic process[116]. In the frequency domain, the coherence analysis is the correlation that describes the strength of the relationship between input signal (i.e. MABP) and output signal (i.e. CBF). Coherence values range from 0 to 1, where 0 indicates intact cerebral autoregulation and 1 suggests implies absence of cerebral autoregulation. The transfer function analysis is another frequency-domain method where gain quantifies the extent to which a waveform is transferred from an input signal (i.e. MABP) to an output signal (i.e. CBF). Low gain indicates intact cerebral autoregulation and high gain suggests high CBF variability in proportion to high variability in MABP.

The time-domain analysis is a statistical measurement of linearity between MABP and CFB where the outcome variables are correlation and regression. In this thesis, correlation between systemic pressure and CBF was performed using time domain analysis. The characteristics of this method will be discussed in more details in the section 2.3.2 and Chapter 4, section 4.4.2 of this dissertation.

In neonates, Tsuji et al. (2010) were the first to describe the coherence between ΔHbD (a NIRS derived signal and surrogate measurement of CBF, $\Delta HbD = \Delta HbO_2 - \Delta Hb$), and MABP as a measure of cerebral autoregulation. They described a higher rate of GMH-IVH in the group of infants where coherence between ΔHbD and MABP was

above 0.5[117]. O'Leary et al. (2009), using transfer function analysis, studied a cohort of preterm infants born < 32 weeks and demonstrated that higher MABP-HbD gain was associated with the likelihood to develop early GMH-IVH[81]. However, HbD is not an ideal parameter to measure continuous CBF, because it requires offline analysis and is more sensitive to changes in cerebral blood volume (CBV). On the other hand, the tissue oxygenation index (TOI) has been shown to be a more robust surrogate of CBF[118].

The development of spatially resolved NIRS allowed the use of continuous parameters of cerebral oxygenation (known as the tissue oxygenation index (TOI) or regional oxygen saturation (rSO_2), depending on the NIRS device) as surrogate measure of CBF to assess cerebral autoregulation. TOI and rSO_2 have been applied to measure cerebral autoregulation instead of HbD[119]. Wong et al. (2009) were the first to show that changes in TOI correlate with changes in CBF in both time and frequency-domain analysis. TOI strongly reflected changes in CBF during fluctuations in MABP over periods longer than 10 seconds (Figure 2.8)[118]. Higher coherence between MABP and TOI was observed in more premature and sick infants and in those who died or had severe IVH[78].

2.3.2. Measurements of cerebral autoregulation: lessons from adult neurocritical care

The 'Lassen's curve of cerebral autoregulation was based on static measurements of CBF and MABP. However, cerebral autoregulation is a dynamic process; therefore in clinical practice continuous measurement of cerebral autoregulation depends on the spontaneous response of CBF to spontaneous fluctuations in CPP or MABP (dynamic autoregulation). Haemodynamic oscillations that last between 20 seconds to 3 minutes are the best for the assessment of cerebral autoregulation[120]. Oscillations faster than 20 seconds are too fast to initiate vasodilation or vasoconstriction, which can be reliably measured. Oscillations longer than three minutes, in clinical practice can be contaminated too much by medication, nursing and changes in cerebral metabolic rate. Several invasive and non-invasive methods to assess CBF have been applied for research or clinical purpose. Some monitoring modalities, such as Xe^{133} washout technique, CT perfusion, MRI and PET, measure direct perfusion but can only offer

static measurements; other modalities such as transcranial Doppler, NIRS (both non-invasive), ICP via intraparenchymal probe or external ventricular drainage and invasive brain oxygen monitoring ($PbtO_2$) measure surrogate markers of CBF or CBV and usually provide more continuous measurements[121-131].

In neonates, invasive methods to assess CBF are currently not ethically accepted for either research or clinical use, although some physiological studies have used more invasive methods such as Xe^{133} and PET in the past[132, 133]. This section will focus on invasive and non-invasive studies that applied similar methodology used in the clinical measurements included in this dissertation.

Cerebrovascular pressure reactivity is one of the key mechanisms responsible for cerebral autoregulation. In adult patients with traumatic brain injury a continuous computational analytic approach to monitor cerebrovascular pressure reactivity was first described by Czosnyka et al. (1997)[130]. By using time-domain analysis to calculate continuous moving linear Pearson's correlation coefficient between slow waves of ICP and MABP, they proposed an index of cerebrovascular reactivity, the pressure reactivity index (PRx). If pressure reactivity is intact, an increase in MABP will lead, within approximately 5-15 seconds, to a vasoconstriction with reduction in CBV and thus ICP will decrease. On the other hand, if pressure reactivity is impaired, CBV will passively increase with rising MABP and ICP will consequently rise. The correlation between spontaneous fluctuations in MABP and ICP waves will result in values of PRx between -1 and +1, where negative values reflect normal or intact cerebrovascular reactivity and positive values reflect disturbed vasoreactivity (Figure 2.11). PRx has been shown to be a strong independent predictor of outcome; prolonged positive values of PRx have been associated with death in adults with traumatic brain injury[114, 130].

Figure 2.11 Pressure reactivity index (PRx)

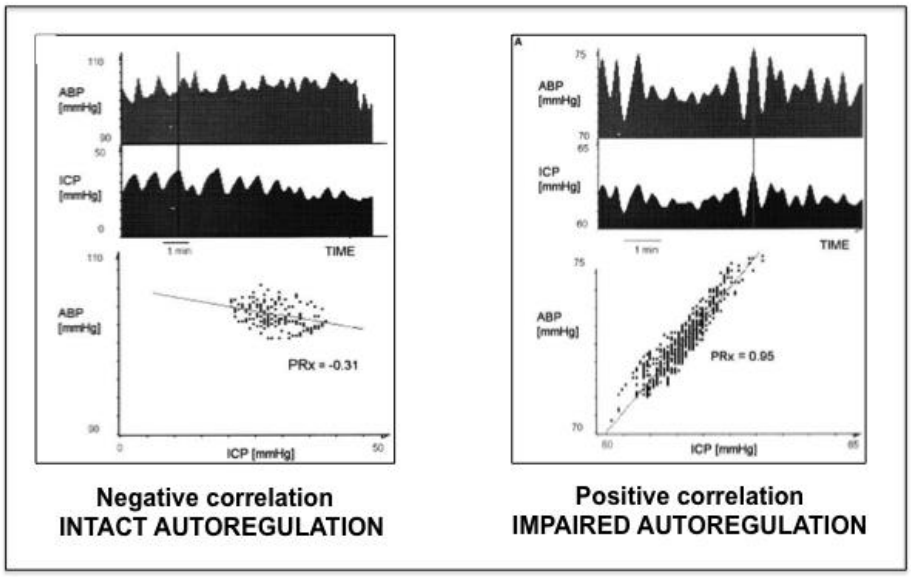

The figure shows the correlation between slow waves in intracranial pressure and arterial blood pressure. Intact cerebral autoregulation is demonstrated by negative PRx and impaired cerebral autoregulation by positive PRx. Adapted from *Czosnyka et al. (1997)*[130].

Based on the methodology used to calculate PRx, other indices of cerebrovascular reactivity and cerebral autoregulation using non-invasive techniques have been suggested and validated against invasive methods.

Using the transcutaneous Doppler technique, Czosnyka et al. (1998) have described an index of cerebrovascular reactivity between slow waves of MABP and flow velocity in the middle cerebral artery, the mean flow index (Mx). This index has been extensively used to assess cerebral autoregulation in patients with traumatic brain injury. However, some limitations to the use of Mx as a continuous measure of cerebral autoregulation include the difficulty to record prolonged monitoring periods and operator dependent variability[134, 135].

NIRS is a non-invasive technique that provides surrogate measurements of CBF and CBV. Brady et al. (2007) using NIRS in a piglet model, described an index of cerebrovascular reactivity derived from the linear moving correlation coefficient between spontaneous slow waves of CPP and cerebral oxygen saturation, the COx (cerebral oximetry index)[129]. COx was sensitive for loss of autoregulation caused by

induced hypotension in this animal model and it has been validated against invasive methods using laser Doppler and ICP monitoring[129, 136]. Thresholds of COx above 0.36 had high sensitivity (73% to 99%) and moderate specificity (around 63%) for detecting loss of cerebral autoregulation[129]. COx is an attractive method of pressure autoregulation monitoring in neonates, because it can be non-invasive measurement of cerebral autoregulation. Gilmore et al. (2011) defined COx as the correlation coefficient between slow waves of MABP and cerebral oxygenation and studied a cohort of preterm infants (born ≤ 30 weeks) during their first four days of life (Figure 2.12). They observed that lower MABP was associated with more frequently impaired cerebral autoregulation (Cox > 0.5); however no difference in COx was observed between infants with or without GMH-IVH[137].

Figure 2.12 Cerebral oximetry index in preterm infants

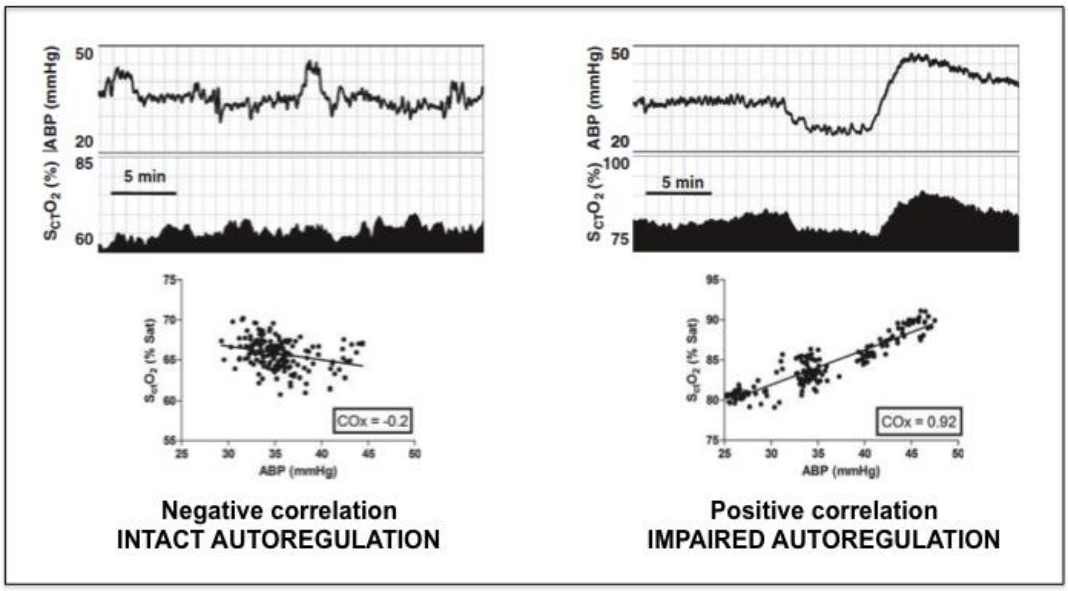

Intact cerebral autoregulation is demonstrated by negative COx and impaired cerebral autoregulation by positive COx. Adapted from *Gilmore et al. (2011)*[137].

More recently, Eriksen et al. (2014) used COx to investigate the association between dopamine and cerebral autoregulation. In a cohort of 60 preterm infants (born ≤ 32 weeks), where 13 received dopamine within the first days of life, COx was higher in the dopamine group compared to those who did not received hypotension treatment[138].

The haemoglobin volume index (HVx) is another NIRS-derived index of cerebrovascular reactivity. The HVx is a moving correlation coefficient between slow waves of total haemoglobin (rTHb), a surrogate of CBV measured with NIRS, and MABP[139]. HVx has a strong correlation with PRx and it has been used to identify lower limits of autoregulation in animal models[140].

More recently, Mitra et al. (2014) described the tissue oxygenation heart rate reactivity index (TOHRx) based on the correlation between slow waves of TOI and heart rate (HR) (Figure 2.13). This methodology is based on the fact that changes in cardiac output (CO) in preterm infants may rely mainly in changes in heart rate. Strong coupling between cardiac output and TOI may be interpreted as a failure of regulation of CBF. Higher TOHRx (impaired cerebrovascular reactivity) was observed in infants with worse neonatal score of mortality and morbidity (more severely sick infants). TOHRx was also higher in infants with lower MABP. However, similarly to COx, TOHRx also failed to show association with outcome of mortality or GMH-IVH[141].

Figure 2.13 Tissue oxygenation heart rate reactivity index (TOHRx)

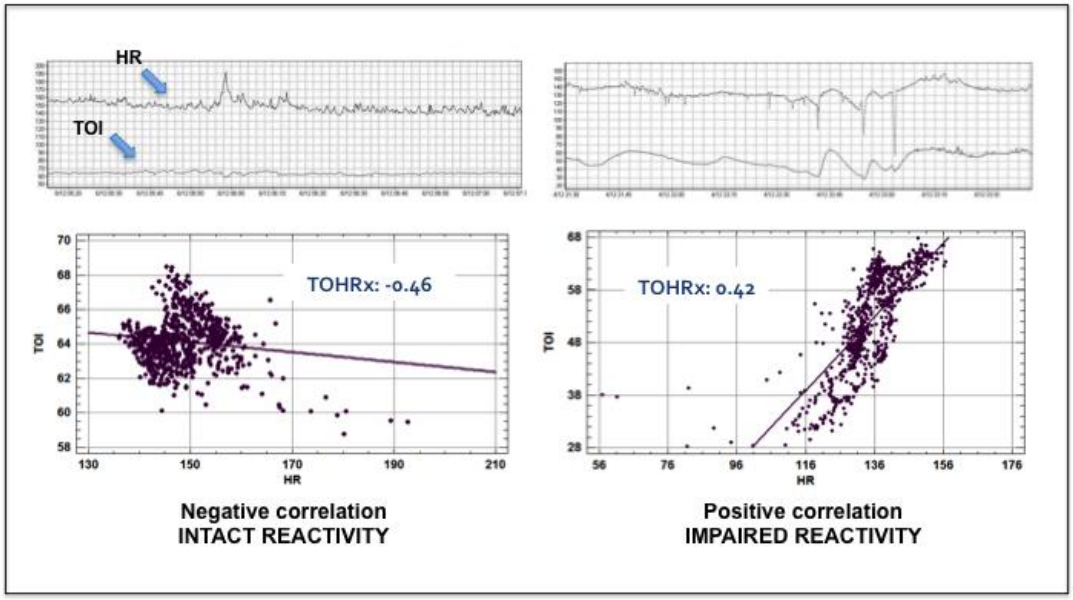

Intact cerebrovascular reactivity is demonstrated by negative TOHRx and impaired cerebrovascular reactivity by positive TOHRx. Adapted from *Mitra et al (2014)*[141].

2.4. CIRCULATORY ADAPTATION AFTER BIRTH

2.4.1. Fetal and early postnatal circulation

The transition from fetal to newborn life is marked by significant changes in the circulatory physiology. The fetal circulation is characterised by low systemic vascular resistance (SVR), with high systemic blood flow, high pulmonary vascular resistance and low pulmonary blood flow (Figure 2.14). The placenta is responsible for oxygen and blood supply to the fetus. Both right and left cardiac outputs contribute to the systemic blood flow. This combined cardiac output is markedly higher in the fetus (in the range of 400-450 mL/kg/min) compared to the systemic blood flow after birth (about 200 mL/kg/min). The right ventricle is the main cardiac chamber and pumps about 65% of the cardiac output to the systemic circulation bypassing the lungs - that only receive 5-10% of the combined cardiac output (CO) - through a channel between main pulmonary artery and descending aorta, known as the ductus arteriosus. In contrast, the left cardiac output supplies mostly the brain and upper body[142-144].

Figure 2.14 Fetal circulation

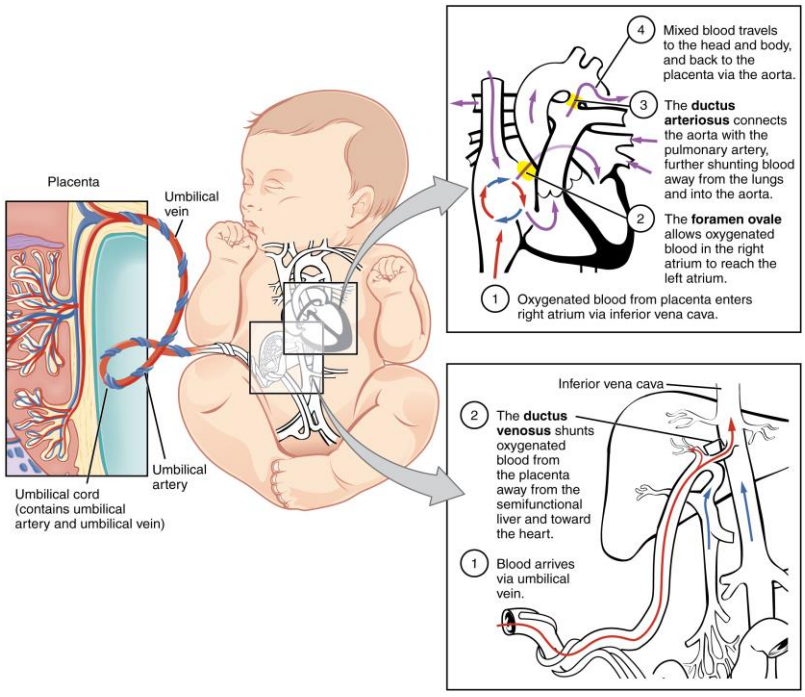

The figure shows the vital three shunts during fetal life: foramen ovale, ductus arteriosus and ductus venosus (Adapted from *https://en.wikipedia.org/wiki/Fetalcirculation*).

In term infants, the normal transition from fetal to postnatal circulation is characterised by an increase in SVR following the removal of the placenta, cord clamping and the release of catecholamines and other hormones. The pulmonary vascular resistance drops, following the first breath and subsequent lung expansion and increase in the partial pressure of oxygen. The antenatal channels usually close within the first 24 hours of age, which also contribute to the increase in SVR. On the other hand, in preterm infants or in pathological situations the circulatory changes following birth may not be complete for days or weeks[142]. This is mainly due to the inability of the immature myocardium to adapt to the increased ventricular workload and the persistence of the antenatal channels, known clinically as the persistent ductus arteriosus (PDA) and persistent foramen ovale (PFO)[145, 146]. Haemodynamic instability may occur and the distribution of systemic blood flow may preserve the vital organs (brain, heart and adrenals) at the expense of non-vital organs[142, 147].

Figure 2.15 Transitional circulation in a healthy term infant

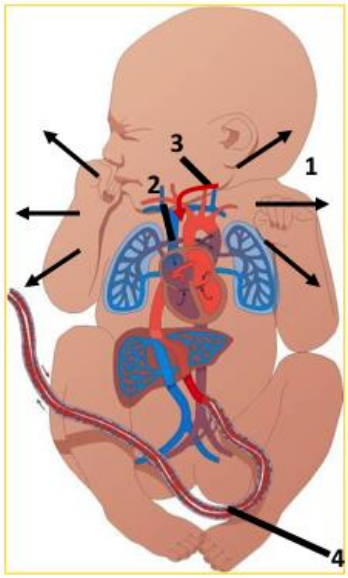

1. The opening of airways and pulmonary vasculature induces a fall in pulmonary resistance.
2. Increased pulmonary venous return leads to functional closure of foramen ovale.
3. The increase in partial pressure oxygen promotes the closure of ductus arteriosus.
4. Cutting of umbilical cord will result in increased in systemic resistance.

As previously discussed, following preterm birth, cardiac output and CBF are low and both rise over the first days of life[65, 148]. $CMRO_2$ is also low immediately after birth. It is unknown whether the low perfusion just reflects low demand or $CMRO_2$ is low as a result of the low output state. It may be possible that the infant effectively lowers its metabolic rate as a protective mechanism during this transitional phase. The complex interaction between systemic blood flow, blood pressure and end organ perfusion during the transitional circulation following preterm birth is shown in Figure 2.16.

Figure 2.16 Interaction between blood flow, vascular resistance, blood pressure and cellular metabolic demand

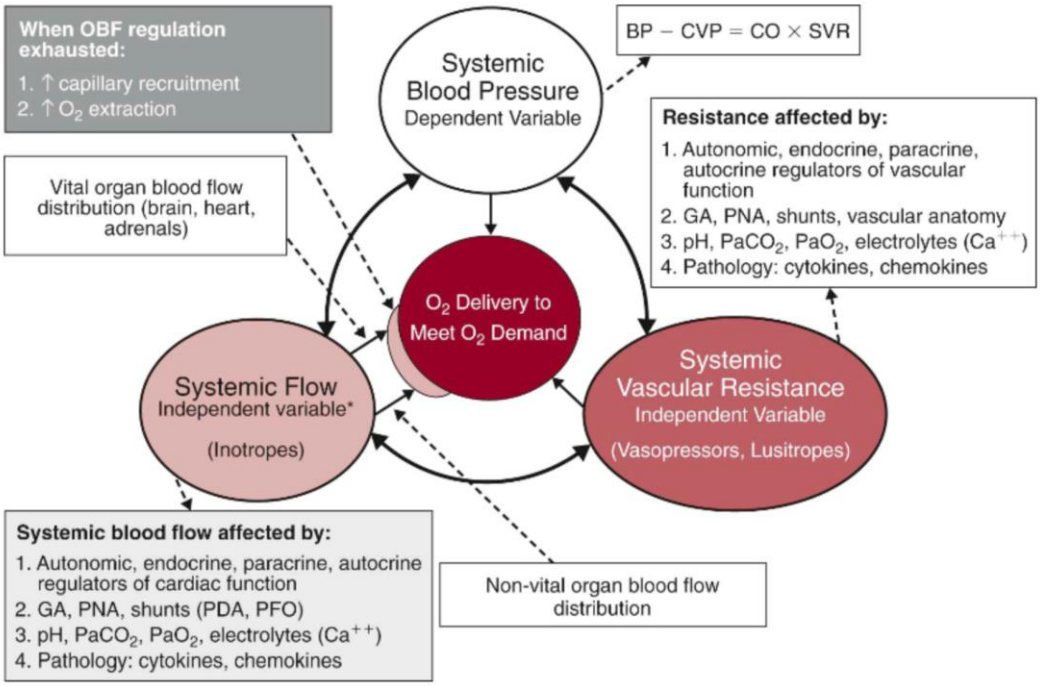

Coupling of oxygen supply and demand plays an important role on the control of microcirculation. OBF: organ blood flow, BP: blood pressure, CO: cardiac output, SVR: systemic vascular resistance, GA: gestational age, PNA: postnatal age (Adapted from *Noori et al, Principles of developmental cardiovascular physiology and pathophysiology, 2012*)[142].

2.4.2. The controversies around "normal" blood pressure in preterm infants

Strategies for preventing cerebral injury in preterm infants have emphasized the importance of maintaining a "normal blood pressure" to ensure adequate perfusion of the brain. However, the definition of hypotension or hypertension in this population remains uncertain. The current management of hypotension in preterm infants in the

first few days of life does not combine quantitative information about blood flow and tissue oxygen delivery[149, 150]. The dynamic nature of the cardiovascular system during the first hours and days of life with spontaneous increase in blood pressure and the evidence that blood pressure and systemic blood flow are not necessarily related are usually neglected [145, 151].

Mean arterial blood pressure (MABP) is determined by the interaction between cardiac output (CO) and systemic vascular resistance (SVR)

Equation 2-10

$$MABP = CO \times SVR$$

Cardiac output (CO) is determined by stroke volume and heart rate.

$$CO = SV \times HR$$

Normative data on blood pressure

Several studies have attempted to define normal ranges of blood pressure in neonates during the transitional period; however, there is not yet a consensus on the definition of normal thresholds. The majority of studies are of small populations, retrospective in design and included both invasive and non-invasive measurements of blood pressure[47, 151, 152]. Moreover, the evidence that hypotension in newborn infants is associated with poor outcome remains controversial, especially in the preterm population, as discussed below.

The current clinical practice remains based mainly on recommendations from the Joint Working Group of the British Association of Perinatal Medicine published in 1992 where MABP should be maintained at or greater value (in mmHg) than the gestational ages in weeks[153]. Another well-adopted concept is to accept the value of 30 mmHg as the critical lower limit of blood pressure in preterm infants regardless the gestational age. The threshold of ≤ 30 mmHg for hypotension has been suggested based on a few studies assessing the lower limits of cerebral autoregulation and reporting that preterm infants who had mean values of MABP below 30 mmHg were

more likely to develop brain injury[151, 154, 155]. In addition, several neonatal guidelines define hypotension as MABP below the 5th-10th percentile according to age and birth weight reference values[156] (Figure 2.17).

Figure 2.17 Predicted MABP for infants during the first 72 hours of life

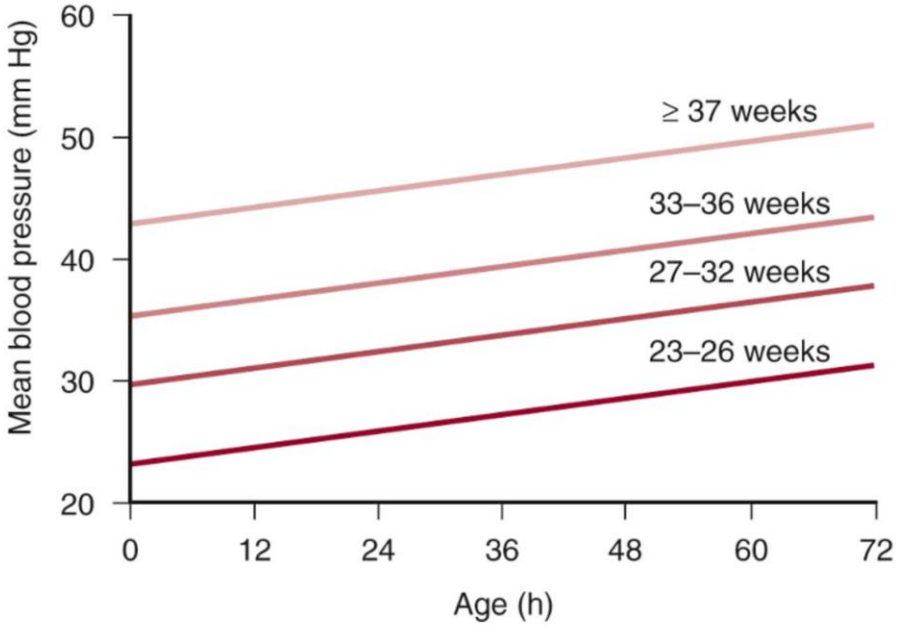

The graph shows the lower limit of 80% confidence interval of MABP for each gestational age group for a cohort of 103 infants born between 23 to 43 weeks. The difference of values between term and preterm infants and the increase in MABP over the first 72 hours of life can be observed. (Adapted from *Nuntnarumit et al, Clini Perinatol. 1999*)[156].

Relationship between hypotension and outcome in neonates

Several studies have associated hypotension with increased mortality and development of GMH-IVH and PVL. Most of them had important limitations such as small sample sizes, non-consistent blood pressure thresholds and different ways to measure the duration and magnitude of hypotension[151, 157 47, 49, 158]. However, despite the differences in methodologies, early studies by Miall-Allen et al. (1987), Bada et al. (1990) and Cunningham et al. (1990) all showed an association between "low blood pressure" and severe GMH-IVH, supporting the relationship between hypotension and brain injury[47, 155, 158].

The association between systemic hypotension and low CBF and decreased oxygen delivery may explain the relationship between low blood pressure and brain injury in

preterm infants[80, 154, 159]. Impaired cerebral autoregulation in preterm infants may lead to a direct relationship between MABP and CBF, putting these babies at risk of hypoxic-ischaemic brain injury[78, 160]. Moreover, the configuration of the cerebral vasculature in preterm infants may increase the risk of white matter brain injury. The vascular end zone in the white matter not fully developed, making this area more sensitive for falls in cerebral perfusion pressure and ischemia[8, 51] (seen in Chapter 2, section 2.2).

More recent studies have not found an association between hypotension (established according to the current definitions) and short or long-term outcomes[161-163]. Some studies have shown that efforts to raise and treat hypotension had no improvement on outcome, or suggested that inotropes and vasopressors may be deleterious[164 165]. Dempsey et al. (2009) observed that preterm infants with MABP below the gestation age in weeks but showing signs of good organ perfusion (such as good capillary refill time < 3 seconds, normal lactate and good urine output) who did not receive treatment had short-term outcome as good as those with "normal" blood pressure[164]. Moreover, Alderliesten et al. (2014) have demonstrated that MABP below the gestational age alone was not associated with lower cerebral oxygenation or worse neurodevelopmental outcome at 18 and 24 months' corrected age[163].

2.5. DEFINING OPTIMAL CEREBRAL PERFUSION PRESSURE AND OPTIMAL ARTERIAL BLOOD PRESSURE BASED ON THE STRENGH OF AUTOREULATION

Optimising CPP or MABP according to the strength of cerebral autoregulation is a concept that has been suggested for the management of adult patients with traumatic brain injury. More recently, several studies in the context of paediatric traumatic brain injury, intra-operative monitoring during cardiac surgery and cardiac arrest have applied this same concept of individualised brain monitoring targeting optimal CPP or optimal MABP[166-169]. This is an attractive method, as it combines haemodynamic measurements of systemic blood flow with end organ perfusion.

Steiner et al. (2002) were the first to demonstrate that by using PRx it is possible to define an optimal value for CPP where cerebral autoregulation is strongest (CPP_{OPT}). Data from adult patients with traumatic brain injury, admitted to a neurocritical care unit, who had continuous invasive measurements of MABP and ICP recorded and analysed using ICM+ software[170]. The determination of CPP_{OPT} for each individual patient was possible as CPP values were divided into bins of 5 mmHg and PRx values were averaged within these bins. The values were accepted when more than 2.5% of the data set was included and when the graph showed a distinct minimum value for PRx (Figure 2.18). The difference between CPP_{OPT} and mean CPP for the whole monitoring period was calculated. Patients whose mean CPP values were maintained close to the values of CPP_{OPT} had better outcome compared to those who had mean values away from the optimal. These findings led to a suggestion that the management of patients with traumatic brain injury should include individual CPP measurements[171]. However, the data published by Steiner et al. (2002) were obtained through retrospectively analysis of the recordings of ICP for the whole monitoring period, thus they were not necessarily applicable for a more real-time management of CPP. Subsequently, Aries et al. (2012) validated an algorithm for automated and continuous updating of CPP_{OPT} derived from time windows of 4 hours[172]. Using this new method, they were able to define CPP_{OPT} in 83% of patients and confirmed that the patients who were treated with values of CPP away from CPP_{OPT} were more likely to have bad outcome, defined as death and severe disability[173]. Recently, a

prospective pilot study conducted in a single European centre, in which adult patients with traumatic brain injury were managed according to continuous monitoring of CPP_{OPT} targets, demonstrated that the methodology published by Aries et al. (2012) is feasible for real-time bedside monitoring (Figure 2.18)[174]. However, the methodology has yet to be refined in order to be applied in randomised control trials.

Figure 2.18 Optimal cerebral perfusion pressure

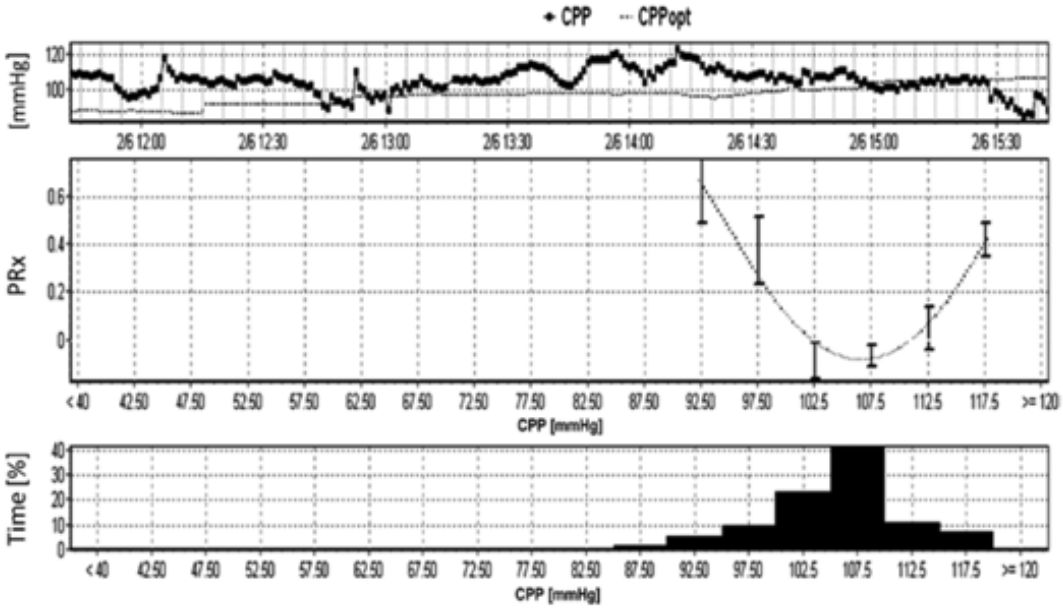

The first graph shows the actual CPP and CPP_{OPT} measurements for a 4-hour-window of data. The second graph shows the CPP_{OPT} defines by U-shape curve. The CPP_{OPT} is the value of CPP where PRx is more negative (strongest cerebral autoregulation). The bottom graph is a frequency histogram of all CPP measurement for this 4-hour-window of data for one single patient. Adapted from *Aries et al. (2012)*[172].

A non-invasive equivalent method of optimising MABP published by Zweifel et al. (2010) made an important contribution to cerebral monitoring of patients whose invasive measurement of ICP was not indicated or feasible. Using the total haemoglobin index (THx) – a NIRS derived index – they were able to define levels of MABP where cerebral vascular reactivity was strongest ($MABP_{OPT}$). They also compared values of $MABP_{OPT}$ with CPP_{OPT} assessed with THx and PRx, respectively and demonstrated significant agreement between the two indices (Figure 2.19). Recently, a feasibility pilot study including twenty adult patients who were admitted to an intensive care unit following cardiac arrest defined $MABP_{OPT}$ based on another

non-invasive NIRS-derived index of cerebral oximetry (COx)[166]. Although the sample size was small, $MABP_{OPT}$ curves were defined for all patients.

Figure 2.19 Invasive and non-invasive measurements of CPP_{OPT} and $MABP_{OPT}$

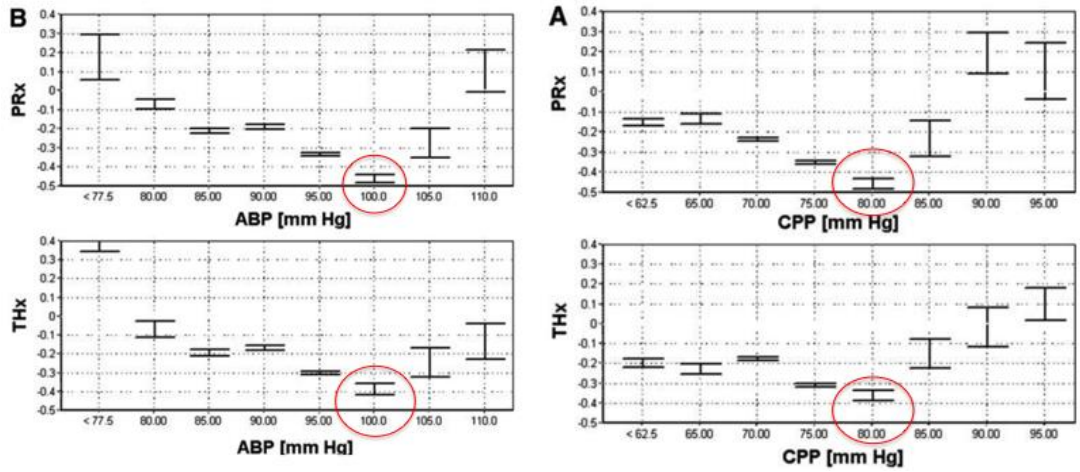

The lower the value for PRx and THx the stronger the cerebrovascular reactivity. ABP is equivalent to MABP. Adapted from *Zweifel et al. (2010)*[175].

In paediatric traumatic brain injury, Young et al. (2016) published a single centre study on continuous monitoring of PRx and CPP_{OPT}. They observed that the time spent with CPP values close to CPP_{OPT} was longer in those children who survived compared to those who died. In neonates, a non-invasive index of cerebral blood volume (HVx) has been to define $MABP_{OPT}$ during therapeutic hypothermia treatment and rewarming in infants who had hypoxic-ischaemic injury[176]. Burton et al. (2015), in an pilot study, showed that infants who spent more time with MABP below $MABP_{OPT}$ during rewarming phase, had greater impaired motor and cognitive outcome at two years of age[177].

3. NON-INVASIVE ASSESSMENT OF CEREBRAL AND SYSTEMIC CIRCULATION

3.1. NEAR-INFRARED SPECTROSCOPY (NIRS)

NIRS is a technique that can provide real time monitoring of cerebral oxygenation at the bedside. NIRS was first described by Jobsis (1977) and first applied in newborn infants in 1985 to study cerebral blood flow and oxygenation[178, 179]. Since then this technology has been extensively used to assess cerebral haemodynamics in adults, children and neonates[180, 181 182].

NIRS technology is based on two fundamental phenomena: the relative transparency of biological tissue to light in the near-infrared spectrum (wavelength between 600 and 1000nm) and the presence of light-absorbing molecules, or chromophores, in biological tissue. The NIRS technique can monitor a variety of chromophores that are found in the living tissue. Some of them, such as melanin, bilirubin and water, remain relatively constant over a certain period of time. Other chromophores such as oxyhaemoglobin (HbO_2), deoxyhaemoglobin (Hb) and oxidised cytochrome oxidase (CtOx) are more physiologically interesting as their oxygenation status is not constant and so will show variation in light absorption over short time periods[183].

In the visible part of the spectrum the interaction between the haemoglobin molecule and oxygen can be visualised: the arterial or oxygenated blood appears red because all colours of visible light except red are strongly absorbed by HbO_2 and venous blood appears more purple or blue as Hb absorbs red light more strongly. In the near-infrared region the light absorption by both chromophores decreases but the absorption spectra of HbO_2 and Hb remain significantly different, allowing the spectroscopic separation of the components. Light at 850nm will be absorbed more by HbO_2 and less by Hb; conversely light at 750nm will be absorbed predominantly by Hb. The isobestic point (the wavelength at which HbO_2 and Hb molecules have the same absorption properties) is seen at 800nm and can be used to calculate the haemoglobin concentration independent of oxygen saturation (Figure 3.1)[184].

Figure 3.1 Light absorption spectra of the most common chromophores present in the human tissue

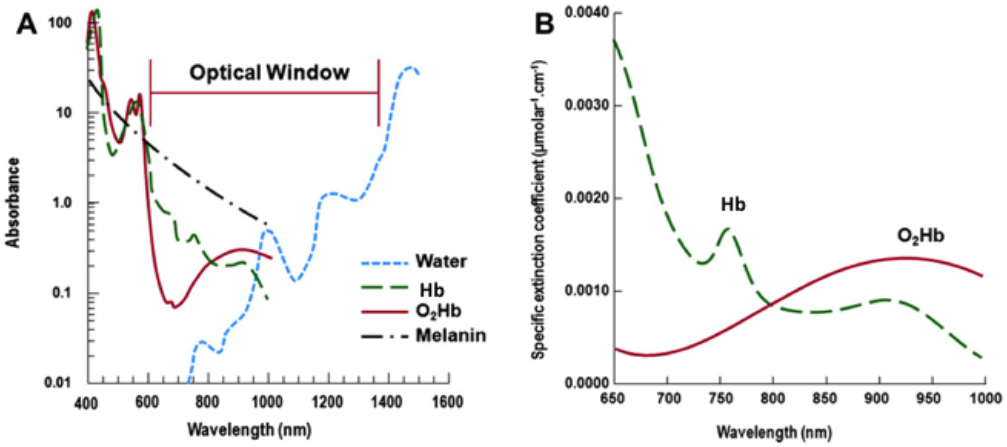

A: Light absorption by water is predominantly above 1000 nm wavelength. Below 1000 nm, the chromophores that mainly absorb light are Hb, HbO2 and melanin. B: Changes in light absorption by Hb and HbO_2 in the near-infrared region. At the isobestic point (800 nm) Hb and HbO_2 spectra of absorption is the same.

Light that has traversed up to 8 cm of a biological tissue can be detected, however this propagation of light depends on the combination of reflectance, scattering and absorption effects[178]. Conventional NIRS is based on the Beer-Lambert Law, which states that attenuation of light passing through a volume containing absorbing components (i.e. chromophores) dissolved in a non light-absorbing medium, is proportional to the concentration of the components and the distance travelled by the light (Figure 3.2). Therefore, the concentration of the chromophores in the medium can be calculated by measuring intensity of the emitted light and the detected light and the distance travelled by the light through the medium.

Figure 3.2 The Beer-Lambert law and the modified Beer-Lambert law used in NIRS

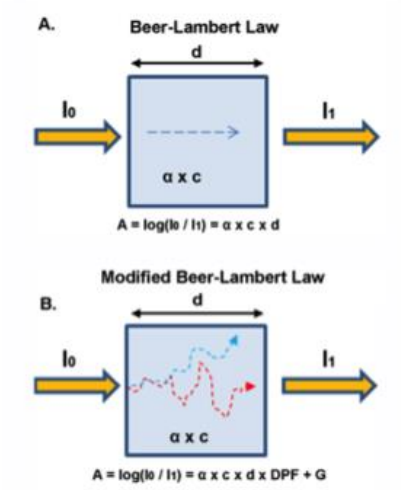

Schematic diagrams representing the (A) Beer- Lambert and the (B) modified Beer-Lambert law.

In both cases α is the specific per chromophores extinction coefficient [μmol/cm] while c is the concentration of the chromophores [μmol/cm].

The α x c is known as the absorption coefficient. When multiple chromophores are present the combined absorption coefficient is the linear sum of all the absorption coefficients.

A – attenuation, I0 – intensity of the light entering the medium, I1 – intensity of the light exiting the medium. Courtesy of Peter Smielewski

The Beer-Lambert law is valid for a homogeneous and isotropic medium, which assumes photons travel in a straight line. However, in a scattering medium, such as the biological tissue, which is nonhomogeneous and anisotropic, the Beer-lambert law has to be modified to take into account the scattering losses and the subsequent increased optical pathlength due to scattering. In a highly scattering medium, photons will travel a mean distance that is greater than the geometrical pathlength (*d*), which is the true optical distance and it is defined as the geometrical pathlength (DP). The scaling factor is defined as the differential pathlength factor (DPF) (Equation 3-1)[185].

Equation 3-1 Modified Beer-Lambert Law

$$A = \lg Io \text{ , } I = a \times c \times d \times B + G$$

Where A is the attenuation measured in optical density (OD). I_0 and I represent the incident and transmitted light in the medium, respectively. α is the specific extinction coefficient of the absorbing compound in the solution measured in μmolar $^{-1}$.cm^{-1}. c is the concentration of the absorbing compound in the solution measured in μmolar. d is the distance between the points where the light enters and leaves the solution measured in cm (geometrical distance). B is the differential pathway factor. G for scattering losses factor.

Conventional NIRS systems using the modified Beer-Lambert law, is able to measure changes in the concentration of HbO_2 and Hb; absolute quantification of CBF and CBV is possible by either the manipulation of inspired oxygen or injection of optical

dye indocyanine green[180, 186]. Real time continuous and quantitative measurements of CBF and CBV are not possible due to the inability to resolve the attenuation due to scattering of light in the medium and the presence of chromophores in all tissues located between the source of light and detector (optode), such as the skin, subcutaneous tissue, bones of the skull, meninges, cerebral fluid, cerebral cortex and white matter. This problem limited NIRS to clinical research studies because off-line processing of the data was required to calculate CBF and CBV[180]. Therefore, a method that relies on the photon diffusion theory, rather than the modified Beer-Lambert law, has been developed, known as spatially resolved spectroscopy (SRS), which provides a continuous quantitative measurement of cerebral oxygenation (Figure 3.3). By using a single light source that emits three to four wavelengths of light within the near-infrared region and multiple closely spaced detectors, the slop of light attenuation versus distance is measured. By applying photon diffusion theory, the scattering component of light attenuation can be accounted for and an absolute assessment of the ratio of HbO_2 and total haemoglobin can be made and expressed as percentage oxygen saturation[187].

Figure 3.3 Spatially resolved spectroscopy (SRS)

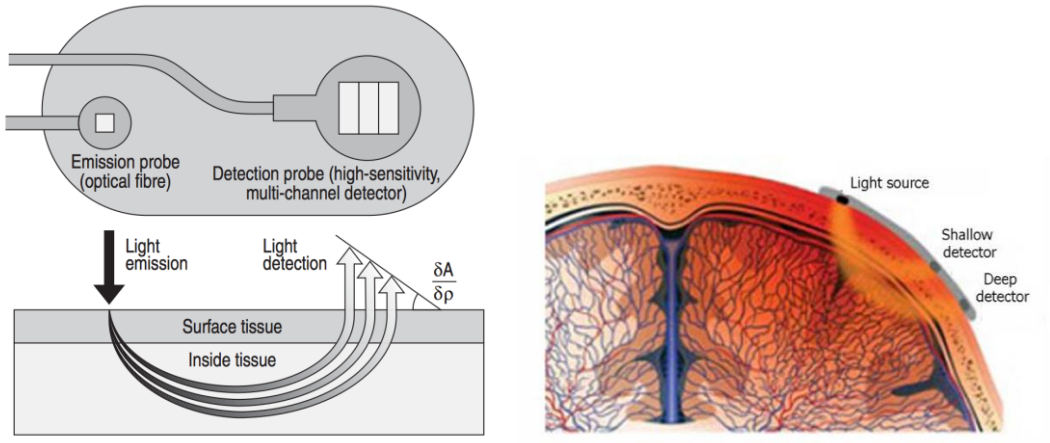

The figure on the right shows the principle of SRS. δA/δρ is the rate of light attenuation over distance (Adapted from *Valipour, European Respiratory Journal, 2002*)[188]. The figure on the left shows an example of NIRS probe with a light emittent and two detectors (NIRO 200NX probe, Hamamatsu, Japan).

The equation below demonstrates the principal of SRS.

Equation 3-2

$$\frac{\partial A}{\partial \rho} = \frac{1}{ln10} \times \left(\sqrt{3\mu a \times \mu s'} + \frac{2}{\rho} \right)$$

Where A is attenuation, ρ the distance from light impulse source and μa means absorption coefficient and μs' the reduced scatter coefficient[187].

The NIRS measurements included in this dissertation were performed using the NIRO 200NX (Hamamatsu, Photonics Japan). The NIRO 200NX monitor works with a laser photodiode emitting three wavelengths of light in the near-infrared spectrum (775, 810 and 850 nm) coupled with a set of three photodiode detectors (separated by 1 mm from each other). The NIRO 200NX measures HbO_2 and Hb using the modified Beer-Lambert law, and the tissue oxygenation index (TOI) and tissue haemoglobin index (THI) using SRS. Because in the first order approximation the scatter coefficient (μs') can be treated as a constant (k) with respect to the wavelength, the relative concentrations of oxygenated and deoxygenated haemoglobin can be obtained (k*HbO_2 and k*Hb, respectively) and resolved to the desired depth of the detector, i.e. giving the possibility of resolving the cortical influence from the skin, skull and meninges[187, 189].

TOI is calculated as the formula below and it is expressed as a percentage (%).

Equation 3-3

$$TOI = HbO_2 / HbO_2 + Hb \times 100\%$$

Where TOI indicates the Tissue Oxygenation Index, while Hb and HbO_2 indicate deoxygenated and oxygenated haemoglobin respectively.

THI is calculated as the formula below and expressed as a relative value, representing a change from the baseline measurement at the start of the study.

Equation 3-4

$$THI = HbO_2 + Hb$$

Where THI indicates the Tissue Haemoglobin Index. Hb and HbO_2 indicate deoxygenated and oxygenated haemoglobin respectively.

The SRS algorithm has been validated for monitoring of cerebral haemodynamics. Al-Rawi et al. (2001) studied a cohort of adult patients undergoing carotid endarterectomy and showed that sensitivity of TOI intracranial and extracranial changes was 85.7% and 0% respectively and specificity was 100% and 0% respectively[190]. Wong et al. (2009) demonstrated that TOI has concordance with CBF in a lamb model, supporting the clinical use of TOI for studies on cerebral haemodynamics[118].

3.1.1. Precision, accuracy and limitations of NIRS technology

Several NIRS monitors have been designed over the last two decades, using the multi-distance detector approach to provide a continuous quantitative assessment of cerebral oxygenation. Different instruments use different terminologies and methods to estimate cerebral oxygenation. The two most common NIRS monitors used in the neonatal environment are: the NIRO 200NX from Hamamatsu, Photonics K.K, Japan (which uses the SRS method described above), and the INVOS 5100c (Somanetics/Covidien, Mansfield, USA). The INVOS instrument has a transducer containing one LED light emitting source with two different wavelengths (730 and 810 nm) and two photodiode detectors at a distance of three and four centimetres from the emitting source, respectively. The INVOS monitor uses a formula that subtracts the light absorbed by the nearest detector (assuming this detector light absorbed only by shallow regions as the akin and skull) from the more distal detector; it estimates the regional cerebral oxygen saturation (rSO_2), diminishing the contribution of extra-cerebral tissue. TOI and rSO_2 measure the oxygen saturation

across veins (70-80%), capillaries (5%) and arteries (20-25%) and both have been validated against the jugular saturation as well as against each other[191, 192].

The comparison between measurements using different devices remains an important limitation to the use of NIRS as a clinical tool. The reproducibility of measurements between different NIRS monitors has been assessed in several studies. The validity of any monitoring instrument depends in its precision and accuracy. Sorensen & Greisen (2006) studied the precision of TOI using the NIRO 300 monitor and observed that the variation in measurements within infant was 5.2% and between different infants, was 6.9%[193]. Pocivalni et al. (2011) compared the NIRO 300 and INVOS 5100 instruments and reported a 10% difference between the two monitors with the NIRO reading lower values for cerebral oxygen saturation[194]. A similar, but smaller discrepancy, was documented by Schneider et al. (2014) comparing the NIRO and INVOS (2.9% difference)[195]. The reasons for these discrepancies are complex and multifactorial; different manufacturers use different algorithms to calculate the saturation values, moreover there is no calibration standard. In addition, several studies have used adult sensors to measure cerebral oxygenation in infants. The difference between adult and neonatal sensors can reach 15%[196].

The proportion of approximately 70% venous saturation and 25% to 30% arterial is based on studies comparing positron emission tomography (PET) and NIRS[197]. However, significant variation between individual cerebral arterial/venous ratio should be considered. Different physiological or pathological status may contribute to changes in this proportion, nevertheless the use of NIRS as a trend monitor can minimise this limitation[198]. The skull, the presence of high extra-cerebral fluid and hair can also contribute to the attenuation of light and reduce the accuracy of NIRS measurements[199-201]. However, in preterm infant the thickness of the skull is thinner than in adults and the amount of hair is negligible, which may not cause a major influence in the continuous trend measurements. Single channel NIRS provide regional cerebral oxygenation (reflectance more) and assumptions of global brain perfusion and haemodynamics should be cautiously considered. Using two channels, one in each side of the infants' head or changing the optodes from one side to the other every few hours may minimise this limitation.

3.1.2. Fractional tissue oxygen extraction

The balance between oxygen delivery and oxygen consumption can be investigated using a relative measurement of fractional tissue oxygen extraction (FTOE) (Equation 3-5).

Equation 3-5

$$FTOE = SaO_2 - rScO_2 / SaO_2$$

Where SaO_2 is peripheral arterial oxygen saturation and $rScO_2$ is regional cerebral oxygenation.

Increased FTOE may indicate a reduced oxygen delivery with constant cerebral oxygen consumption or a higher consumption than oxygen delivery. On the other hand, decreased FTOE may reflect a reduction in oxygen extraction due to decrease in oxygen consumption with rise in oxygen delivery[202].

3.1.3. Clinical applications of NIRS in neonates

NIRS has been increasingly applied as a trend monitor of cerebral oxygen delivery and perfusion. This technology has been routinely used during cardiac surgery in many centres[182]. In infants undergoing cardiac surgery, an association between intraoperative low cerebral oxygenation and poor neurodevelopmental outcome at one year of age has been described[203]. More recently, some neonatal intensive care units in North America and in Europe have adopted the use of NIRS in term infants with hypoxic ischaemic encephalopathy (HIE) undergoing hypothermia treatment. The rationale to use NIRS in this population is its possible prognostic value on long-term neurodevelopmental outcome. Higher cerebral oxygen saturation with lower FTOE at 24 hours of age has been observed in infants who died or had adverse motor and cognitive impairment compared to infants with more favourable outrome[204, 205]. In small studies using MRI (magnetic resonance imaging), cerebral oxygenation had strong positive correlation with CBF in infants with severe HIE[206]. In addition infants who had any degree of brain injury shown on the MRI done on day 10 of life had higher cerebral oxygenation on the first day of life compared to infants who had

normal MRI[207]. However, larger studies are necessary to define the thresholds of cerebral oxygenation in this population and to understand the physiology of brain haemodynamics in infants undergoing hypothermia treatment.

In the preterm population, several studies have used NIRS to assess cerebral oxygenation and cerebral autoregulation. A lack of consensus on "normal cerebral oxygenation thresholds" and the evidence that monitoring cerebral haemodynamics during the first days of life may improve long-term neurological outcome have delayed the use of NIRS as a routine cotside monitoring.

Cerebral oxygenation in preterm infants

Data from early animal studies and small cohorts originally suggested a "normal range" for cerebral oxygenation between 55% and 85%. According to these studies, neuronal injury occurs when cerebral oxygenation is below 35%[208]. Over the last decade, several groups have used NIRS to monitor cerebral oxygenation in small and large cohorts of infants over the first days of life[209-211]. Alderliesten et al. (2016) have recently proposed gestational age-specific reference curves for cerebral oxygenation (rSO_2) and FTOE during the first three days of life in a cohort of 999 preterm infants born at less than 32 weeks (Figure 3.4). They suggested that lower thresholds are seen in infants with lower gestational age and that postnatal age, haemodynamically significant PDA and in-utero growth restriction may have an impact on levels of rSO_2[210]. Despite being a valid study to elucidate the questions about rSO_2 thresholds, there were a number of limitations. Infants with different morbidities were included in the overall analysis; most infants had rSO_2 recorded with a small adult sensor (as mentioned, differences between adult sensors and neonatal sensors can reach 15%) and data were collected in a single level III neonatal unit[210].

Figure 3.4 Reference values of cerebral oxygenation in preterm infants

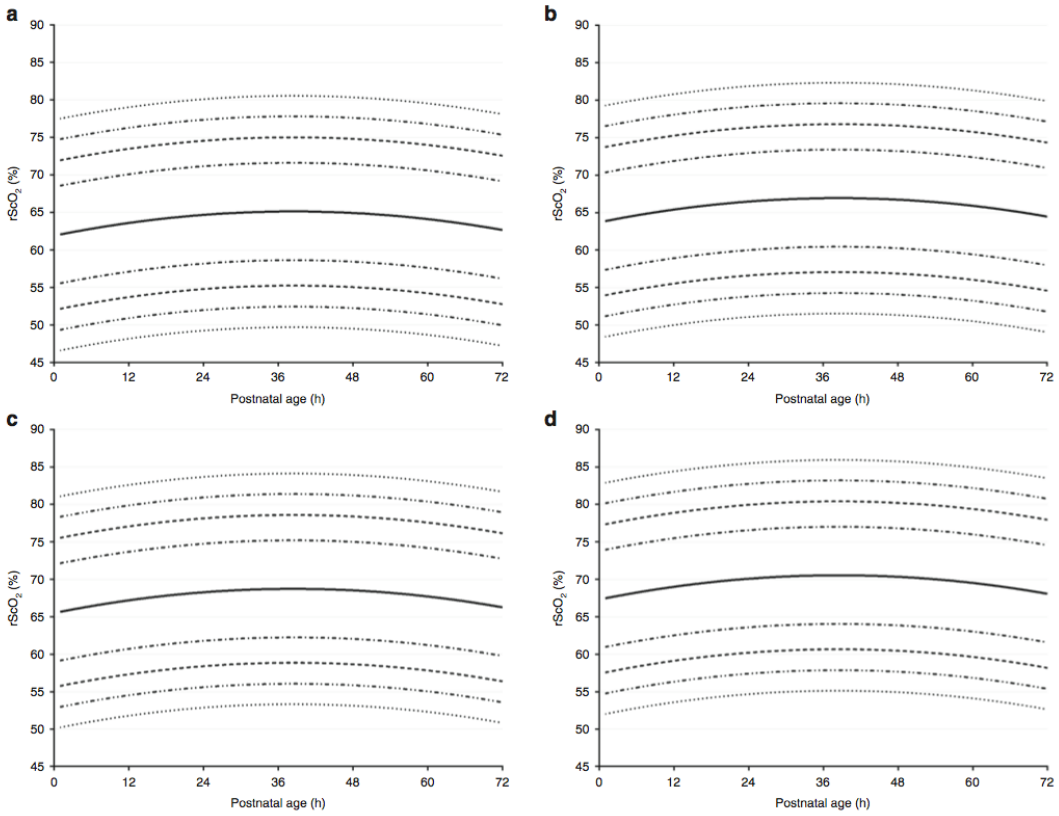

Each graph shows references and percentiles values for different ranges of gestational age at birth: a 24-25 weeks, b 26-27 weeks, c 28-29 weeks and d 30-31 weeks. Adapted from *Alderliesten et al. (2016)*[210].

The importance of defining thresholds of cerebral oxygenation in preterm infants have increased since a large multi-centre study demonstrated that NIRS could be used to stabilize cerebral oxygenation in extreme preterm infants. The SafeBoosC (Safeguarding the Brains of Our Smallest Children) phase II randomized control trial has shown that the burden of hypoxia and hyperoxia in preterm infants born at less than 28 weeks can be reduced by using continuous monitoring of rSO_2 over the first 72 hours of life. In the 86 infants randomised to the experimental group, where NIRS measurements were visible and a dedicated guideline treatment from rSO_2 below 55% or above 85%, the mean burden (magnitude of deviation from stipulated thresholds) of hypoxia was significantly less than in the 86 infants in the control group, where rSO_2 was blinded (Figure 3.5). Although this trial was not powered to detect differences in short or long-term outcomes, its results have emphasized the importance of including continuous monitoring of tissue perfusion during the

transitional period, when preterm infants are more vulnerable to hypoxic-ischaemic brain injury. However, the SafeBoosC trial had several limitations: different monitors and sensors were used in different centres, and motion artefacts were not completely removed, for example repositioning of the sensors may have induced sudden change in cerebral oxygenation[209]. These limitations should be addressed before a larger phase III trial having primary outcome of death and/or brain injury and secondary outcome of neurodevelopmental outcome is designed.

Figure 3.5 SafeBoosC trial

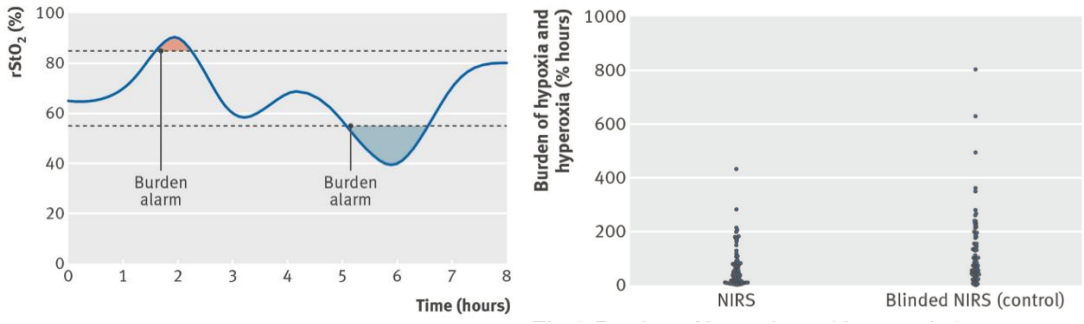

On the right is a schematic illustration of the estimation of burden of hypoxia (below 55%) and hyperoxia (above 85%). On the left is the difference of burden of hypoxia and hyperoxia between groups (NIRS = visible measurements together with guideline treatment, Blinded NIRS = control group). Adapted from *Hyttel-Sorensen et al (2015)*[209].

Several studies have used NIRS to monitor cerebral oxygenation during the immediate transition from birth in term infants[212-214]. However, no definite thresholds have yet been defined.

Cerebral autoregulation

Cerebral autoregulation using NIRS and the different studies using this technology to assess CBF and cerebrovascular reactivity in preterm infants has been described in Chapter 2, section 2.3.1.

3.1.4. Complexity of biological signals as an alternative method to analyse NIRS signals

A complex biological system includes a diversity of regulatory mechanisms that interact in a non-linear way. Most studies using NIRS or systemic signals apply time or frequency-domain analysis. These methods assume linearity or stationarity. However, a non-linear method to analyse biological signals may reveal more accurately the magnitude of changes over time. A complex biological system has the ability to react and adapt to minute changes in its environment. When the complexity of a system is reduced or lost, a pathological status is potentially present. Loss of complexity has been observed in several diseases and aging[215, 216]. It has also been associated with poor outcome in severely sick adults and children[217, 218].

Analysis of entropy is a non-linear measurement of system randomness and unpredictability, which has been suggested as a method to assess the complexity of biological signals in healthy and pathological systems. The entropy of a system increases with greater randomness. In 1991, Pincus introduced the approximate entropy (ApEn) method to assess the irregularity of biological time series[219]. Several studies have shown that ApEn may correlate with subclinical changes that are often undetectable by time-series analysis. Moreover, ApEn changes have been associated with subsequent clinical changes[219]. ApEn has been extensively used in physiological and medical studies. It has been applied to discriminate atypical EEG's and respiratory patterns from normal signals[220, 221]. One decade later, sample entropy (SampEn) was proposed as a modified method, which was less dependent on the length of the time series and less statistically biased[222, 223]. In neonates, Sample Entropy analysis of heart rate variability (HRV) was used to predict the onset of neonatal sepsis 24 hours before clinical diagnosis[222].

More recently, multiscale Entropy (MSE) has been used to provide a more meaningful measure of complexity, exploring calculations of (SampEn) over multiple time scales (Figure 3.6). MSE shows that correlated random signals are more complex than uncorrelated random signals (white noise). Moreover, MSE describes pathological physiology better than simple entropy measures, doing a better differentiation between healthy, complex system and deranged or random

interactions[224]. Since Costa et al., 2002 introduced MSE method; several studies in adults and children have been published using this methodology. MSE has been applied to assess the complexity of cardiac interbeat from an interval time-series; healthy adults had more complex dynamics than adults with congestive heart failure or those with atrial fibrillation[225]. Complexity of intracranial pressure (ICP) measured using MSE has been correlated with clinical outcome. In adults with traumatic brain injury, reduced complexity of mean ICP was associated with poor outcome and increased mortality[226]. In neonates, MSE was significantly reduced in infants with neonatal seizures and later diagnosis of epilepsy when compared to control infants[227].

Figure 3.6 Multi-scale entropy analysis

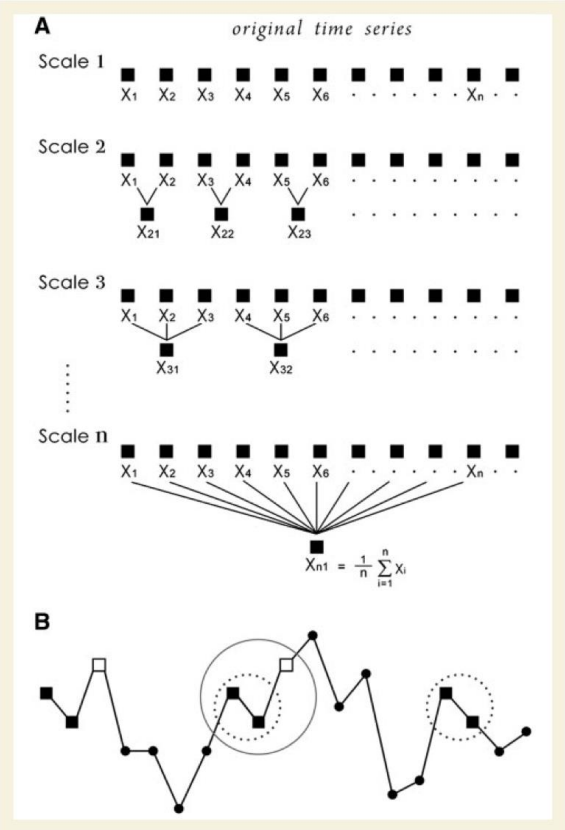

The illustration (A) shows sequences of time series data and (B) sample entropy. For length m = 2, two sequences (dotted circle) match the first two data points and one sequence (circle) matches the first three data points (length m + 1). This matching process is repeated for the next two data points and then all sequences to determine the total number of matches of length m and m + 1. Sample entropy is calculated as the negative natural logarithm of the ratio between the number of length m + 1 matches and the number of length m matches. Adapted from *Lu et al. (2012)*[226].

3.2. NEONATAL FUNCTION ECHOCARDIOGRAPHY

The lack of reliable continuous measurement of systemic blood flow remains an unresolved problem in neonatal intensive care units. Haemodynamic monitoring often relies solely on blood pressure and heart rate measurements. Beyond that, the assessment of cardiovascular function and organ perfusion is based on poorly validated measurements of capillary refill time, skin colour and urine output. Methods of continuous cardiac output measurement, such as thermodilution and electrical impedance monitoring have not yet been well validated for clinical use in neonates, mainly due to the difficulties on assessing the complexity of transitional circulation and the persistence of antenatal channels in preterm infants and sick infants.

Doppler echocardiography is a non-invasive technique that can estimate hemodynamic parameters of systemic blood flow and surrogate measurements of cerebral blood flow (CBF). Over the last 20 years, neonatologists have developed skills to perform targeted functional echocardiography to assess cardiac output, myocardium performance, and the presence and patency of the ductus arteriosus and foramen ovale. This practice has helped the management of infants with hemodynamic compromise and has possibly improved short-term outcome[228, 229]. However, the validity and reliability of measurements between observers remains an important limitation. Intra-observer variability can range from about 10% and inter-observer variability from 15% to 20%[230]. Therefore, functional echocardiographic measurements should be taken in consideration along with the clinical context.

Two-dimensional (2D) echocardiography

2D echocardiography allows the assessment of the structure of the heart and major vessels, giving a subjective impression of myocardium contractility, identifying any thrombus, pericardium effusion, and allows the positioning the cursor to obtain M-mode and Doppler measurements[231]. The most common views to perform functional echocardiography in neonates are: subcostal, apical, long axis parasternal, short axis parasternal (Figure 3.7). These views are used to measure several parameters: left ventricular output (LVO), right ventricular output (RVO), PDA, PFO, myocardium contractility[231, 232].

Figure 3.7 Neonatal echocardiography: standard views

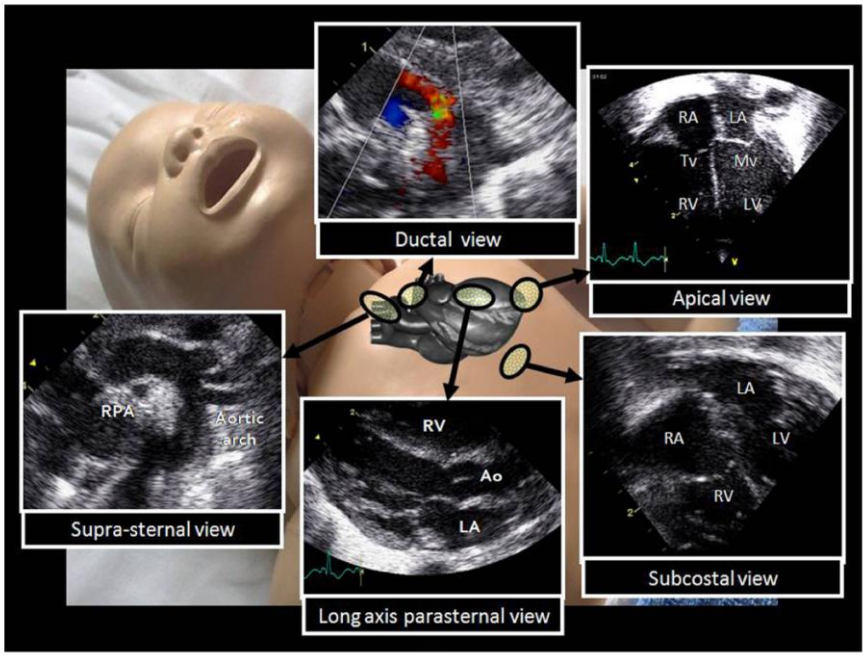

The image shows the five most common views for the assessment of cardiac morphology and function in newborn infants. Adapted from *El-Khuffash et al. (2011)*[229].

M-mode modality assesses the insonated structure over time during the cardiac cycle by displaying consecutive single lines though part of the heart (Figure 3.19). Each line represents the same structure but in a different time. M-mode is useful to get more detailed analysis of chamber size, wall thickness, valvular motion and quantification of myocardium contractility[229, 231, 233].

Doppler ultrasound

The Doppler principle can be applied to ultrasound because frequency changes when sound is reflected from moving objects. Blood flow can be estimated using Doppler ultrasound, because the major reflector is the red blood cell. The velocity of the moving blood can be calculated if the frequency shift is directly proportional to the velocity of the moving object and if the angle of insonation is within 20° of the axis of movement. Increasing angle can lead to underestimated values of flow velocity. By measuring velocity two parameters can be derived. Firstly, the pressure gradient can be determined by using a modified Bernoulli equation (pressure gradient = 4 x velocity^2). Secondly, by measuring the diameter of a vessel as well as the flow

velocity, blood flow can be estimated as flow if the product of mean velocity and cross-sectional area[233, 234].

In neonatal echocardiography, three types of Doppler are usually used:

PW (Pulse wave Doppler): it is the most commonly used type of Doppler. It allows the operator to focus the velocity assessment on a "range gate" on the 2D image. It has the limitation of assessing velocities only up to 2 m/s.

CW (Continuous wave Doppler): it allows the assessment of velocities above 2 m/s, but it assesses the whole path of transmission, being less focused.

CD (Colour Doppler): it is derived from CW. Flow direction and velocity are mapped in colours on a 2D image. Conventionally, flow away from the probe is mapped in blue and flow towards the probe is mapped in red.

3.2.1. Measurements

The measurements described below are the ones obtained during data collection for this thesis and are limited to systemic blood flows and persistent antenatal shunts. Several methods to assess myocardium performance and right ventricle function have been recently described in the literature; however the discussion about these measurements is beyond scope of this thesis.

Left ventricular output

LVO is obtained from the measurement of flow velocity from the ascending aorta from a modified apical five chamber view and diameter of the ascending aorta from the long parasternal view[146 235]. Three different methods to measure aortic diameter have been suggested: between the hinges of the aortic arch (AV)[236, 237], at the aortic sinus (AS)[238, 239] and at the sinotubular junction (STJ)[146]. Mellander et al. (1987) have compared ultrasound methods to measure LVO with thermodilution and observed that measurements using 2D diameter from AV underestimate LVO[240]. Recent work published by Beker et al. (2014) showed that aorta diameter measurement at STJ was more precise and accurate to determine LVO than AV and AS. According to this study, measurements at AV level underestimate LVO and measurements at AS level

overestimate (Figure 3.8)[241]. Most research studies have used the measurement suggested by Evans et al (STJ)[146].

Figure 3.8 Aorta diameter measurements

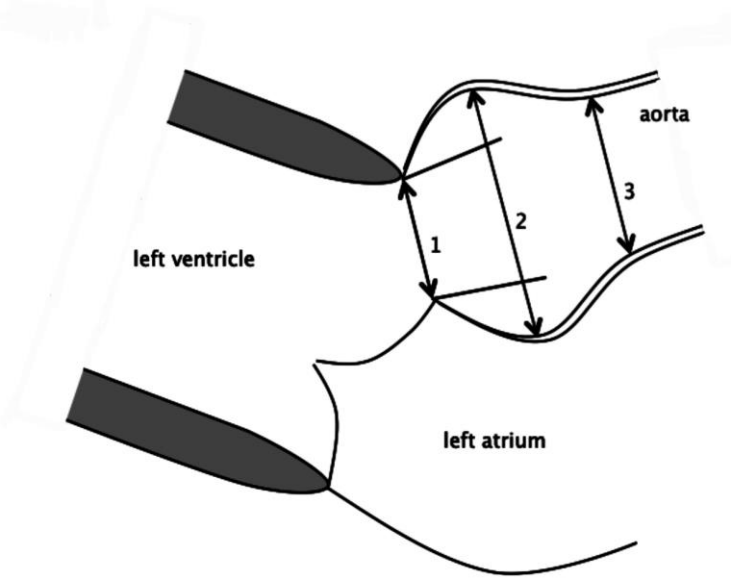

Aortic diameters from 2D (high parasternal long axis view) images for estimation of LVO: 1. between the hinges of the aortic valve (AV). 2. at the level of the aortic sinus (AS). 3. at the level of sinotubular junction (STJ). Adapted from *Beker et al. (2014)*[241].

The methodology suggested by Evans et al. (1996) has been validated against invasive methods such as thermodilution and dye dilution[146, 173, 240]. The accuracy of LVO measurements is variable. Intra-observer variability has been estimated at about 10% and inter-observer variability of 20%. However, this variability may be decreasing with the use of modern ultrasound machines, which offer better quality images and advance software for image reconstruction[232].

The main limitation on the use of LVO as a measure of systemic blood flow is the presence of a PDA with left-to-right flow, particularly in preterm infants. In infants with a closed or restrictive ductus arteriosus, LVO is associated with systemic blood flow and RVO reflects pulmonary blood flow. However, in the presence a PDA with a left-to-right PDA shunt, RVO would better reflect systemic blood flow and LVO pulmonary blood flow, as long as PFO flow is minimal. LVO is usually increased with a significant PDA shunt but RVO may be decreased due to reduced systemic venous return (‘ductal steal’) (Figure 3.9).

Figure 3.9 Systemic and pulmonary blood flows in the presence of PDA

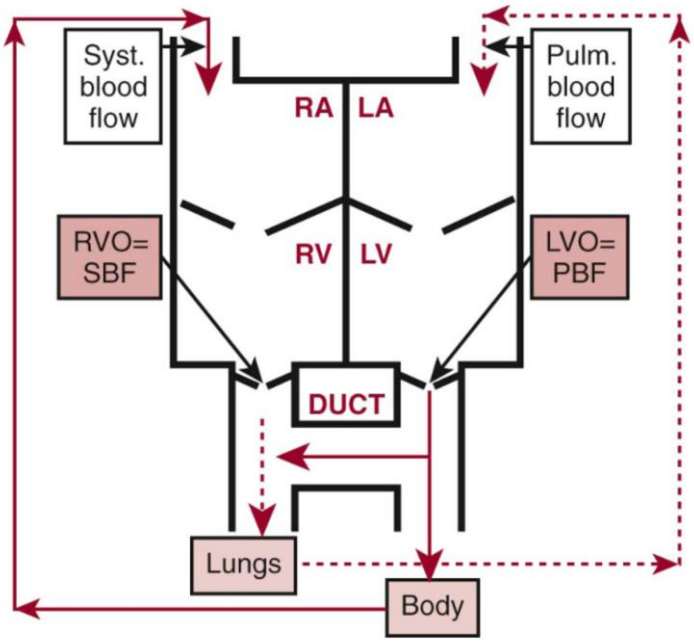

LVO reflects the sum of systemic blood flow and ductal shunt, which is then equal to pulmonary blood flow (PBF). RVO provides an estimated measurement of systemic blood flow (SBF), as long as PFO is negligible. Adapted from *Kleinman, Hemodynamics and Cardiology: Neonatology questions and controversies, 2012*[233].

Figure 3.10 LVO measurements

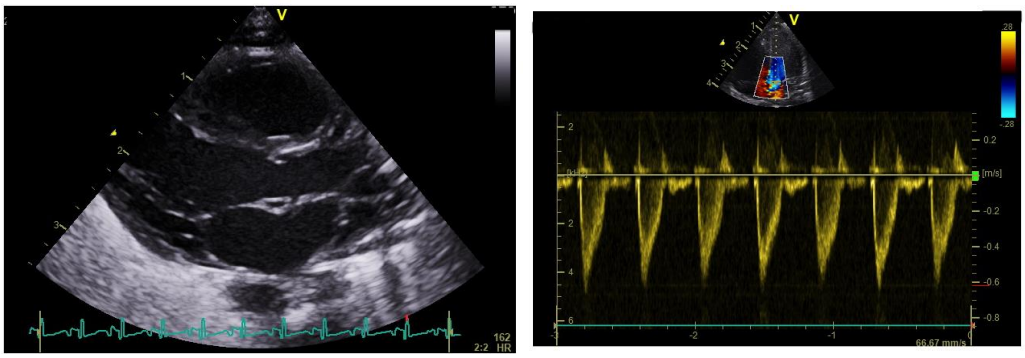

The picture on the left shows the long parasternal axis view at the aorta level for 2D measurement of LVO diameter. On the right, the picture shows the LVO flow taken from modified 5 chambers apical view.

All functional echocardiography images presented in this section were recorded from infants recruited to the studies included in this dissertation. I collected all images and performed all measurements (more details in Chapter 4).

Right ventricular output

RVO is usually measured following the methodology published by Evans & Iyer (1994) in the main pulmonary artery (MPA) from the true parasternal view. Diameter is determined in end systole at the insertion of the pulmonary valve leaflet just before the valve closes. Doppler is performed on the same window, placing the range gate just beyond the valve leaflets. Flow velocity measurements can be difficult to obtain when a large left-to-right ductal shut is present. Moreover, the accuracy of RVO is not clear, as studies comparing RVO with other methods of measuring right-sided cardiac output have not been published. However, in infants with a closed ductus arteriosus and no shunt across the foramen ovale the RVO has been strongly correlated with LVO[242]. RVO measurements may not be accurate in infants with a large PFO; however, atrial shunts are usually not significant within the first 24 hours of age, and therefore RVO is a reasonable measure to assess systemic blood flow in preterm infants with significant PDA in this time period.

Figure 3.11 RVO measurements

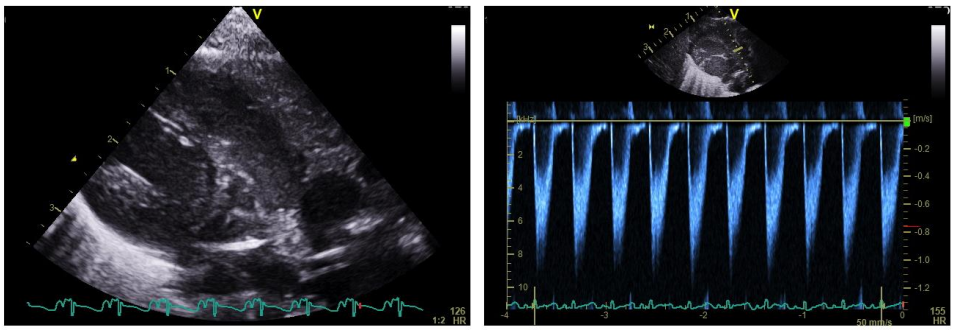

The picture on the left shows the upper long parasternal axis view at the main pulmonary artery level for 2D measurement of RVO diameter. On the right, the picture shows the RVO flow taken from the main pulmonary artery view.

Superior vena cava

SVC flow has been suggested as a surrogate marker of blood flow from the brain and upper body[56]. It was initially proposed as a global measure of systemic blood flow during transitional period because it is not influenced by atrial and ductal shunts. SVC flow velocity is considerably easy to record from low subcostal view but diameter measurements (in most studies are performed using M-mode) can show large variability and be difficult to obtain. Spontaneous respiration and beat-to-beat variability may influence flow velocity since SVC flow is a venous flow. Therefore, the diameter should be taken from an average of 10-15 cardiac cycles. In infants with a closed ductus arteriosus and LVO similar to RVO, SVC has been estimated an average of 37% of LVO[56]. A major limitation in the use of SVC flow in clinical practice is the high intra and inter-observer variability. Lee et al. (2010) have reported mean intra-observer variability of 17% and 29% in inter-observer analysis[243].

SVC flow increases over the first 48 hours of life. Early studies from Evans and Klucow's group have shown an association between low SVC flow (< 40 mL/kg/min) within the first 24 hours and later development of GMH-IVH, death, and poor long-term neurodevelopmental outcome[145, 244]. However, more recent studies have not found the same correlation between low SVC flow and poor outcome. Recent data have reported higher values of SVC measurements within the first 24 hours of age compared to early studies published by Kluckow's group[245, 246].

More recently, Ficial et al. (2017) a modified method to measure SVC flow by obtaining flow velocity from a suprasternal window and by deriving the cross-sectional area from imaging the SVC in short axis and manually tracing the minimal and maximal area. This method had better agreement with MRI-derived SVC flow and better intra and inter-observer variability when compared to the methodology published by Evans and Kluckow in 2000. However, no ranges of normal SVC flow measurements have been yet published using this recent method neither data on short or long-term outcome[247]. The measurements included in this dissertations were based on Kluckow & Evans (2000)[56].

.

Figure 3.12 SVC measurements

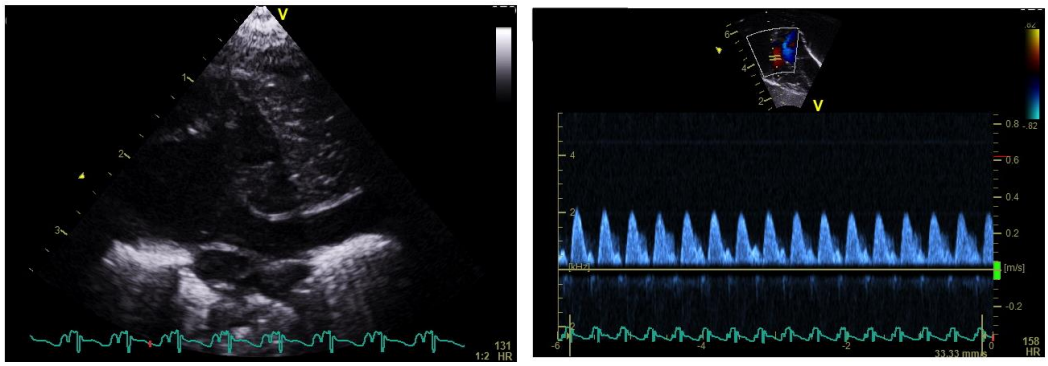

The picture on the left shows the high long parasternal view at the level where SVC enters the right atrium for the measurement of minimal and maximum diameters. On the right, the picture shows the SVC flow obtained from the low subcostal view.

Table 3.1 Values for LVO, RVO and SVC flow in preterm infants

	< 12 hrs of life Mean (SD)	**24 hrs of life Mean (SD)**	**48 hrs of life Mean (SD)**
LVO (mL/kg/min)		240 (60)	260 (60)
RVO (mL/kg/min)		260 (90)	270 (90)
SVC (mL/kg/min)	60 (25)	80 (20)	90 (25)

SD for standard deviation. Values are according to Kluckow et al.[56, 146]

Persistent foramen ovale

The foramen ovale is situated in the mid-portion of the inter-atrial septum. During fetal life, it has the function to divert the blood flow coming from the ductus venosus to the left atrium, and the blood flow from the inferior vena cava into the right atrium (Figure 3.13). Following birth the changes in pressure between left and right ventricle usually induce the closure the foramen ovale over the first few days of life. The PFO is usually present in preterm infants and can be measured from the subcostal view using low scale colour Doppler. Diameter can be measured using either colour flow jet through the atrial septum or by 2D images. PW Doppler can be used to assess the

direction and velocity of flow. PFO can increase RVO measurements when diameter is bigger than 3 mm and it is less likely to influence CBF compared to PDA[233, 242, 248].

Figure 3.13 PFO measurements

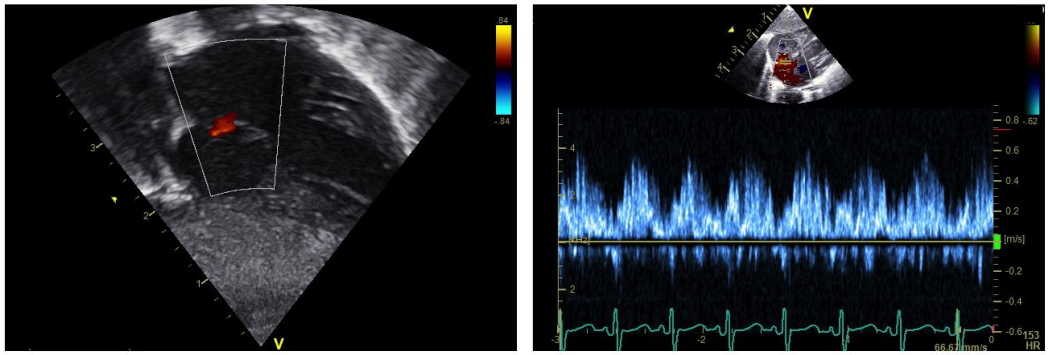

The picture on the left shows the subcostal view at PFO level. On the right, the picture shows the PFO flow obtained also from subcostal view.

Persistent ductus arteriosus

The clinical significance of a PDA and its association with neonatal morbidities has been a controversial subject between neonatologists. Several studies have associated haemodynamically significant PDA (hsPDA) with adverse outcome such as GMH-IVH, necrotizing enterocolitis (NEC), chronic lung disease (CLD) and death [249-251]. However, the definition of what is an hsPDA remains debatable. Different studies have applied different classifications. Time of diagnosis and treatment have not been consistent across studies either, contributing to the uncertainty on when it should be treated, which cases will need management and what is the best treatment option[252-255].

The size of a PDA can be measured directly with 2D ultrasound using modern scans. Old studies have reported ductal size using colour Doppler, but measurements done using this method usually overestimate the diameter. PDA size and flow characteristic are usually obtained from the high left parasternal view. Diameter should be measured on the site of maximal constriction in the end of systole. Some studies have reported diameters measured from the short axis view, however this view does not show all ductal trajectory and the size of the PDA may be overestimated[232, 256].

Clinical signs such as heart murmur, persistent tachycardia, hyperactive precordium, bounding pulses, and evidence of cardiomegaly or pulmonary congestion are not accurate to predict the magnitude of PDA and they are usually not present within the first days of life. Therefore, echocardiographic measurements have been largely used to detect hsPDA[144, 257].

PDA measurements to assess hemodynamic significance:

Ductal diameter: this has been considered the most important parameter to define the degree and severity of PDA shunting. A diameter above 1.5 mm has been associated with higher ratio between pulmonary and systemic blood flow[242, 258].

Figure 3.14 PDA diameter

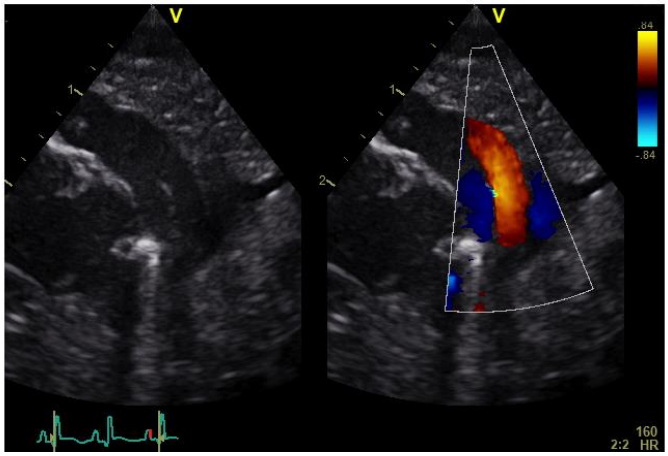

On the left: PDA on 2D image from parasternal view. On the right in red is the PDA colour Doppler flow. The red colour indicates left-to-right shunt.

Ductal flow pattern: Depending on the difference between pulmonary to systemic pressures the ductal flow may have complete right to left flow, bidirectional flow or complete right to left flow. A complete right to left flow is always considered pathological in neonates. A right to left shunt that accounts for more than 30% of the cardiac cycle in a bidirectional shunt is considered a sign of pulmonary hypertension.

Ductal flow pattern can be recorded from high left parasternal view by placing the PW range gate at the pulmonary end the PDA, aiming an angle of insonation below 20° According to the visual appearance the ductal flow pattern can be classified in five different categories[259]:

Pulmonary hypertension:

It is a bidirectional shunt that is usually seen in early postnatal hours in preterm infants and in cases of persistent pulmonary hypertension (high pulmonary vascular resistance).

Figure 3.15 PDA flow pattern – Pulmonary hypertension

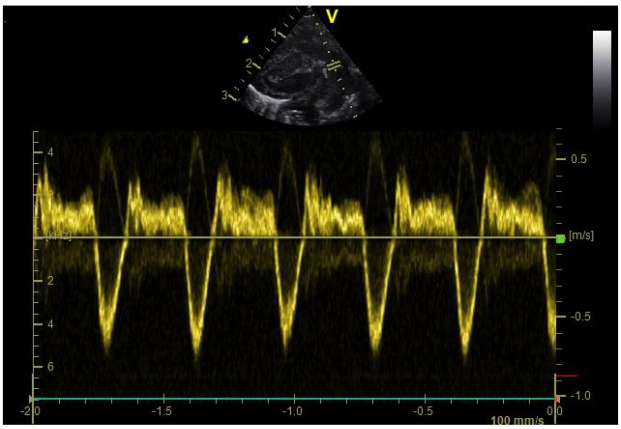

Growing:

This is a transitional flow pattern between pulmonary hypertension and pulsatile flows. It is a bidirectional shunt with predominant left-to-right flow. It represents the falling in pulmonary vascular resistance.

Figure 3.16 PDA flow pattern – Growing

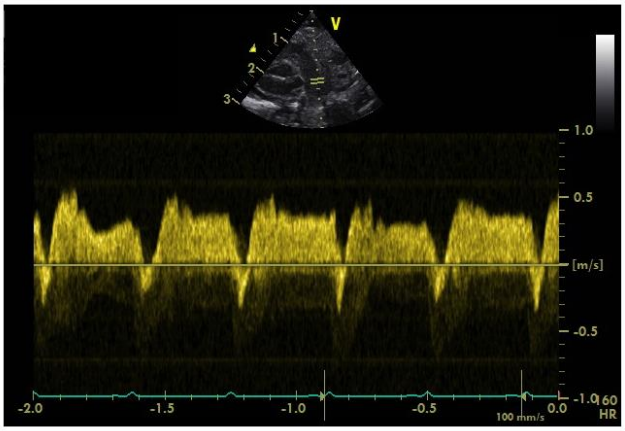

Pulsatile:

It is a complete left-to-right flow with peak velocity of about 1.5 m/sec with rhythmically pulsatile change. This pattern has demonstrated high specificity and sensitivity to predict PDA with clinical signs. Left-to-right flow across the PDA has been associated with severe respiratory distress syndrome and higher incidence of chronic lung disease[260].

Figure 3.17 PDA flow pattern - Pulsatile

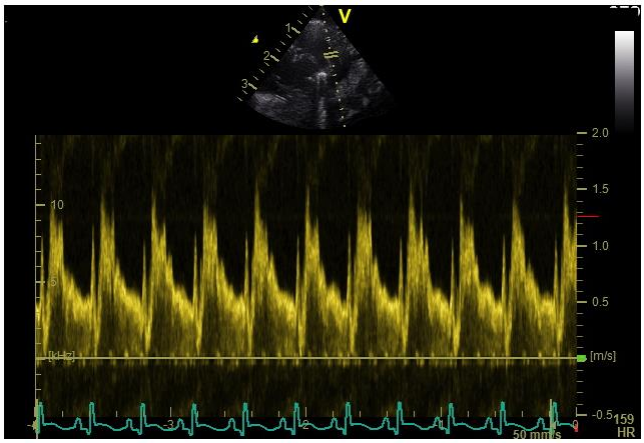

Closing:

Differently from the pulsatile flow, the closing pattern has a continuous left-to-right flow with peak velocity usually ≥ 2m/sec.

Figure 3.18 PDA flow pattern - Closing

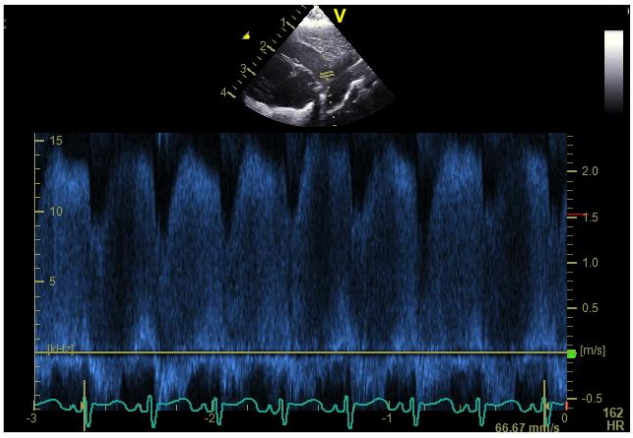

Closed: absence of flow.

Increased LVO:

High LVO (> 350 mL/kg/min) may indicate increased pulmonary flow in infants with a PDA > 1.5 mm. Increased ductal shunting has been associated with low SVC (surrogate of systemic blood flow) with an opposite increase in LVO. Additional evidence that a moderate to large left-to-right PDA may cause low systemic blood flow and possible poor organ perfusion is the fall in celiac artery blood flow despite a rising LVO[261-264].

Ratio between left atrium diameter and aortic root (LA:Ao):

The LA:Ao ratio is one of the first suggested markers of PDA significance[256]. This ratio relies on the principle that a left-to-right ductal shunt may increase the volume load on the left side of the heart, thus the left atrium will dilate in relation to the aortic arch that which remains the unaffected. Several studies have suggested values for LA:Ao that may predict a significant PDA. The most acceptable value in the literature is a LA:Ao ratio above 1.4 – 1.5 . However, it is not an accurate measurement on the first day of life[265, 266].

Figure 3.19 LA:Ao measurement – M-mode

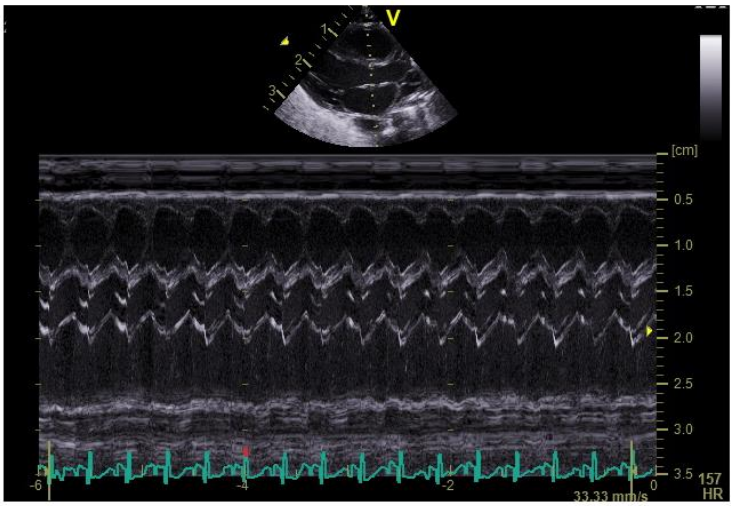

Descending aorta flow:

The flow pattern on the post-ductal descending aorta is normally forward, but with increasing left-to-right shunt across the PDA this flow pattern can become retrograde. This retrograde diastolic flow has also been associated with higher ratio between

pulmonary to systemic blood flow[256]. Goves et al. (2008) measured the blood flow in the descending aorta just proximal to the diaphragm and observed that retrograde flow in descending aorta is a marker of high volume shunt across the PDA; a possible marker of ductal steal and lower body hypoperfusion[267].

Figure 3.20 Reversal end-diastolic flow in the post-ductal aorta

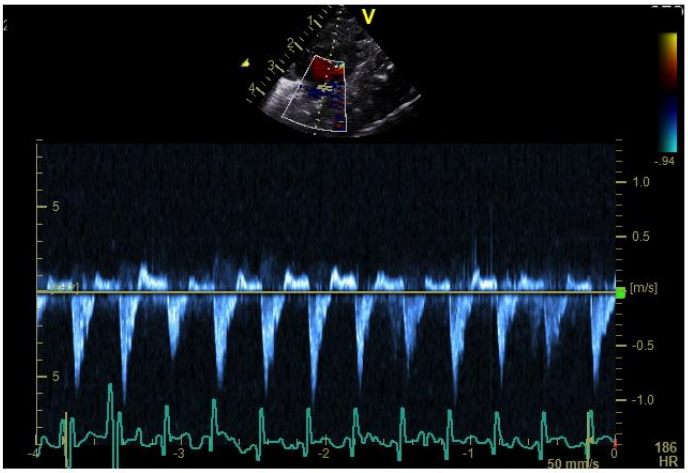

End-diastolic flow velocity in the left pulmonary artery:

Increased diastolic and/or mean velocity in LPA has been associated with the severity of ductal shunt[266]. The flow velocity can be obtained from the same PDA view by placing the PW range gate on the LPA. Normal LPA diastolic velocity has been suggested as above 0.2 m/second[268]. Mean LPA velocity of above 0.43 m/sec has been suggestive of a large ductal shunt[266].

Figure 3.21 LPA end-diastolic flow velocity

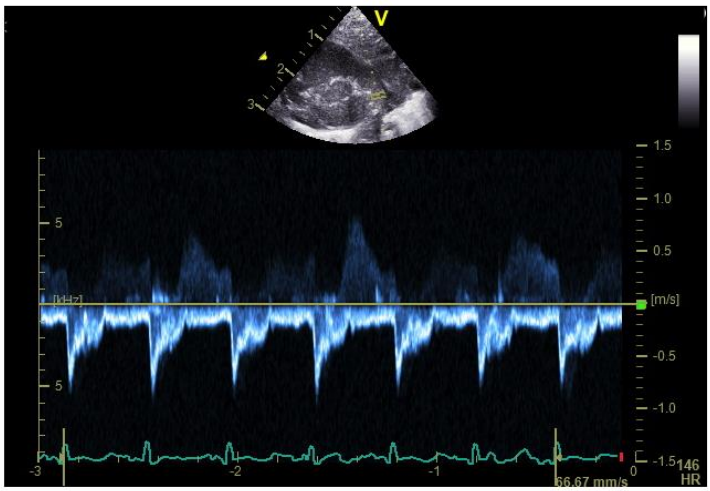

3.2.2. Relationship between NIRS and functional echocardiography measurements

A few studies have attempted to address the correlation between cerebral blood flow and oxygenation with echocardiographic measurements. The challenges and reliability of correlating continuous NIRS signals with static functional echocardiography measurements is discussed in more details in Chapter 8.

4. METHODS

4.1. STUDY DESIGN AND ENROLMENT

The data included in this thesis were collected under two different prospective observational study protocols:

a. **'RUMBA'[1]:** Study into the control of blood flow and oxygen to the brain of preterm infants undergoing intensive care. Data for this cohort were collected between **September 2010 and March 2013**. This study was funded by a project grant from the Evelyn Trust (http://www.evelyntrust.com/projects-weve-funded/all-supported-projects).

b. **'SAMBA'** (Study of Autoregulation Monitoring in Babies)**:** Circulatory function and cerebrovascular control of blood flow and oxygen delivery to the brain in newborn infants undergoing intensive care. Data for this cohort were collected between **May 2013 and October 2015**. This study as well as being the main body of work funded by CAPES/COT received additional funding from SPARKS (www.sparks.org.uk) for a research nurse and computer scientist research associate.

All data were collected at the Neonatal Intensive Care Unit (NICU) at The Rosie Hospital, Cambridge University Hospital Foundation Trust.

[1]'RUMBA' is not an acronym, but the name of the group of infants recruited before 'SAMBA'.

4.1.1. Population

The recruitment criteria were similar for both study protocols:

Inclusion criteria:

Preterm infants born at ≤ 32 weeks gestational age with birth weight < 1.5 kg, who had an indwelling arterial catheter inserted for clinical reasons.

Exclusion criteria:

Infants born with major malformations (e.g. gastroschisis or major cardiac defect), infants who were severely sick or moribund, infants who were more than 72 hours old (for RUMBA) or more than 12 hours old (for SAMBA).

4.1.2. Data collection

RUMBA study:

This study had two data collection phases:

- **Phase 1**: between September 2010 and March 2012

Dr Mitra recruited and collected data from 31 preterm infants. Most of these infants had data collected within the first 72 hours of age, however four infants had data collection between the 4^{th} and 7^{th} day of life. The median (range) age at the start of the study was 44 (7 – 180) hours.

- **Phase 2**: between April 2012 and March 2013

I recruited and collected data from 29 preterm infants. All of them had data collection started before 72 hours of life. The median (range) age at the start of the study was 26 (6 – 74) hours.

SAMBA study:

Data for this study were collected from May 2013 to October 2015. I recruited 61 preterm infants for this study. Five infants were recruited only and no data were

collected due to problems with the connection between software and cotside monitors or clinical indication to remove the arterial catheter before the beginning of data collection. The remaining 56 infants were recruited within the first 24 hours of age. The median (range) age at the start of the study was 5.3 (3.1 – 12.7) hours. All infants had data collected until 48 hours of age, apart from for four infants, whose studies were discontinued due to clinical deterioration, maternal request or removal of UAC before 48 hours of age. 53 (94.7%) infants were inborn; only three infants included in this cohort were transferred from outside neonatal units.

During the data collection period, a total of 95 preterm infants met inclusion criteria, but were not recruited due to the following reasons:

- NIRS monitors were in use for another study (N = 16)
- Parents did no consent for the study after being approach and given verbal and written information (N = 3)
- Research team was not informed (N = 4)
- Research team was not available to recruit (N = 28)
- It was not ethical to approach parents (N = 4)
- Cotside monitor was incompatible with ICM+ (N = 4)
- Arterial line was removed before 12 hours of life (N = 7)
- Parents were not available to give consent (infants were admitted from other neonatal units) (N = 29)

Table 4.1 shows the distribution of the population recruited for ‘RUMBA’ and ‘SAMBA’ according to the different studies included in each chapter of this dissertation.

Table 4.1 Distribution of the population recruited for 'RUMBA' and 'SAMBA' according to the different studies

	'RUMBA' Phase 1	'RUMBA' Phase 2	'SAMBA'
Chapter 5.1	All infants		
Chapter 5.2			All infants
Chapter 6.1	All infants		
Chapter 6.2			Infants < 28 weeks and data collected < 24 hours of age
Chapter 7		Data collected < 24 hours of age	
Chapter 8			Infants who had echocardiography

The rationale for the infants selected for each study is described in the relevant chapters.

4.2. ETHICS

All study protocols included in this thesis were authorized by the Research and Development department of Cambridge University Hospitals NHS Foundation Trust and approved by The East of England Research Ethics Committee (12/EE/0524 for SAMBA and 09/H0306/20 for RUMBA), in accordance with the declaration of Helsinki. All infants were studied following signed informed parental consent.

4.3. MEASUREMENTS

4.3.1. NIRS and systemic physiological measurements

Following enrolment, a neonatal NIRS sensor from a NIRO 200NX near-infrared spectrophotometer (Hamamatsu Photonics, KK, Japan) was placed on one side of the infant's head in the temporo-parietal area. A sensor holder was used to fix the light source at 3 cm away from the receiver diodes and adhesive paper secured the sensor to the infant's skin. A lightproof cover was also used (Figure 4.1). The sensor was changed to the opposite temporo-parietal side of the infant's head every 6 to 8 hours (when the study duration was above 6 hours) to avoid skin marks. NIRS signals (HbO_2, Hb, TOI and THI) were sampled at the rate of 0.5 Hz.

Figure 4.1 NIRS sensor placement

Example of a NIRS sensor placed on an infant's temporal head and lightproof cover.

The following systemic physiological signals were recorded simultaneously and continuously from the neonatal intensive care monitors (Solar 8000; Carescape B850, GE Healthcare, Milwaukee, Wisconsin):

- Full resolution of arterial blood pressure waveform: sampling frequency of 120Hz (Solar) and 100Hz (Carescape).
- Peripheral oxygen saturation (SaO_2): sampling frequency of 1Hz.
- Heart rate (HR): sampling frequency of 1Hz.

Transcutaneous carbon dioxide (tCO_2) data were collected from TCM400 monitor (Radiometer) at a frequency rate of 1Hz.

Both NIRS and physiological signals were collected, synchronised and stored using ICM+ software® (http://www.neurosurg.cam.ac.uk/icmplus), a Cambridge University enterprise bedside software designed by Dr Smielewski and Prof Czosnyka and used extensively in adult neurocritical care in Cambridge and in nearly 100 neurocritical care units worldwide. The ICM+® program records raw signals from intensive care monitors, ventilators and different cerebral monitors, and calculates time trends of selected brain and systemic parameters. The software allows simple data display in a variety of ways, including time trends and more sophisticated statistical analysis (examples of raw data, trends and more sophisticated data display using ICM+® are shown latter in this chapter and in the following chapters of this dissertation[269].

Figure 4.2 Cotside monitoring and data collection

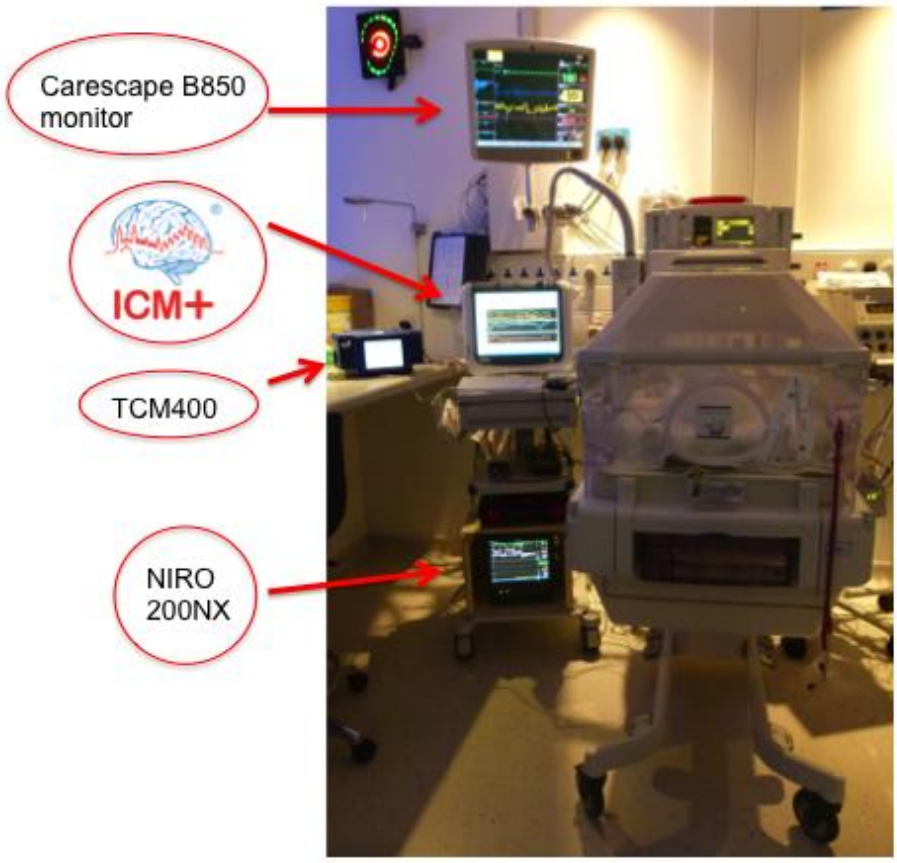

Data from all monitors were collected on ICM+ software®. The same software was used for retrospective analysis.

4.3.2. Clinical data and outcome

Clinical data within the study period and data on outcome were collected from the medical notes. A separate study chart was kept at the cot-side during the study period. This chart was used by nurses and the research team to record the date and time of events, such as handling/care, examination, procedures, changes on drug infusions or any other interventions. Clinical decision-making was at the sole discretion of the attending neonatal consultant.

CRIB II (Clinical Risk Index for Babies II) score of mortality and morbidity was calculated for all infants included in this dissertation[270]. The CRIB II score is a neonatal risk-adjusted score used worldwide. It takes into account gender, gestational age, birth weight, temperature at admission to the neonatal unit and worse base excess

within the first 12 hours of life. The range of possible CRIB II scores is from zero to 27, and lower the score, better is the predicted outcome[270].

Cranial ultrasonography scans were performed at the start of the study and repeated every 12-24 hours until third day of life and then every 1-3 weeks until corrected gestational age at term. GMH-IVH was defined according to Papile et al. (1978) and the greatest grade of haemorrhage during the admission period was used for analysis[14].

Data on mortality were included for all those infants who died before 40 weeks of corrected gestational age. Two infants included in the SAMBA study died after this age cut-off (one died at corrected age of 50 weeks due to complications of chronic lung disease and pulmonary hypertension and the other died at 6 months of age at home due to possible sudden death).

According to the neonatal unit guideline, all preterm infants were screened for sepsis and antibiotics were started within the first hours after birth. Infants were divided in two groups:

- No-sepsis group: included those with no clinical signs of sepsis, normal c-protein reactive (CRP), negative blood culture or antibiotics given only for the first 48 hours of life

- Sepsis group: included those with presumed sepsis (CRP moderately high, negative culture and antibiotics for 5-7 days), clinical sepsis (high CRP, clinically unwell, negative culture and antibiotics for 7-14 days) or confirmed sepsis (clinical sepsis with positive culture)

Confirmed necrotizing enterocolitis (NEC) was defined as either clinical or radiological signs of NEC and treatment for 7-10 days of antibiotics.

4.3.3. Functional echocardiography

Data on cardiac function and ductal patency were collected only from infants recruited for the SAMBA study. Anonymised echocardiographic images were recorded using Vivid S5/Vivid E9 (GE Healthcare) at around 6, 12, 24 and 48 hours

of age. All measurements were done retrospectively using EchoPAC clinical workstation software. In order to avoid inter-observer variability, I was the only investigator who collected the images and retrospectively performed the measurements. A senior neonatologist with cardiology expertise reviewed the images and measurements.

The following measurements were collected:

- PFO: 2D diameter (mm), flow pattern (left-to-right, right-to-left or bidirectional) and flow velocity were obtained from subcostal view[248].

- SVC flow: SVC diameter was measured from the upper parasternal view using M-mode. Measurements were averaged from three to five cycles, as diameter can have a mean variability of 22% throughout the cardiac cycle. Flow was measured from low subcostal view. Velocity time integral (VTI) was calculated and averaged from and 10 cycles. SVC = (VTI x (π x (mean SVC diameter^2/4) x heart rate)/weight[56].

- LVO: Aorta diameter was ascending aorta from the long parasternal view sinotubular junction (STJ). Flow velocity measurement was obtained from modified five chamber view. VTI was calculated and averaged from three to five cycles. LVO = stroke volume (π x (aorta diameter)^2/4 x VTI) x heart rate/weight[146 235].

- RVO: diameter of the main pulmonary artery was measured from the parasternal view and determined in end systole at the insertion of the pulmonary valve leaflet just before the valve closes. Flow velocity was performed on the same window, placing the range gate just beyond the valve leaflets and averaged from three to five cycles. RVO = stroke volume (π x (aorta diameter)^2/4 x VTI) x heart rate/weight[242].

- PDA measurements: diameter was estimated from 2D image and colour Doppler flow (mm), flow pattern (left-to-right, right-to-left or bidirectional), end diastolic flow velocity in the LPA (LPA EDF vel), presence of reversal diastolic flow in the post-ductal aorta at the abdominal level (Ao). Details and references for these measurements were described in Chapter 3, section 3.2).

All measurements were described in more details in Chapter 3, section 3.2.

4.4. DATA ANALYSIS

4.4.1. NIRS data pre-processing

Data collected at the full frequency resolution from the previously described cotside monitors were then retrospectively analysed using ICM+[269].

Figure 4.3 Example of real-time data display at the cotside using ICM+ software

The figure shows real-time data before artefact removal. The artefact circled on the arterial blood pressure signals are the result of arterial line sampling for either calibration or blood sampling. The two artefacts circled on the TOI signal were due to handling or changing the probe position.

Artefacts were identified and manually removed from the raw data (Figure 4.4 and Figure 4.5). Most of the artefacts were the result of umbilical arterial line sampling, infants being handled or movements. Annotations from the nurses regarding cares and handling allowed me to manually exclude periods of data with invalid measurements or with transients induced by external interventions. Artefacts were removed with the 'global artefact removal' function in ICM+ software®, which means for every artefact removed from arterial blood pressure signal the data from all other signals at the same

date and time stamp were removed, and vice-versa. To date there is no universal, validated method for automatic robust removal of data artefacts.

Figure 4.4 Example of a common artefact in the blood pressure raw data

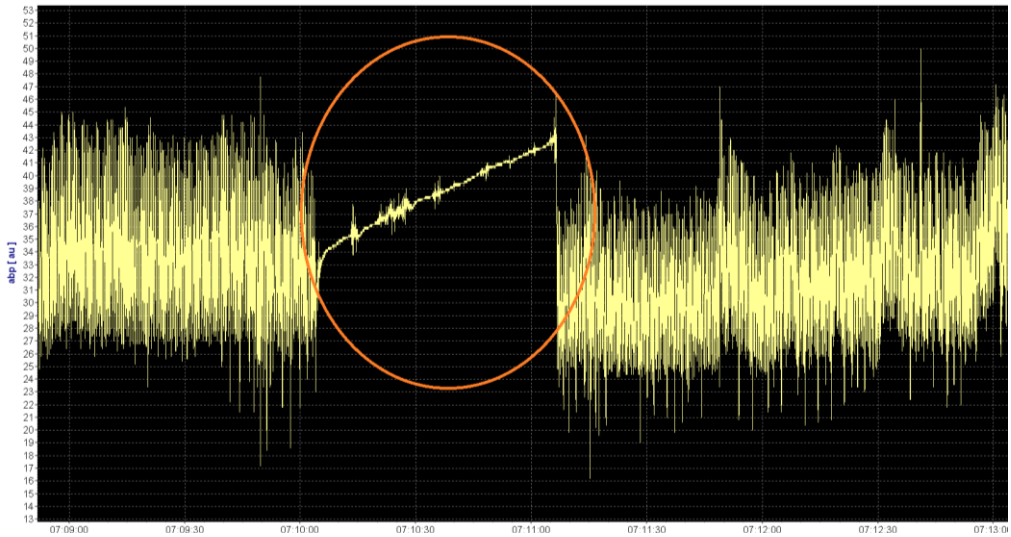

The figure shows the trace for raw arterial blood pressure data. The circled area is an artefact caused by arterial central line sampling.

Figure 4.5 Example of a common artifact in the NIRS raw data

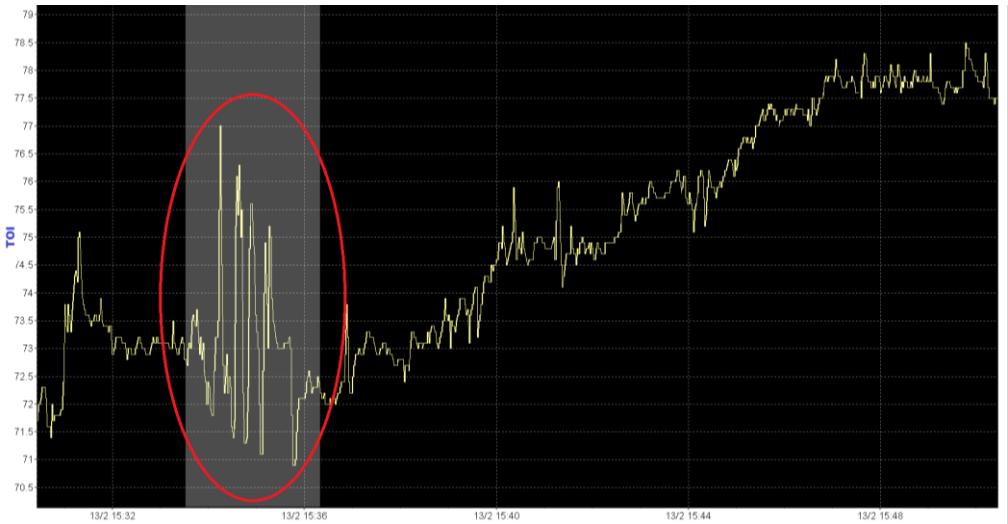

The figure shows the trace for raw TOI data. The circled and shaded area is an artefact potentially caused by handling of infant's head of sensor.

Subsequently all the recorded physiological variables were treated with a moving average filter of 10 seconds length and down-sampled to frequency of 0.1Hz. This effectively removed all the components associated with pulse and respiratory activities while retaining waves in the low and very low frequency range (<0.02Hz), thus focusing further analysis entirely on the cerebrovascular and systemic regulatory responses.

4.4.2. Measurements of cerebrovascular reactivity and cerebral autoregulation

TOHRx was calculated from moving correlation-coefficient analysis, using 5-minute windows between 10-seconds average values of TOI and HR (Figure 4.6). The same method was used to calculate TOx (moving correlation-coefficient analysis between TOI and MABP), as shown in Figure 4.7. The 5-minute window calculation for TOHRx and TOx has its origin in the physiology of "slow brain waves" and inertia of the CBF autoregulation. To supress any "high-frequency" waves that are passed partially through the autoregulation "filter", the measured data are first low-pass filtered and down-sampled to give 1 sample every 10 seconds. This results in 6 samples per minute, therefore the subsequent correlation analysis requires at least several minutes of data to minimize the variance of the calculated index. In contrast, increasing the data buffer size increases the changes of error caused by baseline drifts related to the independent physiological fluctuations (e.g. thermal or metabolic).

Figure 4.6 Correlation coefficient between TOI and HR to calculate TOHRx

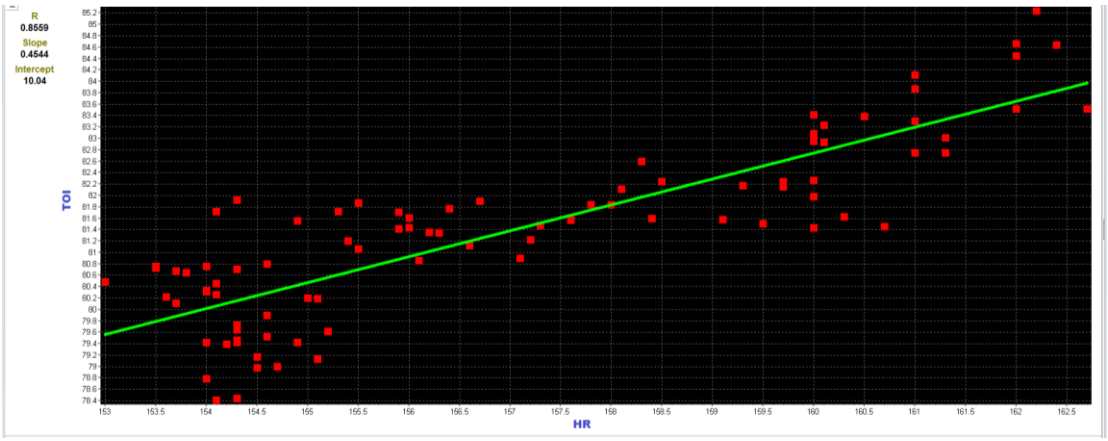

Figure 4.7 Correlation between TOI and MABP to calculate TOx

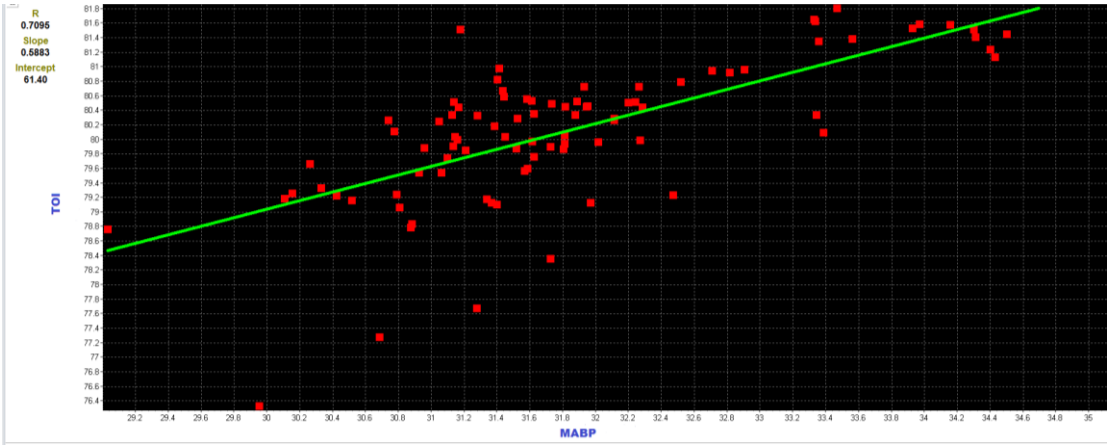

4.4.3. Multiscale entropy analysis (MSE)

We applied MSE to investigate the complexity of NIRS and systematic physiological signals. Details on MSE analysis are described in detail in Chapter 7.

4.5. STATISTICAL ANALYSIS

Statistical analysis was done using SPSS software package version 23 and 25 (SPSS, Inc., Chicago, IL, USA). Data distribution was assessed for normality using Shapiro-Wilk test. Depending on the distribution, either parametric or non-parametric tests were used.

The specific statistical methods used in each study included in this thesis are described in detail in the respective chapters.

A statistical test was considered significant if P value was < 0.05 (two-tailed) for all studies included in this dissertation.

5. MONITORING OF CEREBRAL OXYGENATION AND CEREBROVASCULAR REACTIVITY IN PRETERM INFANTS UNDERGOING INTENSIVE CARE

5.1. CONTINUOUS COTSIDE MONITORING OF BRAIN AND SYSTEMIC PHYSIOLOGICAL SIGNALS: DEMOGRAPHIC DATA AND CASE REVIEWS

5.1.1. Introduction

Major changes in cerebral and systemic circulation occur within the first 12 to 24 hours of life. In preterm infants, the fluctuations in cerebral blood flow and oxygenation are associated with ischaemic and haemorrhagic brain injury, as discussed in Chapter 2. Therefore, monitoring of brain and systemic physiological signals from early hours following birth could provide valuable information on the cerebrovascular reactivity and circulatory function during the transitional circulation in preterm infants, and indicate those who are at an increased risk to develop a poor outcome.

Data collected from cerebral NIRS and systemic signals are susceptible to noise, which are usually due to artefacts. The quality of cerebral and systemic signals should be impeccable in order to be meaningful. Therefore, the use of software that combines simultaneously data collection, data visualisation and data analysis is important. The physiological and NIRS data collected for all studies included in this thesis were recorded and analysed using ICM+ software®. This section of this dissertation will provide an overview of the physiological data collected and specific cases will highlight the value of combining this software to the standard cotside monitoring in the care of preterm infants undergoing intensive care.

5.1.2. Aims

The aim of this section is to describe the general characteristics of the population recruited for both 'RUMBA' and 'SAMBA' cohorts and the incidence of GMH-IVH and mortality in these two cohorts. We further aimed to demonstrate the importance of cotside monitoring by describing four cases from the 'SAMBA' population.

5.1.3. Methods

All preterm infants who were recruited for 'RUMBA' and 'SAMBA' cohorts and had demographic and NIRS data collected were included in the data presentation and analysis (as described in Chapter 4, section 4.1.1, five infants were recruited for 'SAMBA' but data was not collected). The recruitment details, ethics, population and pre-processing data analysis, including the methodology to calculate TOx and TOHRx, were described in Chapter 4.

5.1.4. Results

Table 5.1 shows the characteristics of the 116 infants recruited in the 'RUMBA' and 'SAMBA' cohorts. Table 5.3 shows the frequency of intraventricular haemorrhage (IVH) grades of all infants.

Table 5.1 General characteristics of the all infants recruited for 'RUMBA' and 'SAMBA'

Variables	Total (N = 116)
Gestational age	26+0 (23+2 – 32 +1)
Birth weight	795 (445 – 1440)
Male/Female	55/61
CRIB II	11 (4 – 17)
GMH-IVH	44 (38%)
Mortality	20 (17.2%)

Gestational age, birth weight and CRIB II (Clinical Risk Index for Babies II) values are presented as median (range). Remaining variables are presented as frequency.

More detailed demographic data were collected for the 'SAMBA' cohort. Table 5.3 shows the antenatal and postnatal characteristics and complications for infants recruited for 'SAMBA'.

Table 5.2 Antenatal and postnatal data from 'SAMBA' cohort

Variables	Total (N = 56)
PPROM	23 (41%)
Antenatal Steroids	55 (98.2%)
$MgSO_4$	15 (26.8%)
SVD/C-section	32/24
Male/Female	21/35
Inborn	52 (92.8%)
Total doses of Surfactant	2 (1-4)
Apgar 5 min	7 (1-9)
Caffeine	51 (91%)
Morphine	24 (42.9%)
Ventilated at start of study	100%
Extubated during the study	27 (48.2%)
PPHN on NO	4 (7.1%)
Early onset of sepsis	36 (62.2%)
Confirmed NEC	7 (12.5%)

PPROM is for premature prolonged rupture of membranes. SVD is for spontaneous vaginal delivery. C-section is for caesarean section. Inborn is for infants delivered at The Rosie Maternity. PPHN is for persistent pulmonary hypertension of the newborn. NO is for nitric oxide. NEC is for necrotizing enterocolitis (confirmed NEC was defined as either clinical or radiological signs of NEC and treated for 7-10 days of antibiotics). Data on 'Total doses of Surfactant' and 'Apgar at 5 min' are shown as median and range. The remaining data are shown as frequency.

Twelve mothers received an incomplete course of antenatal steroids (one dose) and 43 received complete course (two doses). Twelve infants had suspected NEC (defined as clinical signs of suspected NEC but no abnormalities found on the abdominal x-ray and antibiotics given for ≤ 5 days).

Table 5.3 Degrees of IVH for infants recruited for 'RUMBA' and 'SAMBA'

IVH Grades	Total (N = 116)
No-IVH	72 (62.1%)
Grade I (GMH)	9 (7.8%)
Grade II	20 (17.2%)
Grade III	8 (6.9%)
Grade IV	7 (6%)

GMH is for germinal matrix haemorrhage

Only one infant developed PVL. This infant was included in the 'SAMBA' cohort and the case is described in the 'Case Reviews' section (Case 2).

Infants recruited for 'SAMBA' cohort had cranial ultrasound performed regularly at the start of the study and repeated every 12 to 24 hours. Eighteen infants included in the 'SAMBA' cohort developed an IVH. In 13 of them, the IVH was diagnosed after 24 hours of life. In the other five infants the IVH was diagnosed at the ultrasound scan done at 12 or 24 hours of life (two of these 5 infants had an IVH diagnosed at the start of the study).

As most infants in the 'SAMBA' cohort had an IVH diagnosed at around or after the first 24 hours of life, three studies included in this thesis focused on the data collected from only in the first 24 hours of life. The rationale was that understanding the pathophysiology behind the development of a GMH-IVH before the haemorrhage occurred could potentially identify those infants who are at a greater risk of developing the brain injury.

Table 5.4 shows the age and cause of death for all infants included in the 'RUMBA' and 'SAMBA' cohorts. None of the studied infants included in both cohorts died within the data collection period. Only 8 infants who died had developed IVH, and the presence of IVH was not statistically associated with death (P = 1.0). Infants died due to a variety of complications such as necrotising enterocolitis (NEC), sepsis or multi-organ failure. Although brain injury visible on cranial ultrasound scan was not directly the cause of death for these infants, most of them had a degree of perinatal ischaemia or early postnatal cerebral or systemic hypoperfusion.

Table 5.4 Age and cause of death for infants recruited for RUMBA and SAMBA

Infant	Cohort	GA at Birth	GA at Death	Cause of Death
01	RUMBA	24+1	26+6	Pulmonary haemorrhage and clinical deterioration
02	RUMBA	24+2	37+1	Fulminant NEC
03	RUMBA	28+2	30+1	*Staphylococcus Aureus* sepsis and Pulmonary haemorrhage
04	RUMBA	25+5	26+5	Clinical deterioration, multi-organ failure
05	RUMBA	27+1	30+0	Fulminant NEC
06	RUMBA	26+2	31+3	Fulminant NEC
07	RUMBA	26+6	28+2	Pulmonary hypoplasia, PPNH
08	RUMBA	26+2	29+0	Severe renal failure
09	RUMBA	24+0	34+6	Fulminant NEC
10	RUMBA	27+0	30+4	Multi-organ failure
11	RUMBA	24+1	36+0	CMV infection
12	RUMBA	25+5	28+4	Severely ill from birth – IVH grade IV, pulmonary haemorrhage, NEC
13	RUMBA	28+0	28+2	Pulmonary hypoplasia, severe hypotension
14	SAMBA	26+2	28+3	Twin-twin transfusion, severe antenatal brain and heart hypoxia, multi-organ failure
15	SAMBA	24+4	25+2	Severe antenatal hypoxia, IVH and multi-organ failure
16	SAMBA	30+2	37+2	Fulminant NEC
17	SAMBA	26+3	31+2	*Pseudomonas aeruginosa* sepsis and meningitis – severely sick from birth, IVH grade IV
18	SAMBA	24+1	25+5	Fulminant NEC
19	SAMBA	24+2	28+4	PPROM, cord prolapse, fungal infection
20	SAMBA	23+5	24+0	Clinical deterioration, immature lungs and grade III IVH

GA is for gestational age. NEC is for necrotising enterocolitis. CMV is for cytomegalovirus. PPROM is for premature prolonged rupture of membranes. The infant numbers are not related with study identification.

5.1.5. Case Reviews

The following cases demonstrate the cotside motoring of a stable infant, an infant who developed PVL and an infant with severe hypoxic-ischaemic injury. In Chapter 6, section 6.2, the case of an infant who developed an IVH is discussed.

1) Stable infant

The Figures 5.1 and 5.2 show examples of continuous NIRS and physiological signals monitoring from a male preterm infant who was born at 25+5 weeks of gestational age, weighing 720 grams. He was born by emergency C-section due to cord presentation. Apgar score was 1 at 1 minute and 6 at 5 minutes of life. There was an antenatal history of maternal vaginal bleeding at 23 weeks, premature prolonged rupture of membranes (PPROM) for 40 hours prior to delivery and maternal pyrexia. A full course of antenatal steroids (betamethasone) was given 13 days before delivery. He was a breech presentation and was intubated and received one dose of surfactant at 10 minutes of age. CRIB II score was 13. He remained stable during the study period and did not require inotropes, saline boluses or blood products. Sepsis was suspected due to prematurity but his blood culture and infection markers were unremarkable. He was extubated at 13 hours of age and remained on continuous positive airway pressure (CPAP). He did not develop an IVH. He did not develop NEC and was discharged home at corrected age of 37 weeks, self-ventilated in air and on full bottle-feeding.

Figure 5.1 NIRS and physiological signals in a stable infant (TOx)

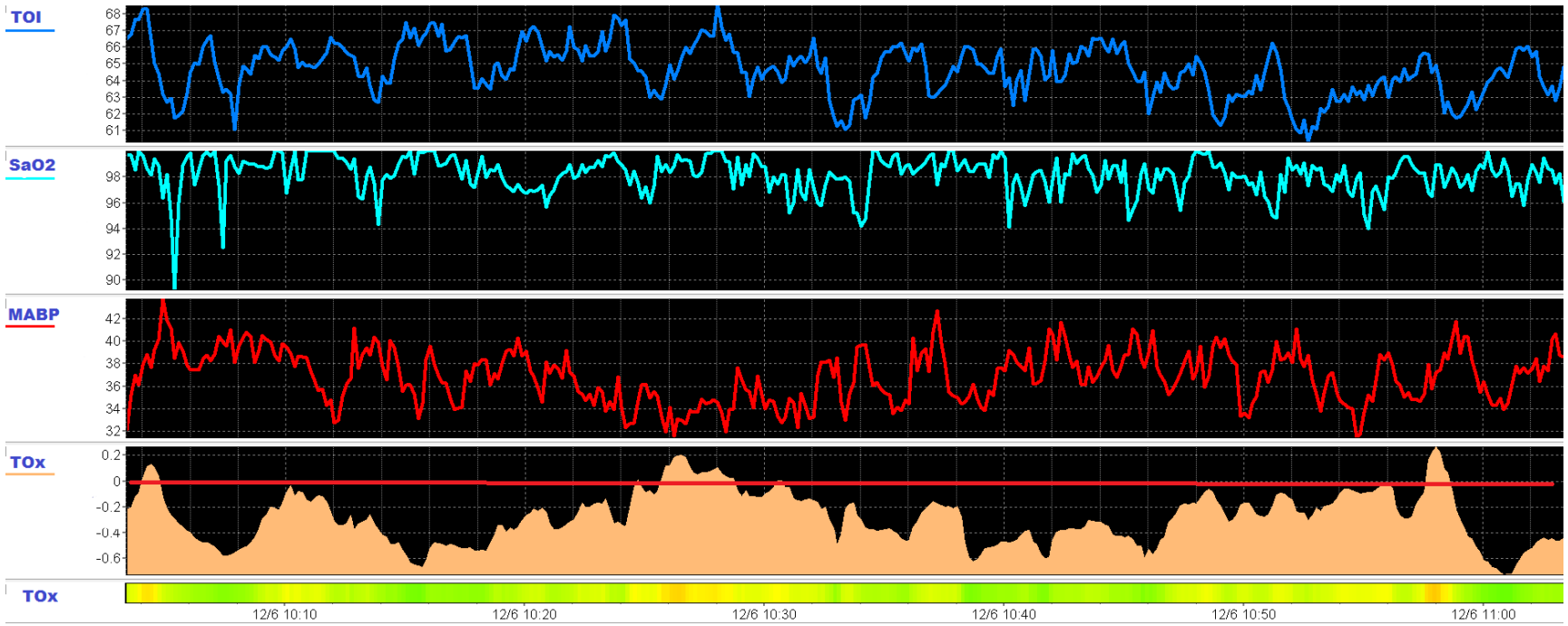

The figure shows graphs of continuous monitoring of TOI, MABP, SaO_2 and TOx signals for 1-hour-window interval. The infant's age at this 1-hour-window was between 39 and 40 hours of life. The bottom chart is a 'risk chart': colours changed from green (more negative TOx or more intact cerebral autoregulation) to red (more positive TOx or more impaired cerebral autoregulation). TOx is mainly negative for this window interval and remained mainly negative throughout the study. Mean TOI, SaO_2, MABP and TOx for this 1hour-window interval was 64, 98%, 37 mmHg and -0.28, respectively.

Figure 5.2 NIRS and physiological signals in stable infant (TOHRx)

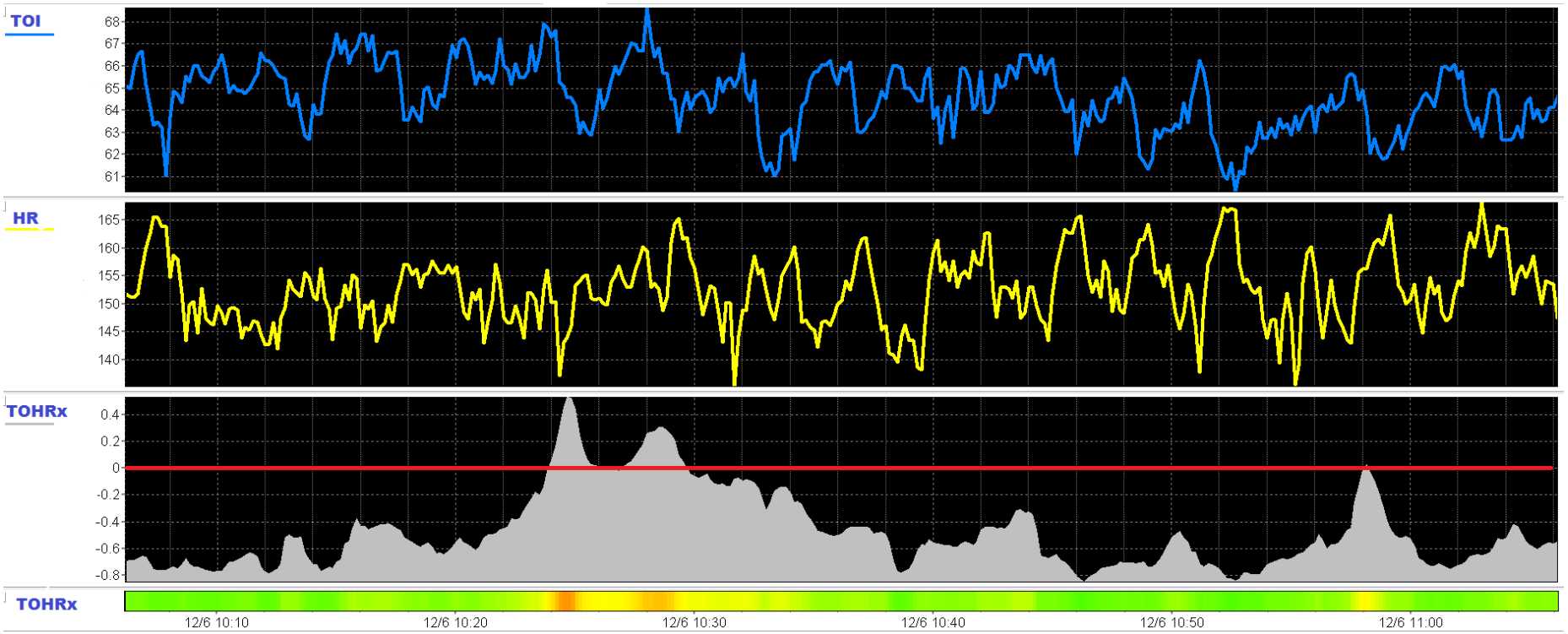

The figure above shows the graphs of continuous monitoring of TOI, HR and TOHRx for the same 1-h-window interval shown in Figure 5.1. TOHRx is also mainly negative (more green areas on the bottom 'risk chart') for this 1-h-window interval and remained mainly negative throughout the study. Mean HR and TOHRx for this window interval was 152 bpm and -0.46, respectively.

2) Infant who developed PVL

The Figures 5.3, 5.4 and 5.5 show NIRS and physiological data from a 3-hour-window interval from an infant who had normal cranial ultrasound images within the first week of life, which only showed some mild degree of periventricular flare, but developed PVL, which was diagnosed on day 15 of life (Figure 5.7).

This female preterm infant was born at 28+2 weeks of gestational age, with a birth weight of 1115 grams and delivered by spontaneous vaginal delivery. Her Apgar score was 6 at 1 minute and 8 at 5 minutes of life. There was an antenatal history of maternal pyrexia and no intra-partum antibiotics were given. Her mother received full course of antenatal steroids (betamethasone), but no $MgSO_4$ was given. She was intubated at birth and received one dose of surfactant. Her CRIB II score was 8. She was extubated at 10 hours of age and remained on CPAP throughout the rest of the study period. She did not require boluses of saline, blood products or inotropic support during the first 48 hours of life. She was noted to be agitated and had several episodes of high-pitched crying and irritability during the study period, which was observed by the research and clinical team.

She was between 25 and 28 hours of age in the 3-hour-window interval shown in Figure 5.3 and 5.5. She was on CPAP and her arterial blood gas showed $PaCO_2$ between 3.9 kPa and 4.6 kPa for this window interval. The fluctuations in the MABP signal were only observed because the data was displayed on ICM+® on 1-4 hour-window intervals. Observations only from the usual neonatal monitors would not show this interesting pattern.

Figure 5.4 shows 45-minute-window interval extracted from the 3-hour-window data shown in Figure 5.3, demonstrating the degree of pressure passive circulation. We can observe that changes in TOI follow changes in MABP with no influence from SaO_2. Figure 5.6 shows the raw arterial blood pressure signal (ABP). We can notice the same sinusoid pattern observed in the figures 5.3, 5.4 and 5.5.

Figure 5.3 NIRS and physiological signals for an infant who developed PVL (TOx)

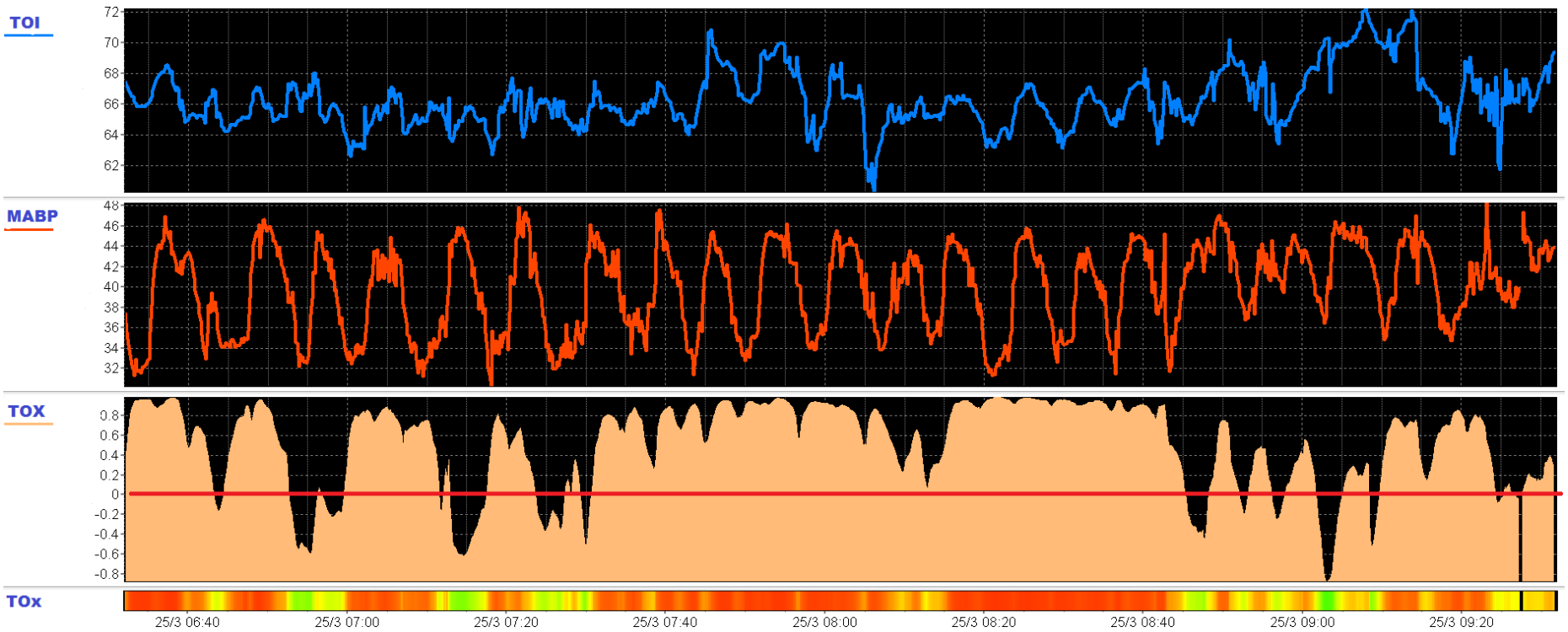

The figure above shows the graphs of continuous data for TOI, MABP and TOx. The bottom figure is a 'risk chart': colours changed from green (more negative TOx or more intact cerebral autoregulation) to red (more positive TOx or more impaired cerebral autoregulation). Observe the variability in the MABP signal and the amount of time that cerebral autoregulation was impaired (predominantly red areas on the 'risk chart'). Mean TOx for this 3h-window was +0.51, mean MABP was 40 mmHg and mean TOI was 67.

Figure 5.4 Pressure passive pattern in an infant who developed PVL

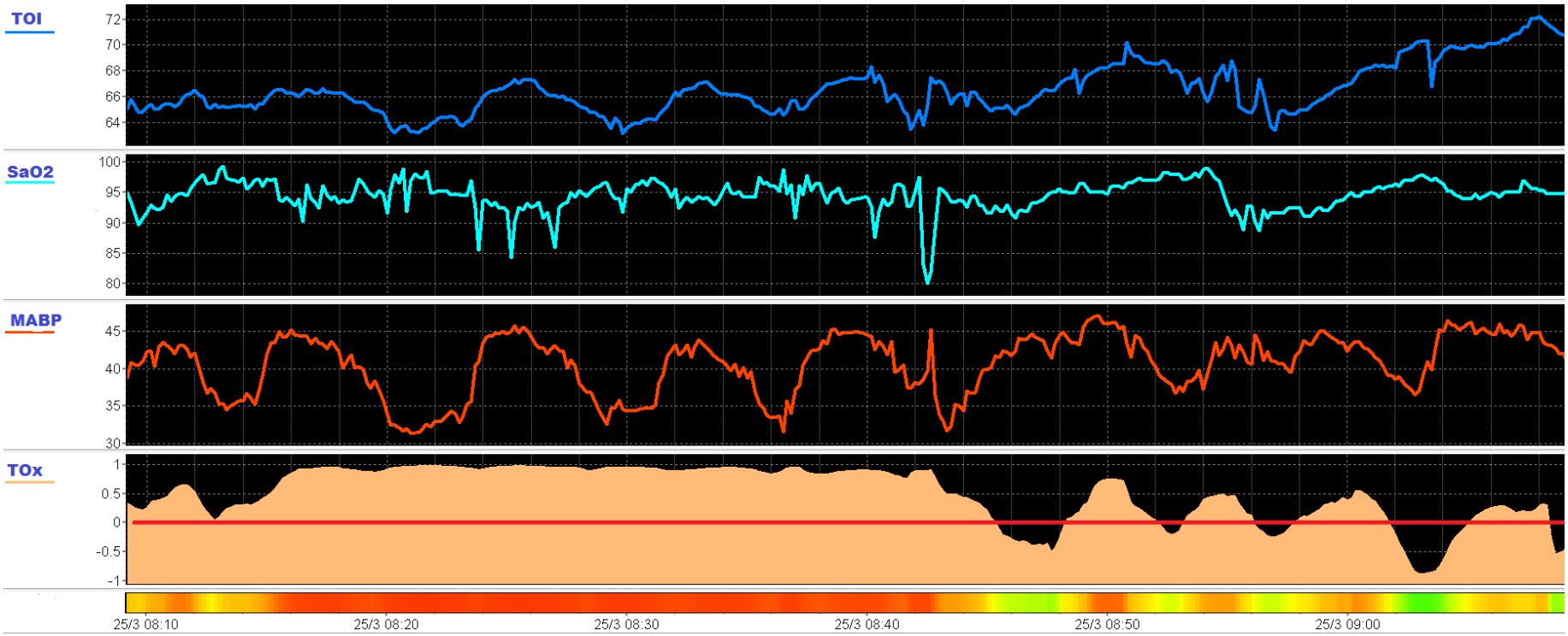

The figure above shows a 45-minute-window extracted from the previous 3h-window shown in Figure 5.3. We can observe that changes in TOI follow mainly the changes in MABP and not frequently the changes in SaO_2. The degree of pressure-passive circulation can be observed from the TOx graph and from the 'risk chart' (prolonged period of red area or more positive TOx).

Figure 5.5 NIRS and physiological signals for an infant who developed PVL (TOHRx)

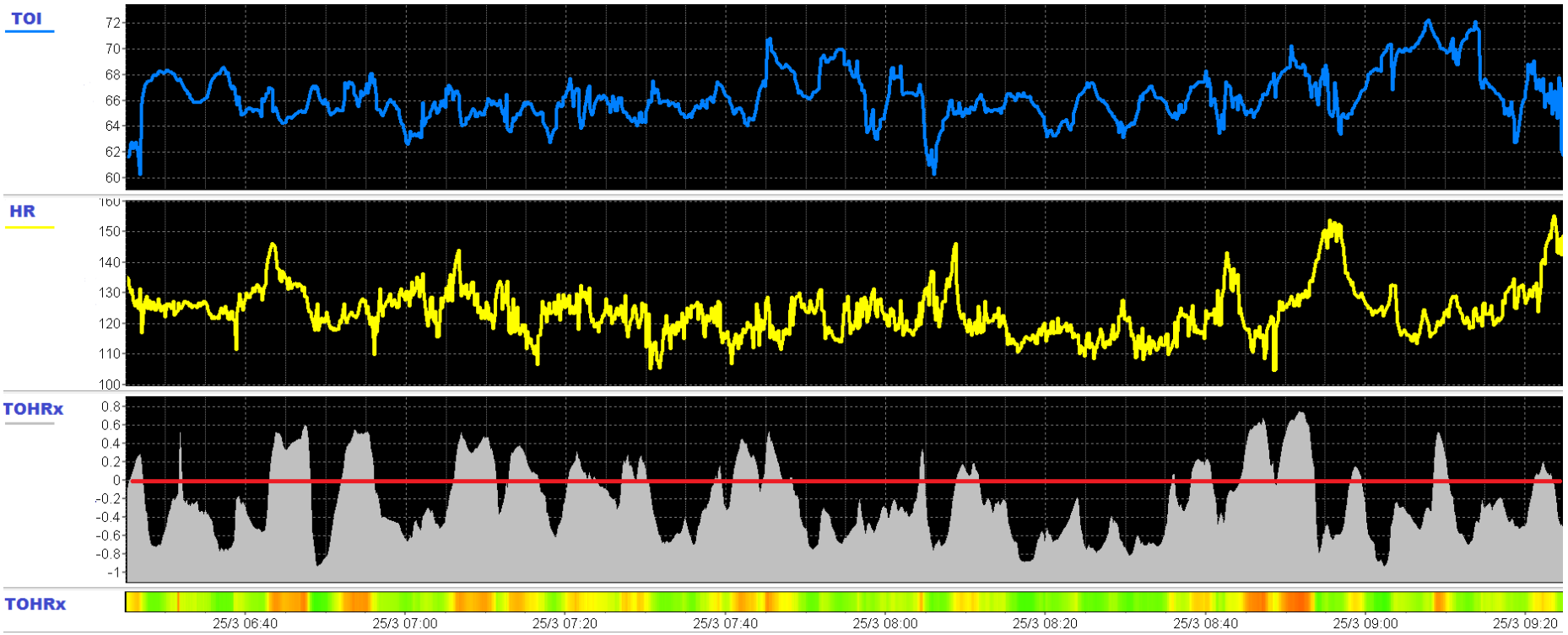

The figure above shows the graphs for continuous data of TOI, HR and TOHRx for the same 3-h-window interval shown in Figure 5.3. The 'risk chart' on the bottom shows predominant areas of more intact cerebrovascular reactivity (yellow to green TOHRx). Mean TOHRx value for this 3-h-window interval was -0.12.

Figure 5.6 Raw arterial blood pressure (ABP) data

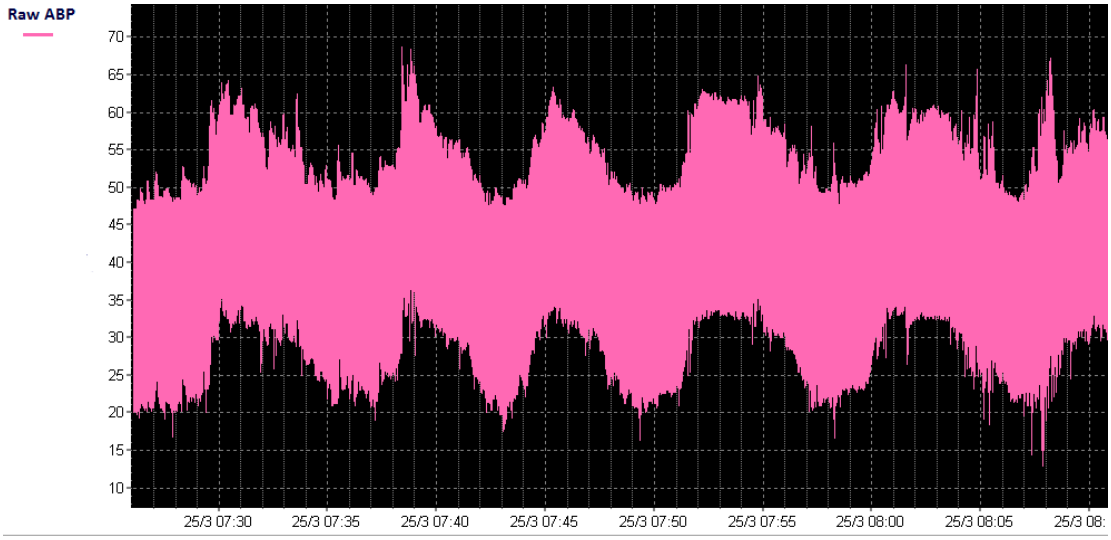

The figure above shows an interval of 45 minutes of raw arterial blood pressure (ABP) data within the same 3-h-window shown in Figure 5.3.

Figure 5.7 Cranial Ultrasound images

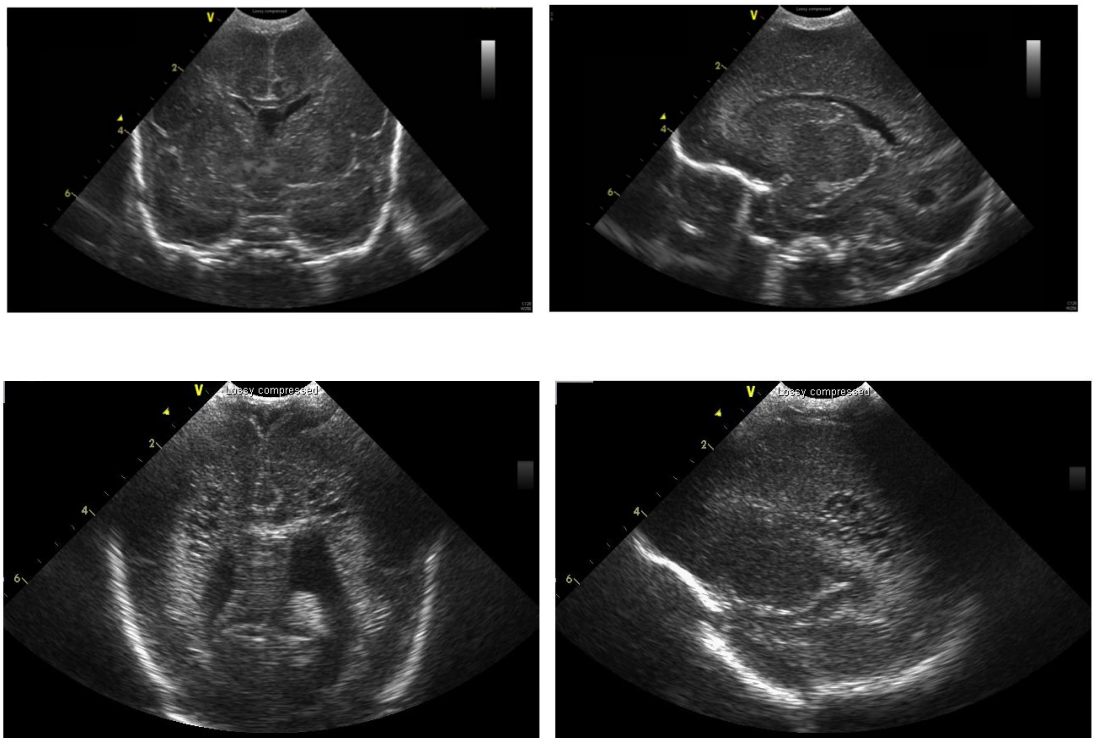

The top two images are the coronal and sagittal views of the normal cranial ultrasound at 24 hours of age. The bottom two images are the sagittal and coronal views at day 15 of life, showing bilateral cystic PVL. *I performed the cranial ultrasound scans and recorded the images above as part of the data collection for this thesis.*

3) Infant with signs of severe hypoxic ischaemic injury from birth

The examples below show two figures of 1-hour-window each of continuous NIRS and physiological data from an infant who had normal cranial ultrasound images during the first 48 hours of life, but developed a grade II IVH on day three and died on day four of life.

This female preterm infant was born at 24+4 weeks of gestational age with a birth weight of 775 grams and was delivered by spontaneous vaginal delivery. Her Apgar score was 1 at 1 minute and 2 at 5 minutes of life. Her mother received only one dose of antenatal glucocorticoid (betamethasone) four hours before delivery and no $MgSO_4$ was given (the infant was recruited before the standard protocol for antenatal $MgSO_4$ was placed into practice). She was born in poor condition, requiring intubation and resuscitation with chest compressions. She received only one dose of surfactant, which was given after intubation in the delivery unit. She remained ventilated throughout admission. Her CRIB II score was 16. She had persistent metabolic acidosis within the first 6 hours of life and received multiple infusions of sodium bicarbonate to correct her base deficit. Dopamine and dobutamine were started within the first 24 hours of life. An echocardiogram showed poor myocardium contractility. The presence of a bulging anterior fontanelle was described during the first 24 to 48 hours of life.

She was between 22 and 23 hours of age in the 1-hour-window interval shown in the figures 5.8 and 5.9. We can observe that cerebral autoregulation and cerebrovascular reactivity were mostly impaired within the period shown in this interval (both ‘risk charts’ had mainly orange to red colours). This pattern was persistent over the entire study period.

Figure 5.8: NIRS and physiological signals for an infant with signs of hypoxic ischemic encephalopathy (TOx)

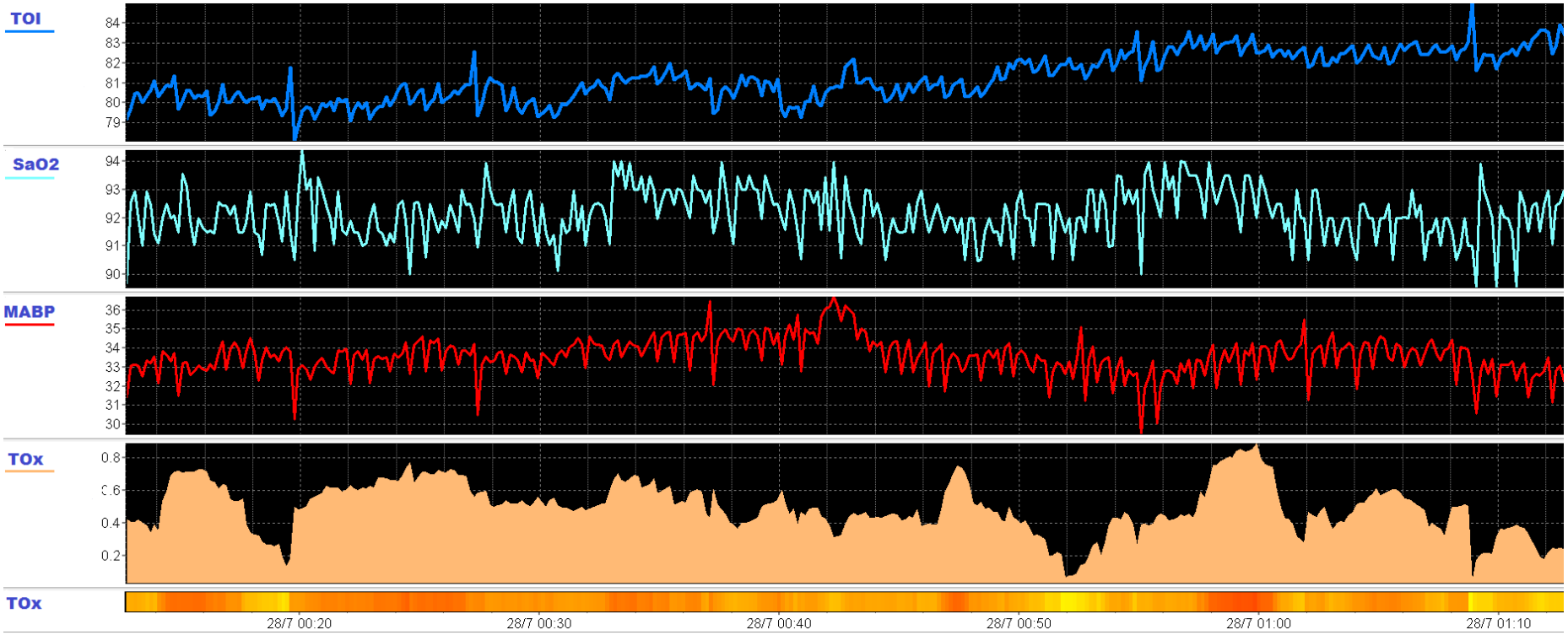

The figure above shows the graphs of continuous data of TOI, SaO_2 MABP and TOx. The bottom 'risk chart' shows predominantly severe impaired cerebral autoregulation. Values for TOx were positive for this entire period. Mean TOx for this 1h-window was +0.50, mean MABP was 33 mmHg, SaO_2 was 92% and mean TOI was 81. High values of TOI may reflect the hypoxic ischaemic injury.

Figure 5.9: NIRS and physiological signals for an infant with signs of hypoxic ischemic encephalopathy (TOHRx)

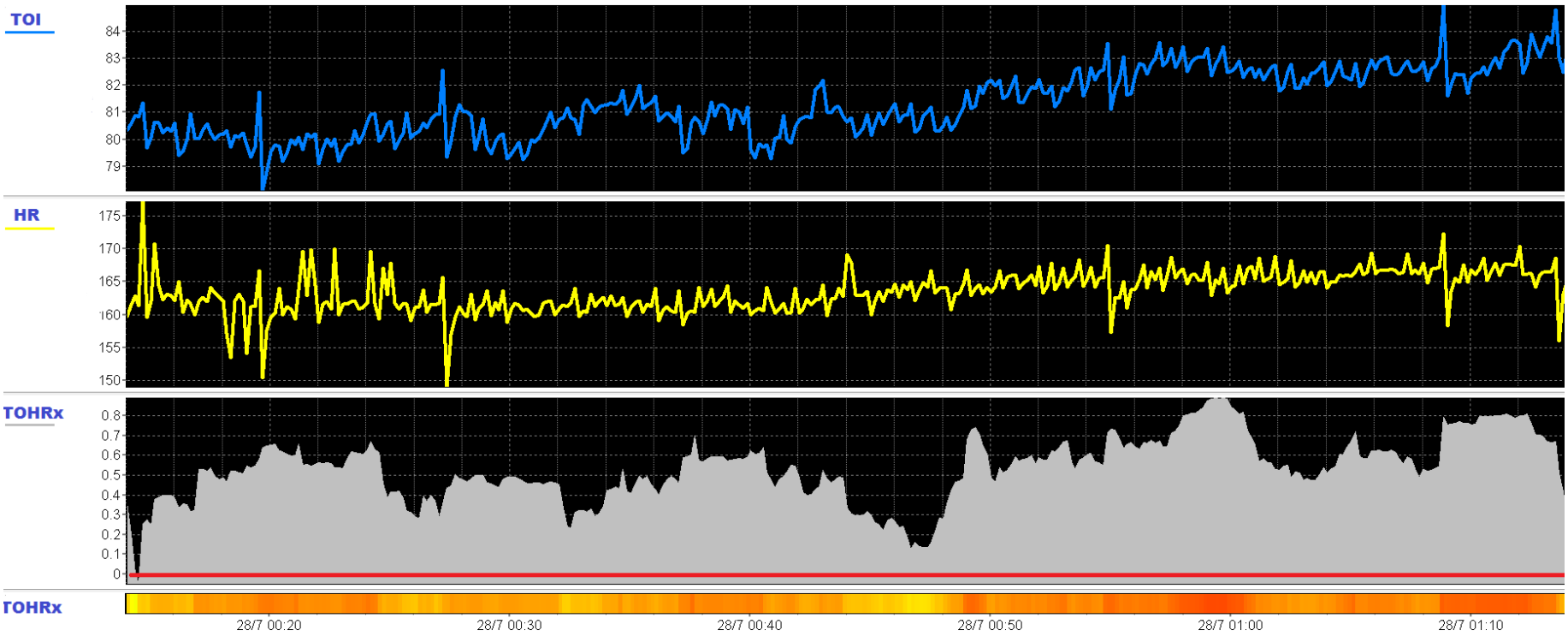

The figure above shows the graph of continuous data of TOI, HR, TOHRx for the same 1h-window shown in Figure 5.8. The bottom 'risk chart' also shows predominantly impaired cerebrovascular reactivity. TOHRx was also mainly positive for the entire period. Mean TOHRx for this 1-h-window was +0.52 and mean HR was 163 bpm.

5.1.6. Discussion

Recruitment challenges and the impact on outcome data

The recruitment of preterm infants soon after birth is challenging. Getting consent from parents when they are emotionally fragile requires the sensitivity to understand when it is not ethical to approach them regarding research studies. In addition, sick preterm infants require a huge amount of work and concentration from the clinical team. Therefore the addition of extra tools to the standard neonatal care, such as NIRS monitors and computers for data collection, may not be well accepted by the medical and nursing team. The recruitment criteria and study design for the 'RUMBA' study allowed our research team to recruit infants and at any time within the first 72 hours of life and collect data for short periods of time initially. This allowed me to introduce the idea of studying infants from early hours of life and using extra monitors as a positive concept. The 'RUMBA' study was well accepted in the neonatal unit in Cambridge. Nurses and doctors became familiarised with the NIRS monitor and ICM+® software, allowing me to expand the duration of data collection for the 'SAMBA' study.

Most infants recruited for both 'RUMBA' and 'SAMBA' studies were inborn infants. In the 'SAMBA' cohort only three infants were born in other smaller neonatal units and transferred to the tertiary unit in Cambridge before 12 hours of life. This may have had an impact on our results, as inborn infants tend to have less morbidities and better outcome. Centralising care in specialist centres and in-utero transfer of preterm infants born between 23 to 26 weeks' gestational age to tertiary hospitals have been associated with reduced mortality, lower rates of GMH-IVH and less morbidity for those who survive[271, 272].

The use of antenatal medications, such as glucocorticoids and $MgSO_4$ has also contributed to reduce the incidence of brain injury and improve neurodevelopmental outcome[273-276]. In the fetus, endogenous levels of glucocorticoids increase late in gestation to enable organ maturation, fetal growth and survival after birth. Preterm infants may not be adequately exposed to endogenous glucocorticoids, predisposing them to develop IVH, respiratory distress syndrome (RDS) or necrotizing

enterocolitis NEC[277, 278]. Nearly 100% of the infants recruited for 'SAMBA' received at least one dose of antenatal glucocorticoids. Since 1995 the use of antenatal glucocorticoids has been recommended for the prevention of RDS, GMH-IVH and neonatal death[279, 280]. A Cochrane review published in 2006, which included 13 studies with a total of 2872 infants born at less than 36 weeks, showed a significant decrease in perinatal mortality, morbidity and incidence of GMH-IVH and PVL. Since then, the administration of synthetic glucocorticoids to women who are likely to deliver preterm infants below 34 weeks has become a common practice in developed countries[273, 274].

The two most common synthetic glucocorticoids used in pregnancy are betamethasone and dexamethasone. They are 25 times more potent than cortisol and freely able to cross the placenta and enter the fetal circulation[281]. Because they are usually administered before the natural endogenous cortisol surge, they trigger the glucocorticoid signalling in the developing brain. This may prevent the negative consequences of preterm birth but may potentially increase the risk of metabolic, cardiovascular and neuropsychiatric disorders in adult life[277, 278]. Infants included in the 'SAMBA' cohort most likely received betamethasone as most of them were inborn and the protocol of preterm labour at The Rosie hospital has included the use of betamethasone for several years. Betamethasone has been associated with decreased mortality, reduced risk of periventricular leukomalacia and less side effects compared to dexamethasone; therefore betamethasone is currently the preferred choice of synthetic glucocorticoids in several maternity hospitals[281-284]. However, it is difficult to precise how many infants included in this dissertation have received betamethasone or dexamethasone, as protocols were not the same in the different hospitals and infants may have received antenatal glucocorticoids in their local units before being in-utero or ex-utero transferred to Cambridge.

The exact mechanism of glucocorticoids in neuroprotection remains elusive, but data from animal studies have suggested that antenatal glucocorticoid suppresses the vascular endothelial growth factor (VEGF) and angiogenesis, contributing to the stabilization of the germinal matrix vasculature and, hence, reducing its propensity to haemorrhage[285]. The use of antenatal betamethasone has been associated with an increase by 1.5 fold to 2 fold in the fibronectine expression, which may provide

vascular stability and a reduction in the risk of GMH-IVH. In the near term fetal sheep, antenatal glucocorticoids have been associated with a decrease in cerebral blood flow, increase in arterial blood pressure and peripheral vascular resistance[286-288].

Half way through the data collection for the 'SAMBA' study, the antenatal guideline on the use of $MgSO_4$ was implemented, and since then a high percentage of the infants recruited for the study received the medication. $MgSO_4$ has been widely used in Obstetrics for treatment of preeclampsia and tocolysis, but successive studies have shown that secondary outcomes of mothers given $MgSO_4$ improved neurological outcomes in their infants. In moderate to severe eclampsia, $MgSO_4$ has been effective in reducing the risk of maternal seizures[289, 290] In 2009, a Cochrane review found a reduction in cerebral palsy and gross motor dysfunction with no increase in risk of paediatric mortality[275, 276]. Although data from meta-analyses and some randomised trials are compelling, unlike glucocorticoids, the use of $MgSO_4$ is not universal for a number of reasons. Information on therapeutic dose of $MgSO_4$ for neuroprotection and data on fetal toxicity remain scarce. Moreover, major randomized control trials have used different doses, timing and different gestational ages at randomization. Currently, the international consensus is to use of $MgSO_4$ for neuroprotection prior delivery at less than 30 weeks[291, 292].

The exact mechanism of $MgSO_4$ in neuroprotection in preterm infants is unknown, but animal data have suggested that $MgSO_4$ may reverse the effects of hypoxic/ischaemic injury by blocking N-methyl-D-aspartic acid (NMDA) receptors in oligodendrocytes and acting as a calcium antagonist (reducing the calcium influx into the cells)[293, 294]. Extremely preterm infants have an increased risk to develop hypoxic-ischaemic injury and associated complications, such as neonatal seizures, compared to term infants[295]. Bennet et al. (2018) have recently demonstrated that the duration, burden and amplitude of seizures was significantly reduced in preterm fetal sheep who received $MgSO_4$ after an acute in utero asphyxial insult, with greater impact in male compared to female fetuses[296]. $MgSO_4$ may also be implicated in improving vascular instability, reducing inflammation, acting against free radical activity, stabilizing the neuronal cell membrane and having anti-apoptotic actions[294, 297-299].

Galinsky et al. (2016) have demonstrated that $MgSO_4$ may increase flow in the peripheral vasculature in fetal sheep during acute hypoxic-ischaemic insults[300].

The use of antenatal glucocorticosteroids and, potentially, the use of $MgSO_4$ may improve the clinical condition of infants following preterm delivery. Currently in neonatal practice most preterm infants whose mothers received a full course of antenatal glucocorticosteroids, are usually born in good condition and do not require mechanical ventilation and invasive monitoring of MABP. However, for both 'RUMBA' and 'SAMBA' studies, the presence of an indwelling arterial catheter to continuously monitor MABP was an inclusion criterion. This may have had an impact on the characteristics of the population included in all studies in this dissertation, the current guideline in the neonatal unit at The Rosie Maternity recommends the insertion of umbilical arterial lines only in preterm infants who either require mechanical ventilation at birth or are started on CPAP but are small and fragile. Therefore, the population recruited for our studies could have been, potentially, sicker compared to other studies published on assessment of cerebrovascular reactivate and cerebral oxygenation in infants, although most infants were inborn and had received antenatal steroids.

The percentage of severe IVH (grade III and IV) for both 'RUMBA' and 'SAMBA' cohort was similar to studies using larger database, although the recruitment for our studies included mainly inborn infants and those who had indwelling arterial line in situ[20]. The age and cause of death for all infants included in the 'RUMBA' and 'SAMBA' studies were described in Table 5.4. The discussions about mortality in the following chapters will refer back to the results presented in this table.

Monitoring cerebral and systemic signals at the cotside

'RUMBA' and 'SAMBA' were prospective observational studies. One of the real challenges of observational data on preterm infants is the heterogeneity of the studied population and complexity of the physiological data. Interesting information and insights about the physiology of these infants can be lost by grouping them together for data analysis. Outliers are usually present and may affect the statistical analysis,

but at the same time they may contain interesting information (more details about outliers are discussed in section 5.2). A wealth of information can be obtained from the large amount of data collected from a unique individual and some observations described in the case reviews demonstrated the importance and the beauty of 'individualised medicine'. ICM+® software allows data collection and real-time analysis at the cotside, which could add information on the clinical management of the patients, as the current intensive care monitors have limited options to visualize data, especially retrospective values and trends. During data collection and retrospective analysis, trends could be identified, artefacts were cleaned and events, such as increase or decrease of inotropes and vasopressors, handling and procedures, were highlighted. This allowed the data analysis to be more meaningful for each individual patient and a decrease in bias and confounders caused by artefacts and drug administration.

The cases described in this section demonstrate the value of having cotside software that allows clinicians to visualize the changes in the pattern of cerebral and systemic signals and the real-time analysis of indices of cerebrovascular reactivity. The pattern of changes in the MABP signal shown in 'Case 2' could be easily missed with standard monitoring. The loss is cerebral autoregulation was clearly observed as changes in MABP correlated with changes in TOI. The 'risk charts' also provide clear information regarding periods of intact and impaired cerebrovascular reactivity.

'Case 2' showed that whilst impaired cerebral autoregulation was predominant, as demonstrated by predominant positive correlation between MABP and TOI (positive TOx), the correlation between HR and TOI was mainly intact (negative TOHRx). Although TOHRx has been suggested as an index of cerebrovascular reactivity based on the principle that cardiac output is mainly regulated by changes in HR, the inverse correlation between MABP and HR with TOI observed for that infant during that 3-h-window of data shown in the Figures 5.3 and 5.5 may suggest that TOHRx could potentially be influenced by baroreflex sensitive[141]. However, studies on baroreflex sensitive in preterm infants are complex and difficult to be designed, as the HR component of baroreflex in preterm infant is immature and maturates with gestational age and postnatal age[301-304]. Studies on the correlation between autonomic nervous

system and cerebrovascular control may require a large cohort of preterm infants; therefore it is not in the scope of this dissertation.

5.2. CEREBRAL AUTOREGULATION, CEREBROVASCULAR REACTIVITY AND CEREBRAL OXYGENATION IN PRETERM INFANTS DURING EARLY TRANSITIONAL CIRCULATION

5.2.1. Background

Decreased cerebral oxygenation and impaired cerebrovascular reactivity within the first days of life have been associated with poor outcome in preterm infants, as described in Chapter 2. In addition, the degree of pressure passivity increases with decreasing gestational age, making extremely preterm infants more susceptible to the fluctuations in cerebral blood flow [40, 305].

Measurements of cerebrovascular reactivity and cerebral autoregulation in preterm infants using NIRS have been mainly described using the frequency domain method. More recently studies have suggested that time-domain analysis could be a more robust method to describe cerebral autoregulation[306]. However, indices of cerebral autoregulation and cerebrovascular reactivity derived from time-domain analysis have failed to show a strong association with outcome[137, 141].

5.2.2. Aims

The aim of this study was to describe the measurements of cerebral oxygenation (TOI), cerebral autoregulation (TOx) and cerebral vascular reactivity (TOHRx) within the first 48 hours of life and their relationship with outcome of IVH and mortality. We further investigated the correlation between mean values of TOI, TOx and TOHRx averaged within the first 24 hours of life with gestational life, MABP, CRIB II and the use of inotropes.

5.2.3. Methods

This prospective observational study included preterm infants who were recruited for ‘SAMBA’ cohort, because these infants had more continuous NIRS data within the first 48 hours of life. The recruitment details, ethics, population and pre-processing

data analysis, including the methodology to calculate TOx and TOHRx, were described in Chapter 4.

NIRS data were averaged within the first 24 hours of life, and between 24 and 48 hours of life. Infants were included in the 'inotrope' group if they had dopamine, dobutamine or adrenaline started before 24 hours of life.

Preliminary analysis showed a difference in the distribution of the data for infants who were born < 28 and ≥ 28 weeks of gestational age. Therefore, a further analysis including only the subgroups of infants born < 28 weeks was performed.

Pearson coefficient correlation (r) or Spearman's correlation (r_s) were used to assess the relationship between indices of cerebral autoregulation (TOx), cerebrovascular reactivity (TOHRx) and cerebral oxygenation (TOI) with gestational age, CRIB II score and MABP. Independent samples T-test (φ) or Mann-Whitney test (§) were used for comparisons of mean TOx, TOHRx and TOI between outcome groups (IVH and mortality) and 'inotropes' groups, depending on the data distribution.

5.2.4. Results

The characteristics of all infants included in this study are shown in Table 5.5.

Table 5.5 Characteristics of the enrolled infants

Variable	Total (56)	No-IVH (38)	IVH (18)	P	Survived (49)	Died (7)	P
Gestational Age (weeks + days)	25+7 (23.43-31)	25.85 (23.57-31)	25.74 (23.43-29.29)	0.23§	25.86 (23.43-31)	24.57 (23.71-30.29)	0.24§
Birth weight (grams)	760 (520 – 1350)	760 (540-1350)	762 (520-1320)	0.86§	760 (540-1350)	760 (520-1180)	0.63§
Gender (Male/Female)	21/35	16/22	5/13	0.38Ω	20/29	1/6	0.24Ω
CRIB II	11 (5-16)	11 (5-16)	12 (9-16)	**0.043§**	11 (5-16)	14 (8-16)	0.23§
Inotropes*	27	21 (55%)	8 (44%)	0.57Ω	23 (47%)	6 (85%)	0.10 Ω
Sepsis	37	22 (58%)	15 (85%)	0.08Ω	31 (63%)	6 (86%)	0.40Ω

Data on gestational age, birth weight and CRIB II (Clinical Risk Index for Babies II) are show as median (range). Data on gender, inotrope use and sepsis are shown as frequency. § Mann-Whitney test. Ω Chi-square test. ***'Inotropes' group (total numbers)**: dopamine only (3), dopamine + dobutamine (16), dopamine + hydrocortisone (1), dopamine + dobutamine + hydrocortisone (2) dopamine + dobutamine + adrenaline + hydrocortisone (2), dobutamine only (3).

5.2.5. Cerebral Oxygenation

Mean TOI was predominantly above 70% within the first 48 hours of life. There was no difference in mean TOI between 0-24 and 24-48 hours (P = 0.62[§]).

Figure 5.10 Distribution of TOI within the first 48 hours of life

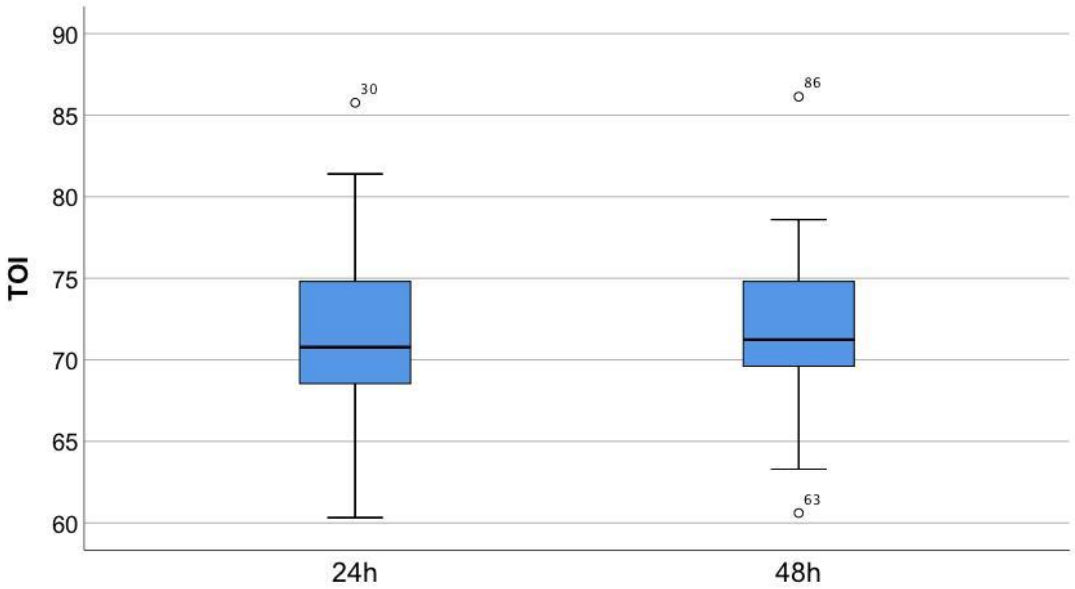

Median (Interquartile Range) TOI for 0-24h interval was 72 (6.4)% and for 24-48h interval was 72 (5.3)%.

Mean TOI within the first 24 hours had no correlation with gestational age at birth, MABP or CRIB II (Table 5.6).

Table 5.6 Correlation between TOI and GA, MABP and CRIB II

	All infants (N = 56)		Infants < 28 weeks (N = 44)	
	TOI	**P**	**TOI**	**P**
GA	0.130	0.34	0.208	0.18
MABP	-0.155	0.25	-0.018	0.91
CRIB II	-0.071	0.60	-0.128	0.41

GA for gestational age in weeks. CRIB II for Clinical Risk Index in Babies II. All Pearson correlation-coefficient.

Association between TOI and IVH

Including the whole cohort, no difference between mean TOI averaged between 0-24 hours and IVH groups was observed, however, mean TOI averaged between 24-48 hours was significantly lower in the IVH group (Figure 5.11).

Figure 5.11 Association between TOI and IVH for the whole cohort

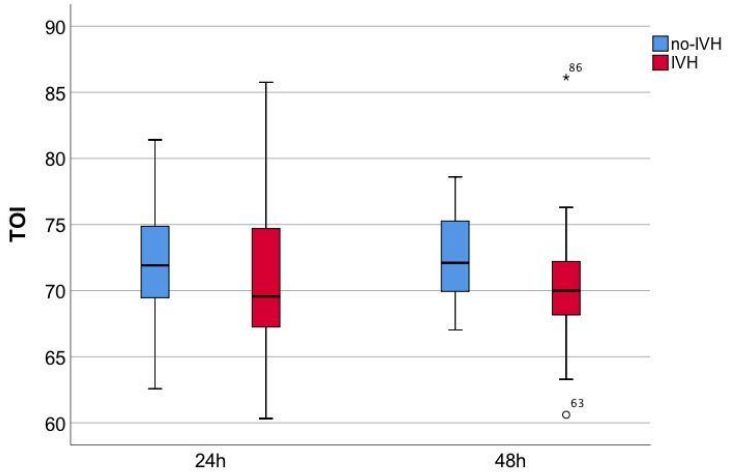

Figure shows the difference in mean TOI between IVH groups for 0-24h (P = 0.25 [φ]) and 48h (P = 0.028[§]) intervals (N = 56).

Including only infants < 28 weeks, mean TOI was significantly lower at 0-24 and 24-48 hours intervals in the IVH group, as shown in Figure 5.12.

Figure 5.12 Association between TOI and IVH in infants < 28 weeks

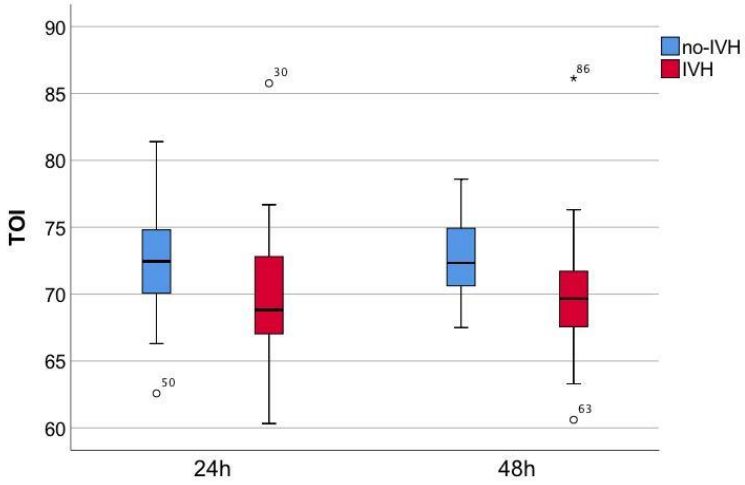

Figure shows the difference in mean TOI between IVH groups for 0-24h (P = 0.040[§]) and 48h (P = 0.012[§]) intervals. Only infants born at less than 28 weeks were included (N = 44).

Association between TOI and Mortality

Mean TOI averaged between 0-24 and 24-48 hours had not association with mortality for the whole cohort (P = 0.38[§] and P = 0.90[§]) or only infants < 28 weeks (P = 0.63[§] and P = 0.93[§], respectively).

Measurement of cerebral autoregulation (TOx)

Mean TOx was predominantly positive within the first 48 hours of life as shown in Figure 5.13.

There was no difference in mean TOx between these two time intervals (P = 0.34[φ]).

Figure 5.13 Distribution of TOx within the first 48 hours of life

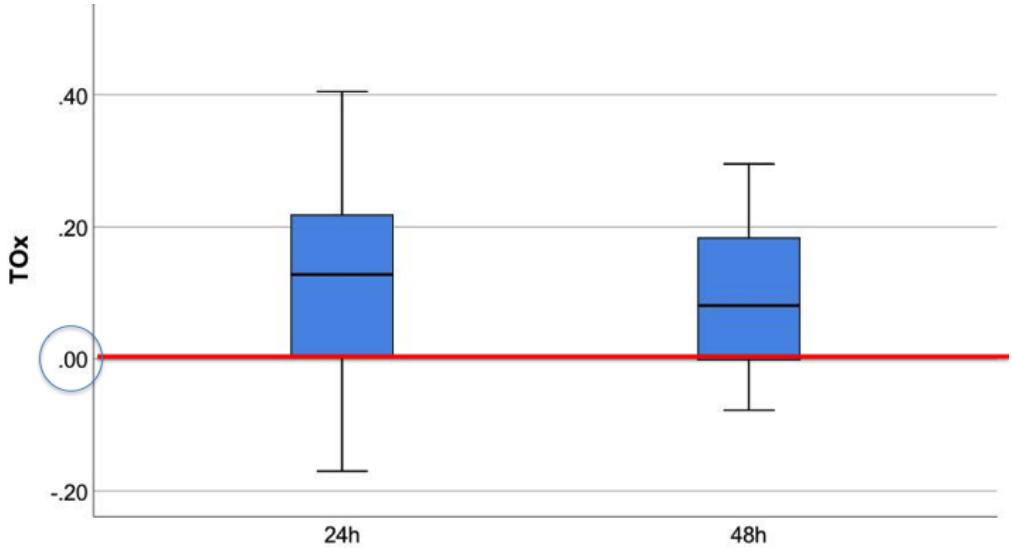

Median (Interquartile Range) TOx for 0-24h interval was 0.13 (0.21) and for 24-48h interval was 0.08 (0.18).

Distribution of mean TOx within the first 24 hours of life and correlation with other variables

Mean TOx within the first 24 hours of age for each individual infant was below zero for only 13 infants (23.2%). None of the infants had mean TOx ≥ 0.5. Figure 5.14 shows a frequency histogram for three different thresholds of TOx.

Figure 5.14 Distribution of the mean TOx averaged over first 24 hours of life

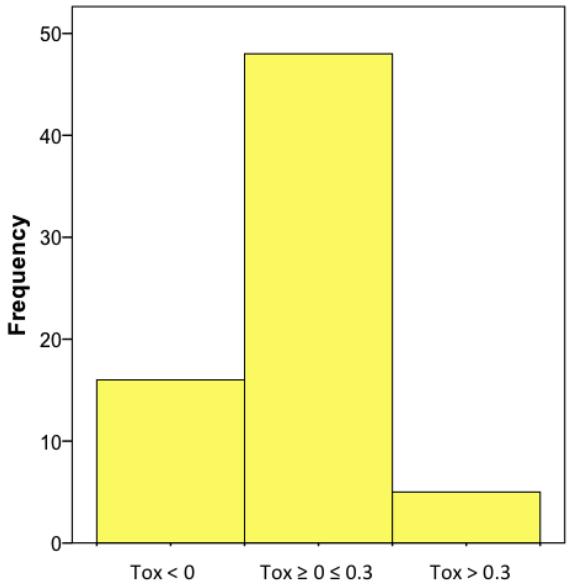

The threshold of TOx > 0.3 for impaired cerebral autoregulation was suggested by Brady et al., (2007)[129].

Mean TOx had no correlation with gestational age at birth (Table 5.7). However, we can observe in Figure 5.15 that the pattern of the correlation between TOx and gestational is different for infants born < 28 weeks and for those born ≥ 28 weeks. When only infants born at less than 28 weeks were included in the analysis, mean TOx had a negative correlation with gestational age (Table 5.7).

Figure 5.15 Correlation between mean TOx and gestational age

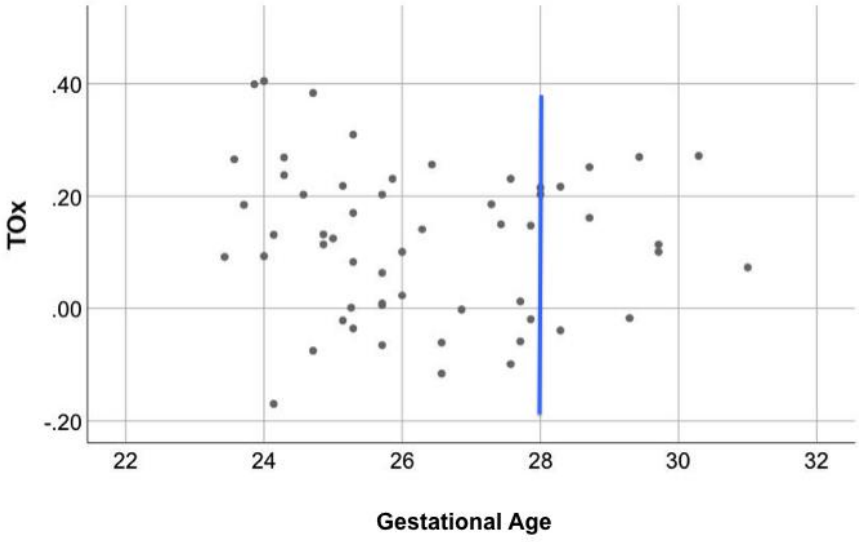

Mean TOx over the first 24 hours of life and gestational age at birth in weeks

The pattern of correlation between TOx and gestational age at birth was the opposite from the correlation between MABP and gestational age for infants born < 28 weeks, as shown in Figure 5.16. MABP had a significant positive correlation with gestational age for infants born < 28 week (r = 0.472, P = 0.001), following the physiological norms. However, there was no correlation between MABP and gestational age for those born ≥ 28 weeks (r = -0.219, P = 0.50).

Figure 5.16 Correlation between MABP and gestational age

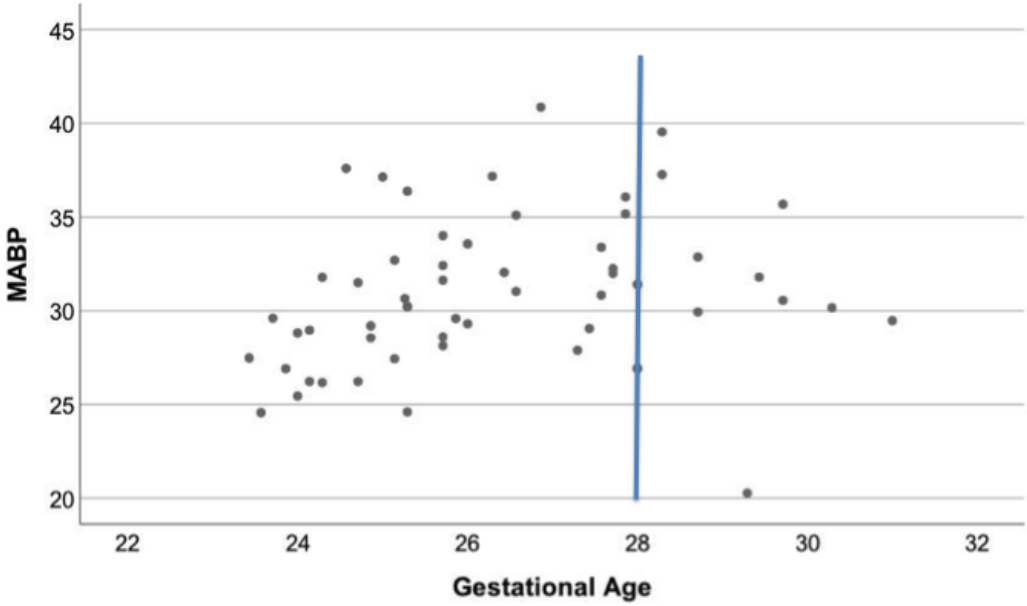

Mean MABP over the first 24 hours of life and gestational age in weeks.

Mean TOx had a negative correlation with MABP as shown in Figure 5.17 and this negative correlation was stronger when only infants born < 28 weeks were included (Table 5.7).

Figure 5.17 Correlation between TOx and MABP

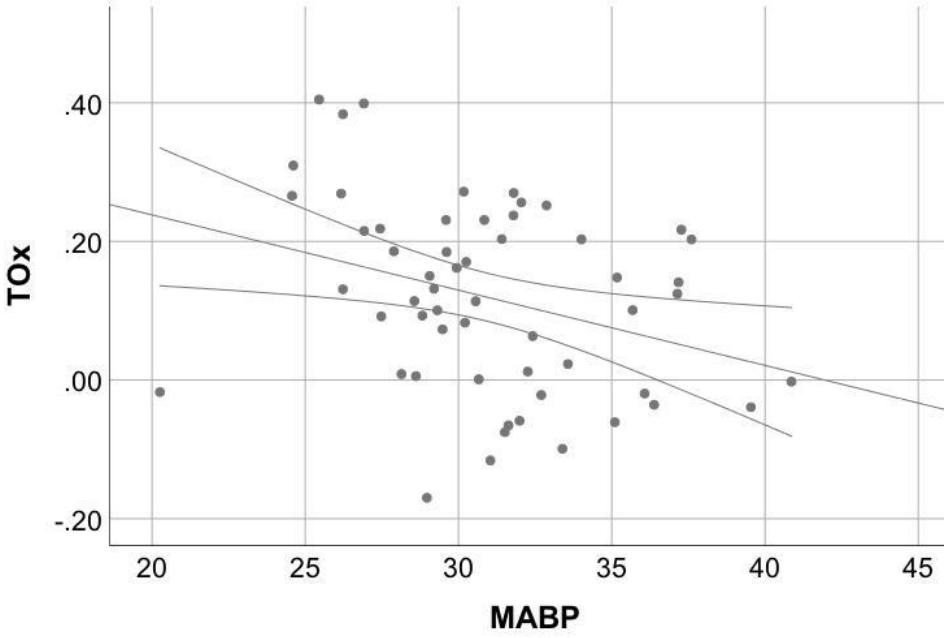

Mean TOx and mean MABP (mmHg) averaged within the first 24 hours of life.

Mean TOx had no correlation with CRIB II, but when only infants born < 28 weeks were included, a positive correlation was observed (Table 5.7).

Table 5.7 Correlation between TOx and gestational age, MABP, CRIB II and TOI

	All infants (N = 56)		**Infants < 28 weeks (N = 44)**	
	TOx	**P**	**TOx**	**P**
GA	-0.108*	0.43	-0.345	**0.022**
MABP	-0.322	**0.015**	-0.444	**0.003**
CRIB II	0.165	0.22	0.311	**0.040**
TOI	0.10	0.94	0.25	0.87

GA for gestational age in weeks. CRIB II for Clinical Risk Index in Babies II. *Spearman rank correlation, the remaining correlations were Pearson correlation-coefficient.

Association between TOx and IVH

Including the whole cohort (N = 56), no difference between the mean TOx and IVH groups was observed for 0-24h and 24-48h intervals (P = 0.71[φ] and P = 0.28[φ] respectively).

Including only infants born < 28 weeks, the difference in mean TOx between groups remained non-significant (Figure 5.18).

Figure 5.18 Association between TOx and IVH in infants born < 28 weeks

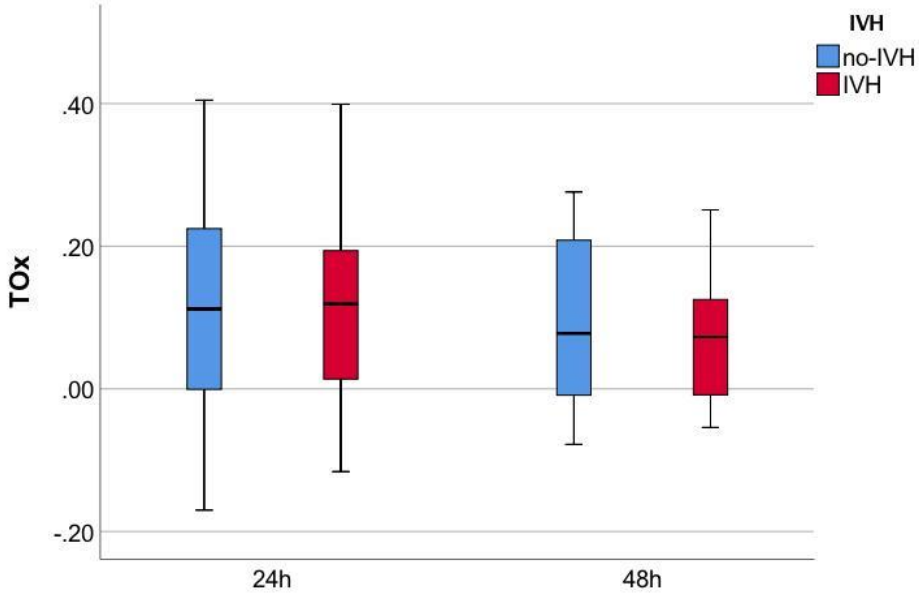

Figure shows the difference in TOx between infants who did not have and had IVH for 0-24h (P = 0.094[φ]) and 24-48h (P = 0.55[φ]) intervals. [φ]Independent samples t-test.

Association between TOx and mortality

Including the whole cohort (N = 56), there was no difference in the mean TOx within the first 24 hours of life between mortality groups (P = 0.17[§]). However, the mean TOx within 24-48 hours tended to be significantly higher in those infants who died (P = 0.052[§]).

Including only infants born < 28 weeks, an outlier was observed as shown in Figure 5.19. When this outlier was removed from the analysis, mean TOx remained non-

significant between groups at for the 0-24h interval (P = 0.054[§]), but it was significantly higher in the group of infants who died for 24-48h interval (P = 0.040[§]) (Figure 5.19).

Figure 5.19 Association between TOx and mortality in infants < 28 weeks

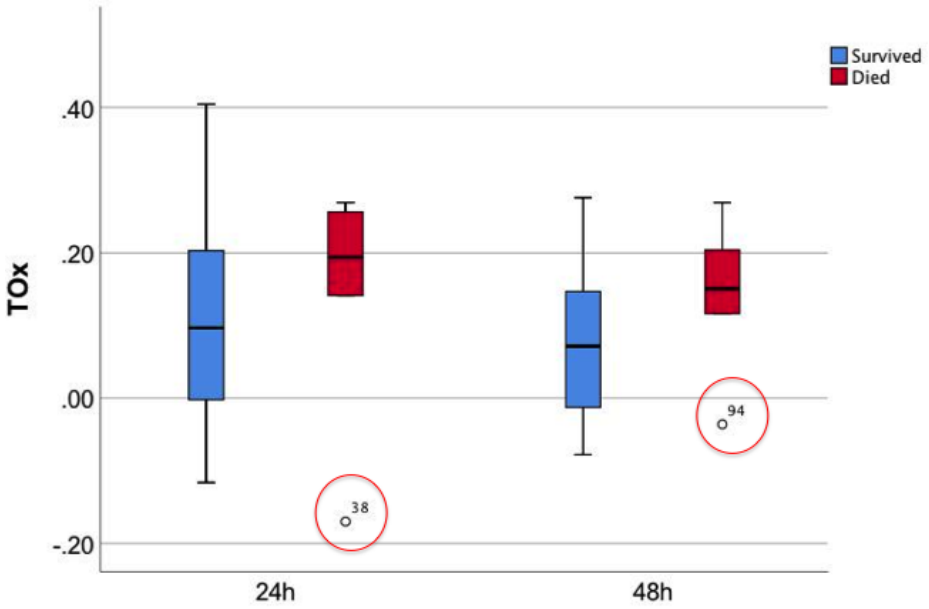

Figure shows the difference in TOx between infants who died and survived. The outlier was the same in both intervals: a female infant born at 24+1 week's gestational age who was stable within the first 24 hours of age, did not require inotropes, had no early sepsis and did no develop IVH. However, this infant developed fulminant NEC with bowel perforation and died on day 11 of life.

Association between TOx and inotropes

Mean TOx averaged within the first 24 hours of life was significantly higher for infants who were started on inotropes compared to the 'no-inotropes' group, for the whole cohort analysis (P = 0.002[φ]). The difference between groups was significantly higher when only infants < 28 weeks were included (P < 0.001[φ]) as shown in Figure 5.20.

Figure 5.20 Association between TOx and the use of inotropes in infants < 28 weeks

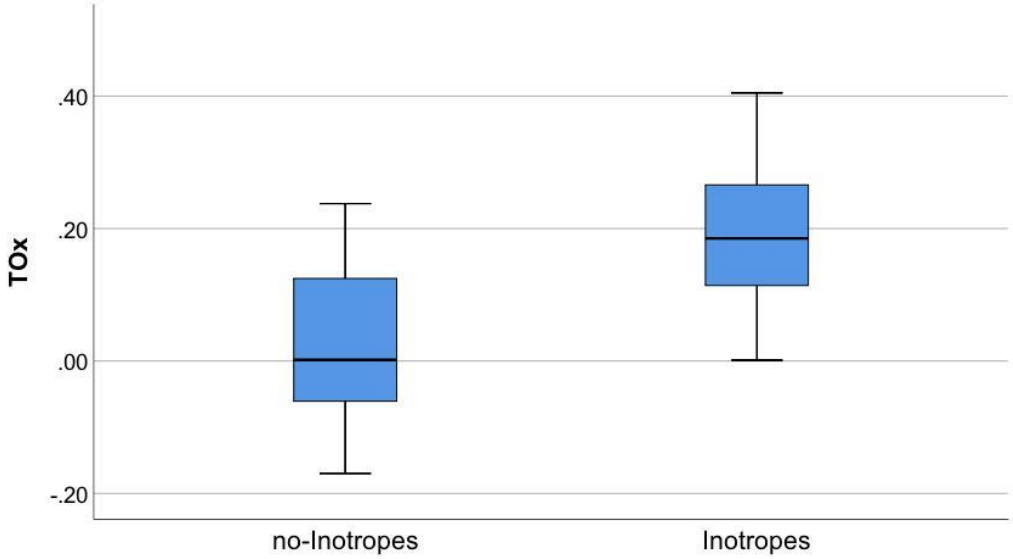

Median (Interquartile Range) TOx for 'no-Inotropes' group was 0.002 (0.19) and for 'Inotropes' group was 0.18 (0.16), N = 44.

Measurement of cerebrovascular reactivity

Mean TOHRx was predominantly negative within the first 24 hours of life and within 24 to 48 hours as shown in Figure 5.21. There was no difference in mean TOHRx between these two time intervals (P = 0.96$^{\varphi}$).

Figure 5.21 Distribution of TOHRx in the first 48 hours of life

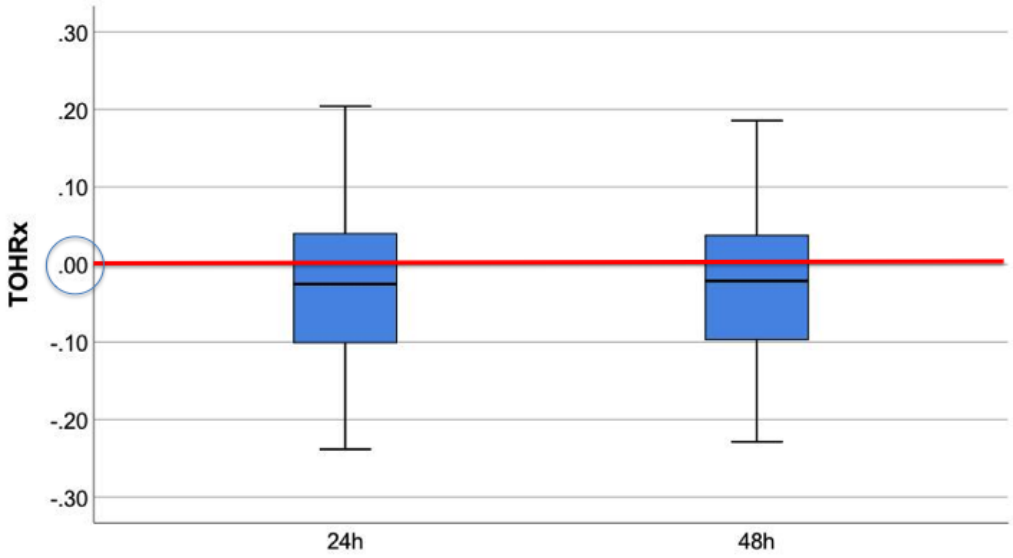

Median (Interquartile Range) TOHRx for 0-24h interval was -0.025 (0.14) and for 24-48h interval was -0.021 (0.13).

Distribution of mean TOHRx within the first 24 hours of life and correlation with other variables

Thirty-four infants (60.7%) had a mean TOHRx < zero and no infants had mean TOHRx ≥ 0.5 within the first 24 hours of life (Figure 5.22).

Figure 5.22 Distribution of the mean TOHRx averaged over first 24 hours of life

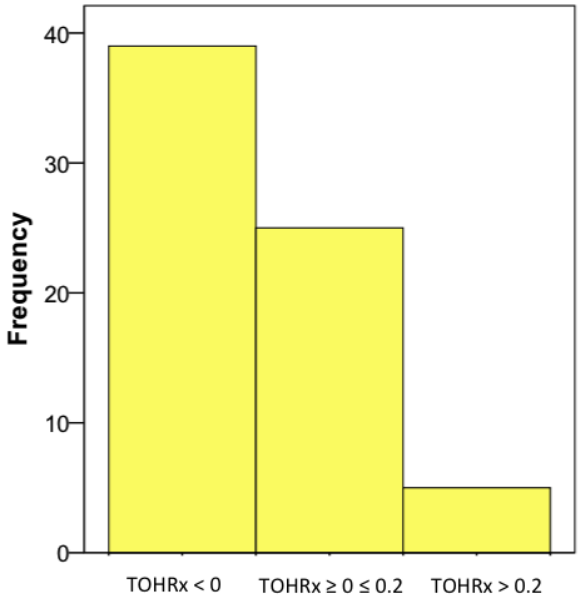

No thresholds of TOHRx for impaired cerebrovascular reactivity have yet been reported in the published literature. The threshold of 0.2 was chosen after observing the data distribution for the first 24 hours.

Mean TOHRx had negative correlation with gestational age at birth when the whole cohort was included in the analysis and remained significant when only infants < 28 weeks were included (Table 5.8 and Figure 5.23). HR had similar correlation with gestational age (Figure 5.24).

Including the whole cohort, mean TOHRx had a negative correlation with MABP. Including only infants below 28 weeks this correlation became insignificant (Table 5.8). However, three outliers were identified. When they were removed from the analysis, the correlation became significant r = - 0.446, P = 0.004 (Figure 5.25).

Mean TOHRx had positive correlation with CRIB II (Table 5.8)

Figure 5.23 Correlation between TOHRx and gestational age

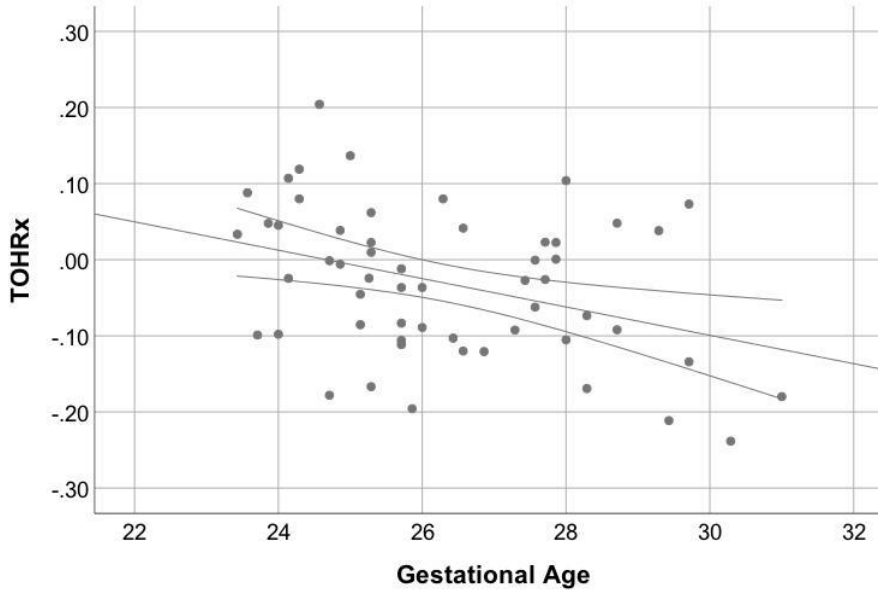

Mean TOHRx within the first 24 hours of life and gestational age at birth in weeks (r = -0.367, P = 0.005).

Figure 5.24 Correlation between HR and gestational age

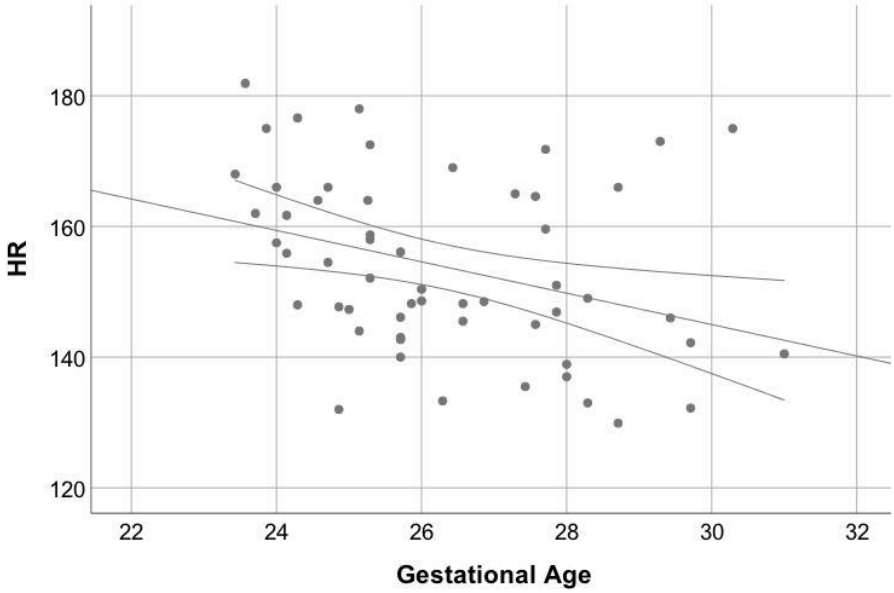

Mean HR within the first 24 hours of life and gestational age at birth in weeks (r = -0.339, P = 0.010).

Figure 5.25 Correlation between TOHRx and MABP in infants < 28 weeks

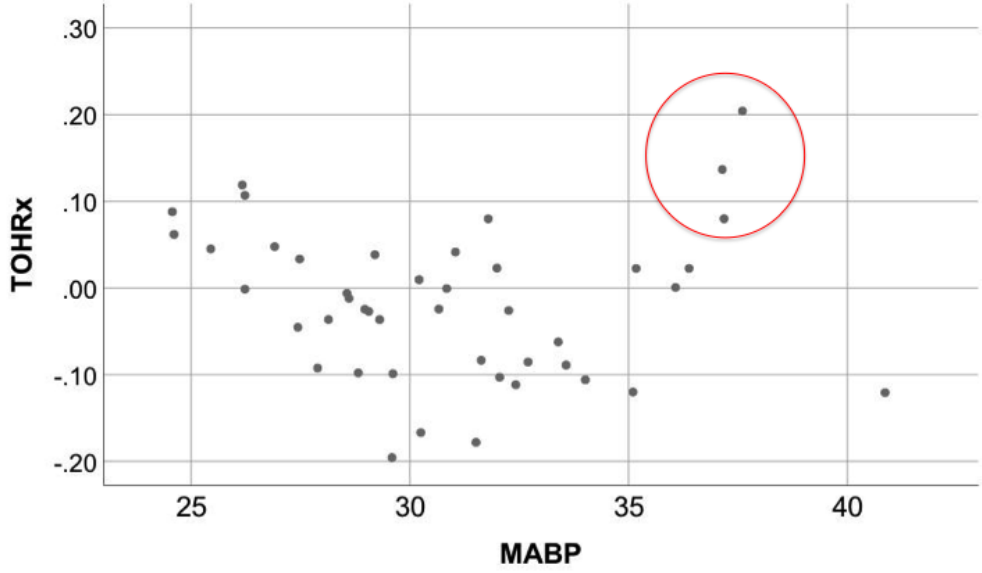

All outliers were infants who had severe antenatal hypoxia. Two outliers were infants who were severely sick soon after birth and died two weeks of age. The third one was high MABP and very low TOI within the first 24 hours of age and developed bilateral grade III IVH after the 1st day of life.

Table 5.8 Correlation between TOHRx and GA, MABP, CRIB II, TOI and TOx

	All infants (N = 56)		**Infants < 28 weeks (N = 44)**	
	TOHRx	**P**	**TOHRx**	**P**
GA	**-0.367**	**0.005**	**-0.304***	**0.045**
MABP	**-0.289***	**0.031**	-0.202*	0.19
HR	0.213	0.11	0.218	0.16
CRIB II	**0.404**	**0.002**	**-0.370**	**0.013**
TOI	0.030*	0.82	-0.195	0.20
TOx	0.146	0.28	0.288*	0.058

GA for gestational age in weeks. CRIB II for Clinical Risk Index in Babies II. *Spearman rank, the remaining correlations are Pearson correlation-coefficient.

Association between TOx and IVH

Including the whole cohort, there was no difference between mean TOHRx between IVH groups for the 0-24h interval (P=0.27$^{\varphi}$). However, mean TOHRx was significantly higher in infants who had an IVH for the 24-48h interval (P = 0.045$^{\varphi}$) as shown in Figure 5.26.

Figure 5.26 Association between TOHRx and IVH for the whole cohort

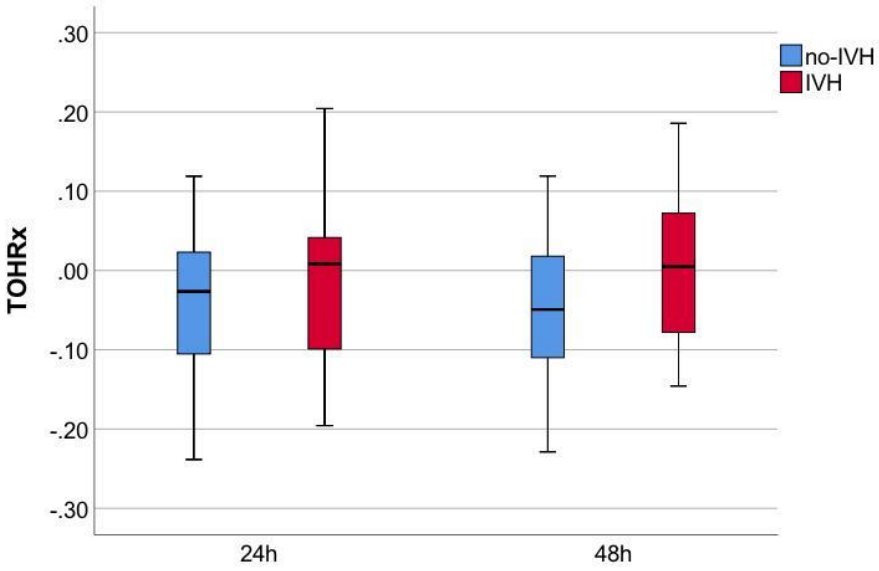

Figure shows the difference in mean TOHRx between IVH groups for 0-24h and 24-48h intervals. All infants included (N = 56).

Including only infants < 28 weeks, there was no difference in mean TOHRx between IVH groups for the 0-24h (P=0.58$^{\varphi}$) and for the 24-48 intervals (P = 0.20 $^{\varphi}$).

Association between TOx and mortality

There was no difference in mean TOHRx averaged within 0-24 hours between those infants who died and survived (P = 0.68$^{\varphi}$). When only infants < 28 weeks were included, the difference between groups remained non-significant (P = 0.34$^{\varphi}$). The difference between mortality in the groups remained non-significant when TOHRx was averaged between 24-48 hours (P = 0.41$^{\varphi}$). However, when only infants below 28 weeks were included, mean TOHRx (24-48h) was significantly higher in those infants who died (P = 0.008$^{\varphi}$) as shown in Figure 5.27.

Figure 5.27 Association between TOHRx and mortality in infants < 28 weeks

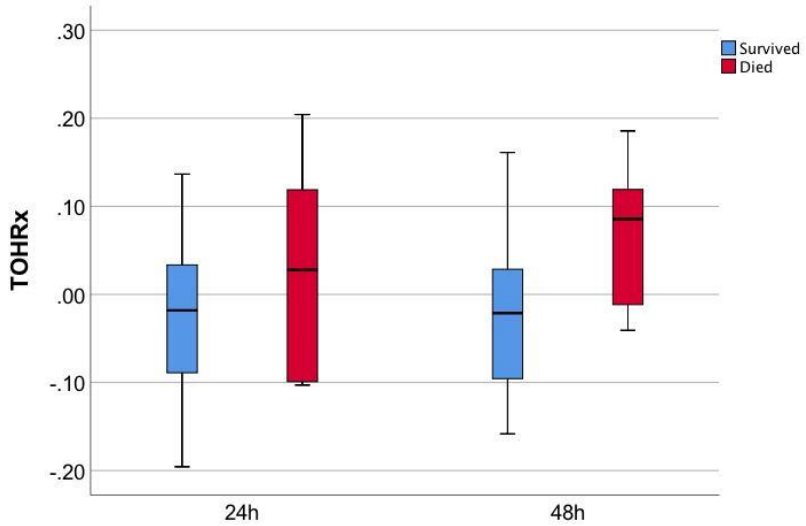

Figure shows the difference in mean TOHRx between IVH groups for 0-24h and 24-48h intervals. Only infants born at less than 28 weeks were included (N = 44).

Association between TOHRx and inotropes

Mean TOHRx was significantly higher for infants who were started on inotropes compared to 'no-inotropes' group for the whole cohort analysis (P = 0.040[φ]). Mean TOHRx tended to be higher in the 'inotropes' group in infants < 28 weeks (Figure 5.28), but the difference between groups did not reach statistical significance (P = 0.051[φ]).

Figure 5.28 Association between TOHRx and the use of inotropes in infants < 28 weeks

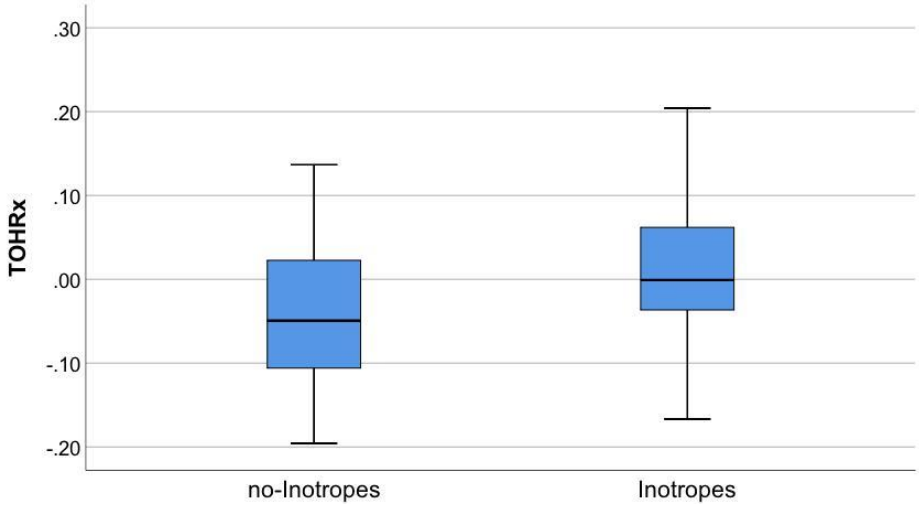

Median (Interquartile Range) TOHRx for 'no-Inotropes' group was -0.05 (0.13) and for 'Inotropes' group was -0.0009 (0.10), N = 44.

5.2.6. Discussion

Cerebral oxygenation within the first 48 hours of life and its relationship with outcome

In this study, no statistically significant difference in mean TOI averaged between the first 24 hours of life and between 24 and 48 hours was observed. Mean TOI had a better correlation with IVH when only infants born < 28 weeks' gestational age were included in the analysis. Cerebral oxygenation was lower for infants who developed an IVH but no difference was observed in mean TOI between infants who died or survived. Several studies have already reported increased cerebral hypoxia and hypoperfusion within days of life in infant who later developed IVH[77, 145, 307]. It is well known that hypoperfusion-reperfusion injury is the key mechanism in the development of brain injury in preterm infants. The amount of cerebral hypoxia or low cerebral blood flow has been suggested as the main factor associated with the development of GMH-IVH[36]. However, to date there are no studies on the best approach to monitor cerebral oxygenation at the cotside in order to prevent the development of brain injury in neonates. The SafeBoosC trial demonstrated that it is possible to stabilise cerebral oxygenation, however thresholds of "normal" TOI remain uncertain, as discussed in Chapter 3[209]. Mean TOI alone may not be a robust method to assess changes in cerebral circulation. The time-domain correlation between TOI and other signals may provide more robust information on changes in cerebrovascular reactivity at the cotside.

Pressure passive circulation and cerebrovascular reactivity

In this study we observed that preterm infants, especially those born at less than 28 weeks of gestational age, had mainly positive TOx within the first 48 hours of life. However, cerebrovascular reactivity, assessed by TOHRx, was possibly more preserved (negative TOHRx) in more than 50% of the cohort. Regulation of CBF may be determined by other factors than blood pressure alone. Several physiological and biochemical mechanisms may have strong influence in the regulation of CBF, especially in the preterm population [308-310].

Thresholds of intact cerebral autoregulation and preserved cerebrovascular reactivity in preterm infants have not yet been consistently defined. Brady et al. (2007) described the loss of cerebral autoregulation when COx was above 0.3 in a piglet model of hypotension[129]. Gilmore et al., 2011 used the percentage of time of COx above 0.5 as a threshold of impaired cerebral autoregulation in preterm infants[137]. In our study, none of the infants had a mean TOx or mean TOHRx above 0.5, and only about 50% of had a mean TOx above 0.3 within the first 24 hours of life.

Cerebrovascular reactivity in extremely preterm infants

In our study, nearly 80% of the infants were born at less than 28 weeks gestation. According to studies in preterm lambs, the musclaris layers of cerebral arteries and arterioles develop approximately after 63% of the gestation, which is equivalent to approximately 25 weeks in humans. In lambs, cerebral autoregulation is active from the late stage in pregnancy, time equivalent to 36 weeks in humans[311]. Clinical studies have shown that cerebral autoregulation improves with increasing gestation age[305]. However, some degree of vasoreactivity may be present before cerebral autoregulation is established or even in those infants whose cerebral autoregulation is absent. In our study, TOHRx had negative correlation with gestational age, which may demonstrate that more immature infants had more impaired cerebrovascular reactivity. However, HR had very similar correlation with gestational age, showing the normal physiological maturation in HR with advance in gestational age and the possible limitation in the correlation of TOHRx with gestational age. Mean TOHRx over the first 24 hours of age was mainly positive for those infants born at less than 26 weeks. On the other hand, TOx only had a significant negative correlation with gestational age for infants < 28 weeks' gestation, showing that impaired cerebral autoregulation increased with decreasing gestational age. The lack of correlation between TOx and gestational age for those infants ≥ 28 weeks' gestation may be related with the underlying pathology affecting those infants, instead of the normal transitional adaptation following birth. It is possible that preterm infants born > 28 weeks actually may present more periods of intact cerebral autoregulation but this mechanism may become impaired when they are sick. In addition, TOHRx had no correlation with TOx, which may support the suggestion that some infants who are

passive to arterial blood pressure may have some degree of intact cerebrovascular reactivity.

The small number of infants born above 28 weeks of gestation who were included in this study were sick enough to have an umbilical arterial line inserted following birth, therefore the negative correlation between MABP and gestation age may represent the pathological status of this small proportion of all infants included in the analysis instead of normal physiological changes. On the other hand, the positive correlation between MABP and gestational age in extremely preterm infants follows the norms for MABP and it may reflect mainly physiological changes in this population. However, any assumption considered for the group of infants with more than 28 weeks of gestational age should be cautiously considered, as only 12 infants were included in this sub-group.

The correlation of indices of cerebral autoregulation and cerebrovascular reactivity with outcome

The correlation between TOHRx and CRIB II was similar to the work previously published by our research group[141]. More impaired cerebrovascular reactivity (more positive TOHRx) was observed in infants with worse clinical score of mortality and morbidity. The correlation between TOx and CRIB II was positive only in preterm infants > 28 weeks. In addition, more impaired cerebral autoregulation and cerebrovascular reactivity was observed with lower levels of MABP. These findings were similar to the work described by Gilmore et al., 2011 which showed that infants with a lower MABP had higher percentage of time with levels of COx (equivalent to TOx) above 0.5, in a small cohort of preterm infants born at ≤ 30 weeks' gestational age[137].

There was no correlation between mean TOx and IVH at any time interval. However, mean TOHRx was more positive between 24-48 hours of life in infants who developed IVH. This may reflect the loss of cerebrovascular reactivity after the bleeding occurred, because, as described in section 5.1.4, most infants developed IVH around or after 24 hours of age.

Cerebral autoregulation and cerebrovascular reactivity was more impaired in the extremely preterm infants who died compared to those who survived. Mean TOHRx was higher between 24-48 hours of life in extremely preterm infants who died. Mean TOx was higher in extremely preterm infants who died only when an outlier was removed from the data analysis. Although the outlier has made the statistical analysis non-significant, it has contributed to highlight the complexity of the relationship between indices of cerebrovascular reactivity and mortality. The outlier described in Figure 5.19 was a preterm infant who died at 11 days of life due to perforated NEC, but had a stable first 48 hours of life and did not develop an IVH. The mean TOx for the first 0-48 hours of life was negative for that infant, showing that cerebral autoregulation was intact and brain perfusion was protected, perhaps at the expense of non-vital organs. In this case, gut perfusion may have been compromised with redistribution of blood flow to the vital organs (brain, heart and adrenal glands). Although all infants in this cohort died after 48 hours of life due to other causes apart from brain injury (See Table 5.4) unlike the 'outlier', most of them were sick from early postnatal age, but any correlation between mortality and cerebrovascular reactivity should be considered cautiously, as number of infants who died is small and the causes of death are heterogeneous. The association between impaired cerebral autoregulation and mortality has been previously described. Wong et al., 2008 using coherence analysis, described an association between impaired cerebral autoregulation within the first days of life and subsequent mortality in preterm infants born $\leq$ 32 weeks[78].

Cerebrovascular reactivity and inotropes

In our study, mean TOx was higher in infants who were started on inotropes within the first 24 hours of life. However, it is difficult to establish whether the relationship between inotropes and impaired cerebral autoregulation is purely due to the effects of the drugs or due to the fact that infants who received inotropes were sicker and more hypotensive. As discussed before, TOx had a negative correlation with MABP. Several studies have already reported that hypotension may be associated with impaired autoregulation[78, 137, 312]. More recently, Eriksen et al. (2014) have reported that mean COx was higher in a group of preterm infants who received dopamine within the first 24 hours of life compared to infants who did not received dopamine[138].

In this study, they did not found correlation between COx and gestational age, CRIB II or mortality. However, data were collected for short period of time (mean 2.5 hours only) and it was not clear if those infants who did not receive dopamine had received any other treatment for hypotension such as volume expansion, inotropes or vasopressors. TOHRx was slightly more positive in the 'inotropes' groups compared to the 'no-inotrope' group when all infants were included in the analysis. However, no difference between these two groups was observed when only preterm infants < 28 weeks were included.

Limitations

In this study we used averaged values of TOI, TOx and TOHRx over approximately 24-hour time intervals. Data on percentage of time spent above thresholds of cerebrovascular reactivity may offer a better correlation with outcome. However, definite thresholds of cerebral autoregulation and cerebrovascular reactivity in extremely preterm infants have not yet been well defined, which limited our analysis to averaged values. Other factors related to changes in CBF, such as changes in CO_2, could have had an impact on the final results. In our study, data on continuous transcutaneous CO_2 were collected for some infants, however values were not always reliable and could not be used in the final analysis. Moreover, changes in peripheral oxygenation, especially below 85%, can contribute as a confounder. However, major episodes of arterial oxygen desaturations were removed from the data during manual artefact removal, reducing this confounding factor.

6. OPTIMAL MEAN ARTERIAL BLOOD PRESSURE IN PRETERM INFANTS

6.1. MONITORING OF CEREBRAL VASCULAR REACTIVITY FOR DETERMINATION OF OPTIMAL BLOOD PRESSURE IN PRETERM INFANTS

The results presented in this section have been published in *The Journal of Pediatrics*[313].

6.1.1. Introduction

Disturbances in cerebral perfusion have been implicated in the pathophysiology of hemorrhagic and ischaemic brain lesions in preterm infants, as described in Chapter 2, section 2.1.3. Strategies for preventing cerebral injury in preterm infants have emphasized the importance of maintaining a "normal blood pressure" to ensure adequate perfusion of the brain. However, the definition of hypotension or hypertension in this population remains uncertain. The current management of hypotension in preterm infants does not combine quantitative information about organ perfusion. Nevertheless, regulation of CBF must be a crucial mechanism to ensure survival and avoid ischemic or haemorrhagic injury. The concept of optimizing CPP or MABP according to the strength of cerebral autoregulation (described in Chapter 2, section 2.3.2) could provide an individualized and quantitative approach to the management of hypotension in preterm infants.

6.1.2. Aims

In this study, we hypothesized that using NIRS we could define levels of MABP where cerebrovascular reactivity is strongest ($MABP_{OPT}$). Furthermore, we hypothesized that deviations from $MABP_{OPT}$ values would correlate with outcome of mortality and IVH.

6.1.3. Methods

This prospective observational study included preterm infants born at ≤ 32 weeks gestational age who were recruited to the 'RUMBA' cohort only. The recruitment details, ethics, population and pre-processing data analysis were described in Chapter 4. In this study we used TOHRx as an index of cerebrovascular reactivity. The method to calculate TORHx was described in Chapter 4, section 4.4.1.

Optimal blood pressure calculation

The methodology applied to define $MABP_{OPT}$ in this cohort of preterm infants was similar to the method previously used by Aries et al to define $MABP_{OPT}$ in adults with traumatic brain injury[172]. In adults, different windows have been analyzed, and the optimum of 5-minute windows for the autoregulation index and a 4-hour window for $MABP_{OPT}$ proved to be the optimal (also showing the strongest association with outcome after traumatic brain injury)[172]. The four-hour window for calculation of $MABP_{OPT}$ in adults is a trade-off between increasing the range of MABP variation (generally increasing with increased window) required to "probe" the $MABP_{OPT}$ and making the index available as soon as possible, to be clinically relevant. The $MABP_{OPT}$ for individual infants was determined by dividing MABP, recorded within a 1-hour period, into 3 mm Hg bins and averaging TOHRx within those bins. An automatic U-shape curve-fitting method was applied to determine the MABP value with the lowest associated TOHRx value, which corresponds to maximal cerebrovascular reactivity, following the method described by Aries at al. In our study $MABP_{OPT}$ was defined as the MABP where TOHRx was lowest.

Divergence from optimal blood pressure

The absolute value of the difference between mean MABP from the total monitoring time and mean $MABP_{OPT}$ also from the total monitoring time was defined as 'ABS' (absolute deviation) and was calculated for each individual patient.

Statistical analysis

A non-parametric (Kruskall-Wallis) test was used to investigate the difference between 'ABS' and mortality. One-sample t test between proportions was used to determine whether there was significant difference between deviation from MABP and mortality rate and grades of IVH. Pearson correlation coefficient (r) was used to correlate the expected MABP thresholds based on gestational age in weeks with $MABP_{OPT}$.

6.1.4. Results

The median (range) age of the 60 preterm infants the beginning of the study was 34 (5-228) hours, and the median time of recorded data was 2 (1-24) hours. Demographic data are shown in Table 6.1.

Table 6.1 Characteristics of the enrolled infants

Variables	Total (n=60)
Gestational age (weeks)	26+2 (23+2 – 32+1)
Birth Weight (grams)	845g (445g – 1440g)
Male:Female	1.4:1
CRIB II	11 (4 – 17)
IVH	27(45%)
Inotrope medication	31 (51%)
Mortality	11 (18%)

Gestational age, birth weight and CRIB II (Clinical Risk Index for Babies II) values are presented as median (range). Remaining variables are presented as frequency

Figure 6.1 Example of TOHRx over MABP plot to determine the $MABP_{OPT}$ in a single infant

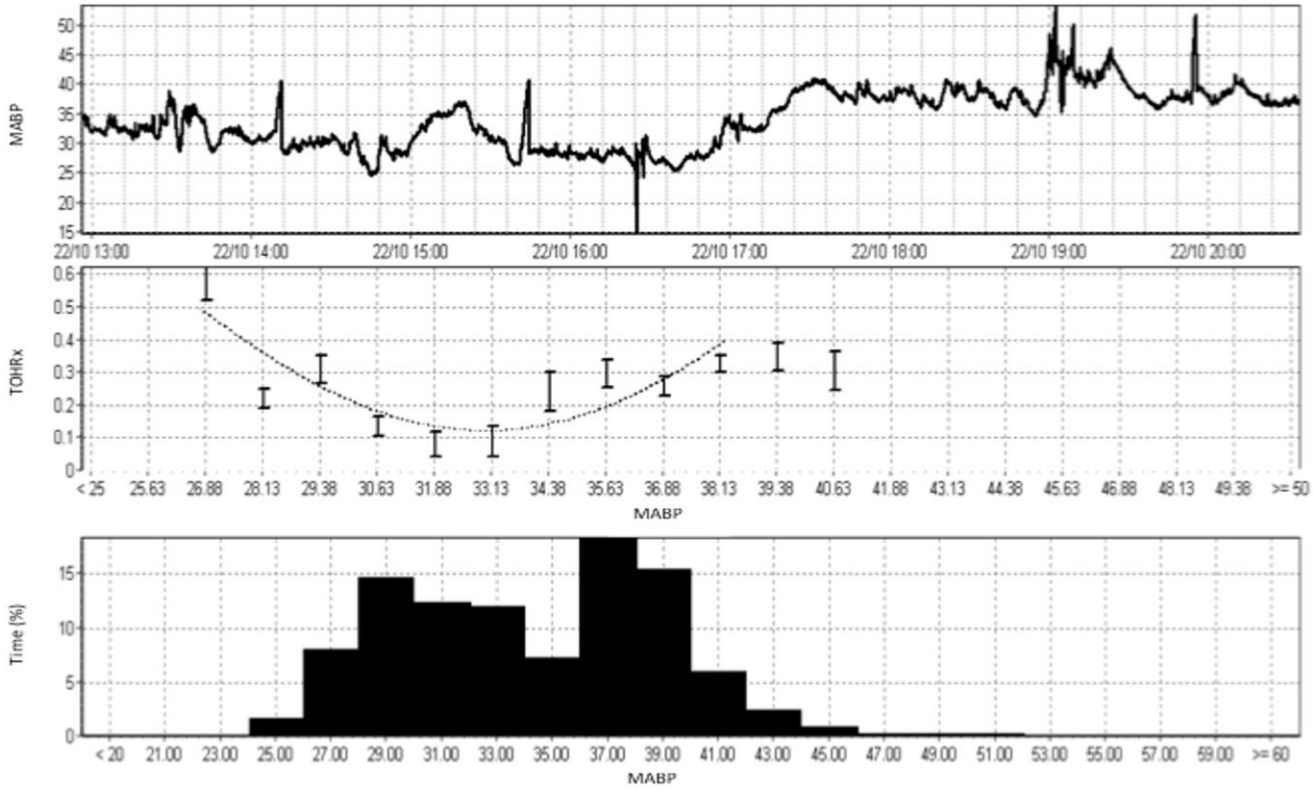

A male infant born at 25+2 weeks' gestational age with a birth weigh of 860 grams who was studied within the first 36 hours of life for 23 hours. This infant was ventilated and was not on inotropes during the recording study period. The first graph shows the infants actual MABP. The second graph shows $MABP_{OPT}$ curve. The frequency histogram shows the percentage of time spent in each value of MABP. Adapted from *da Costa, et al. (2015)*[313].

Figure 6.1 shows an example of the $MABP_{OPT}$ graph for a single infant and a histogram of MABP, normalized by the total number of data samples. The $MABP_{OPT}$ is the minimum value of the U-shape curve fitted to the mean TOHRx versus mean MABP data pairs.

The determination of individual $MABP_{OPT}$ using a sliding 1-hour window was possible in 49 (81.6%) infants from a total of 60. In 11 (19.3%) infants, the $MABP_{OPT}$ was not identified possibly due to the short period of recording data (< 3hours) or the presence of frequent artifacts. The mean $MABP_{OPT}$ averaged from the 1-hour window was 35 +/-6.4 mm Hg (mean +/-SD). The $MABP_{OPT}$ increased with increasing gestational age ($r = 0.390$; $P < 0.005$) as shown in Figure 6.2.

The measurement of divergence from the $MABP_{OPT,}$ ABS, was greater in those infants who did not survive. Infants who survived had a mean ABS of 2.1 (CI 1.64, 2.56) mmHg, whereas those who did not survive had a mean ABS of 4.2 (CI 3.44, 4.96) mmHg $P = 0.013$ (Figure 6.3).

Infants who had a MABP lower than $MABP_{OPT}$ by at least 4mmHg had greater mortality rate (40%) than those with MABP close to or above $MABP_{OPT}$ (13%), $P = 0.049$. Infants with MABP greater than $MABP_{OPT}$ by at least 4 mmHg had significantly greater IVH score (grades 3 and 4) ($P = 0.042$).

Expected MABP threshold (gestation age in weeks) was only moderately correlated with $MABP_{OPT}$ ($r = 0.42$; $P < 0.002$), with $MABP_{OPT}$ values greater than expected MABP by 9 mm Hg on average ($P < 0.001$).

Figure 6.2 Correlation between $MABP_{OPT}$ and gestational age in weeks

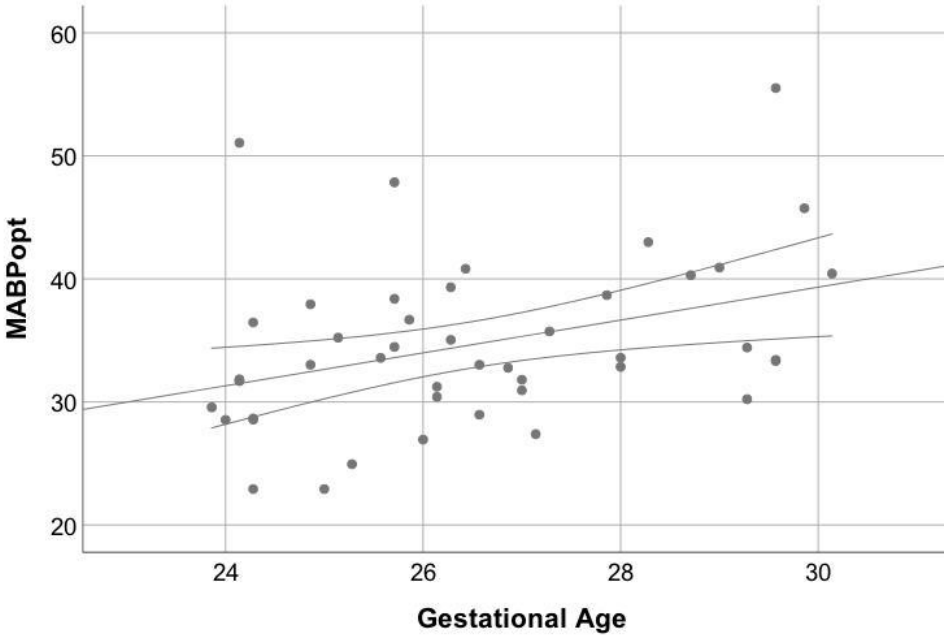

Mean $MABP_{OPT}$ averaged for the entire recording period for each individual infant and gestational age at birth in weeks.

Figure 6.3 Difference between ABS and outcome groups

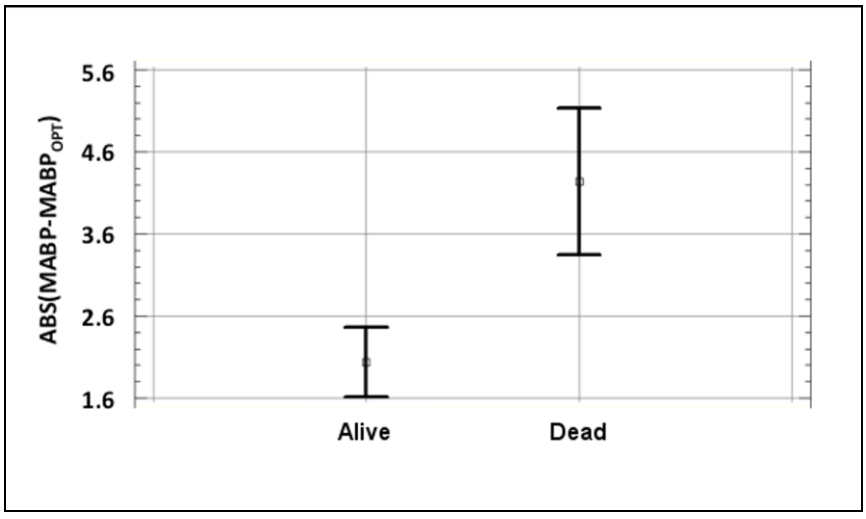

Mean ABS was 2.1 (95% CI 1.64 – 2.56) mmHg for those infants who survived and 4.2 (95% CI 2.44 – 4.96) mmHg for those who died (non-parametric test), P=0.013

6.1.5. Discussion

In this study, using TOHRx as a marker of cerebrovascular reactivity, we were able to define retrospectively $MABP_{OPT}$ in over 80% of the infants studied. In addition, we observed a significant correlation between divergence from $MABP_{OPT}$ values and adverse outcome. We observed an expected increase in the $MABP_{OPT}$ with increase in gestational age, as MABP also increases with gestational age in the human fetus and in several other species[314-319] [152, 156]. The value of $MABP_{OPT}$ is a unique measurement for each infant, determined by their own physiology rather than population norms.

Work published by Wong et al. (2012), using coherence spectrum analysis, observed that impaired autoregulation and pressure-passive perfusion can be present even with only small fluctuations in blood pressure in critically ill preterm infants[82]. In our study we observed that, although the values of ABS were small, they significantly correlated with mortality, suggesting that small fluctuations in arterial blood pressure can have a detrimental impact on outcome, probably by breaching autoregulatory limits. An increase in TOHRx with both lowering and increasing MABP below or above $MABP_{OPT}$ may be conceptually visualized as a moving 'working point' of the autoregulatory Lassen curve, similar to the explanation given in the experimental study of Brady et al. (2008)[136].

Similar to other cerebrovascular indices reported, TOHRx is a dimensionless index, which relates the reactivity of the cerebral circulation to changes in the systemic circulation. In a previous study, we found that TOHRx was significantly correlated with the Clinical Risk Index for Babies II (CRIB II)[141]. As described in a previous study from our group, we did not find a high coherence between TOI and MABP (previously described as COx or TOx) in this cohort of preterm infants within the very low frequency band-with range (0.0002-0.05Hz), selected for its highest sensitivity to detect autoregulatory responses. The results of our previous study suggested that TOI-HR passivity increased with arterial hypotension[141]. This finding is in line with the literature on autoregulation theory. In adults, CBF is not related to cardiac output, but in preterm infants a positive correlation between CBF and left cardiac output has been suggested[320, 321].

Howlett et al. (2013), using the haemoglobin volume index (HVx) that is based on the correlation between the tissue hemoglobin index (THI) and MABP, were able to define $MABP_{OPT}$ in over 77% of term infants with hypoxic-ischaemic encephalopathy during rewarming phase of therapeutic hypothermia. They showed that infant who had moderate to severe MRI abnormalities spent a greater proportion of time with MABP below $MABP_{OPT}$ when compared to those infants with no brain injury brain injury[322].

In adult patients with traumatic brain injury, a greater divergence from CPP_{OPT} has been associated with poor outcome. Mortality increased when the median CPP fell below the CPP_{OPT} values and the likelihood of severe disability increased when the median CPP was above CPP_{OPT}[170, 172, 175]. In our study, mortality rates were higher in preterm infants with a MABP below $MABP_{OPT}$. In adults, targeting an individualized CPP during management of severe traumatic brain injury has been suggested to improve outcome and the data from several studies have supported the need for a clinical randomized controlled trial.

Blood pressure monitoring alone is not a reliable predictor of brain injury in preterm infants[323, 324]. However, fluctuations in MABP combined with immature vasculature and pressure passive cerebral vascular circulation in sick preterm infants has been associated with IVH[81]. Several studies have associated low cerebral perfusion with the development of IVH, suggesting a 'reperfusion' injury as the main pathophysiological mechanism[24, 66, 325]. In our study, preterm infants who had MABP values higher than $MABP_{OPT}$ had more severe IVH, suggesting that a diminished autoregulatory capacity can be found in infants who developed a severe IVH. Although we could demonstrate a correlation between deviations from $MABP_{OPT}$ and outcome of IVH and mortality, we were not able to predict the development of an IVH, as some infants already had established IVHs when the study was performed. In order to investigate the haemodynamic and autoregulatory pattern of infants who go onto develop an IVH, a studying monitoring preterm infants in the first 24 hours of life would be necessary.

Individualised hemodynamic management of the preterm infant is complex, with many variables and output. In this research study we obtained an objective 'individualised' measurement of MABP based on the strength of cerebrovascular

regulation. Clearly targeting hemodynamic management to optimize cerebral perfusion and oxygenation is critically important given the risk of haemorrhagic and ischaemic brain injury in this population group.

Limitations

We could not define $MABP_{OPT}$ in all patients because the present methodology requires a minimum of 2 to 4-hour windows of continuous data to create a u-shape curve. Shorter recordings could not produce any satisfactory information regarding optimal values of MABP. In order to calculate $MABP_{OPT}$ using this methodology it is necessary to have spontaneous fluctuations in MABP, HR and TOI, which may not occur in infants where autoregulation is completely lost or in infants with intact autoregulation. The percentage of time an infant remains at a particular blood pressure will determine the confidence interval of the average value of cerebrovascular reactivity associated with that pressure level. In most cases, however, infants' MABP followed a Gaussian distribution and may have incomplete coverage of the autoregulatory range. Moreover, values of $MABP_{OPT}$ were calculated retrospectively and to be clinically useful, these values will need to be calculated and displayed in near-real time at the cotside. If an automatic calculation of $MABP_{OPT}$ from a running 1-hour period is used, then these values at the cotside may be available for making clinical decisions in 'real time'. This would enable clinical prospective trials of $MABP_{OPT}$ versus conventional treatment to be carried out.

In this cohort of infants we studied the relationship between continuous physiological variables but continuous measurements of $PaCO_2$ was not available, although $PaCO_2$ was monitored through arterial blood gases and kept fairly stable during the study period. We cannot exclude an effect of fluctuating $PaCO_2$ our data and therefore we acknowledge this limitation. For future studies we would like to explore different models looking at the impact of transcutaneous $PaCO_2$ on cerebrovascular reactivity and $MABP_{OPT}$.

Another confounding factor is the potential instability of SaO_2. Fluctuations of SaO_2 within the frequency range of slow waves (20 sec to 3 min of period) are rarely seen and they did not cause coherent changes in TOI. Incidents of deeper desaturations (below 90%) often caused changes in TOI. However, the total time of such

desaturations was less than 5%, therefore contributing very little to calculated running TOHRx index. When we analysed the data excluding these events, it did not change the main results, but just contributed to a shorter overall detection time of optimal MABP.

6.2. OPTIMAL MEAN ARTERIAL BLOOD PRESSURE IN EXTREMELY PRETERM INFANTS WITHIN THE FIRST 24 HOURS OF LIFE

6.2.1. Background

Major changes in systemic and cerebral haemodynamics occur within the first 12 to 24 hours following birth. As discussed in Chapter 2, section 2.2, a decrease in CBF within the first 24 hours of life has been associated with brain injury in preterm infants. Most infants included in the SAMBA cohort developed GMH-IVH around or just after 24 hours of life, as shown in Chapter 5, section 5.1. Therefore, defining $MABP_{OPT}$ and deviations from optimal values before infants develop GMH-IVH may help to identify those who are at risk and provide a better understanding of its pathophysiology.

6.2.2. Aims

In this study, we aimed to define $MABP_{OPT}$ using NIRS in infants born less than 28 weeks' gestational age within the first 24 hours of life. We hypothesized that using a more refined methodology and with more prolonged periods of continuous NIRS data we could define $MABP_{OPT}$ in a higher proportion of infants at the most vulnerable time in life in terms of developing IVH. Furthermore, we hypothesized that deviations below or above $MABP_{OPT}$ would have associations with outcome of mortality and IVH.

6.2.3. Methods

This prospective observational study included data from infants born at < 28 weeks gestational age recruited for the 'SAMBA' cohort. Only NIRS and physiological data recorded within the first 24 hours of life were included in the analysis. The recruitment details, ethics, population and pre-processing data analysis were described in Chapter 4. Similar to our previous study, we used TOHRx as an index of cerebrovascular reactivity to calculate $MABP_{OPT}$. Deviations below or above $MABP_{OPT}$ values were included in the configuration profile and were calculated

analysis along with $MABP_{OPT}$ values during retrospective data analysis. The mean deviations below or above for the entire study period were correlated with outcome.

Optimal blood pressure calculation

The methodology applied to define $MABP_{OPT}$ in this cohort of preterm infants was similar to the method used in our previous study. However, the configuration was adjusted to take into account the different variability in MABP within the first 24 hours of age in extremely preterm infants. Range of MABP between 15 and 60 mmHg were chosen as the analysis of the MABP for each single infant demonstrated that 20% of the population spent at least 5% of the time with MABP between 15 and 20 mmHg. The configuration was also adjusted for the calculation of $MABP_{OPT}$ not to be re-started after a short period of missing data.

Statistical Analysis

Pearson correlation coefficient or Spearman's rank order correlation were used to investigate the correlation between CRIB II and TOHRx, and the correlation between $MABP_{OPT}$ and gestational age in weeks. Data distribution was assessed as described in Chapter 4. The non-parametric Mann-Whitney test was used to compare mean $MABP_{OPT}$ and mean deviations below or above $MABP_{OPT}$ with outcome of mortality and IVH. Independent samples t-test was used to compare mean MABP between these two groups.

6.2.4. Case reviews

Figure 6.3 shows an example of the $MABP_{OPT}$ graph for a single infant and a histogram of MABP normalized by the total number of data samples. The $MABP_{OPT}$ is the minimum value of the U-shape curve fitted to the mean TOHRx versus mean MABP data pairs. The $MABP_{OPT}$ for the infant in Figure 6.3 within that 4-h-window was around 32 – 35 mmHg.

Figure 6.4 Example of $MABP_{OPT}$ curve for a 4-hour-window data in a single infant

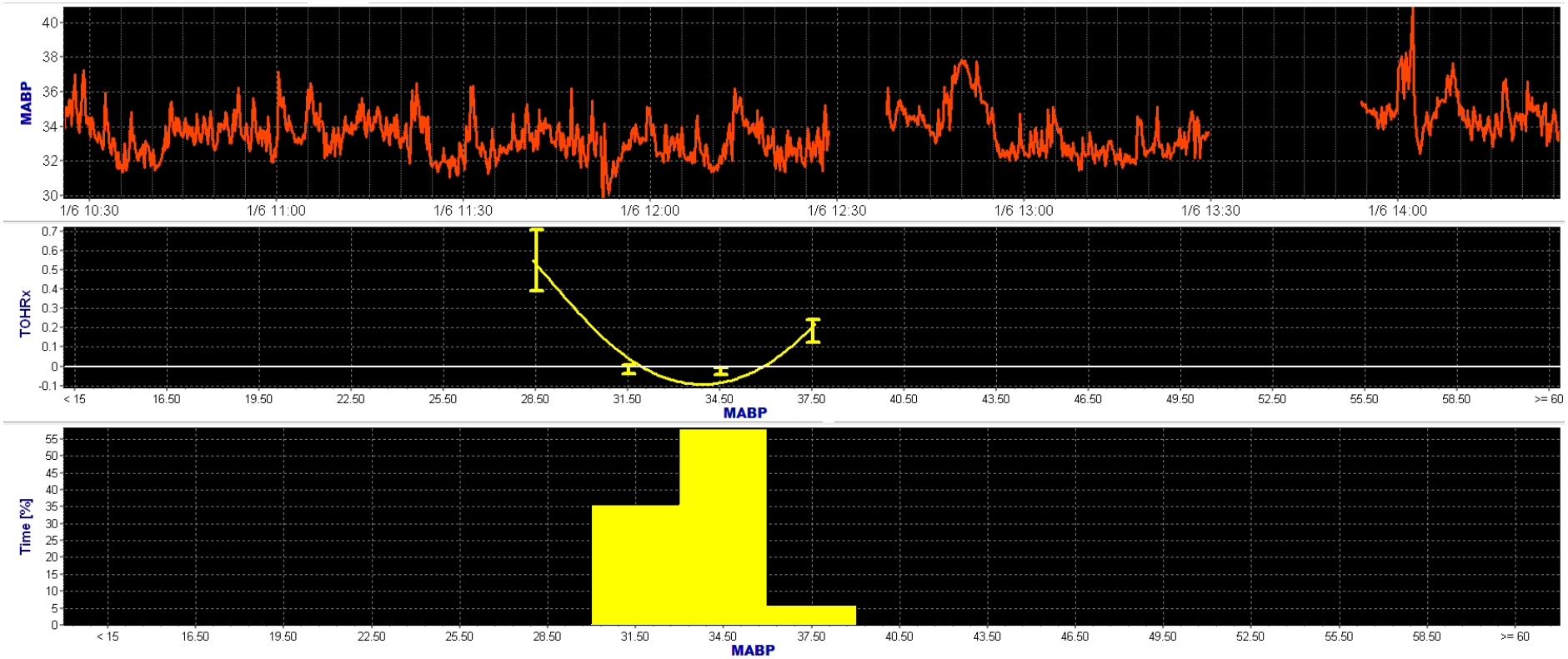

A female infant born at 27+6 weeks' gestational age with a birth weight of 1120 grams, CRIB II = 8. Her mother was given a complete course of antenatal steroids but no antenatal $MgSO_4$. She received one dose of surfactant at birth and was successfully extubated at 15 hours of age. No inotropes or transfusions were given over the first 48 hours of life. She did not have sepsis and received prophylactic antibiotics for 48 hours only. She was between 12 - 16 hours old at the above 4-h window. The first graph shows the infant's actual MABP. The second graph shows the $MABP_{OPT}$ curve. The frequency histogram shows the percentage of time spent in each value of MABP. This infant survived and had no IVH and normal cranial ultrasound at term corrected gestational age.

Figure 6.5 shows a 4-h-window of MABP and $MABP_{OPT}$ for a female infant born at 26+3 weeks' gestational age with a birth weight of 980 grams, CRIB II = 11. She was an IVF pregnancy, and had PPROM from 24+3 weeks; her mother completed a course of antenatal steroids, which was given 16 days before delivery when she was admitted with vaginal bleeding and threatened labour. She was born by emergency caesarean section (inborn), and was a breech presentation. She was intubated at birth and a total of two doses of surfactant were given (1^{st} at 12 minutes of age and 2^{nd} within the first 24 hours of life). She developed PPHN and received NO during her first three days of life. She was on dobutamine and dopamine infusions during the study period and received boluses of saline and sodium bicarbonate. She received antibiotics for presumed sepsis for seven days. Blood and CSF cultures were negative. She received three blood transfusions and one transfusion of fresh frozen plasma during the first 48 hours of life. She had a possible small GMH at her scan at 24 hours of life, but developed grade IV IVH between 24 and 48 hours of life. This infant died at corrected gestational age of 31+2 week's gestational age due to *pseudomonas aeruginosa* sepsis and meningitis.

Figure 6.5 Cranial ultrasound at 24 hours age for the case described above

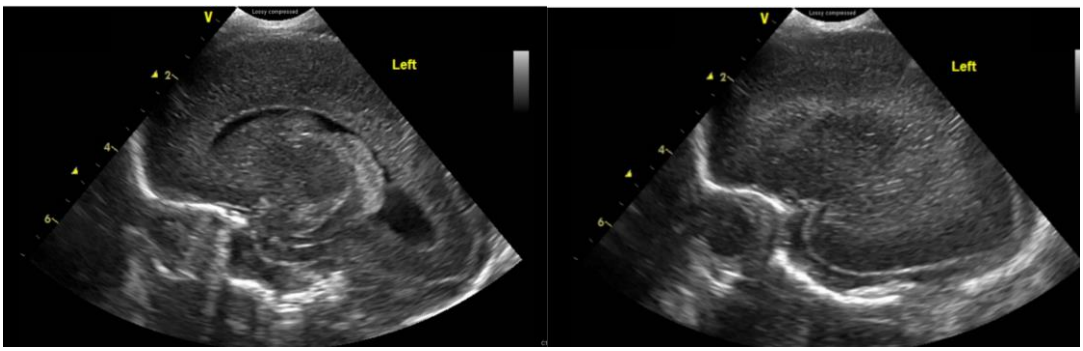

The sagittal images above show the cranial ultrasound performed at 24 hours of life with possible small GMH with some periventricular brightness. All images were recorded as part of the data collection for 'SAMBA' study.

Figure 6.6 $MABP_{OPT}$ graph for a 4-hour-window data for a single infant

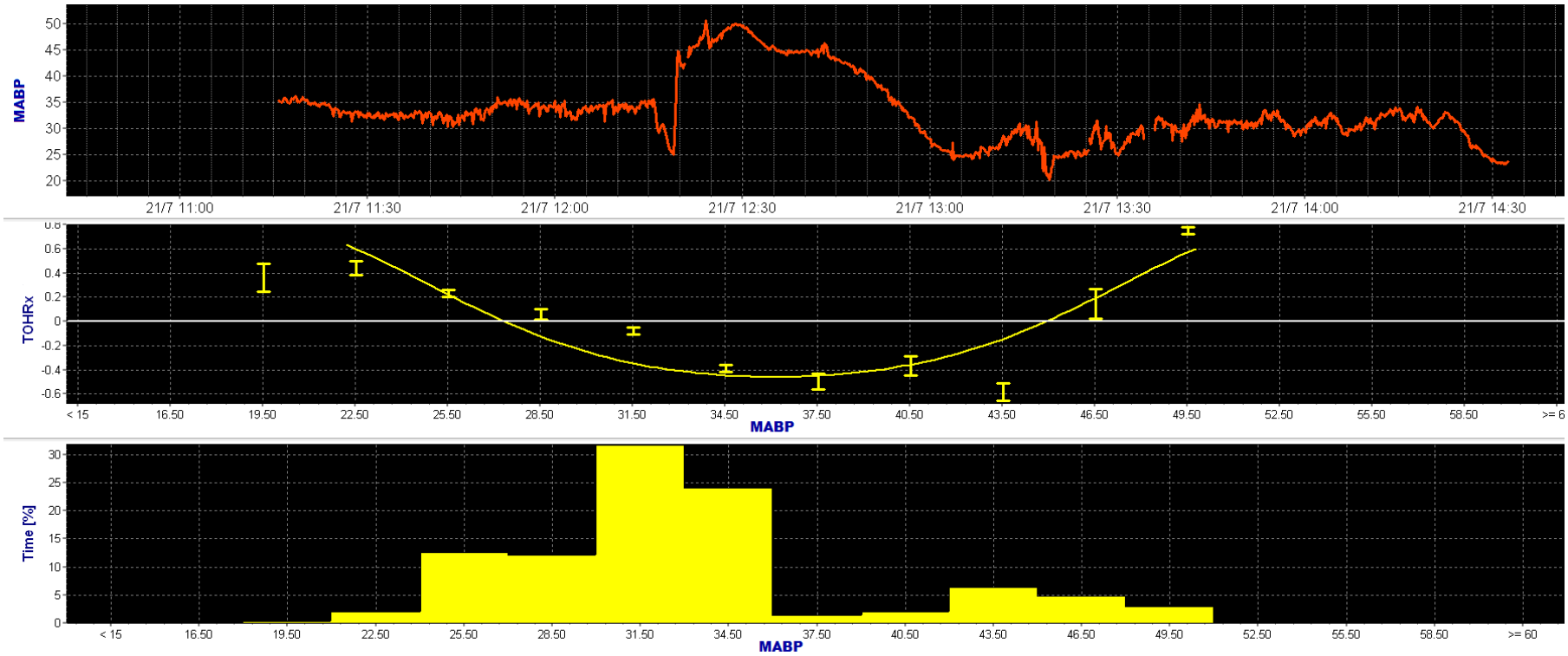

Infant's age at this 4-h-window was 20-24 hours of life. The first graph shows the infants actual MABP. The sudden increase in MABP seen at 12:20 (21/07) on the first graph followed an increase in dopamine infusion from 15 to 20 mcg/kg/min. The second graph shows $MABP_{OPT}$ curve. The frequency histogram shows the percentage of time spent in each value of actual MABP. The $MABP_{OPT}$ for this infant at this 4-h-window was around 35 mmHg. The frequency histogram for this 4-h-window shows that the percentage of time that the actual MABP was below $MABP_{OPT}$ was greater than the percentage of time spent with values $\geq MABP_{OPT}$. We can observe that the infant's MABP was around 35 mmHg (which was approximately the value for $MABP_{OPT}$) for this 4-h-window. A sudden drop on MABP was followed by an increase in dopamine, which may have shifted the MABP to values away from $MABP_{OPT}$ value.

Figure 6.7 TOI, HR and TOHRx signals for a 4-hour-window data for a single infant

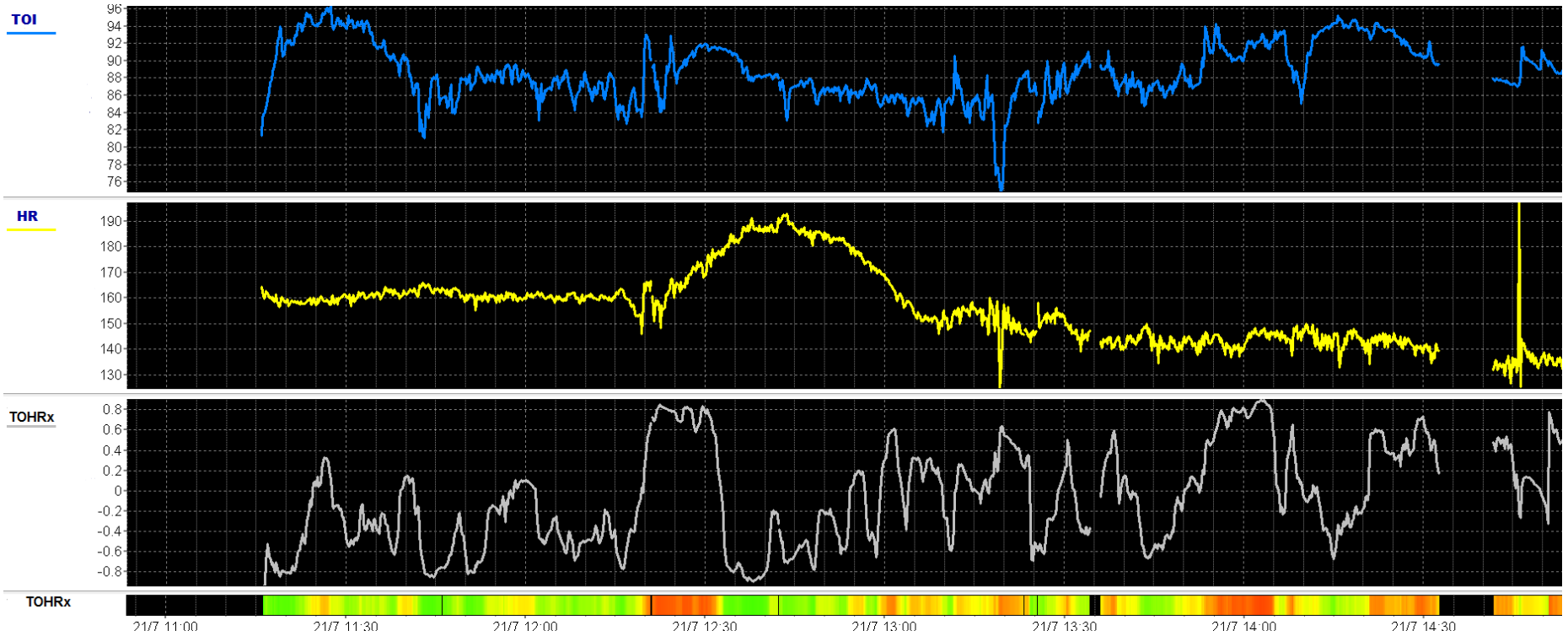

The figure above shows readings of TOI and TOHRx, respectively, for the same infant at same 4-h-window used to calculate $MABP_{OPT}$ shown Figure 6.5. The bottom image shows a 'risk chart' where colours change from green (TOHRx close to -1) towards red (TOHRx close to +1). The sudden increase in the TOHRx trace seen at 12:20 (21/07) followed an increase in dopamine infusion. Comparing Figure 6.5 and Figure 6.6, we observe that the actual MABP was within the $MABP_{OPT}$ values. A sudden fall in MABP and the subsequent increase in dopamine infusion may have resulted in an acute increase in MABP along with impaired cerebrovascular reactivity. The high values of TOI for this infant may reflect the use of NO for PPHN.

Figure 6.7 shows another 4-h-window of MABP and $MABP_{OPT}$ data for this same infant at around 30 hours of life.

Figure 6.8 $MABP_{OPT}$ graph at around 30 hours of age

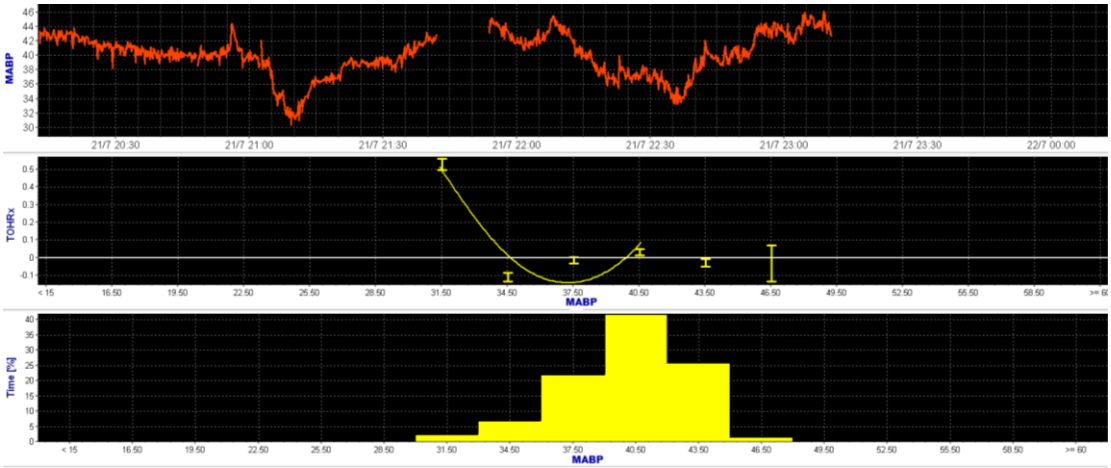

The $MABP_{OPT}$ value for this 4-h-window is around 38 mmHg. The frequency histogram with the percentage of time spent on actual MABP by this infant during this 4-h-window is slightly shifted to values above $MABP_{OPT}$.

The cranial ultrasound performed for at 48 hours of life showed extensive bilateral IVH with HPI (grade IV) as shown in Figure 6.8.

Figure 6.9 Cranial ultrasound at 48 hours

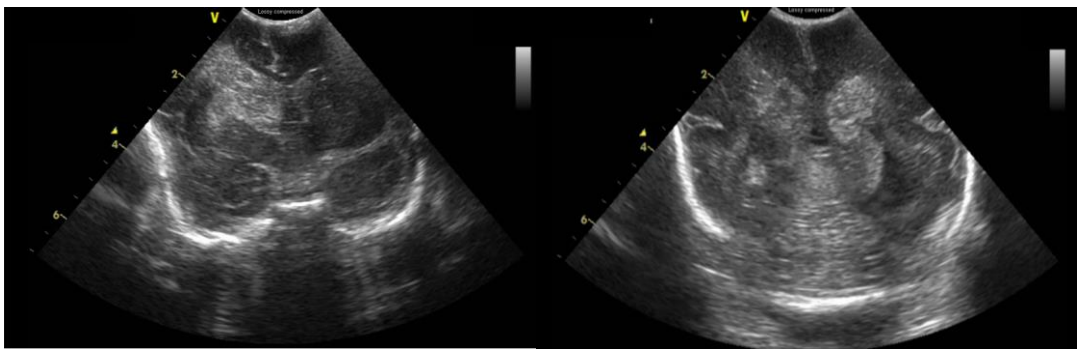

The coronal views above show bilateral IVH grade IV. All images were recorded as part of the data collection for 'SAMBA' study.

6.2.5. Results

The characteristics of all infants included in this study and differences between outcome groups are shown in Table 6.2. The median (range) age of the 44 infants at the start of the study was 5.5 (3.1 - 12.6) hours and the median (range) duration was 18.4 (6.5 – 21) hours.

Table 6.2 Characteristics of the infants included in the study

Variable	Total (44)	No-IVH (28)	IVH (16)	P	Survived (38)	Died (6)	P
Gestational Age (week+days)	25+4 (23+3 – 27+6)	25+2 (23+4 – 27+6)	25+3 (23+3 – 27+4)	0.70[§]	25+3 (23+3 – 27+6)	24+3 (23+5 – 26+3)	0.18[φ]
Birth weight (grams)	755 (520 – 1335)	755 (550-1335)	762 (520-1180)	0.73[§]	755 (550 - 1335)	737 (550 - 1180)	0.60[§]
Gender (M/F)	15/29	16/22	5/13	0.18[Ω]	15/23	0/6	0.08[Ω]
CRIB II	11 (5-16)	12 (8-16)	13 (9-16)	0.24[φ]	12 (8 - 16)	14 (9 - 16)	0.19[φ]
Inotrope	21	15 (53%)	7 (44%)	0.75[Ω]	17 (45%)	4 (67%)	0.40[Ω]
Sepsis	31	17 (61%)	14 (87%)	0.09[Ω]	25 (65%)	5 (83%)	0.65[Ω]

Gestational age, birth weight and CRIB II values are presented as median (range). Remaining variables are presented as frequency.
[φ] Independent samples T-test
[§] Mann-Whitney test
[Ω] Chi-square test

The determination of $MABP_{OPT}$ was possible in 44 infants (100%). Worse clinical status was associated with more impaired cerebrovascular reactivity, demonstrated by the positive correlation between TOHRx and CRIB II score: r = 0.370, P = 0.013. TOHRx had negative correlation with gestational age (GA) at birth, r = - 0.304, P = 0.045.

The mean (standard deviation) $MABP_{OPT}$ was 31.3 (±4.7) mmHg. $MABP_{OPT}$ increased with increasing gestational age, r = 0.424, P=0.004 (Figure 6.10).

Figure 6.10 Correlation between $MABP_{OPT}$ and gestational age

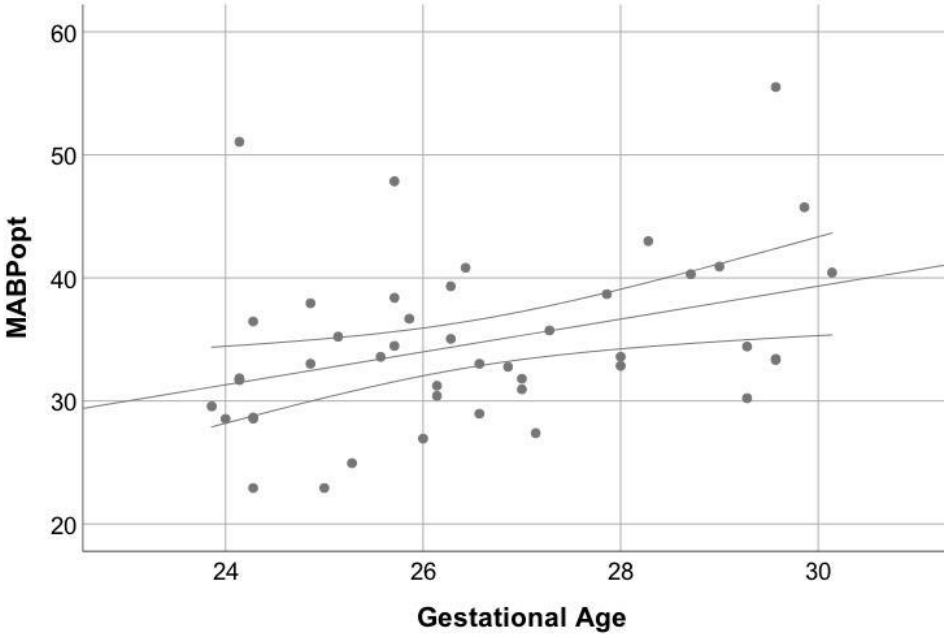

Mean $MABP_{OPT}$ within the first 24 hours of life for each individual infant and gestational age in weeks.

Association between $MABP_{OPT}$ and outcome

The deviation below $MABP_{OPT}$ was higher in the group of infants who developed IVH as shown in Figure 6.11.

Figure 6.11 Association between deviation below $MABP_{OPT}$ and IVH

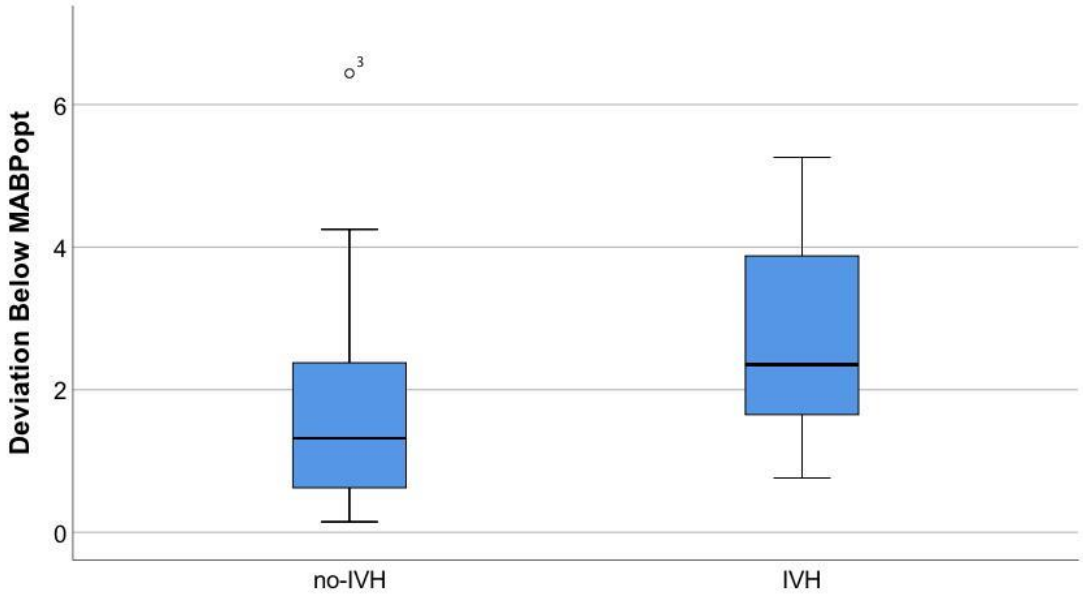

Median (Interquartile Range) deviation below $MABP_{OPT}$ was 1.3 (1.8) for 'no-IVH' group and 2.4 (2.4) for 'IVH' group. P = 0.006 (N = 44). Mann-Whitney test.

The deviation below $MABP_{OPT}$ was significant higher in infants who died compared to those who survived (P = 0.015) (Figure 6.12).

Figure 6.12 Association between deviation below $MABP_{OPT}$ and mortality

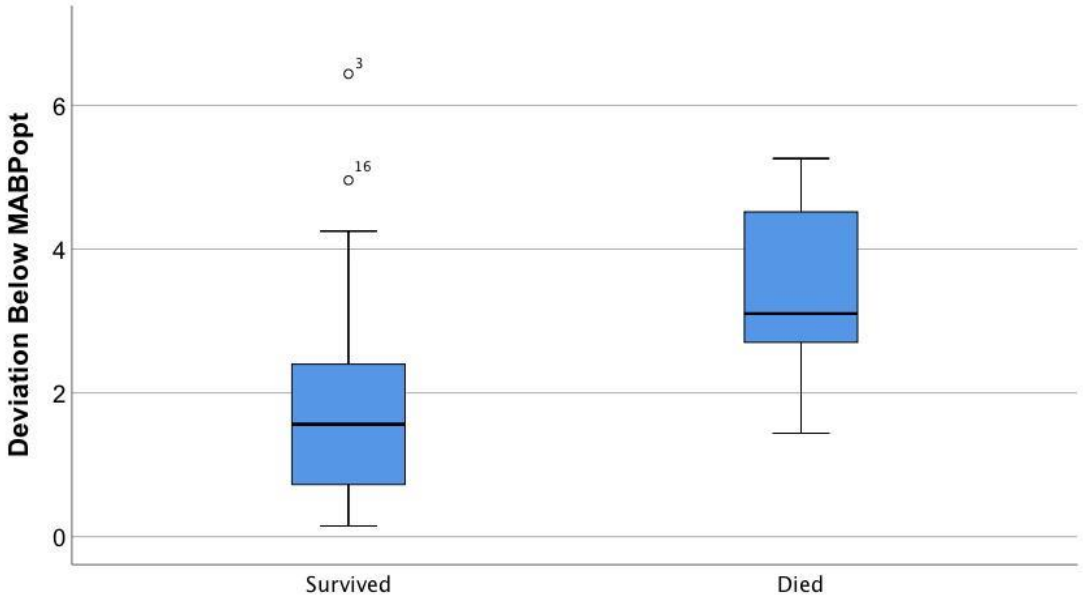

Median (Interquartile Range) for those who survived was 1.6 (1.7) and for those who died was 3.1 (3.8), P = 0.015 (N = 44). Mann-Whitney test.

The median deviation above $MABP_{OPT}$ was higher in the group of infants who did not develop IVH: median (range) 1.8 (0.10 – 3.5) for those infants who did not have IVH was 1.08 (1.37) and for those who developed IVH was 1.2 (0.33 – 3.7), P = 0.026[φ].

There was no difference between mean deviation above $MABP_{OPT}$ and mortality (P = 0.21[φ]).

The differences between mean MABP and mean $MABP_{OPT}$ between infants who developed IVH and did not develop IVH are shown in Table 6.3. There was no difference between mean MABP or mean $MABP_{OPT}$ between infants who died and survived (P = 0.27 [φ] and P = 0.34[§], respectively).

Table 6.3 Association between MABP, $MABP_{OPT}$ and IVH

Mean MABP		
no-IVH Median (range)	**IVH** Median (range)	**P**
30 (24 – 41)	31 (27 – 38)	0.12 [φ]
Mean $MABP_{OPT}$		
no-IVH Median (range)	**IVH** Median (range)	**P**
30 (24 – 48)	33 (27 –39)	0.016[§]

[φ] Independent samples T-test. [§]Mann-Whitney test.

Relationship between $MABP_{OPT}$ and inotropes

MABP was lower in infants who were started on inotropes within the first 24 hours of life (P = 0.001[§]). Similarly, $MABP_{OPT}$ was lower in infants who received inotropes as shown in Figure 6.13.

Figure 6.13 Difference in $MABP_{OPT}$ between inotrope groups

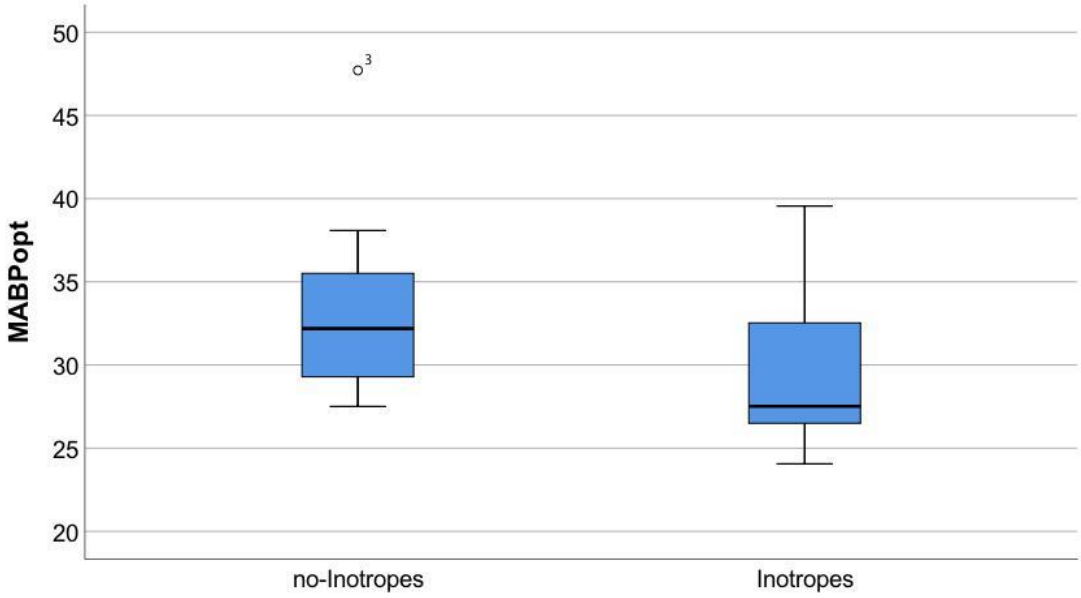

Median (Interquartile Range) for $MABP_{OPT}$ in infants who did not receive inotropes was 32 (6.5) mmHg and 27 (6.2) mmHg for those who received inotropes (P = 0.006). Mann-Whitney test.

There was no statistically significant difference in mean deviation below and above $MABP_{OPT}$ between those infants who received inotropes and did not receive inotropes (Table 6.4).

Table 6.4 Difference between deviation below and above $MABP_{OPT}$ and inotrope

	no-Inotropes Median (range)	**Inotropes** Median (range)	**P**
Mean Deviation Below $MABP_{OPT}$	1.9 (0.2 – 6.4)	1.4 (0.15 – 5.3)	0.79[§]
Mean Deviation Above $MABP_{OPT}$	1.3 (0.1 – 3.4)	1.8 (0.2 – 3.7)	0.14[φ]

[§] Mann-Whitney test [φ] Independent samples T-test

6.2.6. Discussion

In this study, we used TOHRx to define $MABP_{OPT}$ in a different cohort of preterm infants from our previous study. More prolonged periods of continuous NIRS and physiological data were analysed, which allowed us to refine our methodology and, thus, obtain $MABP_{OPT}$ values for 100% of the infants included in this study. $MABP_{OPT}$ was defined in 18.4% more infants compared to our previous study using 'RUMBA' cohort (Chapter 6, section 6.1).

Only data recorded within the first 24 hours of life were included in the data analysis, as the main transitional changes in systemic and cerebral blood flow leading to end organ hypoperfusion may occur within the first hours of life. Moreover, fluctuations in MABP are usually more dynamic within this period[40, 56, 77]. As described in Chapter 5, section 5.1, most infants included in the 'SAMBA' cohort developed IVH just before or after 24 hours of life. Some authors speculate that an IVH that occurs before 12 hours of age could be related to antenatal or perinatal events, such as infection and inflammation, and an IVH that occurs after 12 to 24 hours of age are often related to haemodynamic changes such as fluctuations in MABP and impaired cerebral vascular-reactivity[77, 249, 326]. Therefore, any associations between deviations from

$MABP_{OPT}$ values before 24 hours of age found in our analysis may have a more meaningful relationship with the underlying pathophysiology and outcome.

In this study, we observed that $MABP_{OPT}$ increased with gestational age, following the physiological norms for MABP, as observed in our previous study (Chapter 6, section 6.1)[152, 156, 313]. Mean MABP averaged over the first 24 hours of life had no correlation with IVH or mortality. Several studies have investigated the correlation between MABP and outcome of mortality, brain injury and neurodevelopmental outcome. The majority of these studies found no association between hypotension, which is usually defined as any value of MABP below the gestational age in weeks, and outcome[162, 163, 327]. Dempsey et al. (2009) have suggested that permissive hypotension in extreme preterm infants is not associated with poor outcome, as long as clinical signs of poor tissue perfusion are absent [164]. Studies from more than a decade ago, such as the work published by Bada et al. (1990), observed that infants who developed IVH had larger variability in MABP but only a trend to lower MABP within the first 48 hours of life[158]. On the other hand, the work published by Miall-Allen et al. (1987) showed that infants who had severe IVH and died had lower MABP compared to infants with no brain injury or survived[157]. However, these both studies defined hypotension as any value of MABP below 30 mmHg and none of them correlated MABP with CBF or tissue perfusion[157, 158].

In our study, $MABP_{OPT}$ was significantly higher in the 'IVH group' compared to 'no-IVH group'. Steiner et al. (2002) observed similar relationship in adult patients with traumatic brain injury (TBI). CPP_{OPT} was higher in patients with unfavourable outcome, defined as death or severe disability. They have speculated that higher values of CPP_{OPT} in this group of patients could be related with the severity of the brain injury, as PRx was also higher in patients with poor outcome[170]. Burton et al. (2015) defined $MABP_{OPT}$ in a group of term infants with HIE undergoing therapeutic hypothermia and have also reported higher $MABP_{OPT}$ during rewarming phase in infants who developed motor and cognitive impairment[177]. In our cohort, there was no difference between TOHRx and the outcome of mortality or IVH. However, compared to this study, there is an important difference in both the data collection and time of injury in the populations from the studies from Steiner et al. (2002) and Burton et al. (2015). The assessment of $MABP_{OPT}$ in patients post TBI, in patients

following resuscitation for cardiac arrest and in infants with HIE is based on data recorded after the brain injury occurred whereas in our population data were collected mainly before the IVH occurred. Nevertheless, the difference in $MABP_{OPT}$ between IVH groups in our population could indicate that regulatory vascular mechanism in the brain tissue and possible vascular resistance may have already been impaired before the haemorrhage started.

In our previous study, using data from 'RUMBA' cohort, we observed that mean absolute deviation away from $MABP_{OPT}$ values was higher in infants who died compared to those who survived. We also observed that 40% of those infants who died had MABP below $MABP_{OPT}$ by at least 4 mmHg (average for the entire recording period)[328]. In this new cohort of infants recruited for 'SAMBA' we were able to more consistently define the direction of the deviation away from optimal values. Mean deviation below $MABP_{OPT}$ within the first 24 hours of life was higher in infants who died. The association between deviation below CPP_{OPT} and mortality has been reported in different studies. In adult and paediatric patients with TBI, hypoperfusion was associated with death[168, 170, 172]. Patients who survived and had a good outcome maintained MABP or CPP values close to optimal values. Data on mortality from our study should be considered with caution as all infants died beyond 48 hours of life and the presence of an IVH had no statistical association with mortality. Most infants died due to multi-organ failure or complication of necrotizing enterocolitis (NEC); pathologies that could be related with early hypotension and systemic hypoperfusion (as shown in Chapter 5).

Deviations below $MABP_{OPT}$ have also been associated with brain injury. In infants with HIE undergoing therapeutic hypothermia, higher time and degree of deviation below values of $MABP_{OPT}$ was associated with worse injury to white matter[176]. In our study, mean deviation below $MABP_{OPT}$ was higher in infants who developed IVH and mean deviation above $MABP_{OPT}$ was higher in infants who did not have IVH. In contrast, data from our previous study showed that infants with MABP greater than $MABP_{OPT}$ by at least 4 mmHg had significantly greater IVH scores. However, the main difference between these two cohorts was the age at the start of the data collection. In this 'SAMBA' cohort only data collected before 24 hours of age were analysed, whereas in our previous study ('RUMBA' cohort) the majority of the

infants had data collected after 24 hours of age (median age at the start of the study was 34 hours). It is possible that MABP may increase to levels above $MABP_{OPT}$ just before, during and after the IVH occurs, as suggested by the data shown in the 'Case Reviews'. The frequency histogram described in Figure 6.6 show that actual MABP was below $MABP_{OPT}$ before the haemorrhage started, but around the approximated time when the IVH occurred or it is evolving, the percentage of time of actual MABP spent above $MABP_{OPT}$ is greater (mainly data after 24 hours), as shown in Figure 6.8. Given that hypoperfusion-reperfusion injury is possibly the main mechanism related to development of IVH in preterm infants, the degree of deviations below $MABP_{OPT}$ may represent the level of hypoperfusion injury and deviation above could potentially represent the hyper-perfusion injury. Moreover, mean TOI was lower in extremely preterm infants who developed an IVH (data shown in Chapter 5, section 5.2), supporting the idea that low cerebral blood flow and higher degree of hypoperfusion is present in those infants who subsequently developed brain injury. However, the exact time of bleeding differs from each individual infant, hence, it may be complex to associate the magnitude of deviation above $MABP_{OPT}$ with IVH.

Sick preterm infants show more dynamic variability in MABP and shifts between autoregulatory curves compared to more stable infants. The $MABP_{OPT}$ curve in Figure 6.4 (stable infant) is narrower than the $MABP_{OPT}$ curve shown in Figure 6.6 (unstable infant).

Infants who were started on inotropes had lower mean MABP compared to those who did not required any inotropic support. Similarly, $MABP_{OPT}$ was lower in the group of infants who received inotropes. No difference in deviations above or below from $MABP_{OPT}$ was observed between infants who were started on inotropes and those who did not.

Similar to our previous study, we were unable to use TOx as a marker of cerebral autoregulation to define $MABP_{OPT}$ in this cohort. Observing the data pattern, we noticed that in the cases where a U-shaped curve was created, the TOx values were mainly positive. Preterm infants, especially those born < 28 weeks' gestational age, may possibly be pressure passive within the first 24 hours of age, as shown in Chapter 5, section 5.2. This may have contributed to the failure in obtaining meaningful

$MABP_{OPT}$ curves and correlation between mean $MABP_{OPT}$ and deviations from $MABP_{OPT}$ with outcome.

The relationship between cerebral autoregulation and systolic and diastolic phases of the cardiac cycle may be distinct in preterm infants. Some authors have suggested that in preterm infants, CBF is passive to diastolic blood pressure or could even reach near-zero flow during this phase[329]. Cerebral autoregulation would be more robust during the systolic phase of the cardiac cycle, although pressure reactivity to systolic and MABP may not be observed until 26 to 28 weeks' gestation, according to animal studies. Giving the fact that extremely preterm infants are mainly pressure passive within the first 24 to 48 hours of life, TOHRx may reflect the direct changes in cardiac output through changes in HR.

Limitations

Although the determination of $MABP_{OPT}$ values were obtained for all infants included in this study, the presence of $MABP_{OPT}$ curve was variable during the study and for some infants it was present only in a small percentage of the recording time. A similar problem has been addressed in studies on CPP_{OPT} in patients with TBI[170, 172]. Low MABP variability, impaired cerebral autoregulation and interference with sedative or vasoactive drugs have been associated with failure in the method to obtain CPP_{OPT}[330]. Recent work published by Weersink et al. (2015) investigated the clinical and physiological events that may contribute to failure in obtaining CPP_{OPT} values in a group of patients with TBI. They observed that persistent high values of PRx (severe impaired cerebral autoregulation) were associated with failure in the method to obtain values of CPP_{OPT} in patients with TBI[330]. Consistently positive values of PRx, TOx or TOHRx may preclude the existence of a Lassen autoregulation curve and, therefore, the determination of $MABP_{OPT}$. Moreover, the use of dopamine and dobutamine in nearly half of our population may have contributed to the failure in obtaining consistent values of $MABP_{OPT}$ and the association with outcome. Weersink et al. (2015) have also suggested that vasoactive drugs may have an impact on the calculation of CPP_{OPT}[330]. To improve the percentage of time we can obtain reliable $MABP_{OPT}$ values, recent work published by Liu et al. (2017) has suggested the use of multi-window and weighting calculation algorithm for calculation of CPP_{OPT}. By using this method, more continuous and stable CPP_{OPT} curves were obtained without

changing the relationship between difference in actual CPP and CPP_{OPT} and outcome[331].

Carbon dioxide (CO_2) is a vasodilator and a potential confounder in studies assessing cerebral autoregulation[92]. In our study, continuous monitoring of transcutaneous CO_2 was attempted; however obtaining reliable values was a challenge. Data on transcutaneous CO_2 was not acquired for all infants due to technical problems or due to fragile skin conditions in the very small and immature infants. Regular arterial blood gases were performed and $PaCO_2$ was maintained as stable as possible. Similar to our previous study, we cannot exclude an effect of CO_2 on our data. It is possible that if cerebral vascular reactivity is impaired due to CO_2 this may have had an impact on the calculation of $MABP_{OPT}$ curves and, thus, contributed to the problem on obtaining $MABP_{OPT}$ curves. Future studies should improve the methods to obtain reliable CO_2 measurements and include them to the methodological model of $MABP_{OPT}$ calculation.

Fluctuations on peripheral blood oxygen saturation (SaO_2) could be a confounder factor as we used TOI as a surrogate measure of CBF. Moreover, hypoxia is a powerful vasodilator. However, major episodes of profound desaturations (SaO_2 < 90%) were removed from the data during manual artefact removal and short periods of desaturations did not interfere with the final $MABP_{OPT}$ calculation as observed during a small sub-analysis of the data.

7. COMPLEXITY OF BRAIN AND SYSTEMIC SIGNALS IN PRETERM INFANTS UNDERGOING INTENSIVE CARE

The results presented in this section have been published in *Journal of Cerebral Blood Flow and Metabolism*[332].

7.1. COMPLEXITY OF BRAIN SIGNALS IN PRETERM INFANTS IS ASSOCIATED WITH OUTCOME

7.1.1. Background

Biological systems are characterised by complex regulatory mechanisms that interact in a non-linear way. Therefore, a non-linear method to assess physiological signals may reveal more accurately the magnitude of changes over time. As described in Chapter 3, section 3.1.4, Analysis of Entropy has been described as method to measure the unpredictability and randomness of a biological system. More recently, Multiscale Entropy (MSE) analysis has been used to assess the irregularity and complexity of biological time series data.

7.1.2. Aims

The aim of this study was to apply MSE to study the complexity of cerebral NIRS signals and the complexity of systemic physiological signals in a cohort of preterm infants undergoing intensive care. We further hypothesize that the complexity index (CoI) of cerebral NIRS signals and systemic signals, measured using MSE, correlate with IVH and mortality in this population.

7.1.3. Methods

This prospective observational study included data from infants recruited for both 'RUMBA' and 'SAMBA' cohort. Data recorded within the first 24 hours of life was

included in the analysis. The recruitment details, ethics, population and pre-processing data analysis were described in Chapter 4 (Methods).

Multiscale Entropy Analysis[2]

MSE analysis was performed using algorithm published originally by Costa et al[224, 225]. Briefly, the analysis can be divided into three steps: constructing coarse-grained time series, computing sample entropy for each of them, and calculating overall complexity[333]. Coarse-grained time series for scale τ is derived from original time series by averaging its τ samples in a moving (non-overlapping) window. Thus, time series for scale τ is τ times shorter than original time series. Particularly, for scale one we get simply original time series. For each coarse-grained time series sample entropy was computed. Sample entropy estimates the probability that similar sequences of m consecutive points in time series will also be similar when sequences of the length m+1 are considered. To be precise, two sequences containing the same number of points are considered similar if the absolute differences between their corresponding points are smaller than a specified tolerance value r. Sample entropy is calculated as the negative natural logarithm of the ratio of the total number of (m+1)-point template matches to the total number of corresponding m-point template matches [223]. Higher values of sample entropy indicates that time series is more irregular and less predictable. We assumed $m = 2$ and $r = 0.15 \cdot SD$ where SD denotes standard deviation of analysed time series, as originally proposed by Costa et al [225].

MSE was calculated up to scale 20 [224, 226]. It can be presented as a function of scale factor (~~Fig. 2~~). The area under MSE curve, or in other words the sum of sample entropy values for all scales, was defined as the Complexity index (CoI) [226, 333].

[2]The multiscale entropy analysis described in this section was performed by Mr Michal Placek.

7.1.4. Results

Sixty-one preterm infants were included in this study. The mean (SD) age at the start of the study was 8h (± 5h). Fifty-seven (93%) infants had antenatal steroids and all infants were intubated and received surfactant within 10-20 minutes of birth. Thirty-four (55.7%) had a further one to three doses of surfactant after admission. All infants were receiving mechanical ventilation at the start of the study. Demographic data and differences between groups are shown in Table 7.1.

Table 7.1 Demographic data of enrolled infants

Variable	Total (N = 61)	no-IVH (N = 41)	IVH (N = 20)	P	Survived (N =53)	Died (N = 8)	P
Gestational age (weeks + days)	26+6 (23+3 – 31)	26+6 (23+4 – 31)	25+5 (23+3 – 29+2)	0.12[φ]	26 (23+3 – 30+1)	26 (24+1 – 31)	0.88[φ]
Birth weight (grams)	805 (525 – 1355)	805 (525 – 1355)	802 (550 – 1320)	0.98[§]	810 (525 – 1355)	767 (575 – 1180)	0.72[§]
Gender (Male/Female)	26/35	20/21	6/14	0.18[Ω]	23/30	3/5	1.0[Ω]
CRIB II	11 (5 – 16)	10 (5 – 16)	12 (9 – 16)	**0.025[§]**	11 (5 – 16)	12 (8 – 16)	0.33[§]
Inotrope medication	27 (43.3%)	18 (43.9%)	9 (45%)	1.0[Ω]	21 (39.6%)	6 (75%)	0.12[Ω]
Sepsis	37 (60.7%)	21 (51.2%)	16 (80%)	**0.023[Ω]**	30 (56.6%)	7 (87.5%)	0.24[Ω]

Characteristics of enrolled infants and differences between no-IVH (intraventricular haemorrhage) and IVH groups and between infants who survived and died. Gestational age, birth weight and CRIBII (clinical risk index for babies II) are presented as median (range). Gender is presented as absolute numbers. Remaining variables are presented as frequencies.
[φ]Independent samples t-test. [§]Mann-Whitney test. [Ω]Chi-square test

The median (range) gestational age was 26 weeks + 5 days (23+3 -31); 75% were extremely preterm infants (born at less than 28 weeks). Twenty infants (32.8%) developed an IVH; six of them had an IVH diagnosed within the first 24 hours of life. Of those who developed an IVH, 10 infants had a grade II IVH, 4 had IVH a grade III IVH and 6 had a grade IV IVH. Only one infant had minimal bleeding in the germinal matrix (small grade I IVH) and, therefore, this infant was included in the non-IVH group. Eight infants (13.1%) died before term corrected age of 40 weeks. Seven of them were born before 28 weeks of gestational age (extremely preterm infants) and one was born at 30 weeks + 2 days, who was a severe in-utero growth restricted (IUGR) infant and birth weight of 700g. All infants who died had signs of antenatal or perinatal hypoxia, resulting from either: severe IUGR, twin-twin transfusion, cord prolapse or profound hypotension and hypoplastic lungs. Four of those infants who died (50%) also had an IVH diagnosed. There was no statistical correlation between mortality and IVH (P=0.42).

Examples of monitoring of brain and systemic signals are presented in Figure 7.1**A** (infant who died) and Figure 7.1**B** (infant who survived).

Figure 7.1 Monitoring of brain and systemic signals

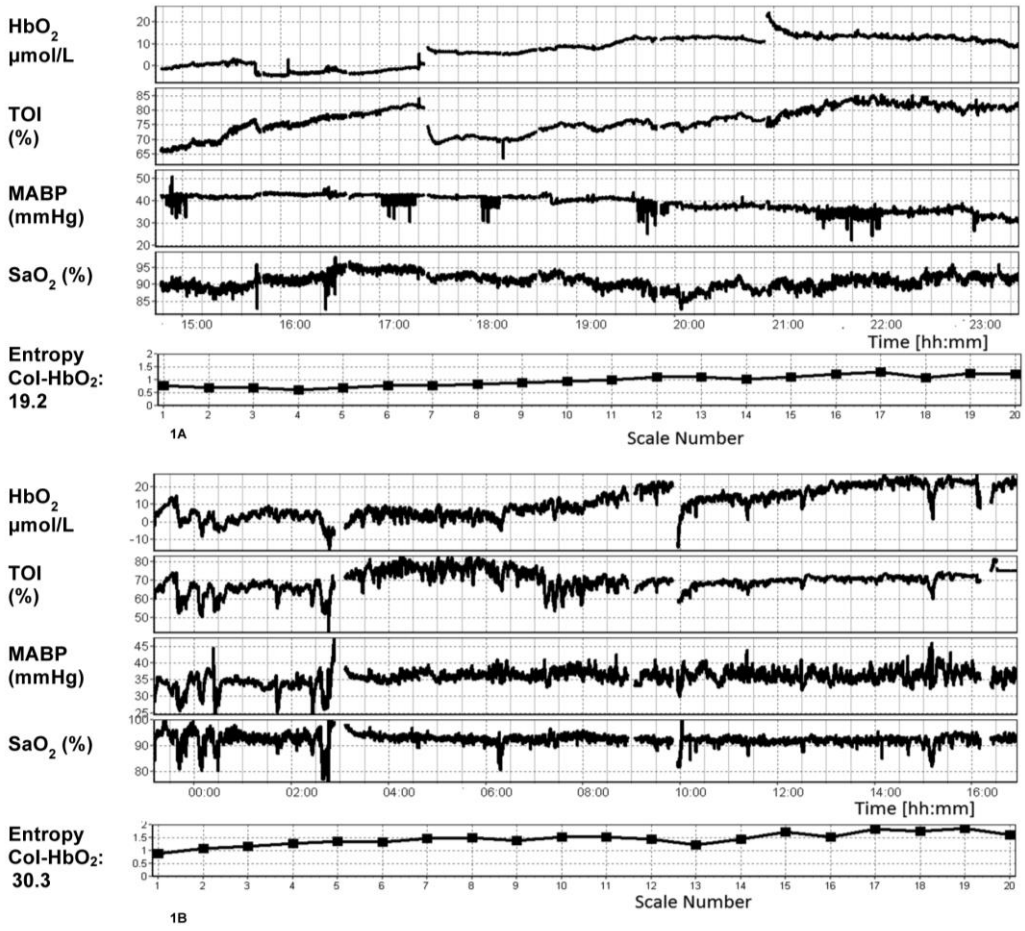

Example of brain and systemic signal monitoring for an infant who died (1A) and survived (1B).

Figure 7.2 shows average MSE plots of HbO_2 and Hb for the whole cohort of patients. Sample Entropy values were averaged individually for each scale and plotted against the scale. This was done separately in groups of those infants who had IVH and did not have IVH, as well as those infants who died and survived. It can be observed through the lower value of sample entropy at each scale factor, resulting in a decrease in overall complexity index, that infants who developed IVH or died had consistently lower entropy in the NIRS signals.

Figure 7.2 Multiscale entropy between outcome groups

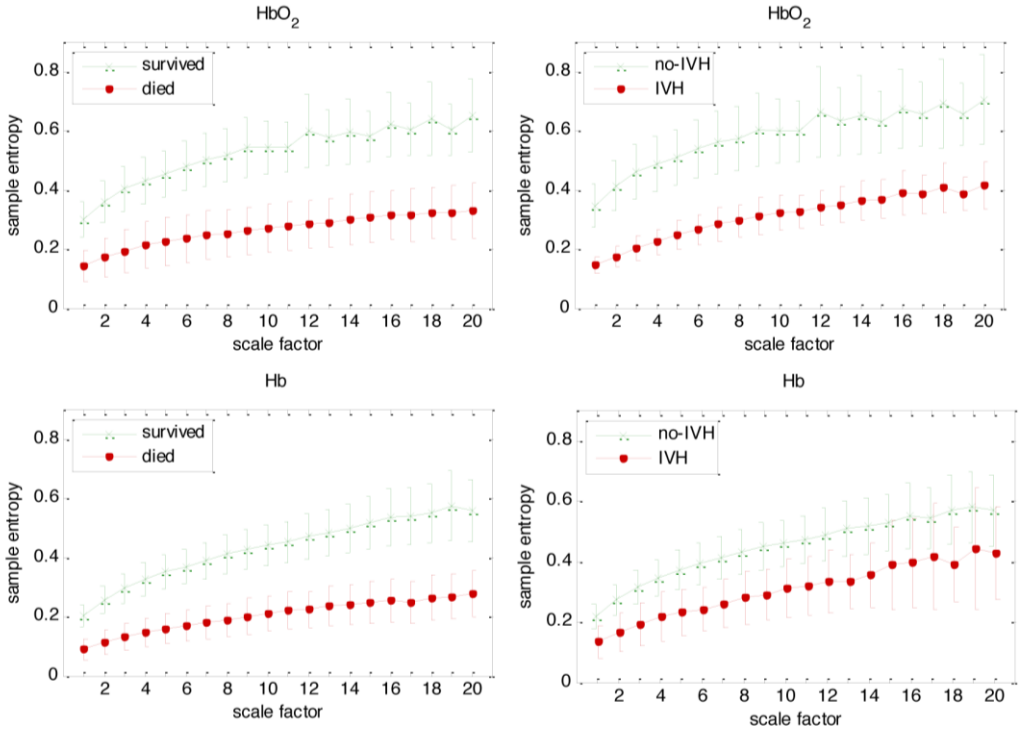

Results are mean ± 1.96 standard error of mean. Oxygenated haemoglobin (HbO_2) and deoxygenated haemoglobin (Hb)

Association between brain and systemic signals with outcome

Lower mean CoI-HbO_2, CoI-Hb and CoI-TOI were observed in those infants who developed IVH compared to those who did not (Table 7.2). However, there was no difference in mean CoI-THI between the two groups (Table 7.2). Mean TOI was not significantly different between infants who had IVH and those who did not have IVH (P=0.38).

Decreased complexity of brain signals was observed in infants who died. Mean CoI-HbO_2 (Table 7.2), CoI-Hb and CoI-THI were lower in those infants who died compared to those who survived (Table 7.2). CoI-TOI just failed to reach statistical significance (P=0.057). There was no difference in mean TOI between these two groups (P=0.52).

There was no difference between mean CoI of mean arterial blood pressure (MABP), mean CoI-HR and mean CoI-SaO_2 between those infants who developed IVH and

those who did not (Table 7.2). Mean MABP, mean SaO_2 and mean HR were not different between these two groups (P=0.52, P=0.46 and P=0.91, respectively). In contrast, mean CoI-MABP was lower in those infants who died compared to those who survived. However, there was no difference in mean CoI-SaO_2 or mean CoI-HR between these two groups (Table 7.2). There was no difference between MABP, SaO_2 and HR between those infants who survived or died (P=0.79, P=0.38 and P=0.20, respectively).

Complexity of brain signals as an independent predictor of IVH

Out of all the studied parameters and demographic data only CRIB II (P=0.031), sepsis (P=0.025) and CoI-HbO_2 (P=0.004) were identified by binary logistic regression analysis as predictors of IVH when individual analysis was performed for each of these variables (Table 7.2). Subsequently these variables were entered as co-variants in a binary logistic regression model. The continuous variables in the model met the assumption of linearity and there were no studentized residuals. Of the three-predictor variables only CoI-HbO_2 remained statistically significant, showing that decreased complexity was independently associated with an increased likelihood of having IVH (Table 7.3 and Table 7.4).

CoI-HbO_2 had no correlation with sepsis (P=0.074) or CRIB II (P=0.138).

Table 7.5 shows the matrix of univariate correlations between CoIs of systemic and brain signals.

Table 7.2 Differences in complexity of brain and systemic signals between outcome groups

	IVH	No-IVH	P	Died	Survived	P
CoI-HbO_2	6.24 (5.02 – 7.45)	11.69 (9.43 -13.96)	0.002	5.30 (3.26 – 7.35)	10.60 (8.74 – 12.45)	0.012
CoI-Hb	6.16 (7.54 –10.71)	9.03 (7.54 –10.71)	0.010	4.09 (2.77-5.36)	8.69 (7.28-10.15)	0.004
CoI-TOI	10.09 (7.62 –12.93)	13.9 (11.94 –16.25)	0.038	8.96 (5.48-13.21)	13.36 (11.43-15.26)	0.057
CoI-THI	4.44 (2.96-6.72)	6.23 (4.64-8.60)	0.242	2.38 (1.48-3.35)	6.16 (4.69-7.97)	0.003
CoI-MABP	17.85 (14.33-21.37)	21.68 (19.12-24.25)	0.82	14.98 (10.305 – 19.722)	21.25 19.24 – 23.41)	0.04
CoI-SaO2	17.43 (14.92-19.94)	18.07 (16.21-19.93)	0.35	16.01 (12.54-19.48)	18.14 (16.52-19.76)	0.16
CoI-HR	18.65 (15.31-21.99)	20.72 (18.34-23.10)	0.31	17.16 (12.58-21.74)	20.47 (18.38-22.57)	0.24

Mean and 95% confidence interval for complexity index (CoI) of NIRS and systemic physiological signals.

Table 7.3 Binary logistic regression for CoI-HbO_2, Sepsis and CRIB II as predictor of IVH – Univariate Model

	B	S.E.	Wald	df	P	Odds Ratio	95% CI for Odds Ratio	
							Lower	Upper
CoI-HbO_2	-0.236	0.082	8.286	1	0.004	0.790	0.637	0.928
Constant	1.247	0.667	3.496	1	0.062	3.481		
	B	**S.E.**	**Wald**	**df**	**P**	**Odds Ratio**	**95% CI for Odds Ratio**	
							Lower	**Upper**
Sepsis	1.574	0.704	4.993	1	0.025	0.207	0.052	0.824
Constant	-0.272	0.332	0.672	1	0.413	0.413		
	B	**S.E.**	**Wald**	**df**	**P**	**Odds Ratio**	**95% CI for Odds Ratio**	
							Lower	**Upper**
CRIB II	0.234	0.108	4.663	1	0.031	1.264	1.022	1.563
Constant	3.371	1.303	6.692	1	0.010	0.034		

Sepsis is for presence of sepsis compared to no sepsis. CoI-HbO_2: complexity index of oxygenated haemoglobin; CRIB II: clinical risk index for babies.

Table 7.4 Binary logistic regression for CoI-HbO_2, Sepsis and CRIB II as predictor of IVH –Multivariate models

	B	S.E.	Wald	df	P	Odds Ratio	95% CI for Odds Ratio	
							Lower	Upper
CoI-HbO_2	-0.216	0.083	6.706	1	0.010	0.806	0.684	0.949
CRIB II	0.249	0.144	2.979	1	0.081	0.248	0.967	1.701
Sepsis	-1.395	0.799	3.049	1	0.081	0.248	0.052	1.186

Sepsis is for presence of sepsis compared to no sepsis. CoI-HbO_2: complexity index of oxygenated haemoglobin; CRIB II: clinical risk index for babies.

Table 7.5 Correlation between complexity index of brain and systemic signals

		CoI-HbO2	CoI-Hb	CoI-TOI	CoI-THI	CoI-SaO2	CoI-MABP	CoI-HR
CoI-HbO2	r_s	1.000	**.696**	**.442**	**.411**	**.301**	**.428**	**.330**
	P		**.000**	**.000**	**.001**	**.018**	**.001**	**.009**
CoI-Hb	r_s	**.696**	1.000	**.358**	**.412**	.242	**.412**	**.290**
	P	**.000**		**.005**	**.001**	.060	**.001**	**.024**
CoI-TOI	r_s	**.442**	**.358**	1.000	**.330**	.238	**.336**	**.307**
	P	**.000**	**.005**		**.012**	.065	**.008**	**.016**
CoI-THI	r_s	**.411**	**.412**	**.330**	1.000	**.262**	**.279**	.223
	P	**.001**	**.001**	**.012**		**.049**	**.035**	.096
CoI-SaO2	r_s	**.301**	.242	.238	**.262**	1.000	**.351**	**.270**
	P	**.018**	.060	.065	**.049**		**.006**	**.035**
CoI-MABP	r_s	**.428**	**.412**	**.336**	**.279**	**.351**	1.000	**.681**
	P	**.001**	**.001**	**.008**	**.035**	**.006**		**.000**
CoI-HR	r_s	**.330***	**.290**	**.307**	.223	**.270**	**.681**	1.000
	P	**.009**	**.024**	**.016**	.096	**.035**	**.000**	

r_s = Spearman's rank correlation coefficient. P values are not adjusted for multiple comparisons. * P<0.05

Correlation between complexity of brain signals and indexes of cerebrovascular reactivity

TOHRx had negative correlation with CoI-TOI (r_s= -0.353, P=0.005), with CoI-MABP (r_s= -0.378, P=0.003) and CoI-HR (r_s= -0.324, P=0.011). In contrast, TOx had no significant correlation with complexity of brain signals. TOx had negative correlation with CoI-HR (r_s = -0.330, P=0.009). TOx had no other significant correlation with the complexity of systemic signals.

7.1.5. Discussion

This study is the first to assess the complexity of cerebral NIRS signals in critically ill preterm infants. We applied MSE to study the complexity of brain and physiological systemic signals in a cohort of preterm infants in the first 24 hours of life. The results revealed an association between complexity of brain signals and outcome.

Several studies have suggested that decreased variability in physiological signals is a sign of failure in complex regulatory system. In perinatal medicine, the 'silent pattern' in fetal ECG is a well-known example of loss of 'natural' variability of vital signs and has been associated with poor neonatal outcome[334]. However, in clinical practice, there is no consensus on which method of intrapartum monitoring is the most effective[335]. Moreover, the continuous monitoring of neonatal vital signs does not take in consideration the non-stationarity characteristic of the biological signals. Entropy analysis has been extensively studied to investigate physiological systems. According to the 'decomplexification' theory of illness, loss of complexity is usually associated with pathological states like diseases or ageing. However, despite being an old concept, assessment of complexity of physiological signals in the neonatal unit is not performed routinely. Moreover, clinicians persist to correlate lack of variability as a sign of clinical stability. In our study, decreased complexity of brain signals was observed in those infants who developed IVH and who died, supporting the 'decomplexification' theory[219, 336]. MSE of HbO_2 and Hb were consistently lower in all scale factors for groups of infants with IVH compared to those who did not have IVH, and for groups of infants who died compared to those who survived. These results are similar to recently published work using MSE to investigate the association

between complexity of EEG and neurological outcome in a cohort of term infants with refractory neonatal seizures[26]. Lower values of MSE were observed in most scales in the group of infants who later developed epilepsy, compared to normal controls, and to those who did not develop epilepsy. In adults with traumatic brain injury, a decrease in entropy of ICP signals across all MSE scales was observed during the development of intracranial hypertension and loss of cerebrovascular reactivity. In this cohort, the CoI was significantly lower in those patients who had moderate and severe disability compared to those who had good outcome [226].

High complexity reflects strong, non-linear interactions between different healthy control systems responding to transient stressors or adapting to changes in the environment. The impairment of those regulatory mechanisms or the breakdown in their interactions is characterized by low complexity of various relevant physiological measurements. This may manifest itself in the total breakdown of (auto and cross) correlations of the measured signals (e.g. instantaneous change in heart rate in atrial fibrillation) or patterns that are overly regular and deterministic in nature (e.g. flat heart rate dynamic seen in chronic heart failure)[216, 337]. Assuming that the impairment of certain physiological control systems occurs before the onset of clinical symptoms of the developing pathology, or even assuming that such impairment could be the potential cause of diseases, a decrease in complexity could serve as an alert of complications like sepsis or poor outcome [226, 338]. In our study, complexity of HbO_2 was an independent predictor of IVH and decreased complexity of brain signals within the first 24 hours of life was observed in those infants who died later during admission, suggesting that the loss of interaction between control systems may be present even before the occurrence of brain injury and death. This could potentially, from early hours of life, divide those infants who are at more risk of poor outcome to those who are more likely to have less morbidity. While the ultimate goal of early analysis of physiological signals would be to identify the 'high risk' infants and develop therapies to prevent IVH and death, identifying those who are 'healthy' could help clinicians to be less invasive and differentiate between normal physiological to pathological adaptation.

The lower complexity of HbO_2, Hb and TOI in those infants who developed IVH may reflect, at least partially, the underlining loss of cerebrovascular reactivity that precedes the occurrence of IVH, as most infants developed IVH after the first 24 hours of life. Changes in cerebrovascular reactivity and loss of autoregulation within the first hours of life have been associated with the incidence of IVH in preterm infants[76, 78, 80]. Several studies have shown that cerebral hypo-perfusion is associated with the pathophysiology of IVH and death[145, 146]. In our study, most infants who died were extremely preterm and all of them had some degree of either antenatal or early postnatal hypo-perfusion or hypoxia. Even those infants who died due to NEC or sepsis were severely sick within the first days of life. Decreased oxygenation has been associated with death as shown in a large cohort of infants included in the BOOST-II trial. In this study, infants with lower oxygen saturation target had higher rate of NEC requiring surgery or causing death[339]. In our cohort, target SaO_2 was kept the same (between 91%-95%) in all groups and there was no difference between mean SaO_2 and CoI-SaO_2 between those infants who died or survived or between those who developed IVH and who did not. However, cerebral hypo-perfusion and loss of cerebrovascular reactivity and may be associated with reduced complexity of cerebral NIRS signals. This hypothesis should be tested in a larger cohort where other factors related with changes in cerebral blood flow, like $PaCO_2$, are also taken into consideration.

In adults, early assessment of complexity of HR and HRV measured by MSE has been used to predict outcome in patients with traumatic brain injury and acute stroke [218, 340]. In neonates, early monitoring of systemic blood flow and cerebral oxygenation has been used to understand the pathophysiology of brain injury in preterm infants [56, 73, 145, 341]. Although the incidence of severe IVH and mortality in this population has decreased in the last 20 years, with improved survival, the prevalence remains high, as does the degree of disability and morbidity in survivors [9]. Preterm infants who develop IVH are at risk of higher morbidity during the neonatal period and later in childhood, including the development of post-haemorrhagic ventriculomegaly, recurrent hospital admissions and mortality. In addition, they may present long-term neurodevelopment and cognitive delays, resulting in increased workload for the health and educational services [4, 7]. Studies using cerebral NIRS have attempted to define

limits of cerebral autoregulation and thresholds of cerebral oxygenation, in order to prevent the occurrence of IVH and improve outcome [137, 141, 210]. However, there is no established threshold of cerebral perfusion and the continuous assessment of cerebrovascular reactivity and oxygenation has not yet been proved to change the outcome of preterm infants. In this context, the analysis of complexity of cerebral NIRS signals may offer a new approach - perhaps an alternative if not a complementary one to the cerebrovascular reactivity assessment - in order to understand the physiological mechanisms involved in the developing brain and to identify those infants who are more likely to be severely sick or even die during the neonatal period.

Complexity of brain signals demonstrated stronger association with outcome than complexity of systemic signals. In our study the complexity of MABP was the only complexity of systemic physiological signals that correlated with outcome. Decreased complexity of MABP was associated with mortality but not with IVH. In clinical practice, the assessment of organ perfusion in preterm infants still relies on indirect measures of systemic blood flow, such as MABP. In adults, the regulation of cerebral perfusion is independent of systemic perfusion. The healthy adult brain has mechanisms that protect its tissue against ischaemic damage. The complexity of cerebral NIRS signals may represent a more direct measure of cerebral perfusion and regulation of blood flow than the complexity of systemic signals. On the other hand, the positive correlation between complexity of systemic and brain signals may suggest that factors associated with loss of cerebral and systemic regulatory mechanisms are related to each other. Further studies are needed to explore the significance of this relationship. Nevertheless, our findings support the idea that the monitoring of brain signals in addition to systemic signals would provide more comprehensive grounds for understanding the physiological mechanisms related to mortality and brain injury in preterm infants.

Limitations

MSE analysis requires a large data set to be able to estimate complexity in a plausible way. The minimum number of samples from time series that allows reasonable MSE calculation rises with the number of scales. It can be estimated that at least 2000 data

samples are required to perform analysis up to scale twenty [342]. In our study, the analysed time series had one sample every 10 seconds, so at least a 6-hour long monitoring period was required to produce meaningful values. Furthermore, MSE analysis is relatively sensitive to outliers and artefacts. Removing a small percentage of them is allowed, however, if the structure of time series is grossly altered due to artefact removal, the value of entropy may also change [225]. The amount of data containing artefacts from our cohort was small, but the artefacts were manually and retrospectively removed. Real-time bedside analysis would require appropriate automatic artefacts detection and removal as well as a criterion for automatic rejection of data segments with too high artefacts content.

Our results of the mortality analysis have to be treated with some caution. Although the association between complexity and mortality was significant, we acknowledge that our sample was small and unbalanced, as only eight infants died. Moreover, most infants in our cohort died later during the neonatal period due to factors which were not necessarily directly related to changes in cerebral perfusion within the first days of life, as sepsis and NEC. However, all infants who died had signs of antenatal or perinatal hypoxia and remained very sick throughout the neonatal admission. Further studies with a larger sample size should be conducted, in order to understand the factors associated with decreased complexity of brain signals in sick preterm infants. However, early recruitment should be taken in consideration to better understand the pathophysiology of brain injury. We aimed to recruit infants before 12 hours of age, but this may have contributed to our limited our sample size, in view of the challenges of getting informed consent from parents soon after the delivery of a sick preterm infant.

8. CARDIAC FUNCTION DURING THE EARLY TRANSITIONAL CIRCULATION IN PRETERM INFANTS

8.1. CHANGES IN SYSTEMIC BLOOD FLOW, CEREBRAL OXYGENATION, CEREBROVASCULAR REACTIVITY AND DUCTAL PATENCY WITHIN THE FIRST 48 HOURS OF LIFE

8.1.1. Background

Preterm infants are at an increased risk to develop low systemic blood flow and poor cerebral oxygenation within the first hours following birth, as described in Chapter 2. Functional echocardiography has been used as a clinical and research tool to assess changes systemic blood flow during the transitional circulation in preterm infants. Measurements of cardiac output, SVC flow and ductal patency have been used to guide clinicians on the management of sick infants, as seen in Chapter 3, section 3.2. However, the correlation between measurements of functional echocardiography and cerebral blood flow and oxygenation remains controversial.

8.1.2. Aims

The aims of this study were:

1) To describe the measurements of systemic blood flow and cerebral oxygenation in a cohort of preterm infants born < 32 weeks within the first 48 hours of life and the relationship of these measurements with outcome of IVH.

2) To investigate the correlation between systemic blood flow and cerebral oxygenation measurements.

3) To investigate the difference in the pattern of changes in systemic blood flow and cerebral oxygenation between infants who had and did not have IVH.

4) To describe PDA measurements during early transitional circulation in sick preterm infants and the relationship between these measurements with outcome, and to further investigate the relationship between a haemodynamically significant PDA and measurements of cerebral oxygenation and cerebrovascular reactivity.

8.1.3. Methods

This prospective observational study included preterm infants who were recruited to the 'SAMBA' cohort only, as these were the only infants who had functional echocardiography after birth. The recruitment details, ethics, population and pre-processing data analysis were described in Chapter 4.

The echocardiographic images and measurements included in this study were described in Chapter 4, section 4.3.3. Measurements of LVO, RVO, SVC and PDA were included in the data analysis. The following NIRS signals were included: TOI, TOEF, TOx and TOHRx. NIRS signals were calculated as described in Chapter 4, section 4.3.1 and section 4.4.1. All NIRS signals were averaged over 45-60 minutes before or before and around the time when echocardiography studies were performed in order to avoid artefacts due to handling or confounders, such as fluid boluses or changes in inotrope/vasopressor infusions.

PDA measurements were considered haemodynamically significant (hsPDA) according to two different criteria:

- PDA 2D size > 1.5 mm or
- PDA > 1.5 mm **AND** LA:Ao ratio > 1.4 or LPA EDF velocity > 2 m/sec or presence of reversal EDF in the post-ductal aorta (**Ao**)

Data distribution was assessed for normality using Shapiro-Wilk test before each statistical test was performed. Independent-samples t-Test (φ) or Mann-Whitney U test (§) were used to investigate the association between mean values of cardiac output and PDA measurements, and mean values of NIRS signals with outcome. Chi-square test (Ω) was used to compare groups with dichotomous variables. Pearson

correlation coefficient (r) or Spearman correlation (r_2) was used to assess the relationship between functional echocardiographic measurement and NIRS signals. ANOVA with Bonferroni correction (δ) and Kruskall-Wallis test (ω) were applied for multiple comparisons between mean values of systemic blood flow and cerebral oxygenation between time intervals.

To provide prediction models for the differentiation between patients with and without IVH concerning pattern of changes across measurements, the relationships between the variables of interest and the different measurement time points were expressed as linear mixed effects models (R package lme4). As fixed effects, we entered the variable of interest and the patient group (condition status: IVH and no-IVH) into the model. As random effects, we had intercepts for the repeated measurement points for each patient. The chi-square and the P-values for comparison of the models were obtained by likelihood ratio tests of the full model with random intercepts against the null model without random intercepts.[3]

8.1.4. Results

General characteristic of the enrolled infants and outcome data

Echocardiographic measurements were performed in 50 infants included in the 'SAMBA' cohort. Cardiac data from two infants were excluded from the analysis because they were diagnosed with cardiac malformations that could affect flow measurements: one infant had a VSD and another had a double SVC. Two infants had normal cardiac morphology within the first 48 hours of life, but developed valve complications later during their neonatal admission: one infant developed aortic stenosis with left ventricle hypertrophy (diagnosed on day 37 of life), and the other infant developed severe pulmonary valve stenosis requiring vavuloplasty. One infant had hypertrophic heart and developed pericardium effusion after 24 hours of life,

[3] The linear mixed model analysis described in this chapter was performed in collaboration with Dr Danilo Cardim.

therefore data from the 48 hours scan were excluded from the analysis. Four infants were diagnosed with PPHN requiring nitric oxide (NO). Nineteen infants did not have echocardiographic measurements at 6 hours of age because the study started around 12 hours of age. Nine infants did not have echocardiographic measurements at 12, 24 or 48 hours either due to clinical deterioration at the time of the scan or because I was not available to perform the scans.

Table 8.1 Demographic data of all infants that had echocardiographic measurements and were included in the data analysis

Variable	Total = 48
Gestational age (weeks + days)	25+5 (23+3 – 31)
Birth weight (grams)	755 (520 – 1350)
Male/Female	15:33
Apgar score at 5 min	7 (1 – 9)
CRIB II	12 (5 – 16)
Antenatal steroids	100%
$MgSO_4$	12 (25%)
Vaginal delivery	26 (54.2%)
Inotropes	26 (54.2%)
NO for PPROM/PPHN	4 (8.3%)
PDA treatment	17 (35.4%)
Sepsis	29 (60.4%)
Confirmed NEC	13 (27.1%)
CLD	24 (50%)
Laser for ROP	4 (8.3%)
IVH	16 (33.3%)
Mortality	7 (14.6%)

Gestational age, birth weight, Apgar score and CRIB II score are presented as median (range). The remaining variables are presented as frequency. NO: nitric oxide. PPROM: premature prolonged rupture of membranes. PPHN: persistent pulmonary hypertension of the newborn. NEC: necrotizing enterocolitis. CLD: chronic lung disease. ROP: retinopathy of prematurity.

Seven infants died before 40 weeks corrected gestational age. These infants died due multi-organ failure due to complications of extreme prematurity, fulminant NEC and sepsis (as described in Chapter 5, section 5.1.4). None of the infants died before 48 hours of age.

Sixteen infants developed IVH; eight of them were classified as severe IVH (grade III or IV).

Seventeen (35%) infants received treatment for their PDA with either ibuprofen (N = 17) or paracetamol (N = 4). Two infants had their PDA surgically ligated: one of them had surgery at 63 days of life and had not received treatment with medication prior to ligation, the other infant had a PDA ligation at 28 days of life and had previously received treatment with paracetamol. The median (range) age at the start of PDA treatment was 13 (2 – 63) days old. Only one infant received treatment during the study (around 36 hours of life). This infant received an incomplete course of ibuprofen in view of clinical deterioration and died just after 48 hours of life.

Measurements of systemic blood flow and cerebral oxygenation within the first 48 hours of life and their correlation with IVH

Mean left and right cardiac outputs and SVC flow increased over the first 48 hours as shown in Table 8.2.

Mean LVO, RVO and SVC was not statistically different between infants who developed or did not develop IVH as shown in Table 8.3.

Table 8.2 Measurement of left and right cardiac outputs and SVC flow within the first 48 hours of life

Measurement	6h (N=27) mean (SD) (range)	12h (N=41) mean (SD) (range)	24h (N=45) mean (SD) (range)	48h (N=40) mean (SD) (range)	P
LVO (ml/Kg/min)	238 (±106) (66-504)	246 (±82) (81-402)	324 (±94) (81-559)	360 (±99) (105-540)	<0.001 δ
RVO (ml/Kg/min)	176 (±75) (52-329)	204 (±81) (67-380)	265 (±78) (101-409)	277 (±72) (145-441)	<0.001 δ
SVC (ml/Kg/min)	80 (±38) (18-162)	90 (±45) (19-188)	104 (±36) (31-183)	110 (±41) (44 -230)	0.006 δ

δOne-way ANOVA with post-hoc analysis (Bonferroni) showed difference between mean LVO at 6h and 24h (P=0.004), 6h and 48h (P<0.001), 12h and 24h (P=0.002) and 12h and 48h (P<0.001). There was no difference between mean LVO at 6h and 12h (P=0.99) or between 24h and 48h (P=0.49). Post-hoc analysis (Bonferroni) showed difference between mean RVO at 6h and 24h (P<0.001), 6h and 48h (P<0.001), 12h and 24h (P=0.003), 12h and 48h (P<0.001). There was no difference between mean RVO at 6h and 12h (P=0.63) and 24h and 48h (P=0.89). Post-hoc analysis (Bonferroni) showed difference between mean SVC at 6h and 48h (P=0.013) only. There was no difference between 6h and 12h (P=0.99), 6h and 24h (P=0.060), 12h and 24h (P=0.40) and 24h and 48h (P=0.99).

Table 8.3 Systemic blood flow, cerebral oxygenation and indices of cerebral autoregulation, cerebrovascular reactivity and IVH groups

Measurement	6h (mean and 95% CI)		P	12h (mean and 95% CI)		P	24h (mean and 95% CI)		P	48h (mean and 95% CI)		P
	no-IVH (N=20)	IVH (N=7)		no-IVH (N=28)	IVH (N=13)		no-IVH (N=30)	IVH (N=15)		No-IVH (N=29)	IVH (N=12)	
LVO (ml/Kg/min)	227 (183-270)	262 (130-395)	0.45 φ	254 (224-283)	218 (164 - 274)	0.20 φ	320 (286-354)	317 (253-382)	0.93 φ	342 (303-381)	367 (298-436)	0.49 φ
RVO (ml/Kg/min)	186 (149-223)	158 (90-225)	0.41 φ	206 (178-234)	191 (131-252)	0.59 φ	272 (244-299)	239 (187-290)	0.20 φ	279 (255-304)	257 (199-314)	0.35 φ
SVC (ml/Kg/min)	80 (63-97)	75 (26-124)	0.76 φ	86 (72-101)	92 (55-129)	0.96§	104 (90-117)	106 (86-127)	0.83 φ	120 (102-138)	97 (76-119)	0.15§
TOI	71 (67-74)	71 (62-78)	0.93§	72 (71-76)	67 (62-73)	**0.033**φ	73 (71-75)	68 (63-73)	**0.013**§	73 (71-76)	69 (64-73)	**0.006**§
TOEF	0.27 (0.23-.30)	0.26 (0.18-0.34)	0.87§	0.22 (0.20-0.25)	0.28 (0.22-0.34)	**0.042** φ	0.23 (0.20-0.25)	0.27 0.22-0.32)	**0.018**§	0.22 (0.19-0.24)	0.27 (0.22-0.31)	**0.006**§
TOx	0.17 (0.06-0.27)	0.22 (-0.08 – +.13)	0.22§	0.10 (0.03-0.18)	0.15 (0.04-0.26)	0.49 φ	0.13 (0.08-0.19)	0.14 (0.04-0.23)	0.98 φ	0.12 (0.07-0.18)	0.12 (0.10-0.23)	0.93 φ
TOHRx	-.46 (-.14 – +.05)	-.11 (-.20 – -.02)	0.29§	-.05 (-.10 – +.01)	-.0.05 (-.14 – +.13)	0.55§	-.02 (-.07 – 0.2)	0.15 (-.08 – 0.11)	0.98	-.032 (-.07 – +.07)	0.15 (-.07 – +.11)	0.23§

§ Mann-Whitney test φ Independent samples T-test

Correlation between cerebral oxygenation and systemic blood flow

Using all data point measurements (N = 154), there was no correlation between LVO and TOI. There was a trend towards a positive correlation between SVC and TOI and a weak statistically significant correlation between RVO and TOI as shown in Table 8.4. Indices of cerebral autoregulation and cerebrovascular reactivity had no correlation with LVO, RVO or SVC (Table 8.4).

Table 8.4 Correlation between systemic blood flow and cerebral oxygenation

		TOI	TOEF	TOx	TOHRx
LVO	r	0.034	-0.096	-0.078	0.081
(mL/kg/min)	P	0.68	0.25	0.34	0.32
RVO	r_s	**0.194**	**-0.227**	0.013	0.009
(mL/kg/min)	P	**0.019**	**0.006**	0.87	0.91
SVC	r_s	0.163	**-0.171**	0.005	0.121
(mL/kg/min)	P	0.054	**0.043**	0.96	0.15

All measurements included (N = 156). r for Pearson correlation-coefficient. r_s for Spearman's correlation.

A strong positive correlation between LVO and RVO was observed when all measurements were included ($r = 0.77$, $P < 0.0001$). Using only measurements when a non-haemodynamically significant PDA (< 1.5 mm) was present, a stronger positive correlation was observed ($r = 0.92$, $P < 0.0001$). A positive correlation between LVO and SVC was observed when all measurements were included ($r = 0.56$, $P < 0.0001$), and remained positive when only measurements with a PDA < 1.5 were included ($r = 0.556$, $P < 0.0001$). All these results are in line with the published literature regarding left and right cardiac outputs and SVC flow measurements discussed in Chapter 3, section 3.2.

Pattern of changes in systemic blood flow and cerebral oxygenation in infants with and without IVH

Although no difference in mean LVO, RVO and SVC was observed between infants who had and did not have an IVH, we investigated whether the *patterns* of changes in cardiac output and SVC flow over the first 48 hours would be different between these two groups. Reviewing the clinical data, we considered that for four infants who received NO for PPHN and the only infant with a hypertrophic myocardium do not reflect the "normal" transitional physiology for preterm infants, and therefore these infants were excluded from the analysis of changes in patterns between groups.

Following the removal of those five infants, LVO, RVO and SVC increased over time with similar mean values and statistical significance as the analysis for the entire cohort, as shown in Table 8.5. The difference in mean LVO, RVO and SVC between infants who developed and did not develop an IVH remained non-significant.

1) Changes in LVO between IVH groups

The Figure 8.1 shows the mean LVO for each time interval for the IVH and no-IVH groups. Infants who did no develop an IVH had a statistically significant increase in mean LVO over the first 48 hours of life ($P < 0.001^{\delta}$). The pattern of increase in mean LVO shows a more steady increase compared to infants who developed an IVH. Although the mean LVO appears lower at 12h and higher at 24h in the IVH group compared to no-IVH group in Figure 8.1, there was no significant statistical difference between groups ($P = 0.27^{\delta}$).

Using mixed model analysis to compare the pattern of change in LVO between infants who had and did not have IVH, no significant difference was observed ($P = 0.66$) for full model analysis.

Figure 8.1 Changes in mean LVO between IVH groups within first 48 hours of life

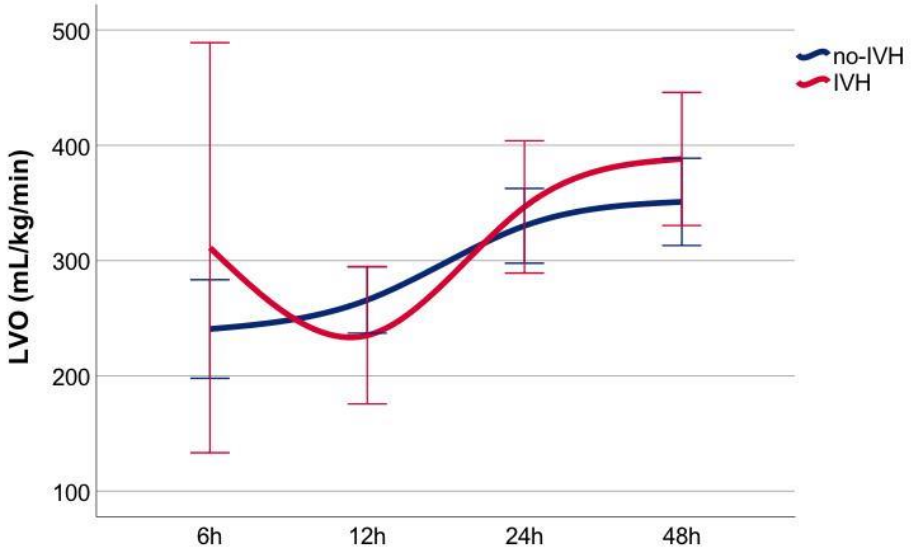

Data are shown as mean and 95% confidence interval. There was no difference in mean LVO at 6h (P = 0.17$^{\varphi}$), 12h (P = 0.27$^{\varphi}$), 24h (P = 0.58$^{\varphi}$) and 48h (P = 0.28$^{\varphi}$) between IVH and no-IVH groups. $^{\varphi}$Independent samples t-test.

Table 8.5 Mean LVO within the first 48 hours of life in the total cohort and in the IVH and no-IVH groups

		6h mean (SD) (range)	12h mean (SD) (range)	24h mean (SD) (range)	48h mean (SD) (range)	P
Total	**LVO (mL/Kg/min)**	257 (±100) (70 – 505)	256 (±76) (113 – 403)	335 (±85) (186 – 560)	361 (±92) (164 – 540)	<0.001$^{\delta}$
no-IVH	**LVO (mL/Kg/min)**	240 (±83) (70 – 379)	265 (±70) (132 – 402)	330 (±82) (186 – 519)	350 (±96) (164 – 540)	<0.001$^{\delta}$
IVH	**LVO (mL/Kg/min)**	311 (±143) (130 – 505)	235 (±88) (113 – 380)	346 (±95) (187 – 560)	388 (±81) (269 – 512)	0.007$^{\delta}$

Total: $^{\delta}$One-way ANOVA with post-hoc analysis (Bonferroni) showed difference in mean LVO between 6h and 24h (P = 0.006), 12h and 48h (P<0.001), 12h and 24h (P = 0.001) and 12h and 48h (P<0.001).
No-IVH: $^{\delta}$One-way ANOVA with post-hoc analysis (Bonferroni) showed difference in mean LVO between 6h and 24h (P = 0.005), 6h and 48h (P<0.001), 12h and 24h (P = 0.040), 12h and 48h (P = 0.002).
IVH: $^{\delta}$One-way ANOVA with post-hoc analysis (Bonferroni) showed difference in mean LVO between 12h and 24h (P = 0.048), 12h and 48h (P = 0.006).
SD is for standard deviation

2) Changes in RVO between IVH groups

The Figure 8.2 shows the mean RVO for each time interval for IVH and no-IVH groups. The pattern of change in mean RVO was similar in both groups. The mean RVO increased over the first 48 hours in the no-IVH group but no statistical significant increase was observed in the IVH group (Table 8.6). Using mixed model analysis, the patterns of change in RVO between IVH groups showed no statistical difference (P = 0.71) for full model analysis.

Figure 8.2 Changes in mean RVO between IVH groups within first 48 hours of life

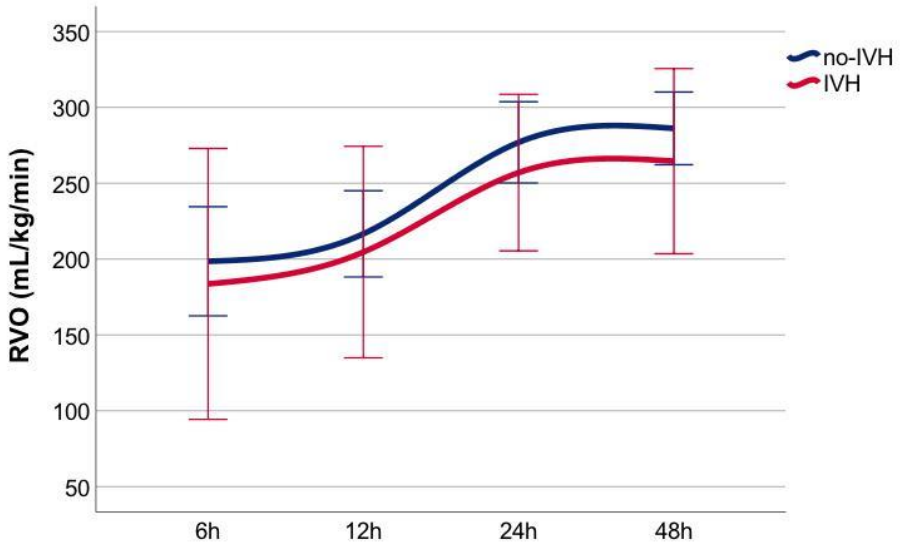

Data are shown as mean and 95% confidence interval. There was no difference in mean RVO at 6h (P = 0.69$^{\varphi}$), 12h (P = 0.68$^{\varphi}$), 24h (P = 0.43$^{\varphi}$) and 48h (P = 0.39$^{\varphi}$) between IVH groups.
$^{\varphi}$Independent samples t-test.

Table 8.6 Mean RVO within the first 48 hours of life in the total cohort and in the IVH and no-IVH groups

		6h mean (SD) (range)	12h mean (SD) (range)	24h mean (SD) (range)	48h mean (SD) (range)	P
Total	**RVO (mL/Kg/min)**	195 (±71) (61 – 330)	213 (±77) (93 – 380)	270 (±73) (142 – 409)	280 (±69) (145 – 441)	<0.001$^{\delta}$
no-IVH	**RVO (mL/Kg/min)**	198 (±72) (61 - 330)	217 (±70) (116 – 347)	277 (±68) (173 – 409)	286 (±59) (155 – 388)	<0.001$^{\delta}$
IVH	**RVO (mL/Kg/min)**	184 (±72) (90 – 253)	205 (±97) (93 – 380)	257 (±85) (142 – 409)	264 (±91) (145 – 441)	0.203$^{\delta}$

Total: $^{\delta}$One-way ANOVA with post-hoc analysis (Bonferroni) showed difference in mean RVO between 6h and 24h (P = 0.001), 12h and 48h (P<0.001), 12h and 24h (P = 0.005) and 12h and 48h (P = 0.001).
No-IVH: $^{\delta}$One-way ANOVA with post-hoc analysis (Bonferroni) showed difference in mean RVO between 6h and 24h (P = 0.001), 6h and 48h (P<0.001), 12h and 24h (P = 0.010), 12h and 48h (P = 0.002).
IVH: $^{\delta}$One-way ANOVA with post-hoc analysis (Bonferroni) showed no difference in mean RVO between intervals.
SD is for standard deviation

3) Changes in SVC flow between IVH groups

Figure 8.3 shows the mean SVC for each time interval for IVH and no-IVH groups. The mean SVC in the no-IVH group had a steadily significant increase over the first 48 hours. Visually the pattern of change in the mean SVC over the first 48 hours was different for those who developed IVH, but the mixed model analysis showed no statistical difference between the patterns of changed in the mean SVC between these two groups (P = 0.84) for full model analysis.

Figure 8.3 Changes in mean SVC between IVH groups within first 48 hours of life

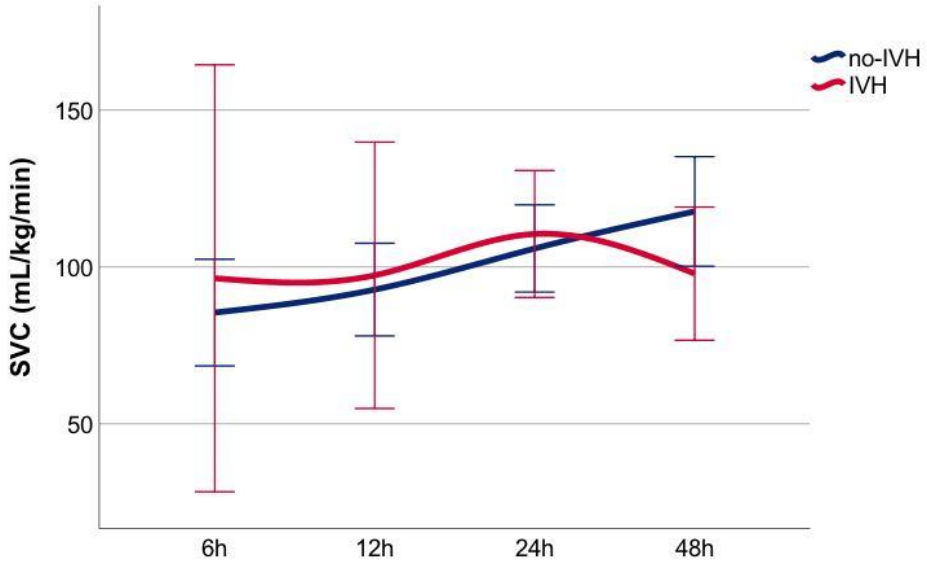

Data are shown as mean and 95% confidence interval. There was no difference in mean SVC at 6h (P = 0.58$^{\varphi}$), 12h (P = 0.94§), 24h (P = 0.69$^{\varphi}$) and 48h (P = 0.17$^{\varphi}$) between IVH groups.
$^{\varphi}$Independent samples t-test. §Mann-Whitney test.

Table 8.7 Mean SVC within the first 48 hours of life in the total cohort and in the IVH and no-IVH groups

		6h mean (SD) (range)	12h mean (SD) (range)	24h mean (SD) (range)	48h mean (SD) (range)	P
Total	**SVC (mL/Kg/min)**	87 (±34) (18 – 163)	94 (±45) (22 – 189)	107 (±34) (44 – 183)	112 (±40) (45 – 195)	0.069$^{\delta}$
no-IVH Group	**SVC (mL/Kg/min)**	85 (±33) (18 - 162)	93 (±35) (50 – 189)	105 (±35) (44– 173)	118 (±42) (58 – 195)	0.025$^{\delta}$
IVH Group	**SVC (mL/Kg/min)**	96 (±43) (55 – 152)	97 (±63) (22 – 175)	110 (±33) (71 – 183)	98 (±32) (45 – 156)	0.86$^{\delta}$

Total: $^{\delta}$One-way ANOVA with post-hoc analysis (Bonferroni) showed no difference in mean RVO between time intervals.
No-IVH: $^{\delta}$One-way ANOVA with post-hoc analysis (Bonferroni) showed difference in mean LVO between 6h and 48h (P = 0.038) only.
IVH: $^{\delta}$One-way ANOVA with post-hoc analysis (Bonferroni) showed no difference in mean LVO between intervals.

4) Changes in TOI and TOEF between IVH groups

Mean TOI was significantly lower at 12, 24 and 48 hours in the IVH group compared to the no-IVH group, and mean TOEF was significantly higher between these two groups in those same time intervals (Figure 8.4 and Figure 8.5). The mean TOI and mean TOEF did not have a statistically significant increase or decrease over the first hours of life in either the IVH or no-IVH groups (Table 8.8 and Table 8.9). However, the mixed model analysis showed that patterns of change in TOI between these two groups were statistically different (P < 0.001) for full model analysis, but the difference in the pattern of changes in TOEF between groups did not reach statistical significance (P = 0.066), for full model analysis.

Figure 8.4 Changes in mean TOI between IVH groups within first 48 hours of life

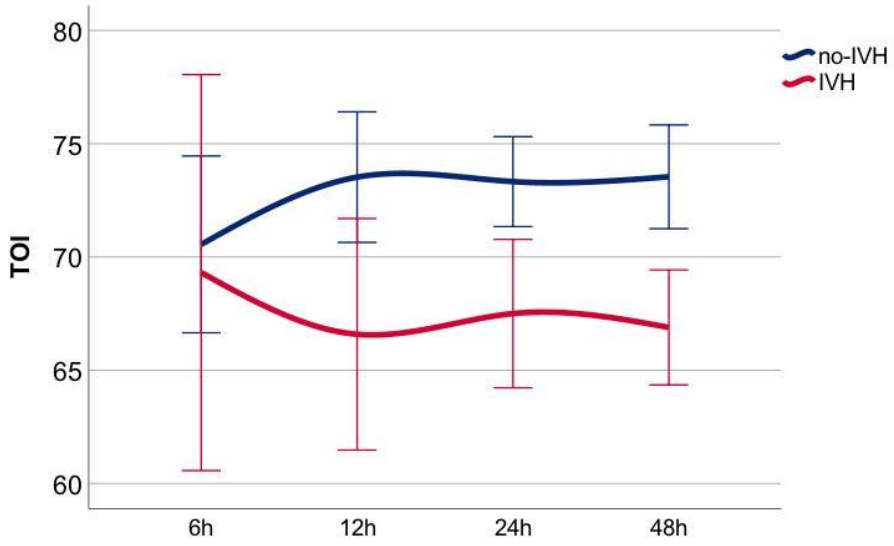

Data are shown as mean and 95% confidence interval. Mean TOI at 12h, 24h and 48h was significantly lower in the IVH group (P = 0.011$^{\varphi}$, P = 0.002$^{\varphi}$, P = 0.001$^{\varphi}$, respectively). There was no difference in mean TOI between groups at 6h (P = 0.75$^{\varphi}$). $^{\varphi}$ Independent samples t-test

Table 8.8 Mean TOI within the first 48 hours of life in the total cohort and in the IVH and no-IVH groups

		6h mean (SD) (range)	12h mean (SD) (range)	24h mean (SD) (range)	48h mean (SD) (range)	P
Total	**TOI (mL/Kg/min)**	70 (±7.5) (58 – 92)	71 (±7.7) (56 – 88)	71 (±5.8) (61 – 84)	72 (±6) (61 – 86)	0.89[δ]
no-IVH	**TOI (mL/Kg/min)**	70 (±7.8) (62 – 92)	73 (±7) (61 – 88)	73 (±5) (64 – 84)	73 (±5.8) (64 – 86)	0.38[δ]
IVH	**TOI (mL/Kg/min)**	69 (±7) (58 – 78)	66 (±7.6) (56 – 80)	67 (±5.4) (61 – 78)	67 (±3.8) (61 – 74)	0.85[δ]

Total: [δ]One-way ANOVA with post-hoc analysis (Bonferroni) showed no difference in mean TOI between time intervals.
No-IVH: [δ]One-way ANOVA with post-hoc analysis (Bonferroni) showed no difference in mean TOI between time intervals.
IVH: [δ]One-way ANOVA with post-hoc analysis (Bonferroni) showed no difference in mean TOI between time intervals.

Figure 8.5 Changes in mean TOEF between IVH groups within first 48 hours of life

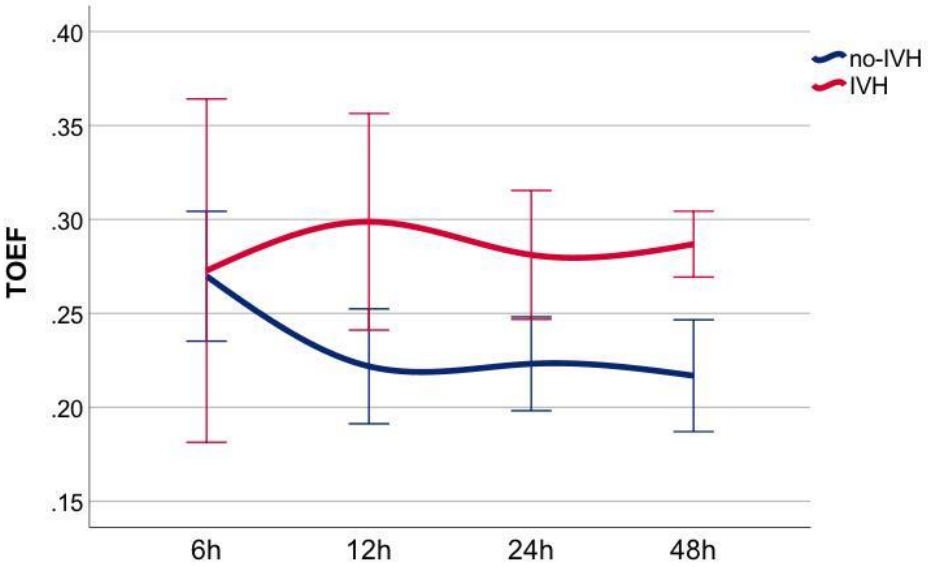

Data are shown as mean and 95% confidence interval. Mean TOEF was significantly lower at 12h, 24h and 48h in the IVH group (P = 0.015[φ], P = 0.07[φ] and P = 0.009 [φ], respectively). There was no difference in mean TOEF between groups at 6h (P = 0.76[§]).
[φ]Independent samples t-test. [§]Mann-Whitney test

Table 8.9 Mean TOEF within the first 48 hours of life in the total cohort and in the IVH and no-IVH groups

	IVH	6h mean (SD) (range)	12h mean (SD) (range)	24h mean (SD) (range)	48h mean (SD) (range)	P
Total	**TOEF**	0.27 (±0.07)	0.24 (±0.08)	0.24 (±0.06)	0.24 (±0.07)	0.39$^{\delta}$
	(mL/Kg/min)	(0.1 – 0.38)	(0.05 – 0.42)	(0.08 – 0.34)	(0.03 – 0.33)	
no-IVH	**TOEF**	0.27 (±0.07)	0.22 (±0.07)	0.22 (±0.06)	0.22 (±0.07)	0.07$^{\delta}$
	(mL/Kg/min)	(0.1 – 0.34)	(0.05 – 0.34)	(0.08 – 0.33)	(0.03 – 0.33)	
IVH	**TOEF**	0.27 (±0.07)	0.30 (±0.08)	0.28 (±0.06)	0.29 (±0.03)	0.86$^{\delta}$
	(mL/Kg/min)	(0.18 – 0.39)	(0.15 – 0.42)	(0.17 – 0.35)	(0.23 – 0.32)	

Total: $^{\delta}$One-way ANOVA with post-hoc analysis (Bonferroni) showed no difference in mean TOEF between time intervals.
No-IVH: $^{\delta}$One-way ANOVA with post-hoc analysis (Bonferroni) showed no difference in mean TOEF between time intervals.
IVH: $^{\delta}$One-way ANOVA with post-hoc analysis (Bonferroni) showed no difference in mean TOEF between time intervals

Mean TOx and mean TOHRx had no significant change within the first 48 hours of life (P = 0.94$^{\delta}$ and P = 0.62$^{\delta}$, respectively) for the full cohort. Mean TOx and mean TOHRx had no difference within the first 48 hours in the no-IVH group (P = 0.65$^{\delta}$ and P = 0.87$^{\delta}$, respectively) or in the IVH group (P = 0.54$^{\delta}$ and P = 0.61$^{\omega}$). Mixed model analysis showed no difference between patterns of changes in TOx (P = 0.57) or TOHRx (P = 0.71) between the IVH groups, for full model analysis.

Correlation between systemic and cerebral blood for each time interval

In order to understand the relationship between systemic blood flow and cerebral oxygenation during the transitional circulation we analysed the correlation between LVO, RVO and SVC with TOI, TOx and TOHRx for each time interval for the total group and for each individual IVH groups independently. A strong positive correlation between systemic and cerebral oxygenation was observed at 24 hours of age in the IVH group only. A negative significant correlation between TOx and LVO was observed, showing that the lower the systemic blood flow, the more impaired was cerebral autoregulation (Table 8.10). No other correlations between systemic blood flow and cerebral oxygenation or cerebrovascular reactivity were observed in any other time intervals in infants in either IVH groups.

Table 8.10 Correlation between systemic and cerebral blood flow at 24 hours of age for infants who developed IVH

		TOI	TOx	TOHRx	TOEF
LVO	r	**0.750**	**-0.570**	-0.022	**-0.802**
(mL/kg/min)	P	**0.003**	**0.042**	0.94	**0.001**
RVO	r_s	**0.703**	-0.358	-0.110	**-0.746**
(mL/kg/min)	P	**0.007**	0.23	0.72	**0.003**
SVC	r_s	0.217	-0.498	0.107	-0.258
(mL/kg/min)	P	0.48	0.084	0.73	0.40

Pearson coefficient-correlation (r), Spearman rank (r_s).

PDA measurements within the first 48 hours of life and the relationship between a haemodynamically significant PDA and cerebral oxygenation

Table 8.11 shows the characteristics of the PDA measurements at 6, 12, 24 and 48 hours. Overall, 105 (68.2%) of all PDA measurements were above 1.5 mm. PDA size did not significantly increase over the first 48 hours of life, but other measurements of haemodynamic significance, such as presence of reversed end diastolic flow (EDF) on the post ductal aorta (Ao), LA:Ao ratio and end diastolic flow velocity on LPA (LPA EDF vel), increased over time. By 48h of life, the flow pattern changed to bidirectional with mainly left-to-right flow or pulsatile. In our cohort, only a small

number of infants had a constricting or closing PDA.

The mean LVO was significantly higher when the PDA was above 1.5 mm. Measurements of haemodynamic significance, such as ‘Ao’, increased ‘LA:Ao ratio’ and ‘LPA EDF vel’ were higher when the PDA > 1.5 mm. There was no difference in the mean TOI, TOEF, TOx or TOHRx between a PDA greater or less than 1.5 mm using all measurement (N = 156) (Table 8.12).

Table 8.11 PDA measurements for each time interval

Measurement	6h (N=27) Median (range)	12h (N=41) Median (range)	24h (N=45) Median (range)	48h (N=41) Median (range)	P
PDA 2D diameter	1.75 (0.95-3.8)	1.7 (1 – 3.3)	1.75 (1.1-3)	1.8 (1 – 3.23)	0.19[ω]
PDA Doppler diameter	2.03 (1.3-1.8)	1.88 (1.05-3.6)	1.8 (1.1-3.9)	2.3 (1.12 -4.4)	0.21[ω]
PDA > 1.5 mm	22 (81%)	23 (56%)	31 (69%)	29 (71%)	0.16[Ω]
Constricting Flow/ No flow	1 (3.7%)	7 (17.1%)	6 (13.3%)	8 (19.5%)	0.34[Ω]
Pulmonary Hypertension type	12 (44.4%)	4 (9.8%)	3 (6.7%)	0 (0%)	**<0.001**[Ω]
Growing	6 (22.2%)	15 (36.6%)	11 (24.4%)	13 (31.7%)	0.51[Ω]
Pulsatile	8 (29.6%)	15 (36.6%)	25 (55.6%)	20 (48.8%)	0.11[Ω]
Ao	2 (7.4%)	4 (9.8%)	9 (20%)	19 (47.5%)	**<0.001**[Ω]
LA:Ao ratio	1.33 (0.83-1.75)	1.3 (0.81-1.86)	1.48 (0.82-1.94)	1.42 (0.83-2.26)	**0.023**[ω]
LPA EDF vel (m/sec)	0.12 (0.03-0.05)	0.08 (0.03-0.25)	0.14 (0.04-0.41)	0.17 (0.01-0.56)	**0.001**[ω]

From 12 hours of life, PDA 2D diameter measurements had a trend to increase over time (r = 0.160, P = 0.073). Pulsatile flow tends to be more frequent from 6 to 24 hours (P = 0.062[Ω]). [Ω]Chi-square analysis. [ω]Kruskall-Wallis test. Ao is for 'presence of reversal flow in the post-ductal aorta. LA:Ao ratio is for left atrium: Aorta ratio. LPA EDF vel is for left pulmonary artery end diastolic flow velocity.

Haemodynamically significant PDA

Table 8.12 shows the differences in systemic blood flow and cerebral oxygenation, cerebrovascular reactivity and markers of haemodynamically significant PDA between an hsPDA defined by size.

Table 8.12 Difference in systemic blood flow, cerebral oxygenation and cerebrovascular reactivity between hsPDA and non-hsPDA according to size

	PDA ≤ 1.5 mm (N=49)	**PDA > 1.5 mm (N=105)**	**P**
LVO (ml/kg/min)	264 (240 – 287)	306 (284 – 328)	**0.010** [φ]
RVO (ml/kg/min)	247 (222 – 271)	228 (211 – 245)	0.21 [φ]
SVC (ml/kg/min)	99 (86 – 111)	99 (90 – 107)	0.70 [§]
LA:Ao	1.3 (1.22 – 1.38)	1.4 (1.4 – 1.5)	**0.003** [φ]
Ao	2%	32%	**0.024** [Ω]
LPA	0.10 (0.08 – 0.12)	0.17 (0.15 – 0.19)	**<0.0001** [§]
Pulsatile	51%	41%	0.30 [Ω]
TOI	73 (71-75)	71 (69-72)	0.18 [§]
TOEF	0.23 (021-0.26)	0.25 (0.23-0.26)	0.85 [§]
TOx	0.16 (0.11-0.21)	0.11 (0.08-0.14)	0.08 [φ]
TOHRx	-.04 (-.08 - +.005)	-.02 (-.05 - +0.01)	0.82 [§]

LVO: left ventricle output, RVO: right ventricle output, SVC: superior vena cava, LA:Ao: Left atrium Aorta ratio, Ao: reversal EDF flow in the post-ductal aorta, LPA: left pulmonary artery. [φ]Independent samples t-test. [§]Mann-Whitney test. [Ω]Chi-square analysis

Including only measurements of a PDA > 1.5 mm, a significant positive correlation between TOI and RVO was observed (r = 0.308, P = 0.003) and between TOI and SVC (r = 0.226, P = 0.033), but there was no correlation between TOI and LVO (r = 0.15, P = 0.16). No correlation was observed between TOx and RVO (r = 0.188, P = 0.074), LVO (r = 0.095, P = 0.37) and SVC (r = 0.188, P = 0.078). No correlation was

observed between TOHRx and RVO (r = -0.054, P = 0.59), LVO (r = 0.024, P = 0.81) and SVC (r = 0.051, P = 0.61).

The 'Ao' was associated with a higher PDA 2D diameter and a higher LVO, suggesting higher ductal steal and haemodynamic significance (Figure 8.6).

Figure 8.6 Differences in mean PDA 2D diameter and mean LVO according to the presence of absence of reversal EDF in the post-ductal aorta

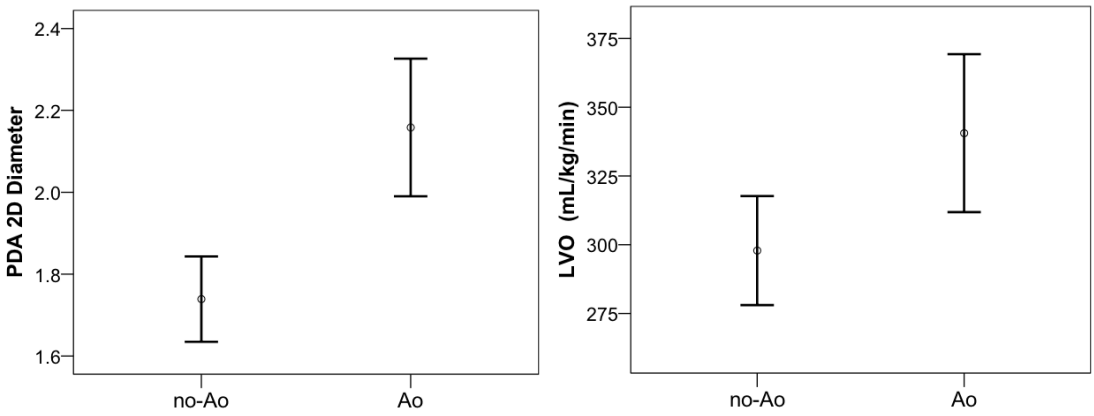

Ao for presence of reverse EDF in the post ductal aorta. Mean (95% CI) for PDA 2D diameter when Ao was present was 2.16 (1.97-2.31) compared to 1.75 (1.65-1.84) in no-Ao measurements, P<0.001[§]. Mean (95% CI) for LVO when Ao was present was 335 (308-362) and for no-Ao was 279 (258-299), P=0.008[§]. [§]Mann-Whitney test.

'LPA EDF vel' had a significant positive correlation with LVO (r_s = 0.372, P<0.001), suggesting that higher velocity was associated with increased ductal steal.

No significant difference was observed in mean TOI, TOEF, TOx or TOHRx when measurements were divided between no-hsPDA and hsPDA according to size and additional criteria described in 'Methods 8.1.3' section of this chapter (Table 8.13).

Table 8.13 Differences between systemic blood flow and cerebral oxygenation and cerebrovascular reactivity between hsPDA groups

	no-hsPDA (N=83)	**hsPDA (N=71)**	**P**
LVO (ml/kg/min)	262 (240 – 284)	328 (304 – 352)	**<0.001**[φ]
RVO (ml/kg/min)	224 (204 – 244)	245 (227 – 264)	0.13[φ]
SVC (ml/kg/min)	93 (83 – 103)	103 (94 – 112)	0.06[§]
TOI	72 (70 – 73)	71 (69 – 72)	0.53[φ]
TOEF	0.25 (023 – 0.27)	0.24 (0.22 – 0.25)	0.40[§]
TOx	0.14 (0.10 – 0.18)	0.11 (0.07 – 0.14)	0.18[φ]
TOHRx	-.04 (-.08 – -.01)	-.02 (-.05 – +0.01)	0.32[§]

hsPDA in this table stands for PDA > 1.5 mm **AND** LA:Ao ratio > 1.4 or LPA EDF velocity > 2 m/sec or presence of reversal EDF in the post-ductal aorta (**Ao**) as described in the Methods section of this chapter.
[φ] Independent samples t-test. [§]Mann-Whitney test

Table 8.14 shows the differences in measurements of haemodynamically significant PDA between IVH groups. Mean LPA EDF vel was higher in the 'no-IVH' group at 12 and 24 hours of life. Reversed EDF in the post ductal aorta (Ao) was higher in the 'no-IVH' group at 24 hours of life.

Table 8.15 shows the difference in cerebral oxygenation, cerebrovascular reactivity and systemic blood flow between PDA groups (according to 2D diameter size only).

Table 8.16 shows the difference in mean pH, $PaCO_2$, lactate, Haemoglobin (Hb), SaO_2, MABP and left ventricle stroke volume (LVSV) between IVH groups. Hb was significantly lower at 12 hours of life in infants who developed an IVH but significantly higher at 48 hours of life in this same group.

Table 8.14 Measurements of haemodynamically significant PDA between IVH groups

Measurements	6h		P	12h		P	24h		P	48h		P
	no-IVH (N=20)	**IVH (N=7)**		**no-IVH (N=28)**	**IVH (N=13)**		**no-IVH (N=30)**	**IVH (N=15)**		**no-IVH (N=27)**	**IVH (N=12)**	
PDA 2D Diameter (mm)	1.91 (0.95-3.8)	2.23 (1.55-3.50)	0.30 $^{\varphi}$	1.67 (1.50-1.83)	1.76 (1.4-2.11)	0.59 $^{\varphi}$	1.82 (1.64-2)	1.78 (1.55-2)	0.74 $^{\varphi}$	1.95 (1.74-2.16)	1.78 (1.5-2)	0.36 $^{\varphi}$
LPA EDF vel	0.14 (0.09-0.19)	0.11 (0.04-0.18)	0.98 §	0.13 (0.10-0.15)	0.074 (0.04-0.11)	**0.08** §	0.18 (0.15-0.22)	0.10 (0.07-0.13)	**0.01** $^{\varphi}$	0.2 (0.15-0.24)	0.18 (0.12-0.25)	0.85 §
Ao	2	0	1.0 $^{\Omega}$	3	1	1.0 $^{\Omega}$	9	0	**0.04** $^{\Omega}$	14	5	0.73 $^{\Omega}$
PDA > 1.5mm	15	7	0.28 $^{\Omega}$	15	8	0.74 $^{\Omega}$	21	10	1.0 $^{\Omega}$	22	7	0.28 $^{\Omega}$
hs PDA	2	8	0.68 $^{\Omega}$	8	5	0.72 $^{\Omega}$	19	5	0.11 $^{\Omega}$	18	6	0.51 $^{\Omega}$

LPA EDF vel for end-diastolic flow velocity in the left pulmonary artery. Ao for presence of reversed flow in the post-ductal abdominal aorta. hsPDA for haemodynamically significant persistent ductus arteriosus. PDA 2D Diameter, LPA EDF vel are shown as mean and 95% confidence interval, the remaining variables as shown as absolute numbers. $^{\varphi}$ Independent samples t-test. §Mann-Whitney test. $^{\Omega}$Chi-square analysis.

Table 8.15 Difference in mean cerebral oxygenation, cerebrovascular reactivity, systemic blood flow and outcome groups between hsPDA groups (according to size) for each time interval

Variables	6h			12h			24h			48h		
	PDA ≤ 1.5 (N = 5)	PDA > 1.5 (N = 18)	P	PDA ≤ 1.5 (N = 16)	PDA > 1.5 (N = 20)	P	PDA ≤ 1.5 (N = 11)	PDA > 1.5 (N = 27)	P	PDA ≤ 1.5 (N = 11)	PDA > 1.5 (N = 27)	P
TOI	72 (58 – 86)	70 (67 – 73)	0.83§	74 (69 – 78)	70 (66 – 73)	0.10φ	72 (68 – 76)	71 (68 – 73)	0.94§	72 (69 – 78)	71 (69 – 73)	0.42φ
TOEF	0.29 (0.24 – 0.35)	0.26 (0.23 – 0.29)	0.34§	0.23 (0.17 – 0.28)	0.26 (0.22 – 0.29)	0.28φ	0.24 (0.18 – 0.29)	0.24 (0.22 – 0.27)	0.72§	0.23 (0.17 – 0.28)	0.23 (0.21 – 0.26)	0.93§
TOx	+0.26 (-0.46 - +0.58)	+0.10 (+0.01 - +0.19)	0.11φ	+0.14 (+0.04 - +0.24)	+0.10 (+0.02 - +0.18)	0.49φ	+0.17 (+0.07 - +0.27)	+0.12 (+0.07 - +0.17)	0.34φ	+0.14 (+0.05 - +0.22)	+0.12 (+0.06 - +0.17)	0.66φ
TOHRx	-0.08 (-0.31 - +0.16)	-0.06 (-0.14 - +0.02)	0.85φ	-0.03 (-0.12 - +0.05)	-0.03 (-0.11 - +0.05)	0.95φ	-0.02 (-0.12 - +0.08)	-0.01 (-0.05 - +0.04)	0.82φ	-0.06 (-0.14 - +0.02)	-0.002 (-0.04 - +0.04)	0.18φ
LVO	237 (119 – 356)	238 (185 – 292)	0.98φ	241 (200 – 281)	251 (211 – 291)	0.67φ	286 (244 – 327)	342 (305 – 379)	0.77φ	309 (250 – 368)	380 (340 – 420)	**0.013**φ
RVO	208 (116 – 299)	168 (132 – 204)	0.36φ	215 (173 – 258)	195 (158 – 232)	0.45φ	272 (225 – 319)	261 (232 – 290)	0.54φ	303 (250 – 356)	267 (239 – 295)	0.50φ
SVC	83 (60 – 105)	79 (59 – 99)	0.82φ	95 (69 – 121)	87 (69 – 105)	0.47φ	107 (84 – 130)	104 (91 – 117)	0.86§	101 (73 – 129)	113 (97 – 131)	**0.37**φ
MABP	33 (29 – 37)	32 (28 – 35)	0.34§	29 (27 – 32)	31 (29 – 34)	0.30φ	33 (29 – 36)	32 (30 – 33)	0.78§	36 (32 – 39)	31 (30 – 32)	**0.005**§

Results are shown as mean (95% confidence interval). φ Independent samples t-test. § Mann-Whitney test

Table 8.16 Differences in mean pH, arterial carbon dioxide ($PaCO_2$), lactate, haemoglobin (Hb), MABP, peripheral arterial oxygenation (SaO_2) and left ventricle stroke volume (LVSV) between IVH groups for each time interval

Measurements	6h		P	12h		P	24h		P	48h		P
	no-IVH (N=20)	IVH (N=7)		no-IVH (N=28)	IVH (N=13)		no-IVH (N=30)	IVH (N=15)		no-IVH (N=27)	IVH (N=12)	
pH (nm/L)	7.33 (7.30 – 7.36)	7.32 (7.26 – 7.37)	0.65 φ	7.30 (7.29 – 7.32)	7.31 (7.27 – 7.35)	0.27 §	7.26 (7.24 – 7.29)	7.28 (7.24 – 7.32)	0.80 §	7.25 (7.23 – 7.27)	7.26 (7.22 – 7.30)	0.64 φ
$PaCO_2$ (kPa)	5.50 (4.84 – 6.15)	5.79 (5.05 – 6.52)	0.43 §	5.60 (5.23 – 5.95)	5.58 (4.91 – 6.25)	0.98 §	6.23 (5.78 – 6.68)	6.29 (5.51 – 7.08)	0.55 §	6.18 (5.74 – 6.61)	5.78 (5.11 – 6.45)	0.28 φ
Lactate (mmol/L)	3.0 (2.0 – 4.0)	4.2 (-0.3 – 8.7)	0.85 §	2.6 (2.3 – 3.0)	4.0 (2.4 – 5.5)	0.60 φ	2.5 (2.2 – 2.9)	2.4 (1.6 – 3.1)	0.31 §	2.54 (2.01 – 3.07)	2.6 (1.82 – 3.40)	0.59 §
Hb (g/L)	147 (134 – 160)	137 (118 – 157)	0.39 φ	155 (147 – 165)	137 (127 – 147)	**0.013 φ**	142 (136 – 149)	132 (123 – 141)	0.19 §	129 (124 – 135)	141 (133 – 150)	**0.012 §**
SaO_2 (%)	94 (91 – 96)	95 (93 – 97)	0.61 §	94 (93 – 95)	97 (93 – 96)	0.69 φ	94 (94 – 95)	94 (93 – 95)	0.31 §	94 (94 – 95)	94 (92 – 95)	0.65 §
MABP (mmHg)	32 (30 – 34)	32 (22 – 43)	0.31 §	30 (28 – 32)	31 (27 – 36)	0.97 §	32 (30 – 33)	32 (30 – 35)	0.61 φ	32 (30 – 34)	32 (29 – 35)	0.91 §
LVSV	129 (108 – 149)	135 (74 – 195)	0.78 φ	133 (118 – 148)	114 (84 – 145)	0.12 §	160 (145 – 174)	167 (132 – 201)	0.77 φ	173 (153 – 192)	169 (139 – 199)	0.82 φ

Results are shown as mean (95% confidence interval). $PaCO_2$ is for partial tension carbon dioxide. Hb is for haemoglobin. SaO_2 is for peripheral arterial oxygen saturation. LVSV is for left ventricle stroke volume.
φ Independent samples t-test. § Mann-Whitney test

8.1.5. Discussion

This study described the relationship between systemic blood flow, cerebral oxygenation and cerebrovascular reactivity in relation to the patency of the ductus arteriosus and their relationship with the presence of IVH, in a cohort of preterm infants undergoing intensive care within the first 48 hours of life.

Changes in systemic blood flow within the first 48 hours of life and its correlation with IVH

The significant increase in left and right cardiac outputs and SVC flow values over the first 48 hours of life as well as the mean (range) values of LVO and RVO were similar to data previously published by several authors[146, 235, 343]. However, the values for SVC were higher than values initially suggested by Evans et al. (2000), although the values for SVC range values were similar[56]. Most studies reporting 'normal' thresholds for LVO, RVO and SVC had data collected from stable term and preterm infants. Our cohort, in contrast consisted mainly of extremely preterm infants, many of whom were ventilated for the majority of time data was collected and half of whom were started on inotropes or vasopressors were commenced within the first 48 hours of life.

Several other authors, in more recent work, have described higher SVC values within the two days of life[245, 344]. Even more recent work published by Kluckow et al. (2009) has shown fewer infants with an SVC flow of ≤ 41 mL/kg/min (described as low flow)[345]. The improvement in neonatal care over the last decade, with more consistent use of volume guarantee ventilation and antenatal steroids may have contributed to this increase in SVC values observed in more recent studies. Low SVC values were associated with IVH in a cohort of preterm infants born at less than 30 weeks' gestational age[145]. Kluckow et al. (2000) observed that infants who developed severe IVH after 24 hours of life had low SVC initially but values improved to normal range just before IVH occurred[145]. This finding may support the hypoperfusion-reperfusion theory and the possible combining effects of systemic and brain haemodynamic changes in this cycle. However, in our study we did not observe a difference in mean SVC values between infants who had or did not have an IVH in any of the four time

intervals within the first 48 hours of life (Table 8.3). Using a threshold of less than 40 or 50 ml/kg/min as 'low SVC', the differences between groups remained unchanged. The patterns of changes in SVC were not significantly different between these two groups. The lack of association between SVC flow and IVH has been described by other research groups in more recent published work[245]. SVC remains a very complex measurement, with high inter-observer variability and questionable reliability. These may be the main reasons why SVC has not been widely applied in clinical practice.

In our population, mean LVO and mean RVO over the first 48 hours of life were not different between the IVH groups. Soon after we started collecting data for our 'SAMBA' cohort in 2013, Noori et al. (2014) published data from a similar cohort of preterm infants, using a similar study design[341]. In their study, they did not find any difference between mean LVO in infants with or without IVH in the first 72 hours of life, but they showed that the pattern of changes in LVO tended to be different between these two groups. In our cohort, we did not find a statistical difference in the pattern of changes in LVO within the first 48 hours of life. However, similarly to those results described by Noori et al. (2014), we observed a trend towards a lower LVO around 12 hours of age in infants who later developed an IVH followed by a significant increase at 24 hours of age to levels above the mean LVO in the group of infants who did not develop an IVH (Figure 8.1). Noori et al. (2014) described this pattern of change in LVO as consistent with hemodynamic changes associated with a hypoperfusion-reperfusion cycle and, as similar to our data, the increase in LVO was observed just before the IVH occurred (around or soon after 24 hours of age for our cohort). They have also observed lower stroke volume and a trend towards a lower MABP at the start of the study in infants who later developed an IVH. Moreover, myocardial performance was better in the IVH group at the time the LVO increased, just before the IVH occurred. In our study, we did not observe differences in mean MABP between the IVH groups and nor was left ventricle stroke volume significantly different (Table 8.16). In the study from Noori et al. (2014), mean $PaCO_2$ was higher in the IVH group at the possible reperfusion phase. In contrast, we did not observe significant difference in mean $PaCO_2$ between these two groups at any time interval. However, the mean Hb was lower at 12 hours of age in the IVH group. This could reflect the initial bleeding in those who had IVH diagnosed at the scan performed

around 24 hours of age and may have had an influence in the lower TOI and LVO observed at 12 hours of age. Interestingly, Hb was significantly higher at 48 hours of age in those who developed an IVH, although this could be related to blood transfusions received between these two time intervals.

Changes in cerebral oxygenation within the first 48 hours its correlation with IVH

In our cohort, cerebral oxygenation was significantly lower and the TOEF was significantly higher from 12 hours of life in infants who developed an IVH (Figure 8.4 and Figure 8.5). Several studies have already reported lower cerebral oxygenation with higher oxygen consumption in infants who had brain injury[73, 341, 346]. In addition to these findings, our study demonstrated that the pattern of changes in the TOI was statistically different between infants who had and did not have IVH. Infants who did not develop an IVH seemed to follow a steady increase in the TOI from 6 hours of age, while infants who had an IVH showed a decrease in the TOI from 6 to 12 hours of age and levels remained lower in this group compared to the no-IVH group throughout the 48 hours. Noori et al. (2014) described an increase in the TOI in the IVH group to levels close to that in the no-IVH group at around 12 to 18 hours of age; we did not observe this in our cohort[341]. In our study, TOI appears to increase from 12 to 24 hours, but this increase was not statistically significant.

Correlation between cerebral oxygenation, cerebrovascular reactivity and measurements of systemic blood flow

In order to explore further the changes in systemic and cerebral haemodynamics and the complex relationship between these two systems in the mechanisms involved in the possible hypoperfusion-reperfusion injury, we investigated the correlation between cardiac output and cerebral oxygenation for each time interval and for each IVH group independently. We observed a strong positive correlation between the TOI and left and right cardiac outputs, and in infants who developed an IVH, a negative correlation between TOx and LVO, at the 24-h interval. Because most infants in our cohort developed an IVH just before or after 24 hours of age, we could speculate that around the same time when reperfusion occurred, cerebral autoregulation and

cerebrovascular reactivity were both impaired. Hence, cerebral oxygenation in those infants who developed IVH became passive to systemic blood flow (cardiac output). In addition, the lower the systemic blood flow (LVO), the more impaired was cerebral autoregulation (more positive TOx) (Table 8.10). As described in Chapter 5, extremely preterm infants are mainly pressure passive within the first 24 hours of age, as observed by the predominantly mean positive TOx. However, some degree of cerebrovascular reactivity seems to be intact as mean TOHRx over the first 24 hours of life was negative for nearly half of the cohort (results shown in Chapter 5, section 5.2). Complete loss of mechanisms involved in vascular reactivity may have occurred either during the reperfusion period or during active haemorrhage.

The correlation between continuous measurements of cerebral oxygenation, using NIRS, with static measurements of systemic blood flow, performed by functional echocardiography, has been applied in several studies but results remain controversial[347-349]. Takami et al. (2010) published a study in a small cohort of 16 very stable preterm infants born at less than 29 weeks' gestational age and small for gestational age and showed a positive correlation between TOI and SVC flow. In addition, they have described a significant decrease in LVO, SVC and TOI from around 6 to 12 hours of age. However there was no discrimination between infants who had or did not have IVH[350]. Dempsey et al. (2009, 2013) have reported different results regarding the correlation between TOI and SVC[349, 351]. In 2009, they reported a positive correlation between TOI and SVC flow in a cohort of infants with a birth weight below 1500 grams. In this same study they described no correlation between TOI and RVO or LVO (all echocardiographic measurements were performed at a mean age of 18 hours of life)[351]. Conversely, in 2013, the same group reported a negative correlation between TOI and SVC at 6 hours of life but no significant correlation between these two measurements at 12, 24 and 48 hours of life[349]. In our study, when measurements from all time intervals were included in the analysis (similar to the analysis done by Takami et al. (2010), RVO had a weak positive correlation with TOI and a weak negative correlation with the TOEF. In addition, SVC had shown a positive trend with the TOI and a weak negative correlation with TOEF. These weak correlations were probably reflecting, at least in part, the strong

correlation between systemic and cerebral oxygenation at 24 hours of life in infants who developed an IVH.

The controversial correlation between cardiac output and cerebral blood flow

The evidence that changes in CO affect CBF is controversial. It has been suggested that CBF is controlled based on integrating mechanisms that would take into account changes in CO. It is already known from basic physiology that optimal organ perfusion is dependent on the relationship between blood pressure and specific organ vascular resistance and that distribution of cardiac output is dependent on the organ's metabolic requirement[352]. There is evidence that dynamic cerebral autoregulation is not affected by acute changes in CO; however, it remains unknown if the plateau or upper and lower limits of autoregulation are changed when CO is altered. Studies in adults have shown that CBF may either be independent or passive of changes in CO[353-356]. In adult patients with stroke, an association between CO and CBF velocity (estimated using Transcranial Doppler) was present in areas affected with ischaemia but not in the unaffected areas[308]. Moreover, there is evidence that CO contributes to the regulation of CBF via sympathetic nervous system[357]. In neonates, there is not much evidence that changes in CO will result in changes in CBF. A short report from Kusaka et al (2005) has shown a positive correlation between CO and CBF in a small cohort of infants undergoing intensive care[320]. It has been suggested that CO would be regulated by changes in heart rate in preterm infants as a compensation for the immature myocardium[142]. In our study we only observed a positive correlation between CBF and CO in infants who had IVH and this correlation was only present around the possible time that reperfusion injury occurred. It is possible that regulatory mechanism may have been disrupted at that same moment, and that cerebral circulation in those infants with susceptibility to develop an IVH may be passive to changes in systemic haemodynamics. However, it will always be difficult to be precise as to the exact time of the start of the injury; therefore it is also possible that CBF became passive to CO during the actual process of bleeding.

The controversial correlation between hsPDA and cerebral blood flow and oxygenation

In studies assessing the relationship between CO and CBF, the presence of a PDA could be a confounding factor. In the presence of a haemodynamically significant PDA (> 1.5 mm and presence of left to right flow), LVO would reflect the pulmonary blood flow and RVO the systemic blood flow. Noori et al. (2014) argued that the differences in LVO patterns in infants with or without an IVH could be related to changes in the PDA rather than systemic blood flow[341]. In our cohort, more than 50% of the infants had a PDA above 1.5 mm before 48 hours of age, however other markers of hemodynamic significance and "ductal steal" such as an increased LA:Ao, presence of reversal flow on the post-ductal aorta, high LPA end diastolic flow velocity and high LVO, increased over the time intervals (Table 8.11), becoming more haemodynamically significant from 24 hours of age. Therefore, it is possible that, within the first 24 hours of life, LVO may still be a reliable trend measure of systemic blood flow and consequently ductal steal may not affect CBF.

The relationship between a PDA and IVH is complex and possibly multifactorial. In our study, no correlation was observed between a haemodynamically significant PDA and the presence of IVH. Several other authors have reported this similar lack of association. The concept that a haemodynamically significant PDA is more frequently observed in infants who develop IVH has been based on findings from relatively old studies. Kluckow & Evans, 1996 were one of the first authors to observe that infants who developed an IVH had a larger PDA than preterm infants with who did not developed IVH. They have also observed that a severe IVH (grades III and IV) was associated with lower RVO, but no association with LVO was found. However, there are some important limitations in these studies. Firstly, in some infants, the PDA measurements were collected *after* the development of the IVH. Echocardiography was performed between 7 and 31 hours of age and they acknowledged this as a possible confounder factor. Secondly, antenatal steroids were not given to all infants, and the lack of antenatal steroids is an independent risk factor for the development of IVH[249]. Jim et al. (2005) have also observed that the incidence of IVH in preterm infants with haemodynamically significant PDA was higher compared to those with non-haemodynamically significant PDA[358]. However, in this study the IVH may have

also occurred before the echocardiogram was performed. Measurements were collected at any time within the first week of life. In addition, possible confounders for fluctuations on cerebrovascular reactivity, such as mean airway pressure and $PaCO_2$ were significantly higher in the group of infants who had a haemodynamically significant PDA[358]. In our study, 100% of the infants who had echocardiography and were included in the data analysis received antenatal steroids. Moreover, most PDA measurements were performed *before* the IVH was detected on cranial ultrasound. In our study, when reviewing the cases of severe IVH, all infants who developed a severe IVH (grade III or IV) had a non-significant PDA within the first 24 hours of age and the PDA became more significant after the haemorrhage occurred.

The impact of a haemodynamically significant PDA on CBF has been assessed in several studies using NIRS[252, 253, 255, 359]. In our cohort, there was no correlation between TOI, TOEF and the presence of a haemodynamically significant PDA. However, the definition of a haemodynamically significant PDA is not the same between different studies. Lemmers et al. (2008) defined a haemodynamically significant PDA (hsPDA) as having 2D diameter above 1.4 mm, LA:Ao ration above 1.4 and LPA > 0.2, and investigated cerebral oxygenation ($rScO_2$, equivalent to TOI) and TOEF before, during and after treatment of infants with a hsPDA with indomethacin. In this study, mean values of $rScO_2$ and MABP were lower and TOEF were higher in infants with a hsPDA compared to infants with no PDA before and during the treatment. After the course of indomethacin was completed, mean values of $rScO_2$ and MABP increased and TOEF decreased to levels similar to the control group. Furthermore, no difference in frequency of IVH in the hsPDA and control groups were observed Interestingly, in this cohort none of the infants had a severe IVH (grade III or IV). Lemmers et al. (2008) attributed the "ductal steal" as the possible cause of low $rScO_2$ in infants with a hsPDA[253]. However, indomethacin may have had a direct influence on the increase in $rScO_2$, as this drug has been shown to enhance cerebrovascular reactivity. Besides that, prophylactic indomethacin has been associated with decrease in severe IVH, which could explain the absence of IVH grade III and IV and reinforce the association between the effects of this drug on cerebral circulation.

In a more recent study, Lemmers' group used a different cohort to investigate the association between the PDA and cerebral oxygenation over the first days of life. The definition of an hsPDA was similar to their previous study from 2008, but in this more recent cohort not all infants received PDA treatment. Using mixed model analysis, they observed that ductal diameter was the only variable related to cerebral oxygenation when gestational age and small for gestational age were included in the model. Again, by applying mixed model analysis, they attempted to use $rScO_2$ as a screening tool to detect an hsPDA, which would not be ideal as $rScO_2$ may be affected by several other parameters than the ones they included in the model. Moreover, NIRS and echocardiographic measurements were performed after the first 12 hours of life up to 6 days of life and within this time interval some infants developed a hsPDA, requiring treatment[252].

The association between cerebral oxygenation and a hsPDA described in those studies published by Lemmers' group had been cited by several authors; however other research groups, using more simple statistical tests and different methodology have found similar results to our study. Petrova et al. (2011) assessed the difference in $rScO_2$ between infants with a 'moderate' PDA (defined as diameter between 1.5 mm to 3 mm) and a 'severe' PDA (diameter above 3 mm) and found no difference in $rScO_2$ and FTOE between the two groups[254]. More recently, van der Laan et al. (2016), using predominant left-to-right flow across the PDA, LA:Ao ratio >1.4, LPA EDF velocity > 0.3 and Ao as markers of hsPDA, and performing measurements at mean (range) 77 (70-107) hours of life found no difference in TOI or TOEF between hsPDA or no-hsPDA. However, they observed that LPA had a positive correlation with TOI and a negative correlation with FTOE. Similar to our results, they found a higher mean ductal diameter in the Ao and higher LPA in Ao. There was no statistical significant difference in the TOI between non-Ao and presence of Ao but the mean TOI was higher in Ao group, which was similar to our findings. No correlation between ductal diameter and TOI or FTOE was observed in that study and no differences in hsPDA and TOI or FTOE were observed either[255].

Limitations

The most important limitation of this study is the comparison between continuous NIRS measurements with static functional echocardiographic measurements. There is no consensus on how to average NIRS data for correlations with cardiac data. We averaged the NIRS around 1-hour interval just before or around the echocardiography measurements, always trying to avoid periods in which drugs or transfusions were given or inotropes and vasopressors were increased or decreased as they may affect CO measurements. Other studies have applied NIRS data averaged only before or only during echocardiographic measurements[341, 349, 350]. Ideally, continuous cardiac output should be applied for studies assessing correlation between systemic and cerebral blood flow. However, the presence of a PDA remains as a major confounder, as all existing methods to measure continuous CO measure surrogate values of LVO.

Our cohort was small and our study was not powered to include multivariate analysis, including several other factors related to development of low systemic blood flow and changes in cerebral oxygenation related to IVH. The immature myocardium has been claimed as one of the major aetiological factors related to the decreased CO and low CBF in preterm infants following birth[360]. However, changes in systemic and cerebral haemodynamics may be influenced by a combination of different factors, such as peripheral vascular resistance, end-organ metabolism regulation, autonomic response and genetic predisposition to IVH. The puppy model of hypoperfusion-reperfusion injury was based on induced hypovolaemia, as well as several other animal studies on cerebral autoregulation[36, 37]. However, in preterm infants other factors such as chorioamnionitis and early onset of sepsis may play an important role in the development of cerebral ischaemia during hypoperfusion phase with not necessarily important decrease in systemic and cerebral blood volume.

9. SUMMARY AND CONCLUSIONS

Early monitoring of cerebral oxygenation, cerebrovascular reactivity and systemic blood flow can provide valuable information on the transitional circulatory function and on the pathophysiology of brain injury in preterm infants. Combining systemic with cerebral NIRS signals to optimise the management of blood pressure by using the strength of cerebrovascular control and information on end-organ perfusion is a feasible way to provide individualised care to preterm infants. Moreover, the complexity of cerebral NIRS signals during early hours of life, measured by using multiscale entropy analysis, can predict those infants who are at increased risk to develop GMH-IVH or die. Finally, the use of functional echocardiography may be a valuable tool to identify those infants with low systemic blood flow and with haemodynamically significant PDA within the first 48 hours of life. However combining static echocardiographic measurements with continuous cerebral NIRS signals was of limited value in predicting those infants at risk of developing brain injury.

9.1. MONITORING OF CEREBRAL OXYGENATION AND CEREBROVASCULAR REACTIVITY IN PRETERM INFANTS UNDERGOING INTENSIVE CARE

In Chapter 5, monitoring brain and systemic signals at the cotside was demonstrated to be feasible and easy to be incorporated to the routine clinical care. Recruiting sick preterm infants within the first hours after birth is challenging. However, the data from cerebral NIRS and systemic signals collected from the very early hours of life offer valuable information on the transitional circulation and could be used to predict which infants are at increased risk to develop IVH or die.

Real time data collection, visualisation and analysis was possible with the use of ICM+®software. Data trends, artefacts and patterns were easily visualised. This made the retrospective analysis of the data more meaningful and individualised before batch and group analysis were performed to differentiate patterns of cerebral oxygenation

and cerebrovascular reactivity between outcome groups. The case reviews demonstrated the different patterns of cerebral NIRS and systemic data and the degree of intact or impaired cerebrovascular reactivity between infants with different pathologies.

Data from all infants recruited for the 'SAMBA' cohort were included in the study shown in section 5.2. The correlation between cerebral autoregulation and cerebrovascular reactivity with the outcome of mortality and IVH, as well as with MABP and with gestational age was stronger in extremely preterm infants. More immature and sicker infants had more impaired cerebral autoregulation and cerebrovascular reactivity. Although most infants were pressure passive within the first 24 hours of life, which was demonstrated by a large number of infants with positive mean TOx, more than half of them had a negative mean TOHRx, showing that some degree of cerebrovascular reactivity may be present when the cerebral pressure regulation is lost. The association of mean values of TOx and TOHRx with outcome of IVH and mortality was affected by the heterogeneity of the data and the presence of outliers. Although none of the infants died before 48 hours of life and the relationship between IVH and death was not statistically significant, most of them had a degree of poor end-organ perfusion within the perinatal and immediate neonatal period.

9.2. OPTIMAL BLOOD PRESSURE IN PRETERM INFANTS

The results from Chapter 6 demonstrated that individual targeting of MABP based on the strength of cerebrovascular reactivity index (TOHRx) was feasible and safe. The combined analysis of cerebral NIRS signals with continuous monitoring of MABP is potentially a more reliable method to estimate end-organ perfusion than the individual analysis of these two signals.

In preterm infants born ≤ 32 weeks, the analysis of the NIRS data collected at any time within the first 72 hours of life showed that lower MABP than $MABP_{OPT}$ was associated with a higher mortality rate, while infants with MABP greater than $MABP_{OPT}$ by at least 4 mmHg had significantly severe IVH, as shown in Chapter 6, section 6.1.

In Chapter 6, section 6.2, the methodology was refined and $MABP_{OPT}$ was calculated from prolonged periods of continuous NIRS and MABP data from extremely preterm infants at less than 24 hours of life. Mean deviation below $MABP_{OPT}$ was significantly higher in infants who developed IVH and infants who died later during neonatal period. $MABP_{OPT}$ was significantly higher in infants who developed an IVH and lower in infants who had inotropes or vasopressors started within the first 24 hours of life. Because the majority of these extremely preterm infants developed an IVH around or after 24 hours of age, the deviations below $MABP_{OPT}$ in the 'IVH group' may represent the degree of cerebral hypoperfusion before the haemorrhage occurred.

The $MABP_{OPT}$ approach would help on individual care based on the strength of cerebral vascular reactivity. Further development of these monitoring techniques and refinement of the methodology should enable the implementation of a bedside tool that could determine $MABP_{OPT}$ in near real time.

9.3. THE ASSOCIATION BETWEEN THE COMPLEXITY OF BRAIN SIGNALS AND OUTCOME IN PRETERM INFANTS

In Chapter 7, multi-scale entropy analysis was applied to assess the complexity of brain and systemic signals in preterm infants undergoing intensive care. NIRS and systemic data collected within the first 24 hours of life were used, and the calculation of complexity index of brain and systemic signals was feasible when at least six hours of continuous data were available.

Decreased complexity of cerebral signals was more strongly associated with outcome of IVH and mortality than the complexity of systemic signals. Infants who died or developed an IVH had lower mean complexity index of HbO_2 and Hb compared to those who did not have an IVH or survived. Furthermore, the complexity index of HbO_2 was independently associated with an increased likelihood of having IVH when binary logistic regression analysis was performed and included CRIB II and presence of sepsis in the model.

Decreased variability in physiological signals is a sign of failure in complex regulatory system. The use of entropy analysis has been extensively studied to investigate physiological systems. However, the continuous monitoring of neonatal vital signs does not take in consideration the non-stationarity characteristic of the biological signals. Therefore, real-time cotside complexity signal analysis could offer more information on infants who are at increased risk to develop brain injury or die and represent a significant advance in the brain oriented care of critically ill newborn infants.

9.4. CARDIAC FUNCTION IN PRETERM INFANTS DURING TRANSITIONAL CIRCULATION

In Chapter 8, functional echocardiography measurements were used to assess the relationship between changes in cerebral and systemic haemodynamics in preterm infants during the transitional circulation. Left and right cardiac output and SVC flow increased significantly over the first 48 hours of life in preterm infants, but there was no significant difference in these measurements between the IVH groups.

The pattern of changes in LVO, RVO and SVC were not different between the IVH groups, however mean LVO tended to be lower in infants who developed an IVH at 12 hours of life with a significant increase from 12 to 24 hours. On the other hand, the pattern of change cerebral oxygenation between IVH groups was significantly different and mean TOI was significantly lower in infant who developed IVH from 12 hours onwards.

The correlation between systemic blood flow and cerebral oxygenation and cerebrovascular reactivity was weak for the group analysis. However, a strong positive correlation was observed between cardiac output and TOI at 24 hours of life in the IVH group. There was also a negative correlation between TOx and LVO at this same time in the IVH group, suggesting that more impaired cerebral autoregulation was present with lower cardiac output. Moreover, this finding may suggest that cerebral blood flow may have become passive to changes in cardiac output around the same time that the haemorrhage occurred, as most infants in the study developed GMH-IVH around or soon after 24 hours of life.

PDA measurements had a significant change within the first 48 hours of life. Measurements of ductal steal such as Ao, LPA EDF velocity and LA:Ao ratio increased between 6 to 48 hours of life. However, the presence of hsPDA had no association with IVH or with cerebral oxygenation. Although our sample size was small, most infants had PDA measurements performed before the haemorrhage occurred, which may suggest the reliability of our results on the lack of significance between 'ductal steal' and IVH.

In conclusion, neonatal functional echocardiography may be a useful tool to assess changes in systemic blood flow and ductal patency in preterm infants during the transitional circulation. However, the lack of correlation between LVO, RVO and PDA with NIRS signals of cerebral oxygenation and cerebrovascular reactivity demonstrates the difficulties in assessing changings between systemic and cerebral haemodynamics using static versus continuous measurements.

10. FUTURE WORK

Future research on early monitoring of brain and systemic signals in preterm infants should ally non-invasive methods to assess cerebral and systemic haemodynamics with advance methods to combine and analyse data.

10.1. EARLY RECRUITMENT AND DATA COLLECTION FROM EXTREMELY PRETERM INFANTS

The work presented in this dissertation showed the importance of monitoring the changes in cerebral and systemic haemodynamics within the first 24 hours of life. Future studies should focus on collecting cerebral and systemic data as soon as preterm infants are admitted to the neonatal intensive care units. However, this will always demand dedicated and motivated research and clinical teams.

Ideally, future studies should stratify the population according the gestational age. Sick preterm infants born ≥ 28 weeks may have a different adaptation from preterm infants born < 28 weeks and the regulation of cerebral blood flow to the brain is possibly different between these two groups. The results showed in Chapter 5, section 5.2 and in Chapter 6, section 6.2 had stronger association with outcome when infants born at less than 28 weeks were included in the analysis.

10.2. THE FUTURE OF NEUROCRITICAL CARE MONITORING

The addition of extra sensors and monitors to the standard care of small and fragile infants are usually seen as a burden from parents and medical and nursing staffing. Ideally, future neonatal intensive care monitors should combine a minimally invasive approach with high technological data analysis. Wireless sensors to monitor heart rate and SaO_2 are under development, but the technology remains unreliable and expensive. Future cotside monitors should offer more information than data averaged every seconds or minutes. In the era of artificial intelligence and big data analysis, our cotside monitors still offer limited information. Ideally, every infant admitted to an

intensive care cot should have a combined software like ICM+®, which collects raw data and allows real-time data analysis and display with easy visualisation for the clinician.

10.3. THE IMPORTANCE OF OPTIMISING BLOOD PRESSURE CONTROL IN PRETERM INFANTS

Feasibility trials on the management of adult patients with traumatic brain injury according to optimal CPP values are currently being undertaken. In neonates, managing preterm infants according to $MABP_{OPT}$ remains a new concept. The methodology used to define $MABP_{OPT}$ is promising however more studies on refining this method and applying the $MABP_{OPT}$ approach on the clinical management of preterm infants should be considered.

10.4. NIRS DATA MAY PROVIDE MORE INFORMATION THAN THRESHOLDS AND TRENDS

Several studies have been published on cerebral NIRS since we started the data collection for the work included in this dissertation. Most of them focused on defining thresholds of cerebral oxygenation and advocated the use of NIRS as cotside tool. However, a few studies applied the combination of NIRS with systemic signals or used more refined methodology to analyse the data. The use of multiscale entropy analysis to define complexity of brain signals and predict outcome is promising. However, future studies using similar methodology should focus on using short period of data and improving artefact detection.

10.5. NON-INVASIVE CARDIAC OUTPUT MONITORING

The relationship between systemic blood flow and cerebrovascular reactivity may be better understood by using measurements of continuous CO. Thoracic electrical impedance (TEI) technology is a continuous non-invasive method of CO monitoring, which is based on the principle that electrical conductivity of blood is higher than that of muscle, fat and air cells[361].This technology has been validated in term and preterm

infants and the accuracy and precision was comparable to echocardiography to estimate CO in term infants [362, 363]. However, further work is required to validate this technique in the preterm population, taking into account the challenges posed by the ductal and atrial shunts.

REFERENCES

1. Blencowe H, Cousens S, Oestergaard MZ, et al. National, regional, and worldwide estimates of preterm birth rates in the year 2010 with time trends since 1990 for selected countries: a systematic analysis and implications. *Lancet*. 2012; 379: 2162-72.

2. Liu L, Johnson HL, Cousens S, et al. Global, regional, and national causes of child mortality: an updated systematic analysis for 2010 with time trends since 2000. *Lancet*. 2012; 379: 2151-61.

3. Mwaniki MK, Atieno M, Lawn JE and Newton CR. Long-term neurodevelopmental outcomes after intrauterine and neonatal insults: a systematic review. *Lancet*. 2012; 379: 445-52.

4. Costeloe KL, Hennessy EM, Haider S, Stacey F, Marlow N and Draper ES. Short term outcomes after extreme preterm birth in England: comparison of two birth cohorts in 1995 and 2006 (the EPICure studies). *Bmj*. 2012; 345: e7976.

5. Younge N, Goldstein RF, Bann CM, et al. Survival and Neurodevelopmental Outcomes among Periviable Infants. *N Engl J Med*. 2017; 376: 617-28.

6. Hodek JM, von der Schulenburg JM and Mittendorf T. Measuring economic consequences of preterm birth - Methodological recommendations for the evaluation of personal burden on children and their caregivers. *Health Econ Rev*. 2011; 1: 6.

7. Mukerji A, Shah V and Shah PS. Periventricular/Intraventricular Hemorrhage and Neurodevelopmental Outcomes: A Meta-analysis. *Pediatrics*. 2015; 136: 1132- 43.

8. Volpe JJ. Intracranial Hemorrhage: Germinal Matrix-Intraventricular Hemorrhage of the Prmenature Infant. *Neurology of the Newborn*. 5th ed. Philadelphia, US: Saunders Elsevier, 2008, p. 517-73.

9. Moore T, Hennessy EM, Myles J, et al. Neurological and developmental outcome in extremely preterm children born in England in 1995 and 2006: the EPICure studies. *BMJ*. 2012; 345: e7961.

10. Stoll BJ, Hansen NI, Bell EF, et al. Neonatal outcomes of extremely preterm infants from the NICHD Neonatal Research Network. *Pediatrics*. 2010; 126: 443-56.

11. Yang D, Baumann JM, Sun YY, et al. Overexpression of vascular endothelial growth factor in the germinal matrix induces neurovascular proteases and intraventricular hemorrhage. *Sci Transl Med*. 2013; 5: 193ra90.

12. Perlman JM. The relationship between systemic hemodynamic perturbations and periventricular-intraventricular hemorrhage--a historical perspective. *Semin Pediatr Neurol*. 2009; 16: 191-9.

13. Volpe JJ. Brain injury in premature infants: a complex amalgam of destructive and developmental disturbances. *Lancet Neurol*. 2009; 8: 110-24.

14. Papile LA, Burstein J, Burstein R and Koffler H. Incidence and evolution of subependymal and intraventricular hemorrhage: a study of infants with birth weights less than 1,500 gm. *The Journal of pediatrics*. 1978; 92: 529-34.

15. Vasileiadis GT. Grading intraventricular hemorrhage with no grades. *Pediatrics*. 2004; 113: 930-1; author reply -1.

16. Leviton A, Kuban K and Paneth N. Intraventricular haemorrhage grading scheme: time to abandon? *Acta Paediatr*. 2007; 96: 1254-6.

17. De Vries LS, Van Haastert IL, Rademaker KJ, Koopman C and Groenendaal F. Ultrasound abnormalities preceding cerebral palsy in high-risk preterm infants. *J Pediatr*. 2004; 144: 815-20.

18. Ballabh P. Intraventricular hemorrhage in premature infants: mechanism of disease. *Pediatr Res*. 2010; 67: 1-8.

19. Morita T, Morimoto M, Yamada K, et al. Low-grade intraventricular hemorrhage disrupts cerebellar white matter in preterm infants: evidence from diffusion tensor imaging. *Neuroradiology*. 2015; 57: 507-14.

20. Bolisetty S, Dhawan A, Abdel-Latif M, et al. Intraventricular hemorrhage and neurodevelopmental outcomes in extreme preterm infants. *Pediatrics*. 2014; 133: 55-62.

21. Inder TE, Huppi PS, Warfield S, et al. Periventricular white matter injury in the premature infant is followed by reduced cerebral cortical gray matter volume at term. *Ann Neurol*. 1999; 46: 755-60.

22. Volpe JJ. Brain injury in the premature infant--from pathogenesis to prevention. *Brain Dev*. 1997; 19: 519-34.

23. Banker BQ and Larroche JC. Periventricular leukomalacia of infancy. A form of neonatal anoxic encephalopathy. *Arch Neurol*. 1962; 7: 386-410.

24. Inder TE and Volpe JJ. Mechanisms of perinatal brain injury. *Semin Neonatol*. 2000; 5: 3-16.

25. Khwaja O and Volpe JJ. Pathogenesis of cerebral white matter injury of prematurity. *Archives of disease in childhood Fetal and neonatal edition*. 2008; 93: F153-61.

26. Volpe JJ. Hypoxic-ischemic Encephalopathy: Neuropathology and Pathogenesis. *Neurology of the Newborn*. 5th ed. Philadelphia, US: Saunders Elsevier, 2008, p. 347-99.

27. Larroque B, Marret S, Ancel PY, et al. White matter damage and intraventricular hemorrhage in very preterm infants: the EPIPAGE study. *J Pediatr*. 2003; 143: 477-83.

28. Woodward LJ, Anderson PJ, Austin NC, Howard K and Inder TE. Neonatal MRI to predict neurodevelopmental outcomes in preterm infants. *N Engl J Med*. 2006; 355: 685-94.

29. Perlman JM. White matter injury in the preterm infant: an important determination of abnormal neurodevelopment outcome. *Early Hum Dev*. 1998; 53: 99-120.

30. Andiman SE, Haynes RL, Trachtenberg FL, et al. The cerebral cortex overlying periventricular leukomalacia: analysis of pyramidal neurons. *Brain Pathol*. 2010; 20: 803-14.

31. Rose J, Butler EE, Lamont LE, Barnes PD, Atlas SW and Stevenson DK. Neonatal brain structure on MRI and diffusion tensor imaging, sex, and neurodevelopment in very-low-birthweight preterm children. *Dev Med Child Neurol*. 2009; 51: 526-35.

32. Hamrick SE, Miller SP, Leonard C, et al. Trends in severe brain injury and neurodevelopmental outcome in premature newborn infants: the role of cystic periventricular leukomalacia. *J Pediatr*. 2004; 145: 593-9.

33. Volpe JJ. Neurobiology of periventricular leukomalacia in the premature infant. *Pediatric research*. 2001; 50: 553-62.

34. Strunk T, Inder T, Wang X, Burgner D, Mallard C and Levy O. Infection-induced inflammation and cerebral injury in preterm infants. *Lancet Infect Dis*. 2014; 14: 751-62.

35. Karen E. Pape JSW. *Haemorrhage, ischaemia and the perinatal brain*. 1979, p.379-82.

36. Goddard-Finegold J, Armstrong D and Zeller RS. Intraventricular hemorrhage, following volume expansion after hypovolemic hypotension in the newborn beagle. *J Pediatr*. 1982; 100: 796-9.

37. Ment LR, Stewart WB, Duncan CC and Lambrecht R. Beagle puppy model of intraventricular hemorrhage. *Journal of neurosurgery*. 1982; 57: 219-23.

38. Perlman JM, McMenamin JB and Volpe JJ. Fluctuating cerebral blood-flow velocity in respiratory-distress syndrome. Relation to the development of intraventricular hemorrhage. *The New England journal of medicine*. 1983; 309: 204-9.

39. Lou HC, Lassen NA and Friis-Hansen B. Impaired autoregulation of cerebral blood flow in the distressed newborn infant. *The Journal of pediatrics*. 1979; 94: 118-21.

40. Soul JS, Hammer PE, Tsuji M, et al. Fluctuating pressure-passivity is common in the cerebral circulation of sick premature infants. *Pediatr Res*. 2007; 61: 467-73.

41. Perlman JM and Volpe JJ. Are venous circulatory abnormalities important in the pathogenesis of hemorrhagic and/or ischemic cerebral injury? *Pediatrics*. 1987; 80: 705-11.

42. Hill A, Perlman JM and Volpe JJ. Relationship of pneumothorax to occurrence of intraventricular hemorrhage in the premature newborn. *Pediatrics*. 1982; 69: 144-9.

43. Salafia CM, Minior VK, Rosenkrantz TS, et al. Maternal, placental, and neonatal associations with early germinal matrix/intraventricular hemorrhage in infants born before 32 weeks' gestation. *Am J Perinatol*. 1995; 12: 429-36.

44. Babnik J, Stucin-Gantar I, Kornhauser-Cerar L, Sinkovec J, Wraber B and Derganc M. Intrauterine inflammation and the onset of peri-intraventricular hemorrhage in premature infants. *Biol Neonate*. 2006; 90: 113-21.

45. Yanowitz TD, Potter DM, Bowen A, Baker RW and Roberts JM. Variability in cerebral oxygen delivery is reduced in premature neonates exposed to chorioamnionitis. *Pediatr Res*. 2006; 59: 299-304.

46. Salhab WA, Hynan LS and Perlman JM. Partial or complete antenatal steroids treatment and neonatal outcome in extremely low birth weight infants < or =1000 g: is there a dose-dependent effect? *J Perinatol*. 2003; 23: 668-72.

47. Cunningham S, Symon AG, Elton RA, Zhu C and McIntosh N. Intra-arterial blood pressure reference ranges, death and morbidity in very low birthweight infants during the first seven days of life. *Early Hum Dev*. 1999; 56: 151-65.

48. Fanaroff JM, Wilson-Costello DE, Newman NS, Montpetite MM and Fanaroff AA. Treated hypotension is associated with neonatal morbidity and hearing loss in extremely low birth weight infants. *Pediatrics*. 2006; 117: 1131-5.

49. Goldstein RF, Thompson RJ, Jr., Oehler JM and Brazy JE. Influence of acidosis, hypoxemia, and hypotension on neurodevelopmental outcome in very low birth weight infants. *Pediatrics*. 1995; 95: 238-43.

50. Takashima S, Becker LE and Chan FW. Retardation of neuronal maturation in premature infants compared with term infants of the same postconceptional age. *Pediatrics*. 1982; 69: 33-9.

51. Borch K, Lou HC and Greisen G. Cerebral white matter blood flow and arterial blood pressure in preterm infants. *Acta Paediatr*. 2010; 99: 1489-92.

52. Greisen G and Borch K. White matter injury in the preterm neonate: the role of perfusion. *Dev Neurosci*. 2001; 23: 209-12.

53. Greisen G, Munck H and Lou H. Severe hypocarbia in preterm infants and neurodevelopmental deficit. *Acta Paediatr Scand*. 1987; 76: 401-4.

54. Wiswell TE, Graziani LJ, Kornhauser MS, et al. Effects of hypocarbia on the development of cystic periventricular leukomalacia in premature infants treated with high-frequency jet ventilation. *Pediatrics*. 1996; 98: 918-24.

55. Shankaran S, Langer JC, Kazzi SN, et al. Cumulative index of exposure to hypocarbia and hyperoxia as risk factors for periventricular leukomalacia in low birth weight infants. *Pediatrics*. 2006; 118: 1654-9.

56. Kluckow M and Evans N. Superior vena cava flow in newborn infants: a novel marker of systemic blood flow. *Archives of disease in childhood Fetal and neonatal edition*. 2000; 82: F182-7.

57. Garfunkel JM, Baird HW, 3rd and Ziegler J. The relationship of oxygen consumption of cerebral functional activity. *J Pediatr*. 1954; 44: 64-72.

58. Kety SS SC. The determination of cerebral blood flow in man by the use of nitric oxide in low concentrations. *American Journal of Physiology*. 1945; 143: 53-66.

59. Greisen G. Cerebral blood flow in preterm infants during the first week of life. *Acta paediatrica Scandinavica*. 1986; 75: 43-51.

60. Altman DI, Perlman JM, Volpe JJ and Powers WJ. Cerebral oxygen metabolism in newborns. *Pediatrics*. 1993; 92: 99-104.

61. Baron JC. Perfusion thresholds in human cerebral ischemia: historical perspective and therapeutic implications. *Cerebrovasc Dis*. 2001; 11 Suppl 1: 2-8.

62. Pryds O and Greisen G. Preservation of single-flash visual evoked potentials at very low cerebral oxygen delivery in preterm infants. *Pediatr Neurol*. 1990; 6: 151-8.

63. Altman DI, Powers WJ, Perlman JM, Herscovitch P, Volpe SL and Volpe JJ. Cerebral blood flow requirement for brain viability in newborn infants is lower than in adults. *Ann Neurol*. 1988; 24: 218-26.

64. Pryds O and Edwards AD. Cerebral blood flow in the newborn infant. *Arch Dis Child Fetal Neonatal Ed*. 1996; 74: F63-9.

65. Meek JH, Tyszczuk L, Elwell CE and Wyatt JS. Cerebral blood flow increases over the first three days of life in extremely preterm neonates. *Archives of disease in childhood Fetal and neonatal edition*. 1998; 78: F33-7.

66. Volpe JJ. Hypoxic-ischaemic encephalopathy: biochemical and physiological aspects *Neurology of Newborn*. Fifth Edition ed. Philadelphia, US: Saunders Elsevier, 2008.

67. Gillian Pocock CDR, David A. Richards. *Human Physiology*. 5th ed.: Oxford, 2017.

68. Jones MD, Jr., Traystman RJ, Simmons MA and Molteni RA. Effects of changes in arterial O2 content on cerebral blood flow in the lamb. *Am J Physiol*. 1981; 240: H209-15.

69. Powers WJ, Press GA, Grubb RL, Jr., Gado M and Raichle ME. The effect of hemodynamically significant carotid artery disease on the hemodynamic status of the cerebral circulation. *Ann Intern Med*. 1987; 106: 27-34.

70. Jones MD, Jr., Rosenberg AA, Simmons MA, Molteni RA, Koehler RC and Traystman RJ. Oxygen delivery to the brain before and after birth. *Science*. 1982; 216: 324-5.

71. Pichler G, Binder C, Avian A, Beckenbach E, Schmolzer GM and Urlesberger B. Reference ranges for regional cerebral tissue oxygen saturation and fractional oxygen extraction in neonates during immediate transition after birth. *J Pediatr*. 2013; 163: 1558-63.

72. Kissack CM, Garr R, Wardle SP and Weindling AM. Cerebral fractional oxygen extraction is inversely correlated with oxygen delivery in the sick, newborn, preterm infant. *J Cereb Blood Flow Metab*. 2005; 25: 545-53.

73. Alderliesten T, Lemmers PM, Smarius JJ, van de Vosse RE, Baerts W and van Bel F. Cerebral oxygenation, extraction, and autoregulation in very preterm infants who develop peri-intraventricular hemorrhage. *J Pediatr*. 2013; 162: 698-704 e2.

74. Miranda MJ, Olofsson K and Sidaros K. Noninvasive measurements of regional cerebral perfusion in preterm and term neonates by magnetic resonance arterial spin labeling. *Pediatr Res*. 2006; 60: 359-63.

75. Borch K and Greisen G. Blood flow distribution in the normal human preterm brain. *Pediatr Res*. 1998; 43: 28-33.

76. Pryds O, Greisen G, Lou H and Friis-Hansen B. Heterogeneity of cerebral vasoreactivity in preterm infants supported by mechanical ventilation. *The Journal of pediatrics*. 1989; 115: 638-45.

77. Meek JH, Tyszczuk L, Elwell CE and Wyatt JS. Low cerebral blood flow is a risk factor for severe intraventricular haemorrhage. *Arch Dis Child Fetal Neonatal Ed*. 1999; 81: F15-8.

78. Wong FY, Leung TS, Austin T, et al. Impaired autoregulation in preterm infants identified by using spatially resolved spectroscopy. *Pediatrics*. 2008; 121: e604-11.

79. Milligan DW. Failure of autoregulation and intraventricular haemorrhage in preterm infants. *Lancet*. 1980; 1: 896-8.

80. Tsuji M, Saul JP, du Plessis A, et al. Cerebral Intravascular Oxygenation Correlates With Mean Arterial Pressure in Critically Ill Premature Infants. *Pediatrics*. 2000; 106: 625-32.

81. O'Leary H, Gregas MC, Limperopoulos C, et al. Elevated cerebral pressure passivity is associated with prematurity-related intracranial hemorrhage. *Pediatrics*. 2009; 124: 302-9.

82. Wong FY, Silas R, Hew S, Samarasinghe T and Walker AM. Cerebral oxygenation is highly sensitive to blood pressure variability in sick preterm infants. *PloS one*. 2012; 7: e43165.

83. Roy CS and Sherrington CS. On the Regulation of the Blood-supply of the Brain. *J Physiol*. 1890; 11: 85-158 17.

84. Koehler RC, Roman RJ and Harder DR. Astrocytes and the regulation of cerebral blood flow. *Trends Neurosci*. 2009; 32: 160-9.

85. Wong FY, Barfield CP, Horne RS and Walker AM. Dopamine therapy promotes cerebral flow-metabolism coupling in preterm infants. *Intensive Care Med*. 2009; 35: 1777-82.

86. Harris AP, Ohata H and Koehler RC. Role of nitric oxide in cerebrovascular reactivity to NMDA and hypercapnia during prenatal development in sheep. *Int J Dev Neurosci*. 2008; 26: 47-55.

87. Kaur C, Ling EA and Wong WC. Development of the various glial cell types in the cerebral cortex of postnatal rats. *Acta Anat (Basel)*. 1989; 136: 204-10.

88. Norman MG and O'Kusky JR. The growth and development of microvasculature in human cerebral cortex. *J Neuropathol Exp Neurol*. 1986; 45: 222-32.

89. Kozberg MG, Ma Y, Shaik MA, Kim SH and Hillman EM. Rapid Postnatal Expansion of Neural Networks Occurs in an Environment of Altered Neurovascular and Neurometabolic Coupling. *J Neurosci*. 2016; 36: 6704-17.

90. Kozberg MG and Hillman EM. Neurovascular coupling develops alongside neural circuits in the postnatal brain. *Neurogenesis (Austin)*. 2016; 3: e1244439.

91. Kaiser JR, Gauss CH, Pont MM and Williams DK. Hypercapnia during the first 3 days of life is associated with severe intraventricular hemorrhage in very low birth weight infants. *J Perinatol*. 2006; 26: 279-85.

92. Kaiser JR, Gauss CH and Williams DK. The effects of hypercapnia on cerebral autoregulation in ventilated very low birth weight infants. *Pediatr Res*. 2005; 58: 931-5.

93. Pryds O. Control of cerebral circulation in the high-risk neonate. *Ann Neurol*. 1991; 30: 321-9.

94. Busija DW and Heistad DD. Factors involved in the physiological regulation of the cerebral circulation. *Rev Physiol Biochem Pharmacol*. 1984; 101: 161-211.

95. Pearce W. Hypoxic regulation of the fetal cerebral circulation. *J Appl Physiol (1985)*. 2006; 100: 731-8.

96. Giussani DA. The fetal brain sparing response to hypoxia: physiological mechanisms. *J Physiol*. 2016; 594: 1215-30.

97. Giussani DA, Spencer JA, Moore PJ, Bennet L and Hanson MA. Afferent and efferent components of the cardiovascular reflex responses to acute hypoxia in term fetal sheep. *J Physiol*. 1993; 461: 431-49.

98. Fletcher AJ, Gardner DS, Edwards CM, Fowden AL and Giussani DA. Cardiovascular and endocrine responses to acute hypoxaemia during and following dexamethasone infusion in the ovine fetus. *J Physiol*. 2003; 549: 271-87.

99. Fletcher AJ, Forhead AJ, Fowden AL, Ford WR, Nathanielsz PW and Giussani DA. Effects of gestational age and cortisol treatment on ovine fetal heart function in a novel biventricular Langendorff preparation. *J Physiol*. 2005; 562: 493-505.

100. Bayliss WM. On the local reactions of the arterial wall to changes of internal pressure. *J Physiol*. 1902; 28: 220-31.

101. Tan CO, Hamner JW and Taylor JA. The role of myogenic mechanisms in human cerebrovascular regulation. *J Physiol*. 2013; 591: 5095-105.

102. Andresen J, Shafi NI and Bryan RM, Jr. Endothelial influences on cerebrovascular tone. *J Appl Physiol (1985)*. 2006; 100: 318-27.

103. Griffith TM, Edwards DH, Lewis MJ, Newby AC and Henderson AH. The nature of endothelium-derived vascular relaxant factor. *Nature*. 1984; 308: 645-7.

104. Furchgott RF and Zawadzki JV. The obligatory role of endothelial cells in the relaxation of arterial smooth muscle by acetylcholine. *Nature*. 1980; 288: 373-6.

105. Wang Q, Pelligrino DA, Baughman VL, Koenig HM and Albrecht RF. The role of neuronal nitric oxide synthase in regulation of cerebral blood flow in normocapnia and hypercapnia in rats. *J Cereb Blood Flow Metab*. 1995; 15: 774-8.

106. Atochin DN, Demchenko IT, Astern J, Boso AE, Piantadosi CA and Huang PL. Contributions of endothelial and neuronal nitric oxide synthases to cerebrovascular responses to hyperoxia. *J Cereb Blood Flow Metab*. 2003; 23: 1219-26.

107. Mandala M, Pedatella AL, Morales Palomares S, Cipolla MJ and Osol G. Maturation is associated with changes in rat cerebral artery structure, biomechanical properties and tone. *Acta Physiol (Oxf)*. 2012; 205: 363-71.

108. Mokri B. The Monro-Kellie hypothesis: applications in CSF volume depletion. *Neurology*. 2001; 56: 1746-8.

109. Fog M. The Relationship between the Blood Pressure and the Tonic Regulation of the Pial Arteries. *J Neurol Psychiatry*. 1938; 1: 187-97.

110. Lassen N. Cerebral blood flow and oxygen consumption in man. *Physiological Reviews*. 1959; 39: 183-238.

111. Boylan GB YK, Penerai RB, Rennie JM, Evans DH. Dynamic cerebral autoregulation in sick newborn infants. *Pediatric research*. 2000; 48: 12-7.

112. Greisen G. Autoregulation of cerebral blood flow in newborn babies. *Early Hum Dev*. 2005; 81: 423-8.

113. Adelson PD, Srinivas R, Chang Y, Bell M and Kochanek PM. Cerebrovascular response in children following severe traumatic brain injury. *Child's nervous system : ChNS : official journal of the International Society for Pediatric Neurosurgery*. 2011; 27: 1465-76.

114. Czosnyka M, Balestreri M, Steiner L, et al. Age, intracranial pressure, autoregulation, and outcome after brain trauma. *Journal of neurosurgery*. 2005; 102: 450-4.

115. Eriksen VR, Hahn GH and Greisen G. Cerebral autoregulation in the preterm newborn using near-infrared spectroscopy: a comparison of time-domain and frequency-domain analyses. *Journal of biomedical optics*. 2015; 20: 37009.

116. Giller CA. The frequency-dependent behavior of cerebral autoregulation. *Neurosurgery*. 1990; 27: 362-8.

117. Tsuji M, Saul JP, du Plessis A, et al. Cerebral intravascular oxygenation correlates with mean arterial pressure in critically ill premature infants. *Pediatrics*. 2000; 106: 625-32.

118. Wong FY, Nakamura M, Alexiou T, Brodecky V and Walker AM. Tissue oxygenation index measured using spatially resolved spectroscopy correlates with changes in cerebral blood flow in newborn lambs. *Intensive Care Med*. 2009; 35: 1464-70.

119. Caicedo A, De Smet D, Naulaers G, et al. Cerebral tissue oxygenation and regional oxygen saturation can be used to study cerebral autoregulation in prematurely born infants. *Pediatr Res*. 2011; 69: 548-53.

120. Czosnyka M, Brady K, Reinhard M, Smielewski P and Steiner LA. Monitoring of cerebrovascular autoregulation: facts, myths, and missing links. *Neurocritical care*. 2009; 10: 373-86.

121. Pickard JD, Matheson M, Patterson J and Wyper D. Prediction of late ischemic complications after cerebral aneurysm surgery by the intraoperative measurement of cerebral blood flow. *J Neurosurg*. 1980; 53: 305-8.

122. Chen A, Shyr MH, Chen TY, Lai HY, Lin CC and Yen PS. Dynamic CT perfusion imaging with acetazolamide challenge for evaluation of patients with unilateral cerebrovascular steno-occlusive disease. *AJNR Am J Neuroradiol*. 2006; 27: 1876-81.

123. Wintermark M, Chiolero R, Van Melle G, et al. Cerebral vascular autoregulation assessed by perfusion-CT in severe head trauma patients. *J Neuroradiol*. 2006; 33: 27-37.

124. Hattingen E, Blasel S, Dettmann E, et al. Perfusion-weighted MRI to evaluate cerebral autoregulation in aneurysmal subarachnoid haemorrhage. *Neuroradiology*. 2008; 50: 929-38.

125. Yundt KD, Grubb RL, Jr., Diringer MN and Powers WJ. Autoregulatory vasodilation of parenchymal vessels is impaired during cerebral vasospasm. *J Cereb Blood Flow Metab*. 1998; 18: 419-24.

126. Yamamoto S, Teng W, Kakiuchi T and Tsukada H. Disturbance of cerebral blood flow autoregulation in hypertension is attributable to ischaemia following subarachnoid haemorrhage in rats: A PET study. *Acta Neurochir (Wien)*. 1999; 141: 1213-9.

127. Powers WJ, Zazulia AR, Videen TO, et al. Autoregulation of cerebral blood flow surrounding acute (6 to 22 hours) intracerebral hemorrhage. *Neurology*. 2001; 57: 18-24.

128. Aaslid R, Huber P and Nornes H. A transcranial Doppler method in the evaluation of cerebrovascular spasm. *Neuroradiology*. 1986; 28: 11-6.

129. Brady KM, Lee JK, Kibler KK, et al. Continuous time-domain analysis of c erebrovascular autoregulation using near-infrared spectroscopy. *Stroke*. 2007; 38: 2818-25.

130. Czosnyka M, Smielewski P, Kirkpatrick P, Laing RJ, Menon D and Pickard JD. Continuous assessment of the cerebral vasomotor reactivity in head injury. *Neurosurgery*. 1997; 41: 11-7; discussion 7-9.

131. Timofeev I, Czosnyka M, Carpenter KL, et al. Interaction between brain chemistry and physiology after traumatic brain injury: impact of autoregulation and microdialysis catheter location. *J Neurotrauma*. 2011; 28: 849-60.

132. Skov L, Pryds O and Greisen G. Estimating cerebral blood flow in newborn infants: comparison of near infrared spectroscopy and 133Xe clearance. *Pediatric research*. 1991; 30: 570-3.

133. Volpe JJ, Herscovitch P, Perlman JM, Kreusser KL and Raichle ME. Positron emission tomography in the asphyxiated term newborn: parasagittal impairment of cerebral blood flow. *Ann Neurol*. 1985; 17: 287-96.

134. Czosnyka M, Richards HK, Whitehouse HE and Pickard JD. Relationship between transcranial Doppler-determined pulsatility index and cerebrovascular resistance: an experimental study. *J Neurosurg*. 1996; 84: 79-84.

135. Czosnyka M, Matta BF, Smielewski P, Kirkpatrick PJ and Pickard JD. Cerebral perfusion pressure in head-injured patients: a noninvasive assessment using transcranial Doppler ultrasonography. *J Neurosurg*. 1998; 88: 802-8.

136. Brady KM, Lee JK, Kibler KK, Easley RB, Koehler RC and Shaffner DH. Continuous measurement of autoregulation by spontaneous fluctuations in cerebral perfusion pressure: comparison of 3 methods. *Stroke; a journal of cerebral circulation*. 2008; 39: 2531-7.

137. Gilmore MM, Stone BS, Shepard JA, Czosnyka M, Easley RB and Brady KM. Relationship between cerebrovascular dysautoregulation and arterial blood pressure in the premature infant. *J Perinatol*. 2011; 31: 722-9.

138. Eriksen VR, Hahn GH and Greisen G. Dopamine therapy is associated with impaired cerebral autoregulation in preterm infants. *Acta Paediatr*. 2014; 103: 1221-6.

139. Lee JK, Kibler KK, Benni PB, et al. Cerebrovascular reactivity measured by near-infrared spectroscopy. *Stroke; a journal of cerebral circulation*. 2009; 40: 1820-6.

140. Lee JK, Yang ZJ, Wang B, et al. Noninvasive autoregulation monitoring in a swine model of pediatric cardiac arrest. *Anesth Analg*. 2012; 114: 825-36.

141. Mitra S, Czosnyka M, Smielewski P, O'Reilly H, Brady K and Austin T. Heart rate passivity of cerebral tissue oxygenation is associated with predictors of poor outcome in preterm infants. *Acta Paediatr*. 2014; 103: e374-82.

142. Noori S ST, Seri I. Principles of developmental cardiovascular physiology and pathophysiology. In: Kleinman C SI, (ed.). *Neonatology questions and controversies: hemodynamics and cardiology*. 2nd ed. Philadelphia, USA: Elsevier Sauders, 2012, p. 3-22.

143. Kiserud T. Physiology of the fetal circulation. *Semin Fetal Neonatal Med*. 2005; 10: 493-503.

144. Gournay V. The ductus arteriosus: physiology, regulation, and functional and congenital anomalies. *Arch Cardiovasc Dis*. 2011; 104: 578-85.

145. Kluckow M and Evans N. Low superior vena cava flow and intraventricular haemorrhage in preterm infants. *Arch Dis Child Fetal Neonatal Ed*. 2000; 82: F188-94.

146. Evans N and Kluckow M. Early determinants of right and left ventricular output in ventilated preterm infants. *Archives of disease in childhood Fetal and neonatal edition*. 1996; 74: F88-94.

147. Azhibekov T, Noori S, Soleymani S and Seri I. Transitional cardiovascular physiology and comprehensive hemodynamic monitoring in the neonate: relevance to research and clinical care. *Semin Fetal Neonatal Med*. 2014; 19: 45-53.

148. Kluckow M and Evans N. Low systemic blood flow in the preterm infant. *Semin Neonatol*. 2001; 6: 75-84.

149. Kluckow M. Low systemic blood flow and pathophysiology of the preterm transitional circulation. *Early human development*. 2005; 81: 429-37.

150. Engle WD. Definition of normal blood pressure: the elusive target. In: Charles Kleinman IS, (ed.). *Neonatology questions and controversies: hemodynamics and cardiology*. 2nd ed. Philadelphia, USA: Elsevier Saunders, 2012, p. 49-72.

151. Watkins AM, West CR and Cooke RW. Blood pressure and cerebral haemorrhage and ischaemia in very low birthweight infants. *Early Hum Dev*. 1989; 19: 103-10.

152. Lee J, Rajadurai VS and Tan KW. Blood pressure standards for very low birthweight infants during the first day of life. *Archives of disease in childhood Fetal and neonatal edition*. 1999; 81: F168-70.

153. Development of audit measures and guidelines for good practice in the management of neonatal respiratory distress syndrome. Report of a Joint Working Group of the British Association of Perinatal Medicine and the Research Unit of the Royal College of Physicians. *Arch Dis Child*. 1992; 67: 1221-7.

154. Munro MJ, Walker AM and Barfield CP. Hypotensive extremely low birth weight infants have reduced cerebral blood flow. *Pediatrics*. 2004; 114: 1591-6.

155. Miall-Allen VM, de Vries LS and Whitelaw AG. Mean arterial blood pressure and neonatal cerebral lesions. *Arch Dis Child*. 1987; 62: 1068-9.

156. Nuntnarumit P, Yang W and Bada-Ellzey HS. Blood pressure measurements in the newborn. *Clinics in perinatology*. 1999; 26: 981-96, x.

157. Miall-Allen VM and Whitelaw AG. Effect of pancuronium and pethidine on heart rate and blood pressure in ventilated infants. *Arch Dis Child*. 1987; 62: 1179-80.

158. Bada HS, Korones SB, Perry EH, et al. Mean arterial blood pressure changes in premature infants and those at risk for intraventricular hemorrhage. *J Pediatr*. 1990; 117: 607-14.

159. Lou HC, Lassen NA and Friis-Hansen B. Low cerebral blood flow in the hypotensive distressed newborn. *Acta Neurol Scand Suppl*. 1977; 64: 428-9.

160. Takashima S and Tanaka K. Development of cerebrovascular architecture and its relationship to periventricular leukomalacia. *Arch Neurol*. 1978; 35: 11-6.

161. Limperopoulos C, Bassan H, Kalish LA, et al. Current definitions of hypotension do not predict abnormal cranial ultrasound findings in preterm infants. *Pediatrics*. 2007; 120: 966-77.

162. Pellicer A, Bravo MC, Madero R, Salas S, Quero J and Cabanas F. Early systemic hypotension and vasopressor support in low birth weight infants: impact on neurodevelopment. *Pediatrics*. 2009; 123: 1369-76.

163. Alderliesten T, Lemmers PM, van Haastert IC, et al. Hypotension in preterm neonates: low blood pressure alone does not affect neurodevelopmental outcome. *J Pediatr*. 2014; 164: 986-91.

164. Dempsey EM, Al Hazzani F and Barrington KJ. Permissive hypotension in the extremely low birthweight infant with signs of good perfusion. *Arch Dis Child Fetal Neonatal Ed*. 2009; 94: F241-4.

165. Batton B, Li L, Newman NS, et al. Early blood pressure, antihypotensive therapy and outcomes at 18-22 months' corrected age in extremely preterm infants. *Arch Dis Child Fetal Neonatal Ed*. 2016; 101: F201-6.

166. Sekhon MS, Smielewski P, Bhate TD, et al. Using the relationship between brain tissue regional saturation of oxygen and mean arterial pressure to determine the optimal mean arterial pressure in patients following cardiac arrest: A pilot proof-of-concept study. *Resuscitation*. 2016; 106: 120-5.

167. Needham E, McFadyen C, Newcombe V, Synnot AJ, Czosnyka M and Menon D. Cerebral Perfusion Pressure Targets Individualized to Pressure-Reactivity Index in Moderate to Severe Traumatic Brain Injury: A Systematic Review. *J Neurotrauma*. 2017; 34: 963-70.

168. Young AM, Donnelly J, Czosnyka M, et al. Continuous Multimodality Monitoring in Children after Traumatic Brain Injury-Preliminary Experience. *PLoS One*. 2016; 11: e0148817.

169. Hori D, Max L, Laflam A, et al. Blood Pressure Deviations From Optimal Mean Arterial Pressure During Cardiac Surgery Measured With a Novel Monitor of Cerebral Blood Flow and Risk for Perioperative Delirium: A Pilot Study. *J Cardiothorac Vasc Anesth*. 2016; 30: 606-12.

170. Steiner LA, Czosnyka M, Piechnik SK, et al. Continuous monitoring of cerebrovascular pressure reactivity allows determination of optimal cerebral perfusion pressure in patients with traumatic brain injury. *Critical care medicine*. 2002; 30: 733-8.

171. Brain Trauma F, American Association of Neurological S, Congress of Neurological S, et al. Guidelines for the management of severe traumatic brain injury. IX. Cerebral perfusion thresholds. *J Neurotrauma*. 2007; 24 Suppl 1: S59-64.

172. Aries MJ, Czosnyka M, Budohoski KP, et al. Continuous determination of optimal cerebral perfusion pressure in traumatic brain injury. *Crit Care Med*. 2012; 40: 2456-63.

173. Chew MS and Poelaert J. Accuracy and repeatability of pediatric cardiac output measurement using Doppler: 20-year review of the literature. *Intensive Care Med*. 2003; 29: 1889-94.

174. Dias C, Silva MJ, Pereira E, et al. Optimal Cerebral Perfusion Pressure Management at Bedside: A Single-Center Pilot Study. *Neurocrit Care*. 2015; 23: 92-102.

175. Zweifel C, Lavinio A, Steiner LA, et al. Continuous monitoring of cerebrovascular pressure reactivity in patients with head injury. *Neurosurg Focus*. 2008; 25: E2.

176. Lee JK, Poretti A, Perin J, et al. Optimizing Cerebral Autoregulation May Decrease Neonatal Regional Hypoxic-Ischemic Brain Injury. *Dev Neurosci*. 2017; 39: 248-56.

177. Burton VJ, Gerner G, Cristofalo E, et al. A pilot cohort study of cerebral autoregulation and 2-year neurodevelopmental outcomes in neonates with hypoxic-ischemic encephalopathy who received therapeutic hypothermia. *BMC Neurol*. 2015; 15: 209.

178. Jobsis FF. Noninvasive, infrared monitoring of cerebral and myocardial oxygen sufficiency and circulatory parameters. *Science*. 1977; 198: 1264-7.

179. Brazy JE, Lewis DV, Mitnick MH and Jobsis vander Vliet FF. Noninvasive monitoring of cerebral oxygenation in preterm infants: preliminary observations. *Pediatrics*. 1985; 75: 217-25.

180. Wyatt JS, Cope M, Delpy DT, Wray S and Reynolds EO. Quantification of cerebral oxygenation and haemodynamics in sick newborn infants by near infrared spectrophotometry. *Lancet*. 1986; 2: 1063-6.

181. Yoxall CW and Weindling AM. Measurement of cerebral oxygen consumption in the human neonate using near infrared spectroscopy: cerebral oxygen consumption increases with advancing gestational age. *Pediatric research*. 1998; 44: 283-90.

182. Denault A, Lamarche Y, Rochon A, et al. Innovative approaches in the perioperative care of the cardiac surgical patient in the operating room and intensive care unit. *The Canadian journal of cardiology*. 2014; 30: S459-77.

183. Horecker BL. The absorption spectra of hemoglobin and its derivatives in the visible and near infra-red regions. *Journal of biological chemistry*. 1943; 148.1: 173-83.

184. Cope M. *The development of a near infrared spectroscopy system and its application for non invasive monitoring of cerebral blood and tissue oxygenation in the newborn infants*. University of London, 1991.

185. Elwell CE. *A pratical users guide to near infrared spectroscopy*. London, UK: Hamamatusu Photonics, 1995.

186. Patel J, Marks K, Roberts I, Azzopardi D and Edwards AD. Measurement of cerebral blood flow in newborn infants using near infrared spectroscopy with indocyanine green. *Pediatr Res*. 1998; 43: 34-9.

187. Matcher SJ and Cooper CE. Absolute quantification of deoxyhaemoglobin concentration in tissue near infrared spectroscopy. *Phys Med Biol*. 1994; 39: 1295-312.

188. Valipour A, McGown AD, Makker H, O'Sullivan C and Spiro SG. Some factors affecting cerebral tissue saturation during obstructive sleep apnoea. *Eur Respir J*. 2002; 20: 444-50.

189. Susumu Suzuki ST, Takeo Ozaki and Yukio Kobayash. A Tissue Oxygenation Monitor using NIR Spatially Resolved Spectroscopy. *SPIE*. 1999; 3597.

190. Al-Rawi PG, Smielewski P and Kirkpatrick PJ. Evaluation of a near-infrared spectrometer (NIRO 300) for the detection of intracranial oxygenation changes in the adult head. *Stroke*. 2001; 32: 2492-500.

191. Nagdyman N, Fleck T, Schubert S, et al. Comparison between cerebral tissue oxygenation index measured by near-infrared spectroscopy and venous jugular bulb saturation in children. *Intensive care medicine*. 2005; 31: 846-50.

192. Thavasothy M, Broadhead M, Elwell C, Peters M and Smith M. A comparison of cerebral oxygenation as measured by the NIRO 300 and the INVOS 5100 Near-Infrared Spectrophotometers. *Anaesthesia*. 2002; 57: 999-1006.

193. Sorensen LC and Greisen G. Precision of measurement of cerebral tissue oxygenation index using near-infrared spectroscopy in preterm neonates. *Journal of biomedical optics*. 2006; 11: 054005.

194. Pocivalnik M, Pichler G, Zotter H, Tax N, Muller W and Urlesberger B. Regional tissue oxygen saturation: comparability and reproducibility of different devices. *J Biomed Opt*. 2011; 16: 057004.

195. Schneider A, Minnich B, Hofstatter E, Weisser C, Hattinger-Jurgenssen E and Wald M. Comparison of four near-infrared spectroscopy devices shows that they are only suitable for monitoring cerebral oxygenation trends in preterm infants. *Acta paediatrica*. 2014; 103: 934-8.

196. Hyttel-Sorensen S, Kleiser S, Wolf M and Greisen G. Calibration of a prototype NIRS oximeter against two commercial devices on a blood-lipid phantom. *Biomed Opt Express*. 2013; 4: 1662-72.

197. Ohmae E, Ouchi Y, Oda M, et al. Cerebral hemodynamics evaluation by near-infrared time-resolved spectroscopy: correlation with simultaneous positron emission tomography measurements. *Neuroimage*. 2006; 29: 697-705.

198. Watzman HM, Kurth CD, Montenegro LM, Rome J, Steven JM and Nicolson SC. Arterial and venous contributions to near-infrared cerebral oximetry. *Anesthesiology*. 2000; 93: 947-53.

199. Germon TJ, Kane NM, Manara AR and Nelson RJ. Near-infrared spectroscopy in adults: effects of extracranial ischaemia and intracranial hypoxia on estimation of cerebral oxygenation. *Br J Anaesth*. 1994; 73: 503-6.

200. Yoshitani K, Kawaguchi M, Miura N, et al. Effects of hemoglobin concentration, skull thickness, and the area of the cerebrospinal fluid layer on near-infrared spectroscopy measurements. *Anesthesiology*. 2007; 106: 458-62.

201. Pringle J, Roberts C, Kohl M and Lekeux P. Near infrared spectroscopy in large animals: optical pathlength and influence of hair covering and epidermal pigmentation. *Vet J*. 1999; 158: 48-52.

202. Naulaers G, Meyns B, Miserez M, et al. Use of tissue oxygenation index and fractional tissue oxygen extraction as non-invasive parameters for cerebral oxygenation. A validation study in piglets. *Neonatology*. 2007; 92: 120-6.

203. Phelps HM, Mahle WT, Kim D, et al. Postoperative cerebral oxygenation in hypoplastic left heart syndrome after the Norwood procedure. *The Annals of thoracic surgery*. 2009; 87: 1490-4.

204. Lemmers PM, Zwanenburg RJ, Benders MJ, et al. Cerebral oxygenation and brain activity after perinatal asphyxia: does hypothermia change their prognostic value? *Pediatr Res*. 2013; 74: 180-5.

205. Toet MC, Lemmers PM, van Schelven LJ and van Bel F. Cerebral oxygenation and electrical activity after birth asphyxia: their relation to outcome. *Pediatrics*. 2006; 117: 333-9.

206. Wintermark P, Hansen A, Warfield SK, Dukhovny D and Soul JS. Near-infrared spectroscopy versus magnetic resonance imaging to study brain perfusion in newborns with hypoxic-ischemic encephalopathy treated with hypothermia. *Neuroimage*. 2014; 85 Pt 1: 287-93.

207. Peng S, Boudes E, Tan X, Saint-Martin C, Shevell M and Wintermark P. Does near-infrared spectroscopy identify asphyxiated newborns at risk of developing brain injury during hypothermia treatment? *Am J Perinatol*. 2015; 32: 555-64.

208. Kurth CD, Levy WJ and McCann J. Near-infrared spectroscopy cerebral oxygen saturation thresholds for hypoxia-ischemia in piglets. *J Cereb Blood Flow Metab*. 2002; 22: 335-41.

209. Hyttel-Sorensen S, Pellicer A, Alderliesten T, et al. Cerebral near infrared spectroscopy oximetry in extremely preterm infants: phase II randomised clinical trial. *Bmj*. 2015; 350: g7635.

210. Alderliesten T, Dix L, Baerts W, et al. Reference values of regional cerebral oxygen saturation during the first 3 days of life in preterm neonates. *Pediatr Res*. 2016; 79: 55-64.

211. Binder C, Urlesberger B, Avian A, Pocivalnik M, Muller W and Pichler G. Cerebral and peripheral regional oxygen saturation during postnatal transition in preterm neonates. *J Pediatr*. 2013; 163: 394-9.

212. Peebles DM, Edwards AD, Wyatt JS, Cope M, Delpy DT and Reynold EO. Changes in human fetal cerebral oxygenation and blood volume during delivery. *Am J Obstet Gynecol*. 1992; 167: 1916-7.

213. Fauchere JC, Schulz G, Haensse D, et al. Near-infrared spectroscopy measurements of cerebral oxygenation in newborns during immediate postnatal adaptation. *J Pediatr*. 2010; 156: 372-6.

214. Kratky E, Pichler G, Rehak T, et al. Regional cerebral oxygen saturation in newborn infants in the first 15 min of life after vaginal delivery. *Physiol Meas*. 2012; 33: 95-102.

215. Goldstein B, Fiser DH, Kelly MM, Mickelsen D, Ruttimann U and Pollack MM. Decomplexification in critical illness and injury: relationship between heart rate variability, severity of illness, and outcome. *Crit Care Med*. 1998; 26: 352-7.

216. Goldberger AL, Amaral LA, Hausdorff JM, Ivanov P, Peng CK and Stanley HE. Fractal dynamics in physiology: alterations with disease and aging. *Proc Natl Acad Sci U S A*. 2002; 99 Suppl 1: 2466-72.

217. Norris PR, Anderson SM, Jenkins JM, Williams AE and Morris JA, Jr. Heart rate multiscale entropy at three hours predicts hospital mortality in 3,154 trauma patients. *Shock*. 2008; 30: 17-22.

218. Riordan WP, Jr., Norris PR, Jenkins JM and Morris JA, Jr. Early loss of heart rate complexity predicts mortality regardless of mechanism, anatomic location, or severity of injury in 2178 trauma patients. *J Surg Res*. 2009; 156: 283-9.

219. Pincus SM. Approximate entropy as a measure of system complexity. *Proc Natl Acad Sci U S A*. 1991; 88: 2297-301.

220. Bruhn J, Ropcke H and Hoeft A. Approximate entropy as an electroencephalographic measure of anesthetic drug effect during desflurane anesthesia. *Anesthesiology*. 2000; 92: 715-26.

221. Engoren M. Approximate entropy of respiratory rate and tidal volume during weaning from mechanical ventilation. *Crit Care Med*. 1998; 26: 1817-23.

222. Lake DE, Richman JS, Griffin MP and Moorman JR. Sample entropy analysis of neonatal heart rate variability. *Am J Physiol Regul Integr Comp Physiol*. 2002; 283: R789-97.

223. Richman JS and Moorman JR. Physiological time-series analysis using approximate entropy and sample entropy. *Am J Physiol Heart Circ Physiol*. 2000; 278: H2039-49.

224. Costa M, Goldberger AL and Peng CK. Multiscale entropy analysis of complex physiologic time series. *Phys Rev Lett*. 2002; 89: 068102.

225. Costa M, Goldberger AL and Peng CK. Multiscale entropy analysis of biological signals. *Phys Rev E Stat Nonlin Soft Matter Phys*. 2005; 71: 021906.

226. Lu CW, Czosnyka M, Shieh JS, Smielewska A, Pickard JD and Smielewski P. Complexity of intracranial pressure correlates with outcome after traumatic brain injury. *Brain*. 2012; 135: 2399-408.

227. Lu WY, Chen JY, Chang CF, Weng WC, Lee WT and Shieh JS. Multiscale Entropy of Electroencephalogram as a Potential Predictor for the Prognosis of Neonatal Seizures. *PLoS One*. 2015; 10: e0144732.

228. Sehgal A and McNamara PJ. Does point-of-care functional echocardiography enhance cardiovascular care in the NICU? *Journal of perinatology : official journal of the California Perinatal Association*. 2008; 28: 729-35.

229. El-Khuffash AF and McNamara PJ. Neonatologist-performed functional echocardiography in the neonatal intensive care unit. *Semin Fetal Neonatal Med*. 2011; 16: 50-60.

230. Hudson I, Houston A, Aitchison T, Holland B and Turner T. Reproducibility of measurements of cardiac output in newborn infants by Doppler ultrasound. *Arch Dis Child*. 1990; 65: 15-9.

231. Jonathan Skinner DA, Stewart Hunter. *Echocardiography for the neonatologist*. Philadelphia, USA: Churchill Livingstone, 2000.

232. de Waal KA. The methodology of Doppler-derived central blood flow measurements in newborn infants. *Int J Pediatr*. 2012; 2012: 680162.

233. Evans NJ. Functional echocardiography in the neonatal intensive care unit. *Hemodynamics and Cardiology: Neonatology questions and controversies*. 2nd ed. USA: Saunders, 2012.

234. Wyllie J. Neonatal echocardiography. *Semin Fetal Neonatal Med*. 2015; 20: 173-80.

235. Mandelbaum-Isken VH and Linderkamp O. Cardiac output by pulsed Doppler in neonates using the apical window. *Pediatr Cardiol*. 1991; 12: 13-6.

236. Groves AM, Chiesa G, Durighel G, et al. Functional cardiac MRI in preterm and term newborns. *Arch Dis Child Fetal Neonatal Ed*. 2011; 96: F86-91.

237. Ficial B, Finnemore AE, Cox DJ, et al. Validation study of the accuracy of echocardiographic measurements of systemic blood flow volume in newborn infants. *J Am Soc Echocardiogr*. 2013; 26: 1365-71.

238. Moritz B, Fritz M, Mann C and Simma B. Nasal continuous positive airway pressure (n-CPAP) does not change cardiac output in preterm infants. *Am J Perinatol*. 2008; 25: 105-9.

239. Patel N, Dodsworth M and Mills JF. Cardiac output measurement in newborn infants using the ultrasonic cardiac output monitor: an assessment of agreement with conventional echocardiography, repeatability and new user experience. *Arch Dis Child Fetal Neonatal Ed*. 2011; 96: F206-11.

240. Mellander M, Sabel KG, Caidahl K, Solymar L and Eriksson B. Doppler determination of cardiac output in infants and children: comparison with simultaneous thermodilution. *Pediatr Cardiol*. 1987; 8: 241-6.

241. Beker F, Davis PG, Sehgal A and Rogerson S. Echocardiographic assessment of left ventricular outflow tract diameter in preterm infants. *Australas J Ultrasound Med*. 2014; 17: 146-9.

242. Evans N and Iyer P. Assessment of ductus arteriosus shunt in preterm infants supported by mechanical ventilation: effect of interatrial shunting. *J Pediatr*. 1994; 125: 778-85.

243. Lee A, Liestol K, Nestaas E, Brunvand L, Lindemann R and Fugelseth D. Superior vena cava flow: feasibility and reliability of the off-line analyses. *Arch Dis Child Fetal Neonatal Ed*. 2010; 95: F121-5.

244. Osborn DA, Evans N, Kluckow M, Bowen JR and Rieger I. Low superior vena cava flow and effect of inotropes on neurodevelopment to 3 years in preterm infants. *Pediatrics*. 2007; 120: 372-80.

245. Holberton JR, Drew SM, Mori R and Konig K. The diagnostic value of a single measurement of superior vena cava flow in the first 24 h of life in very preterm infants. *Eur J Pediatr*. 2012; 171: 1489-95.

246. Bates S, Odd D, Luyt K, et al. Superior vena cava flow and intraventricular haemorrhage in extremely preterm infants. *J Matern Fetal Neonatal Med*. 2016; 29: 1581-7.

247. Ficial B, Bonafiglia E, Padovani EM, et al. A modified echocardiographic approach improves reliability of superior vena caval flow quantification. *Arch Dis Child Fetal Neonatal Ed*. 2017; 102: F7-F11.

248. Evans N and Iyer P. Incompetence of the foramen ovale in preterm infants supported by mechanical ventilation. *J Pediatr*. 1994; 125: 786-92.

249. Evans N and Kluckow M. Early ductal shunting and intraventricular haemorrhage in ventilated preterm infants. *Arch Dis Child Fetal Neonatal Ed*. 1996; 75: F183-6.

250. Kluckow M and Evans N. Ductal shunting, high pulmonary blood flow, and pulmonary hemorrhage. *J Pediatr*. 2000; 137: 68-72.

251. Noori S, McCoy M, Friedlich P, et al. Failure of ductus arteriosus closure is associated with increased mortality in preterm infants. *Pediatrics*. 2009; 123: e138-44.

252. Dix L, Molenschot M, Breur J, et al. Cerebral oxygenation and echocardiographic parameters in preterm neonates with a patent ductus arteriosus: an observational study. *Arch Dis Child Fetal Neonatal Ed*. 2016.

253. Lemmers PM, Toet MC and van Bel F. Impact of patent ductus arteriosus and subsequent therapy with indomethacin on cerebral oxygenation in preterm infants. *Pediatrics*. 2008; 121: 142-7.

254. Petrova A, Bhatt M and Mehta R. Regional tissue oxygenation in preterm born infants in association with echocardiographically significant patent ductus arteriosus. *J Perinatol*. 2011; 31: 460-4.

255. van der Laan ME, Roofthooft MT, Fries MW, et al. A Hemodynamically Significant Patent Ductus Arteriosus Does Not Affect Cerebral or Renal Tissue Oxygenation in Preterm Infants. *Neonatology*. 2016; 110: 141-7.

256. Evans N. Diagnosis of patent ductus arteriosus in the preterm newborn. *Arch Dis Child*. 1993; 68: 58-61.

257. Skelton R, Evans N and Smythe J. A blinded comparison of clinical and echocardiographic evaluation of the preterm infant for patent ductus arteriosus. *J Paediatr Child Health*. 1994; 30: 406-11.

258. Kluckow M and Evans N. Early echocardiographic prediction of symptomatic patent ductus arteriosus in preterm infants undergoing mechanical ventilation. *J Pediatr*. 1995; 127: 774-9.

259. Su BH, Watanabe T, Shimizu M and Yanagisawa M. Echocardiographic assessment of patent ductus arteriosus shunt flow pattern in premature infants. *Arch Dis Child Fetal Neonatal Ed*. 1997; 77: F36-40.

260. Brown ER. Increased risk of bronchopulmonary dysplasia in infants with patent ductus arteriosus. *J Pediatr*. 1979; 95: 865-6.

261. El-Khuffash A, Higgins M, Walsh K and Molloy EJ. Quantitative assessment of the degree of ductal steal using celiac artery blood flow to left ventricular output ratio in preterm infants. *Neonatology*. 2008; 93: 206-12.

262. Hoodbhoy SA, Cutting HA, Seddon JA and Campbell ME. Cerebral and splanchnic hemodynamics after duct ligation in very low birth weight infants. *J Pediatr*. 2009; 154: 196-200.

263. Walther FJ, Kim DH, Ebrahimi M and Siassi B. Pulsed Doppler measurement of left ventricular output as early predictor of symptomatic patent ductus arteriosus in very preterm infants. *Biol Neonate*. 1989; 56: 121-8.

264. Lindner W, Seidel M, Versmold HT, Dohlemann C and Riegel KP. Stroke volume and left ventricular output in preterm infants with patent ductus arteriosus. *Pediatr Res*. 1990; 27: 278-81.

265. Johnson GL, Breart GL, Gewitz MH, et al. Echocardiographic characteristics of premature infants with patient ductus arteriosus. *Pediatrics*. 1983; 72: 864-71.

266. El Hajjar M, Vaksmann G, Rakza T, Kongolo G and Storme L. Severity of the ductal shunt: a comparison of different markers. *Arch Dis Child Fetal Neonatal Ed*. 2005; 90: F419-22.

267. Groves AM, Kuschel CA, Knight DB and Skinner JR. Does retrograde diastolic flow in the descending aorta signify impaired systemic perfusion in preterm infants? *Pediatr Res*. 2008; 63: 89-94.

268. Gournay V, Cambonie G and Roze JC. Doppler echocardiographic assessment of pulmonary blood flow in healthy newborns. *Acta Paediatr*. 1998; 87: 419-23.

269. Smielewski P, Czosnyka M, Steiner L, Belestri M, Piechnik S and Pickard JD. ICM+: software for on-line analysis of bedside monitoring data after severe head trauma. *Acta neurochirurgica Supplement*. 2005; 95: 43-9.

270. Parry G, Tucker J, Tarnow-Mordi W and Group UKNSSC. CRIB II: an update of the clinical risk index for babies score. *Lancet*. 2003; 361: 1789-91.

271. Mohamed MA and Aly H. Transport of premature infants is associated with increased risk for intraventricular haemorrhage. *Arch Dis Child Fetal Neonatal Ed*. 2010; 95: F403-7.

272. Marlow N, Bennett C, Draper ES, Hennessy EM, Morgan AS and Costeloe KL. Perinatal outcomes for extremely preterm babies in relation to place of birth in England: the EPICure 2 study. *Arch Dis Child Fetal Neonatal Ed*. 2014; 99: F181-8.

273. Roberts D and Dalziel S. Antenatal corticosteroids for accelerating fetal lung maturation for women at risk of preterm birth. *Cochrane Database Syst Rev*. 2006: CD004454.

274. Vogel JP, Souza JP, Gulmezoglu AM, et al. Use of antenatal corticosteroids and tocolytic drugs in preterm births in 29 countries: an analysis of the WHO Multicountry Survey on Maternal and Newborn Health. *Lancet*. 2014; 384: 1869-77.

275. Doyle LW, Crowther CA, Middleton P and Marret S. Antenatal magnesium sulfate and neurologic outcome in preterm infants: a systematic review. *Obstet Gynecol*. 2009; 113: 1327-33.

276. Costantine MM, Weiner SJ, Eunice Kennedy Shriver National Institute of Child H and Human Development Maternal-Fetal Medicine Units N. Effects of antenatal exposure to magnesium sulfate on neuroprotection and mortality in preterm infants: a meta-analysis. *Obstet Gynecol*. 2009; 114: 354-64.

277. Moisiadis VG and Matthews SG. Glucocorticoids and fetal programming part 1: Outcomes. *Nat Rev Endocrinol*. 2014; 10: 391-402.

278. Moisiadis VG and Matthews SG. Glucocorticoids and fetal programming part 2: Mechanisms. *Nat Rev Endocrinol*. 2014; 10: 403-11.

279. Patterson RM. Corticosteroids for fetal maturation. *JAMA*. 1995; 274: 943.

280. Effect of corticosteroids for fetal maturation on perinatal outcomes. NIH Consensus Development Panel on the Effect of Corticosteroids for Fetal Maturation on Perinatal Outcomes. *JAMA*. 1995; 273: 413-8.

281. Jobe AH and Soll RF. Choice and dose of corticosteroid for antenatal treatments. *Am J Obstet Gynecol*. 2004; 190: 878-81.

282. Baud O, Foix-L'Helias L, Kaminski M, et al. Antenatal glucocorticoid treatment and cystic periventricular leukomalacia in very premature infants. *N Engl J Med*. 1999; 341: 1190-6.

283. Lee BH, Stoll BJ, McDonald SA, Higgins RD, National Institute of Child H and Human Development Neonatal Research N. Adverse neonatal outcomes associated with antenatal dexamethasone versus antenatal betamethasone. *Pediatrics*. 2006; 117: 1503-10.

284. Lee BH, Stoll BJ, McDonald SA, Higgins RD, National Institute of Child H and Human Development Neonatal Research N. Neurodevelopmental outcomes of extremely low birth weight infants exposed prenatally to dexamethasone versus betamethasone. *Pediatrics*. 2008; 121: 289-96.

285. Vinukonda G, Dummula K, Malik S, et al. Effect of prenatal glucocorticoids on cerebral vasculature of the developing brain. *Stroke*. 2010; 41: 1766-73.

286. Schwab M, Roedel M, Anwar MA, et al. Effects of betamethasone administration to the fetal sheep in late gestation on fetal cerebral blood flow. *J Physiol*. 2000; 528: 619-32.

287. Derks JB, Giussani DA, Jenkins SL, et al. A comparative study of cardiovascular, endocrine and behavioural effects of betamethasone and dexamethasone administration to fetal sheep. *J Physiol*. 1997; 499 (Pt 1): 217-26.

288. Fletcher AJ, McGarrigle HH, Edwards CM, Fowden AL and Giussani DA. Effects of low dose dexamethasone treatment on basal cardiovascular and

endocrine function in fetal sheep during late gestation. *J Physiol*. 2002; 545: 649-60.

289. Duley L, Gulmezoglu AM, Henderson-Smart DJ and Chou D. Magnesium sulphate and other anticonvulsants for women with pre-eclampsia. *Cochrane Database Syst Rev*. 2010: CD000025.

290. Roy J, Mitra JK and Pal A. Magnesium sulphate versus phenytoin in eclampsia - Maternal and foetal outcome - A comparative study. *Australas Med J*. 2013; 6: 483-95.

291. Sarri G, Davies M, Gholitabar M, Norman JE and Guideline Development G. Preterm labour: summary of NICE guidance. *BMJ*. 2015; 351: h6283.

292. Oddie S, Tuffnell DJ and McGuire W. Antenatal magnesium sulfate: Neuro-protection for preterm infants. *Arch Dis Child Fetal Neonatal Ed*. 2015; 100: F553-7.

293. Rouse DJ. Magnesium sulfate for the prevention of cerebral palsy. *Am J Obstet Gynecol*. 2009; 200: 610-2.

294. Zylinska L, Gulczynska E and Kozaczuk A. Changes in erythrocyte glutathione and plasma membrane calcium pump in preterm newborns treated antenatally with MgSO4. *Neonatology*. 2008; 94: 272-8.

295. Manuck TA, Rice MM, Bailit JL, et al. Preterm neonatal morbidity and mortality by gestational age: a contemporary cohort. *Am J Obstet Gynecol*. 2016; 215: 103 e1- e14.

296. Bennet L, Galinsky R, Draghi V, et al. Time and sex dependent effects of magnesium sulphate on post-asphyxial seizures in preterm fetal sheep. *J Physiol*. 2018.

297. Rouse DJ, Hirtz DG, Thom E, et al. A randomized, controlled trial of magnesium sulfate for the prevention of cerebral palsy. *N Engl J Med*. 2008; 359: 895-905.

298. Sugimoto J, Romani AM, Valentin-Torres AM, et al. Magnesium decreases inflammatory cytokine production: a novel innate immunomodulatory mechanism. *J Immunol*. 2012; 188: 6338-46.

299. Hoffman DJ, Marro PJ, McGowan JE, Mishra OP and Delivoria-Papadopoulos M. Protective effect of MgSO4 infusion on nmda receptor binding characteristics during cerebral cortical hypoxia in the newborn piglet. *Brain Res*. 1994; 644: 144-9.

300. Galinsky R, Davidson JO, Drury PP, et al. Magnesium sulphate and cardiovascular and cerebrovascular adaptations to asphyxia in preterm fetal sheep. *J Physiol*. 2016; 594: 1281-93.

301. Mazursky JE, Birkett CL, Bedell KA, Ben-Haim SA and Segar JL. Development of baroreflex influences on heart rate variability in preterm infants. *Early Hum Dev*. 1998; 53: 37-52.

302. Holden K, Morgan JS, Krauss AN and Auld PA. Incomplete baroreceptor responses in newborn infants. *Am J Perinatol*. 1985; 2: 31-4.

303. Fyfe KL, Yiallourou SR, Wong FY and Horne RS. The development of cardiovascular and cerebral vascular control in preterm infants. *Sleep Med Rev*. 2014; 18: 299-310.

304. Andriessen P, Oetomo SB, Peters C, Vermeulen B, Wijn PF and Blanco CE. Baroreceptor reflex sensitivity in human neonates: the effect of postmenstrual age. *J Physiol*. 2005; 568: 333-41.

305. Rhee CJ, Fraser CD, 3rd, Kibler K, et al. Ontogeny of cerebrovascular critical closing pressure. *Pediatr Res*. 2015; 78: 71-5.

306. Eriksen VR, Hahn GH and Greisen G. Cerebral autoregulation in the preterm newborn using near-infrared spectroscopy: a comparison of time-domain and f requency-domain analyses. *J Biomed Opt*. 2015; 20: 037009.

307. Balegar KK, Stark MJ, Briggs N and Andersen CC. Early cerebral oxygen extraction and the risk of death or sonographic brain injury in very preterm infants. *J Pediatr*. 2014; 164: 475-80 e1.

308. Meng L, Hou W, Chui J, Han R and Gelb AW. Cardiac Output and Cerebral Blood Flow: The Integrated Regulation of Brain Perfusion in Adult Humans. *Anesthesiology*. 2015; 123: 1198-208.

309. Nasr N, Czosnyka M, Pavy-Le Traon A, et al. Baroreflex and cerebral autoregulation are inversely correlated. *Circ J*. 2014; 78: 2460-7.

310. Zhang Y, Liu X, Steiner L, et al. Correlation Between Cerebral Autoregulation and Carbon Dioxide Reactivity in Patients with Traumatic Brain Injury. *Acta Neurochir Suppl*. 2016; 122: 205-9.

311. Helou S, Koehler RC, Gleason CA, Jones MD, Jr. and Traystman RJ. Cerebrovascular autoregulation during fetal development in sheep. *Am J Physiol*. 1994; 266: H1069-74.

312. Brady KM, Mytar JO, Lee JK, et al. Monitoring cerebral blood flow pressure autoregulation in pediatric patients during cardiac surgery. *Stroke*. 2010; 41: 1957-62.

313. da Costa CS, Czosnyka M, Smielewski P, Mitra S, Stevenson GN and Austin T. Monitoring of Cerebrovascular Reactivity for Determination of Optimal Blood Pressure in Preterm Infants. *J Pediatr*. 2015; 167: 86-91.

314. Boddy K, Dawes GS, Fisher R, Pinter S and Robinson JS. Foetal respiratory movements, electrocortical and cardiovascular responses to hypoxaemia and hypercapnia in sheep. *J Physiol*. 1974; 243: 599-618.

315. Dawes GS, Johnston BM and Walker DW. Relationship of arterial pressure and heart rate in fetal, new-born and adult sheep. *J Physiol*. 1980; 309: 405-17.

316. Kitanaka T, Alonso JG, Gilbert RD, Siu BL, Clemons GK and Longo LD. Fetal responses to long-term hypoxemia in sheep. *Am J Physiol*. 1989; 256: R1348-54.

317. Macdonald AA, Colenbrander B and Wensing CJ. The effects of gestational age and chronic fetal decapitation on arterial blood pressure in the pig fetus. *Eur J Obstet Gynecol Reprod Biol*. 1983; 16: 63-70.

318. Reeves JT, Daoud FS and Gentry M. Growth of the fetal calf and its arterial pressure, blood gases, and hematologic data. *J Appl Physiol*. 1972; 32: 240-4.

319. Giussani DA, Forhead AJ and Fowden AL. Development of cardiovascular function in the horse fetus. *J Physiol*. 2005; 565: 1019-30.

320. Kusaka T, Okubo K, Nagano K, Isobe K and Itoh S. Cerebral distribution of cardiac output in newborn infants. *Archives of disease in childhood Fetal and neonatal edition*. 2005; 90: F77-8.

321. Bouma GJ and Muizelaar JP. Relationship between cardiac output and cerebral blood flow in patients with intact and with impaired autoregulation. *Journal of neurosurgery*. 1990; 73: 368-74.

322. Howlett JA, Northington FJ, Gilmore MM, et al. Cerebrovascular autoregulation and neurologic injury in neonatal hypoxic-ischemic encephalopathy. *Pediatric research*. 2013; 74: 525-35.

323. Seri I. Management of hypotension and low systemic blood flow in the very low birth weight neonate during the first postnatal week. *Journal of perinatology : official journal of the California Perinatal Association*. 2006; 26 Suppl 1: S8-13; discussion S22-3.

324. Tyszczuk L, Meek J, Elwell C and Wyatt JS. Cerebral blood flow is independent of mean arterial blood pressure in preterm infants undergoing intensive care. *Pediatrics*. 1998; 102: 337-41.

325. du Plessis AJ and Volpe JJ. Perinatal brain injury in the preterm and term newborn. *Current opinion in neurology*. 2002; 15: 151-7.

326. Van Bel F, Van de Bor M, Stijnen T, Baan J and Ruys JH. Aetiological role of cerebral blood-flow alterations in development and extension of peri-intraventricular haemorrhage. *Dev Med Child Neurol*. 1987; 29: 601-14.

327. Logan JW, O'Shea TM, Allred EN, et al. Early postnatal hypotension and developmental delay at 24 months of age among extremely low gestational age newborns. *Arch Dis Child Fetal Neonatal Ed*. 2011; 96: F321-8.

328. da Costa CS, Greisen G and Austin T. Is near-infrared spectroscopy clinically useful in the preterm infant? *Arch Dis Child Fetal Neonatal Ed*. 2015; 100: F558-61.

329. Rhee CJ, Fraser CD, Kibler K, et al. The Ontogeny of Cerebrovascular Pressure Autoregulation in Premature Infants. *Acta Neurochir Suppl*. 2016; 122: 151-5.

330. Weersink CS, Aries MJ, Dias C, et al. Clinical and Physiological Events That Contribute to the Success Rate of Finding "Optimal" Cerebral Perfusion Pressure in Severe Brain Trauma Patients. *Crit Care Med*. 2015; 43: 1952-63.

331. Liu X, Maurits NM, Aries MJH, et al. Monitoring of Optimal Cerebral Perfusion Pressure in Traumatic Brain Injured Patients Using a Multi-Window Weighting Algorithm. *J Neurotrauma*. 2017; 34: 3081-8.

332. Sortica da Costa C, Placek MM, Czosnyka M, et al. Complexity of brain signals is associated with outcome in preterm infants. *J Cereb Blood Flow Metab*. 2017: 271678X16687314.

333. Kang HG, Costa MD, Priplata AA, et al. Frailty and the degradation of complex balance dynamics during a dual-task protocol. *J Gerontol A Biol Sci Med Sci*. 2009; 64: 1304-11.

334. Noren H, Amer-Wahlin I, Hagberg H, et al. Fetal electrocardiography in labor and neonatal outcome: data from the Swedish randomized controlled trial on intrapartum fetal monitoring. *Am J Obstet Gynecol*. 2003; 188: 183-92.

335. Bloom SL, Belfort M, Saade G, Eunice Kennedy Shriver National Institute of Child H and Human Development Maternal-Fetal Medicine Units N. What we have learned about intrapartum fetal monitoring trials in the MFMU Network. *Semin Perinatol*. 2016; 40: 307-17.

336. Buchman TG. Nonlinear dynamics, complex systems, and the pathobiology of critical illness. *Curr Opin Crit Care*. 2004; 10: 378-82.

337. Costa MD, Schnettler WT, Amorim-Costa C, et al. Complexity-loss in fetal heart rate dynamics during labor as a potential biomarker of acidemia. *Early Hum Dev*. 2014; 90: 67-71.

338. Moorman JR, Delos JB, Flower AA, et al. Cardiovascular oscillations at the bedside: early diagnosis of neonatal sepsis using heart rate characteristics monitoring. *Physiol Meas*. 2011; 32: 1821-32.

339. Group BIUKC, Group BIAC, Group BINZC, et al. Oxygen saturation and outcomes in preterm infants. *N Engl J Med*. 2013; 368: 2094-104.

340. Tang SC, Jen HI, Lin YH, et al. Complexity of heart rate variability predicts outcome in intensive care unit admitted patients with acute stroke. *J Neurol Neurosurg Psychiatry*. 2015; 86: 95-100.

341. Noori S, McCoy M, Anderson MP, Ramji F and Seri I. Changes in cardiac function and cerebral blood flow in relation to peri/intraventricular hemorrhage in extremely preterm infants. *J Pediatr*. 2014; 164: 264-70 e1-3.

342. Angelini L, Maestri R, Marinazzo D, et al. Multiscale analysis of short term heart beat interval, arterial blood pressure, and instantaneous lung volume time series. *Artif Intell Med*. 2007; 41: 237-50.

343. Walther FJ, Siassi B, Ramadan NA, Ananda AK and Wu PY. Pulsed Doppler determinations of cardiac output in neonates: normal standards for clinical use. *Pediatrics*. 1985; 76: 829-33.

344. Groves AM, Kuschel CA, Knight DB and Skinner JR. Echocardiographic assessment of blood flow volume in the superior vena cava and descending aorta in the newborn infant. *Arch Dis Child Fetal Neonatal Ed*. 2008; 93: F24-8.

345. Paradisis M, Evans N, Kluckow M and Osborn D. Randomized trial of milrinone versus placebo for prevention of low systemic blood flow in very preterm infants. *J Pediatr*. 2009; 154: 189-95.

346. Baik N, Urlesberger B, Schwaberger B, Schmolzer GM, Avian A and Pichler G. Cerebral haemorrhage in preterm neonates: does cerebral regional oxygen saturation during the immediate transition matter? *Arch Dis Child Fetal Neonatal Ed*. 2015; 100: F422-7.

347. Kissack CM, Garr R, Wardle SP and Weindling AM. Cerebral fractional oxygen extraction in very low birth weight infants is high when there is low left ventricular output and hypocarbia but is unaffected by hypotension. *Pediatr Res*. 2004; 55: 400-5.

348. Victor S, Appleton RE, Beirne M, Marson AG and Weindling AM. The relationship between cardiac output, cerebral electrical activity, cerebral fractional oxygen extraction and peripheral blood flow in premature newborn infants. *Pediatr Res*. 2006; 60: 456-60.

349. Sirc J, Dempsey EM and Miletin J. Cerebral tissue oxygenation index, cardiac output and superior vena cava flow in infants with birth weight less than 1250 grams in the first 48 hours of life. *Early Hum Dev*. 2013; 89: 449-52.

350. Takami T, Sunohara D, Kondo A, et al. Changes in cerebral perfusion in extremely LBW infants during the first 72 h after birth. *Pediatr Res*. 2010; 68: 435-9.

351. Moran M, Miletin J, Pichova K and Dempsey EM. Cerebral tissue oxygenation index and superior vena cava blood flow in the very low birth weight infant. *Acta Paediatr*. 2009; 98: 43-6.

352. Williams LR and Leggett RW. Reference values for resting blood flow to organs of man. *Clin Phys Physiol Meas*. 1989; 10: 187-217.

353. Levine BD, Giller CA, Lane LD, Buckey JC and Blomqvist CG. Cerebral versus systemic hemodynamics during graded orthostatic stress in humans. *Circulation*. 1994; 90: 298-306.

354. Ogoh S, Brothers RM, Barnes Q, et al. The effect of changes in cardiac output on middle cerebral artery mean blood velocity at rest and during exercise. *J Physiol*. 2005; 569: 697-704.

355. Choi BR, Kim JS, Yang YJ, et al. Factors associated with decreased cerebral blood flow in congestive heart failure secondary to idiopathic dilated cardiomyopathy. *Am J Cardiol*. 2006; 97: 1365-9.

356. Berre J, De Backer D, Moraine JJ, Melot C, Kahn RJ and Vincent JL. Dobutamine increases cerebral blood flow velocity and jugular bulb hemoglobin saturation in septic patients. *Crit Care Med*. 1997; 25: 392-8.

357. Cencetti S, Lagi A, Cipriani M, Fattorini L, Bandinelli G and Bernardi L. Autonomic control of the cerebral circulation during normal and impaired peripheral circulatory control. *Heart*. 1999; 82: 365-72.

358. Jim WT, Chiu NC, Chen MR, et al. Cerebral hemodynamic change and intraventricular hemorrhage in very low birth weight infants with patent ductus arteriosus. *Ultrasound Med Biol*. 2005; 31: 197-202.

359. Chock VY, Ramamoorthy C and Van Meurs KP. Cerebral autoregulation in neonates with a hemodynamically significant patent ductus arteriosus. *J Pediatr*. 2012; 160: 936-42.

360. Osborn DA, Evans N and Kluckow M. Left ventricular contractility in extremely premature infants in the first day and response to inotropes. *Pediatr Res*. 2007; 61: 335-40.

361. Keren H, Burkhoff D and Squara P. Evaluation of a noninvasive continuous cardiac output monitoring system based on thoracic bioreactance. *Am J Physiol Heart Circ Physiol*. 2007; 293: H583-9.

362. Ballestero Y, Lopez-Herce J, Urbano J, et al. Measurement of cardiac output in children by bioreactance. *Pediatr Cardiol*. 2011; 32: 469-72.

363. Weisz DE, Jain A, McNamara PJ and A EL-K. Non-invasive cardiac output monitoring in neonates using bioreactance: a comparison with echocardiography. *Neonatology*. 2012; 102: 61-7.